THE UNIVERSITY
of EDINBURGH

Follicular T helper cell populations

Marta Trüb

Thesis submitted for the degree of Doctor of Philosophy

The University of Edinburgh

2016

Declaration

I declare that this thesis has been composed by myself, the work presented within is my own, unless acknowledged otherwise, and it has not been submitted in any other application for a higher degree.

Marta Trüb **Date**

Acknowledgements

I thank my supervisor, Prof. David Gray. He has shown great patience, support and understanding with many problems I have encountered throughout my PhD, both inside and outside the lab. His support has been truly invaluable and many of his advices extended beyond the lab bench (like growing green fingers, or simply not giving up and waiting for the things to work). As a PhD student I have received a lot of freedom, independence, and many opportunities to learn from my own mistakes. For this trust shown by Prof. Gray, for the opportunity to grow as a scientist and a person, I am truly grateful.

I also thank my second supervisor, Prof. Rose Zamoyska, for her support throughout my PhD. I greatly appreciate the support she showed outside the lab in difficult times, and I am especially grateful for being able to attend her lab meetings in the second half of my PhD. I am grateful to all of the members of the Zamoyska Lab for their valuable feedbacks on my own project.

Further, I would like to thank the previous members of the Gray Lab: Dr. Tom Barr, Dr. Stefano Casserta and Sheila Brown, for introducing me to the laboratory techniques and protocols, as well as for the initial input in the project. Many thanks go also to Tom Slocombe and Maartje Cleophas, both of which were sources of helpful advice, reagents and stimulating discussions.

This PhD thesis could not have been completed without the help of collaborators. I would like to express my gratitude to Dr. Stefano Caserta, who has kindly helped with the execution of the RNA isolation protocols, which was crucial for the preparation of the samples for the microarray. The microarray analysis (Chapter 1) was fully performed by Dr. Al Ivens, who has done a truly great work answering all the questions, preparing endless lists and graphs, as well as creating fancy ‘clickable volcano’ plots. The TCR sequencing was a close collaboration with Dr. Graeme Cowan, who has prepared the samples for the sequencing, fully analysed the results and prepared the graphs presented in Chapter 5. I am very thankful to Dr. Cowan for the feedback on the chapter and for numerous discussions that strengthen my understanding of the sequencing techniques. I would also like to thank for the great help that I have received from Dr. Martin Waterfall in multiple sorting experiments.

The bone marrow chimeras, B cell transfer experiments and co-immunisation study were performed with the help of Jordan Rixon. In many experiments large numbers of animals were used and I am grateful to my fellow students and scientists, Cara Bray, Dr. Johanna Knipper, Sharon Campbell and Dr. Shatakshi Sood (Shinny), for their help in dissections and the creation of chimeras, which improved the quality of the experiments. I

also greatly appreciate the constructive feedback from Dr. Johanna Knipper on Chapters 1, 2, 3 and 4.

I am very grateful to my parents, Maria and Jacek Bereska, for their continuous support during the project, especially in the last stages of writing. Furthermore, I thank our wonderful neighbours and friends, Kenny, Heather and Robbie McGibbon, who have helped us on many occasions, including around the arrival of the new members of our family. I also thank my other fellow students, Angela Marley, Georgina Doonan and Caroline Dewar, for sharing the PhD journey. I am grateful to Dr. Kaija Stockner, Dr. Anna Hoy and Dr. Shinny for their help and encouragement.

Throughout my PhD I often heard a sentence: 'I can't imagine doing a PhD and having a child'. My answer always was: 'I can't imagine doing it without'. Here I say a very special 'thank you' to my lucky token and source of never-ending pride, joy and happiness, my daughter Alba. Your hugs and smiles at the end of the day fix everything, even the failed 12 h experiment. And, amazingly, you can always make me laugh, no matter what, and in these moments I am truly happy.

More special thanks go to my little twins, Benjamin and Aurora. You have been there with me during the writing stage, always bringing a smile to my face and warmth to my heart. I am constantly fascinated by your different natures, so easy to recognise form the first days. Importantly, for most of the time you were quite good sleepers, which is the greatest help I could have expected.

Writing a thesis with three little ones is not easy and many of my friends have surprised me with the extent of their help and support for me and my young family, be it by taking Benjamin and Aurora for a walk, coming with a prepared dinner, playing with Alba, organising shopping or giving me some time off. For this, I am truly grateful to Sharon Campbell, Kasia Gawron, Stela MacLachlan, Wiebke Nahrendorf, Cara Bray and Joe. Very many thanks go to Celine Garcia, who regularly and generously gave her time and energy, and who has introduced us to French cuisine.

The last person I would like to thank is my husband, Simon Trüb. This PhD has been a long journey, full of hard work, long hours and many turning points. Thanks to you, Simon, it was a shared journey filled with love, support and faith. We built our family during this time, which made it hard, but also very special. This thesis would not be here if I hadn't had you by my side. Thank you for being my editor and fixing all the 'a's/'the's, removing hyphens and '–ings', and adding dots or comas where needed. And thank you for calling my PD-1$^{HI/LO}$ T_{FH} 'PDF cells' – that made me smile a lot.

Therefore, this journey has come to an end. So… let another adventure begin!

Abstract

Humoral immunity provides protection against subsequent infections. Antigen-specific, high-affinity, class-switched antibodies are produced by B cells through rounds of proliferation, B cell receptor rearrangement and selection in the germinal centres (GC). T cells play an essential and indispensable role in this process and in the recent years the term T follicular helper cells (T_{FH}) was coined to describe this cell subset. The aim of my thesis is to investigate whether there is more than one type of T cells within the T_{FH} population and whether it has important functional consequences.

Firstly, I use sheep red blood cell immunisation (SRBC) and *Salmonella enterica* infection to show phenotypical differences between T_{FH} expressing high and low level of surface molecule PD-1. In order to investigate the relationship between different T_{FH} populations gene profiling was carried out on the microarray platform. Detailed transcriptome analysis revealed the discrete nature of isolated T_{FH} cell subsets and provided an overview of their genetic landscape.

Secondly, I have investigated the dependence of T_{FH} subsets on cognate interactions with B cell in SRBC model by generating BM chimeras. I have demonstrated that generation of PD-1^{HI} T_{FH}, but not of PD-1^{LO} T_{FH}, depends on antigen presentation by B cells. Furthermore, I have shown that provision of wild-type but not MHC II knock-out B cells rescues PD-1^{HI} formation in BM chimeras after SRBC immunisation. Finally, I have explored plasticity within T_{FH} subsets and showed that none of the populations is in a terminally differentiated state, as they can convert into one another.

Thirdly, experiments with *S. enterica* model revealed that the absence of PD-1^{HI} T_{FH} is independent of the splenic architecture disruption present within the first week of the response. Surprisingly, co-immunisation studies showed that PD-1^{HI} population is not only present but even enhanced in the group which received both SRBC and *S. enterica* when compared to single immunisations.

The work presented in the thesis documents that there is a significant and previously unappreciated heterogeneity within T_{FH} subset. This knowledge is

important for designing optimal vaccine strategies and treating autoimmune diseases, as in both processes the antibody production plays a crucial role and its manipulation (either enhancing or blocking antibody production, respectively) can significantly improve clinical interventions.

Abrreviations

Ab	Antibody
Ag	Antigen
AID	Activation Induced Cytidine Deaminase
APC	Allophycocyanin
APC	Antigen Presenting Cell
APRIL	A Proliferation Inducing Ligand
BAFF	B cell-Activating Factor
Bcl-2	B Cell Lymphoma Protein 2
Bcl6	B Cell Lymphoma Protein 6
$Bcl\text{-}_{XL}$	B Cell Lymphoma Extra Large
BCR	B Cell Receptor
Blimp-1	B lymphocyte maturation protein 1
BM	Bone Marrow
BrdU	Bromodeoxyuridine
BSA	Bovine Serum Albumine
BTLA	B and T Lymphocyte Attenuator
CCL	Chemokine CC Ligand
CCR	C-C Chemokine Receptor
CD	Cluster of Differentiation
CDR	Complementarity Determining Region
CFA	Complete Freud's Adjuvant
CFU	Colony Forming Unit
CRE	Cyclization Recombination Enzyme
CSR	Class Switch Recombination
CXCL	Chemokine (C-X-C) Ligand
DC	Dendritic Cell
(d/ss)DNA	(Double /Single Stranded) Deoxyribonucleic Acid

ELISA	Enzyme Linked Immunosorbent Assay
FACS	Fluorescence Activated Cell Sorting
FB	FACS Buffer
FCS	Foetal Calf Serum
FDC	Follicular Dendritic Cell
FITC	Fluorescein Isothiocyanate
Foxp3	Forkhead Box P3
FSC	Forward Scatter
GC	Germinal Centre
GFP	Green Fluorescent Protein
h	hour
HEL	Hen Egg-white Lysozyme
HI	High
HK	Heat Killed
SHM	Somatic Hypermutation
ICOS(L)	Inducible Co-Stimulatory Molecule (Ligand)
IFN α/β/γ	Interferon α/β/γ
Ig	Immunoglobulin
IL	Interleukin
IMDM	Iscove's Modified Dulbecco's Medium
i.p.	intraperitoneal
IRF4	Interferon Regulatory Factor 4
i.v.	intravenous
ITAM	Immunoreceptor Tyrosine-based Activation Motif
ITSM	Immunoreceptor Tyrosine-based Switch Motif
KLH	Keyhole Limpet Hemocyanin
KLRG-1	Killer-Cell Lectin-Like Receptor Subfamily G, Member 1

KO	Knock Out
LCMV	Lymphocytic Choriomeningitis Virus
LO	Low
mAb	Monoclonal Antibody
MAPK	Mitogen-Activated Protein Kinase
MFI	Mean Fluoresnce Intensity
MHC	Major Histocompatibility Complex
min	minute
MPECs	Memory Precursor Effector Cells
MyD88	Myeloid Differentiation Factor 88
NGS	Next Generation Sequencing
NK cell	Natural Killer Cell
NP	4-hydroxy-3nitrophenylacetyl
OVA	Ovalbumin
p:MHC	Peptide:MHC Complex
PAMP	Pathogen-Associated Molecular Pattern
PB	Pacific Blue
PBS	Phosphate Buffer Saline
PD-1	Programmed Death Protein 1
PE	R-Phycoerythrin
PE-/APC- Cy7	Cyanine Dye
PerCP	Peridinin Chlorophyll Protein
p.i.	Post Immunisation
PKC	Protein Kinase C
PSGL1	P-Selectin Glycoprotein Ligand 1
PRRs	Pathogen Recognition Recrptors
RFP	Red Fluorescent Protein
RNA	Ribonucleic Acid

RT	Room Temeprature
SAP	SLAM-associated Protein
SLAM	Signaling Lymphocytic Activation Molecule
SLE	Systemic Lupus Erythematosus
SLECs	Short Lived Effector Cells
SLO	Secondary Lymhoid Organs
SSC	Side Scatter
STAT	Signal Transducer and Activator of Transcription
TCR	T Cell Receptor
TF	Transcription Factor
Th	T Helper Cell
T_{FH}	T Follicular Helper Cells
T_{FR}	T Follicular Regulatory Cells
TGF-β	Transforming Growth Factor-β
TLR	Toll-Like Receptor
TNF–α	Tumor Necrosis Factor-α
Treg	Regulatory T cell
(S)RBC	(Sheep) Red Blood Cell
WT	Wild Type

List of Figures and Tables

Table of Contents:

1 Introduction

1.1 Overview of the immune system

The mammalian immune system has evolved to defend the organism from invading pathogens. Its main purpose is to provide a rapid response to infection, clear the pathogen, repair the damage and establish long-lasting protection. Therefore, the cells of the immune system are able to recognise and be activated by foreign entities while they at the same time remain non-responsive to one's own cells and tissues. The ability to distinguish between self and foreign antigen is one of the crucial aspects of the immune system.

The immune response consists of an innate and an adaptive phase. While the innate response acts early and is not specific to the pathogen, the adaptive response requires time to develop and is highly specific for the infectious agent. The activation of the innate immune cells (macrophages, dendritic cells (DCs), neutrophils, eosinophils and others) initiates the adaptive immune responses (T and B lymphocytes). Following the capture of the pathogen in the tissue, antigen presenting cells (APCs) migrate to the secondary lymphoid organs (SLO) where they process and display the antigen on their surface. The recognition of antigen by T cells (mediated by T cell receptor, TCR) as well as the influence of cytokines secreted by APC leads to T cell activation and differentiation (discussed in detail later). Activated T cells migrate back to the site of the infection to facilitate pathogen clearance and control the magnitude of the immune response at the same time. Additionally, in the SLO specialised T cells support B cell differentiation into either plasma cells, which secrete large amounts of antibodies, or memory B cells, which are the source of a long-lasting immunity to the invading pathogen.

The interplay between the innate and adaptive immune response is incredibly complex, as it involves multiple cell types in various locations of the body over a period of time. The biggest challenges for immunologists is to understand this complicated process in the first place and then to take advantage of it by designing protective vaccines and treatments involving the cells of the immune system.

1.2 Structure of the spleen

The spleen is the largest SLO. It is a major site of haematopoiesis in the mice until the 5th month of gestation at which stage the BM takes over the role. The spleen develops at embryonic day 12 by the formation of the splanchnic mesodermal plate (1). Two and a half days later, after the arrival of the progenitors of the erythroid and myeloid cell lineages, the first haematopoietic stem cell settles in the spleen. Additionally, at this stage inductive signals for the development of other SLO are derived from lymphoid-tissue-inducer cells (LTi), also located in the spleen (1). The anatomically and functionally mature spleen is divided into the red and the white pulp (Fig. 1.1).

1.2.1 Red pulp

The red pulp is a specialised area of the spleen committed to extensive blood filtering. One of the functions of the red pulp is to remove old erythrocytes and recycle iron contained within them. Aged erythrocytes display a stiffening membrane and get stuck to the cords made of fibroblasts and reticular fibres (1). They are later phagocytosed by splenic macrophages located in the same cords. Iron recovered from the old red blood cells is either secreted to the blood stream or is stored inside macrophages in form of insoluble complexes (1). At the same time, macrophages capture the haemoglobin found in the blood stream from the erythrocytes, which were damaged intravascularly in different sites of the body (1). The second important function of the red pulp of the spleen is to capture and limit the spread of systemic pathogens. This function is performed by red pulp macrophages (1). Finally, it is in the red pulp of the spleen where plasmablasts and plasma cells reside and secrete large amount of antibodies, which then enter the bloodstream directly. This localization of plasma cells is mediated by the high concentration of the CXCL12 chemokine in the red pulp and the expression of its receptor, CXCR4, on the plasma cells (2). Therefore, blood entering the spleen (via collective vein) is cleared of old erythrocytes, haemoglobin and pathogen born particles and is supplied with iron and antibodies.

1.2.2 White pulp

The white pulp of the spleen is composed of spatially segregated T and B cell zones. The separation of lymphocytes into discreet compartments is possible due to differences in chemokines produced by non-lymphoid stromal cells and their receptors expressed by lymphocytes. B cells express the CXCR5 chemokine receptor, which binds CXCL13 produced by stromal cells and follicular DCs (FDC) within the B cell follicle (Fig. 1.1, (3-5)). T cells, on the other hand, express in the steady state the CCR7 receptor responding to CCL19 and CCL21 chemokines, produced by fibroblast reticular cells within the T cell zones (6). Additionally, high endothelial venules (HEV) express CCL19 and CCL21 in order to attract and recruit naïve T cells from the circulation (7). The highly organised structure of the white pulp allows for the efficient interactions between naïve T cells and antigen presenting DCs as well as the interaction between activated T and B cells, increasing the probability of interaction between rare antigen-specific cells. As a consequence of this interaction, lymphocytes alter their chemokine receptor expression, which enables migration within the white pulp according to the activation status of the cell (Fig.1.1).

1.2.3 Marginal zone

The marginal zone (MZ) is the interface between the circulation and the lymphoid compartments, flanked by the red and the white pulp of the spleen (Fig. 1.1). The MZ is an entry point for the blood via the marginal sinus (8,9). It is composed of distinct subsets of resident cells, namely MZ macrophages, metallophilic macrophages and MZ B cells.

Two resident MZ macrophage populations can be distinguished by their location and the unique expression of their surface receptors. MZ macrophages expressing SIGN-R1 (C-type lectin receptor, mouse homologue of human DC-SIGN) and MARCO (macrophage receptor with collagenous structure, type I scavenger receptor) receptors form the outer ring of macrophages (1,10). MZ metallophilic macrophages are defined by the expression of Siglec-1 (Sialic acid binding IG-like lectin) and MOMA-1 (Monocyte-Macrophage receptor 1) (1,10,11). Macrophages of the MZ play two important roles, namely pathogen phagocytosis and clearance from

the circulation as well as further activation of the immune system. The first task is possible due to the expression of various pattern recognition receptors (PRRs), such as Toll-like receptors (TLRs), C-type lectin receptors and scavenger receptors (10). PRRs sense pathogen-associated molecular patterns (PAMPs) characteristic for bacteria, viruses and yeast, such as lipopolisaccharide (LPS) or zymosan. Additionally, the bacterial or viral uptake by MZ macrophages limits the spread of pathogens to peripheral organs (12). The second function of MZ macrophages (activation of the immune system) is mediated by the secretion of the cytokines tailored to the invading pathogen (e.g. IFN-α and IFN-β in response to viral antigens, (1)). $CD8^+$ T cell activation can also be initiated through direct interaction between MZ metallophilic macrophages and DCs (10). Additionally, MZ metallophilic macrophages can activate invariant natural killer cells (iNKTs) by the expression of CD1-d, a lipid-binding non-classical MHC molecule (9). Interestingly, the clodronate-mediated depletion of both MZ macrophage populations showed that these cells are dispensable in T cell dependent (TD) responses (10). This is also supported by the observation that neither of the macrophage populations expresses MHC class II, which refutes their role as APCs (1) .

Another resident cell subset of the MZ is MZ B cells. These MZ B cells can be distinguished from follicular B cells by their anatomical location, surface phenotype and function. Unlike follicular B cells, MZ B cells do not enter the circulation (8). High surface expression of IgM, CD1d, CD9, CD21, CD22, CD25 and CD38 and low surface levels of IgD, CD23 and B220 defines MZ B cells phenotypically (8,9). Although MZ B cells are best known for their role in T-cell independent responses (described below), they also take part in TD responses. In fact, MZ B cells express higher surface levels of CD80/86 and MHC class II molecules and are therefore considered to be more potent T cell activators than follicular B cells (8,13,14). Additionally, the regulatory role of MZ B cells is illustrated by the fact that these cells secrete more IL-10 in response to apoptotic cells than follicular B cells (15).

1.3 T cell independent responses

T-cell independent (TI) responses describe B cell activation in the absence of T cell help. This phenomenon is observed most prominently in MZ B cells and B-1b cells subsets.

MZ B cells can readily detect and respond to blood-born pathogens due to their privileged positioning adjacent to the marginal sinus (9,14). The recognition of the infectious agent can be mediated by extensive cross-linking of the B cell receptor (BCR) due to repetitive motifs present on the pathogen surface as well as activation of TLRs (9). In fact, the BCR repertoire of MZ B cells is slightly skewed to recognise such conservative motifs (9,16). Additionally, MZ B cells have a lower activation threshold than follicular B cells, partly due to their strong expression of the complement receptor 2 (CD21) and an enhanced ability to bind immune complexes (14,17). The MZ B cell activation results in cytokine secretion, enhanced antigen presentation and extensive production of class-switched, non-mutated low-affinity antibodies (9,17). The rapid antibody production by MZ B cells can be partially attributed to high levels of transcription factor (TF) Blimp-1 (B-lymphocyte-induced maturation protein 1), essential for the plasma cell formation (9). Impressively, MZ B cells can secrete antigen-specific antibodies as early as day 1 to 3 upon administration of blood–derived antigen, whereas it takes between 5 and 7 days for the GC B cells to start secreting high-affinity antibodies (9,13,17). Therefore, antibodies secreted by MZ B cells are crucial to control the systemic infection in the early phases of the response prior to the generation of high-affinity antibodies in the GC after somatic hypermutation (SHM, (9,13,17,18)).

Another subset displaying TI responses are 'innate-like' B cells – B-1b cells[1]. These cells reside in the peritoneal and the pleural cavity, they also display an enrichment in BCR sequences mediating recognition of repetitive antigens (16). Similarly to MZ B cells, B-1b cells readily produce large amounts of antigen-specific IgM antibodies in response to TLR activation or BCR engagement (14,16,19).

[1] B-1a cells, also found in the pleural and the peritoneal cavity, produce constant low-levels of polyreactive antibodies (against e.g. influenza virus). These are IgM of low or high affinity antibodies directed against conservative motives found on many pathogens.

1.4 TD responses and GC

1.4.1 TD responses

In contrast to TI responses directed mainly towards polysaccharides, protein antigens are TD immune responses. Follicular B cells (termed also B-2b cells) predominate in these responses. Apart from BCR engagement (signal 1), B cells additionally need to receive help from T cells to be fully activated (signal 2). The need for two signals has evolved in order to avoid strong and damaging immune responses to self-antigens by auto-reactive B cells.

Naïve T cells are contained within T cell zones, where the constant probing of DCs loaded with antigen occurs (20). When a naïve T cell encounters a DC presenting the cognate antigen and co-stimulatory molecules such as CD40 and OX40L, it up regulates the CXCR5 chemokine receptor and migrates towards the B cell zone (Fig. 1.1 (21)). Another requirement for the positioning of T cells on the border of the B cell follicle and for the successful entry of T cells into the follicle is the down-regulation of CCR7, as the expression of the CXCR5 receptor *per se* is not sufficient to drive these processes (22).

1.4.2 B cell activation

Antigen-specific $CD4^+$ T helper cells interact with B cells displaying the peptide-MHC class II (p:MHC) complex on their surface. Alongside cognate interaction, a set of activation receptors on the cell surface of both T and B cells needs to be engaged, including ICOS-ICOSL and CD28-CD80/86, respectively. The outcomes of this cell-cell interaction for the B cell are either to become a plasma cell (terminally differentiated cells secreting large amount of antibodies in the extrafollicular zone) or to return to the follicle and seed the GC (Fig. 1.1). The choice between those two fates is thought to be at least partially determined by BCR signal strength, as low affinity B cells will form GC and high will turn into plasma cells (23). Other factors involved in the process might involve the amount of co-stimulatory signals derived by T cells and the level of antigen-receptor engagement (24). On the molecular level, plasma cells and GC B cells can be defined by the expression of two antagonistic TFs: Blimp-1 and B cell lymphoma-6 (Bcl-6), respectively (25,26).

1.4.3 Follicular DCs (FDC)

The GC is a specialized B cell area within the B cell follicle, where SHM, antibody class switch and affinity maturation take place (26,27). The scaffold of the GC is formed by cells of stromal origin called follicular dendritic cells (FDCs, (24,27,28)). FDCs produce the chemokine CXCL13 (also known as B-cell chemoattractant, BLC) and are therefore crucial in maintaining the structure of SLO (Fig. 1.2 (28)). Additionally, FDCs are a potential source of other cytokines supporting GC B cells, namely IL-6 and BAFF (B cell-activating factor belonging to TNF family (29)), although their role in this process is still controversial (30). Most importantly, FDCs capture and retain antigen in the form of spatially organised immune complexes called iccosomes, which are displayed on their surface to naïve B cells in the primary follicle or activated B cells within the GC (27,30,31). The requirement for FDCs in GC response is illustrated by a study showing that selective FDC ablation leads to GC disappearance within 48 h (31).

1.4.4 Dark zone of GC

Some of the activated B cells initiate the GC reaction. They start to proliferate rapidly and are called centroblasts (Fig. 1.2). Centroblasts form the dark zone of the GC and by their expansion naïve B cells (IgM^+ or IgD^+) are pushed to the outer part of the GC, and form a so called follicular mantle (Fig. 1.2 (32)). Centroblasts are undergoing SHM, where mutations are introduced to the variable (V) regions encoding the BCR in order to increase the affinity of the BCR to the foreign antigen (24,32,33). These mutations are targeted to complimentary-binding regions (CDRs), which form an antigen binding site and, therefore, define the specificity and affinity of BCR towards particular antigens (24,32,33). Both somatic hypermutation and class-switch (occurring in the centrocytes, discussed below) are genomic mutations processes mediated by the enzyme called activation-induced cytidine-deaminase (AID) (33). AID mediates the deamination of deoxycytidine residues of the DNA, which can transform a C:G base pair into a U:G base pair and subsequent repair mechanisms fill the abasic site with potentially any nucleotide (32). Additionally, deamination can cause double strand DNA breaks and ultimately lead to the deletion of large DNA regions important in isotype switch recombination (32). During these extensive DNA rearrangements centroblasts do not express BCR on their surface.

1.4.5 Light zone of GC

Once the BCR rearrangement is complete, centroblasts stop dividing and the new receptor is expressed on the surface of B cells termed centrocytes (Fig. 1.2 (32,33)). Thereafter, class-switching takes place. This is a process in which the constant part of the BCR, made of the μ or δ heavy chain in naïve B cells, is exchanged to either the α, γ or ε heavy chain to form (secreted) BCR of different isotype (IgA, IgG or IgE, respectively). The (improved) affinity of the new BCR for foreign antigen is tested in the light zone of the GC by binding to immune complexes on the FDC surface (24,32,33). BCR-mediated signals are essential for the B cell survival. Additional survival signals, delivered by FDC and T follicular helper cells, are also essential for escaping apoptosis but their precise role is still unknown (33). Centrocytes can re-enter the dark zone and undergo secondary rearrangements; there is direct evidence for the bi-directional exchange of B cells between the dark and light zone within the GC (24). Movement between these compartments is mediated by chemokine receptors and their ligands: CXCR4-CXCL12 in the light zone and CXCR5-CXCL13 in the dark zone (32,33).

1.4.6 Termination of GC

Centrocytes, which have undergone a successful BCR rearrangement become either long-lived plasma cells or memory cells (Fig. 1.2). The post-GC differentiation into plasma cells depends on down-regulation of TF Bcl6 and PAX5 (Paired box 5), which is initiated by combined signals from BCR and CD40-ligation (32). As a consequence, Blimp-1 (B Lymphocyte-Induced Maturation Protein 1) is expressed, alongside other important proteins involved in terminal plasma cell differentiation, such as IRF4 (Interferon Regulatory Factor 4) and XBP1 (X-box-binding protein 1) (23,32). The signals initiating the development into memory cells are less well understood. It seems that centrocytes which continue to express PAX5 become memory cells (32). CD40-CD40L interactions are another required signal for the acquisition of memory phenotype (32). The decision whether a cell becomes a plasma cell or a memory cell might also be determined by the affinity of the newly-formed BCR. It was suggested that cells which express a high-affinity BCR preferentially become plasma cells, while memory cells express a low-affinity receptor (32). Long-lived plasma cells migrate to the red pulp of the spleen as well as

the BM, where they can survive in the specialised niches, secreting low-levels of antibodies even for a life time (34). Memory B cells locate to various anatomical sides, including spleen, lymph nodes, or mucosal-associated anatomical tissue; they are also found circulating in the blood (34).

The presence of GC producing high-affinity antigen-specific antibodies is a pre-requisite for the provision of protection from subsequent infections. Therefore, long lasting immunity is a feature absolutely dependent on the successful interaction between T and B lymphocytes. The requirement for sustained contacts between B and T cells is illustrated by the fact that in SAP (SLAM-associated Protein) knock out (KO) mice, where these interactions are disturbed, no GC formation or humoral responses take place (25,35). It is now clear that help to B cells is provided by a specialised subset of T cells and the term 'follicular B helper T cells' (T_{FH}) was coined to refer to this population. The name describes the characteristic localisation in the SLO and the predominant function of this cell subset. T_{FH} cells are the main focus of this thesis and they are therefore discussed in great detail later.

1.5 T cell subsets and differentiation

1.5.1 T cell activation

As discussed earlier, naïve T cells are held in the white pulp of the spleen due to the expression of the CCR7 receptor responding to the CCL19 and CCL21 chemokines produced by fibroblast reticular cells within the T cell zones (6). Here they become activated by the interaction with mature DCs, which have sensed, engulfed and processed the pathogen (36,37).

Immature DCs leave the BM (their site of generation) and migrate to the epithelium, a potential entry site for the pathogens[2]. DCs are highly endocytic cells, dedicated to sampling the environment in order to detect pathogens or host cells damage. Upon encountering PAMPs or danger signals released by injured cells DCs become activated and unresponsive to the environment. They start expressing CCR7, which attracts them to the T cell zones in the SLO. Here they interact with naïve

[2] DCs are a heterogeneous cell subset, here the 'classic', myeloid $CD11c^+$ DC subset is discussed.

T cells by displaying processed antigen on their cell surface on MHC class I or class II molecules. In addition to an antigen specific TCR, co-stimulatory molecules, which are also up-regulated upon DC maturation, are an essential component of efficient activation of a naïve T cell. Furthermore, DCs secrete cytokines essential for differentiation of T cell subsets appropriate to the invading pathogen. Thus, three signals (cognate MHC:TCR interaction, engagement of co-activating receptors and presence of secreted cytokines) are required for the DC-induced T cell differentiation into effector subsets (discussed below) (36,37).

Although DCs play a crucial role in activating T cells in the SLO, other innate cells are important for the activation and support of adaptive responses at the infection site. For example, natural killer cells (NK cells) are an important source of early IFN-γ, supporting Th1 differentiation, basophils influence Th2 responses by secreting IL-4, and γδ T cells enhance Th17 responses by secreting IL-17 (38).

1.5.2 $CD4^+$ T cell differentiation

Different effector $CD4^+$ T helper (Th) cell subsets are generated in order to provide an optimal immune response tailored to the invading pathogen. T cell subsets are usually defined by the expression of a master TF responsible for the acquisition of the stable phenotype and the secretion of the 'signature' cytokine, resulting in their specialised function (Fig. 1.3).

Th1 and Th2 subsets

For a long time Th1 and Th2 cells were recognised as the main Th subsets (39). They are defined by the expression of specific TFs: T-bet (encoded by the gene *Tbx21*) and the selective production of IFN-γ or TF GATA-3 (GATA-binding protein 3) and IL-4, respectively (Fig. 1.3, (39,40,41)). Th1 cells are involved in the response to intracellular pathogens (including bacteria and viruses). This subset is induced by IL-12, secreted by innate immune cells (mainly DCs and macrophages) and IFN-γ, produced by NK cells as well as T cells (41). IL-12 and IFN-γ signalling activates STAT1 and STAT4 (Signal Transducer and Activator of Transcription 1 and 4) pathways as well as T-bet, which starts the Th1 cell differentiation programme (41).

Th2 cells play a role in helminth and worm infections (41). The master TF for this subset is GATA3 and the major signalling pathways involved in the differentiation are signalling via the IL-4 receptor and STAT6 (Fig. 1.3, (41)).

Regulatory T cells (Tregs)

Another T cell subset recognised as a separate lineage are regulatory T cells (Tregs), which express Forkhead Box P3 (Foxp3) TF (Fig. 1.3) (42). Tregs can be generated either in the thymus (and are termed 'natural' nTregs) or induced in the periphery ('inducible' iTregs) under the influence of TGF-β (Transforming Growth Factor- β) (41,43). They play an important role in the suppression of immune responses, which is crucial in preventing and controlling autoimmunity (43). Multiple mechanisms are employed by Tregs to perform their function, such as direct killing of the target cell by the cell-to-cell contact, inhibition of cytokine secretion by other cells (especially IL-2 by cytotoxic T cells) and secretion of the immunosuppressive cytokines such as IL-10 and TGF-β (44).

Th17 cells

Th17 cells are one of the most recently described Th subsets. They are defined by the secretion of IL-17A, IL-17F, IL-21 and IL-22 (39) and the expression of RORγ-T (Retinoic Acid Binding Orphan Receptor γ, Fig. 1.3) (40). Th17 cells play an important role in clearing fungi and extracellular bacteria at the mucosal sites and are also involved in inflammatory diseases (41). This subset seems to display a 'flexible' phenotype, as their conversion to Th1 cells and Tregs cells has been documented (41). Moreover, it seems that the protective or pathogenic role of Th17 cells depends strongly on the environmental cues to which cells are exposed. For example, in the absence of IL-23, Th17 cells can secrete anti-inflammatory IL-10, whereas the presence of IL-23 results in the acquisition of a pathogenic potential and the secretion of inflammatory cytokines (41).

Th9 and Th 22 subsets

Th9 cells have been only recently documented and are quite controversial. Their development requires IL-4 (similarly to Th2 cells) and TGF-β (Fig. 1.3) (38). Other cytokines, such as IL-2, IL-1, IL-33 and IL-25 may also support Th9 differentiation (45). Several TFs are important in the Th9 differentiation, namely Gata3, IRF-4,

STAT6 and PU.1, which would also suggest relationship with Th2 cells. Th9 cells secrete IL-9 alongside other cytokines such as IL-10 and IL-21 (45). The role of Th9 cells is not well defined and is controversial: Th9 cells were shown to play a pathogenic role in allergic lung inflammation and cancer, and a protective or pathogenic role in experimental autoimmune encephalitis (EAE) (45). IL-9 seems to be a difficult cytokine to study, since it shows a pleiotropic character, it can be derived from more than one cell source and its production is transient (45). Clearly much more work needs to be done before Th9 cells become fully recognised as a separate T cell lineage or remain considered a transient developmental phase of other T cell subsets (especially Th2 cells).

The last Th cell subset discussed in current literature (but not yet recognised as a separate lineage) are Th22 cells (Fig.1.3). These cells are found only in humans and are implicated in skin inflammatory conditions, such as psoriasis (38). Th22 cells secrete IL-22 but not IL-17 and seem to be induced by plasmacytoid DC (pDCs) (1,38).

1.5.3 T cell plasticity

Although T cell lineages are considered to display a stable phenotype once differentiation is complete, there is growing evidence of substantial plasticity within T cell subsets (Fig. 1.3). This plasticity can be illustrated by the fact that although each of the subsets produces its 'signature' cytokine, very often it is not an exclusive source of this cytokine. For example, IFN-γ, hallmark of the Th1 programme, can also be made by Th17 cells (40). IL-10, originally thought to be derived from Th2 cells, is produced by many cell types, including Tregs, Th1 cells and cells of the innate system (40). IL-21, the signature cytokine of T_{FH} cells, is also produced by Th17 cells (40). Additionally, in Peyer's patches, Th17 cells can acquire a T_{FH} phenotype and support IgA production from mucosal sites (46). Moreover, the inflammatory environment can push the differentiation of iTreg (generated by TGF-β) into Th17 cells through the presence of IL-6 (38). An extreme example of T cell plasticity is the complete re-programming of Th2 cells into Th1 cells. IFN-α and β, secreted during viral infections, was shown to induce T-bet and IFN-γ expression in Th2 cells, leading to their differentiation into the Th1 subset subset (38,40).

1.6 Phenotype and development of T follicular helper cells (T_{FH})

1.6.1 Inducible Co-Stimulatory Molecule (ICOS)

ICOS is a member of the CD28 family of co-stimulatory and co-inhibitory molecules (47). ICOS is absent from the surface of naïve T cells. Its expression is induced upon activation and, therefore, ICOS is found on activated and memory T cells (48). It binds to the ICOS-ligand (ICOSL) protein receptor, which is constitutively expressed on the surface of B cells (49). ICOS binds phosphatidylinositol 3-kinase (PI3K) and activates protein kinase B (PKB) and phosphoinositide-dependent kinase 1 (PDK1) (48). The kinases PDK-1 and PKB together with glycogen synthase kinase 3 (GSK) regulate numerous events, such as the prevention of cell death, protein translation and up-regulation of cellular metabolism (48).

The indispensible role of ICOS in humoral responses is illustrated by the phenotype of $ICOS^{-/-}$ mice, which exhibit severe impairment in IgG isotype class switching and GC formation in response to TD antigens (50-53). Similar results are obtained when mice are treated with the anti-ICOSL antibody (53). ICOS was found to enhance CD40/CD40L interaction, since CD40 stimulation could restore the isotype class switch in $ICOS^{-/-}$ mice (50). ICOS signalling was also implicated in driving IL-4, but not IFN-γ, secretion (51,52).

Alongside a defect in GC formation, $ICOS^{-/-}$ mice and mice treated with the anti-ICOSL antibody were found to have reduced numbers of $CXCR5^{+}$ $CD4^{+}$ T cells (53) and therefore ICOS-ICOSL interactions were implicated in the T_{FH} development. Furthermore, adoptive T and B cell transfers into SCID mice (Severe Combined Immune Deficiency mice, that is, animals severely deficient in B and T cells, (54)) showed that the frequency of $CXCR5^{+}$ $CD4^{+}$ $ICOS^{+}$ cells is increased in the presence of B cells and depends on the engagement of ICOS on T cells and the ICOSL on B cells (53). In keeping with this finding, studies with B cells exclusively deficient in the ICOS-L (using mice expressing floxed ICOS-L allele and CRE-recombinase driven by the CD19 promoter) confirmed that the impaired generation of the T_{FH} population and GC responses is directly related to the absence of the ICOS-L on B cells (55).

A very recent study by Xu *et al.* provided an important insight into the role of ICOS in the T_{FH} cell development beyond the co-stimulation process (56). The ICOS-ICOSL interactions were found to be essential for the migration of T cells to the T/B cell zone border and the entry into B cell follicles (56). Interestingly, this phenomenon was independent of the expression of CXCR5, CCR7 or Bcl6 (56). DC and cognate B cells were found to be dispensable for the recruitment of T cells to the B cell follicle. Fascinatingly, non-cognate 'bystander' follicular B cells were identified as essential source of the ICOSL (56). This study is in keeping with other published reports that describe normal T cell localisation to B cell follicles in the absence of cognate B cells (57). Therefore, ICOSL deficiency in non-cognate B cells has profound effects on the T cell positioning and results in the inhibition of the T_{FH} development as well as in suboptimal GC responses (56). Additionally, continuous ICOS-ICOSL signalling is essential for retaining T cells in the B cell follicle, as the administration of the anti-ICOSL antibody results in the relocation of fully differentiated T_{FH} from the GC to the T cell zone (58). On molecular levels, ICOS signalling was found to regulate expression of several homing molecules, including *Cxcr5, Ccr7* and *Selplg* (Selectin P ligand, also known as P-selectin glycoprotein ligand 1, PSGL1) (58). Interestingly, TF Krüppel-like factor 2 (Klf2) was shown to act downstream of ICOS signalling and to bind directly to targeted genes, whereas Bcl-6 and Achaete-scute homologue 2 (Ascl-2) TFs were shown to be dispensable in this pathway (58).

Summing up, ICOS-ICOSL interactions are one of the most important cues for T_{FH} differentiation and they mediate almost every step of the process, for instance by engagement during the priming stage, by sustaining the T_{FH} phenotype and by controlling T cell motility within SLO. The exact intracellular events following ICOS-ICOSL engagement still need to be clarified, as this would provide an important insight into the molecular processes governing T_{FH} differentiation.

1.6.2 Programmed Cell Death 1 (PD-1)

Another important member of the CD28 family expressed by T_{FH} is PD-1 (Programmed cell death 1, CD279). Similarly to ICOS, PD-1 is not expressed on resting lymphocytes but is induced upon cell activation in $CD4^+$ T cells, $CD8^+$

T cells, B cells (expressed upon engagement of TCR or BCR), monocytes and natural killer T cells (NK T cells) (49,59,60). It co-localises physically with TCR and CD28 to perform its function (49). The intracellular domain of PD-1 contains the immunoreceptor tyrosine-based inhibitory motif (ITIM) and the immunoreceptor tyrosine-based switch motif (ITSM) (59,61). The inhibitory effect of PD-1 signalling is mediated via the SHP phosphatase (SRC homology 2 (SH2)-domain-containing protein tyrosine phosphatase 2), which upon recruitment dephosphorylates and deactivates molecules involved in the membrane-proximal TCR signalling, including Syk kinase and phosphatydyloinosytol-3-OH-kinase (60). Downstream effects of PD-1 signalling include glucose metabolism limitation, Akt activation (by CD28-mediated activation of PI3K), the limitation of the expression of pro-survival gene Bcl-x_L and inhibition of cytokine mRNA production (49,60,61).

PD-1 binds to PD-L1 (B7-H1, CD274) and PD-L2 (B7-DC, CD273) (49,59,60). PD-L1 and PD-L2 differ in their distribution, with PD-L1 showing a much broader expression than PD-L2. PD-L1 is expressed constitutively and is further up regulated upon activation by T cells, B cells, DCs and macrophages (49,60). It is also expressed in many non-lymphoid tissues, such as the heart, lungs, pancreas, epithelium, liver, brain and muscles as well as immunoprivileged sites such as the eye and placenta (49,60). PD-L2 shows a much more restricted expression pattern, which is limited to DCs, macrophages and cultured BM-derived mast cells (49,61).

The inhibitory character of PD-1 receptor in autoimmunity is illustrated by the phenotype developed by PD-1 deficient mice ($Pd1^{-/-}$). On C57BL/6 background, PD-1 deficiency leads to the development of a late-onset lupus-like proliferative arthritis and glomerulonephirtis with IgG3 deposition (59,61). On BALB/c background, the lack of PD-1 results in autoimmune dilated cardiomyopathy and high levels of IgG directed against cardiac troponin I protein, leading to early and sudden death by congestic heart failure (59,61). Furthermore, the co-inhibitory role of PD-1 in response to foreign antigens is shown by studies using an antagonistic antibody specific for PD-1, in which blockade of PD-1 resulted in enhanced graft vs host disease (GVHD) and hapten-induced contact hypersensitivity in mice (59).

A recent study by Hams *et al*. has identified PD-1:PD-L1 interaction as crucial in limiting humoral responses by controlling the expansion of T_{FH} (62). In this study mice deficient in PD-L1 (B7-H1$^{-/-}$), infected with helminth *Schistosoma mansoni* showed higher titres of total and antigen-specific IgE, IgG1 and IgG2a as well as expanded GC B cells and plasma cell populations, when compared to WT mice (62). B7-H1$^{-/-}$ mice also showed enhanced T_{FH} expansion in response to helminth infection or immunisation with model antigen keyhole limpet hemocyanin (KLH) (62). Additionally, this phenotype (T_{FH} expansion and increased antibody titres) was recapitulated by treatment with anti-PD-L1 or anti-PD-1 (but not anti-PD-L2) antibody (62), which suggests that PD-L1 is a primary receptor for PD-1 expressed by T_{FH} cells. This finding might be surprising considering studies with fusion proteins, which indicated that PD-L2 has a two- to six-fold higher affinity for PD-1 than PD-L1 (49). *In vivo* co-transfer studies have indicated that B cells are a source of PD-L1 involved in limiting T_{FH} expansion and humoral responses, although possible contributions of other subsets expressing PD-L1 have not been fully eliminated (62).

1.7 Cytokine production by T_{FH} cells

1.7.1 IL-21

IL-21 is produced by CD4$^+$ T cells (T_{FH} and T_H17) as well as NK T cells (63). It has pleiotropic effects and impacts cells of both lymphoid and non-lymphoid lineage (63).

The IL-21 receptor (IL-21R) belongs to the common γ-chain family of cytokine receptors, alongside IL-2, -4, -7, -9, -13 and -15 (64, 65). It signals via Jak-1 and Jak-3, as well as STAT1, STAT3 and STAT5 (66), including STAT5a and STAT5b (63). Of these, STAT3 seems to have the most potent effect in IL-21 signalling (63). The MAPK and PI3K pathways have also been implicated in IL-21-mediated proliferation (67). IL-21R is expressed by many cells of the innate and adaptive immune system, including CD4$^+$ T cells, CD8$^+$ T cells, B cells, DC, MF as well as NK cells and non-immune cells such as keratinocytes, fibroblasts and endothelial cells (64). IL-21R$^{-/-}$ mice show an unaltered lymphoid development (64). The expression of IL-21R on CD4 and CD8 T cells, although low in naïve cells, is

increased in response to TCR stimulation or IL-21, revealing the autocrine amplification loop in IL-21 signalling. Similarly, B cells also up regulate IL-21R in response to BCR or IL-21 stimulation (63). B cells show the highest surface levels of IL-21R (even in the resting state) and follicular B cells express more IL-21R than MZ B cells (63). Plasma cells do not express IL-21R (which is in agreement with the non-proliferative state of the terminal differentiation observed in these cells) (63).

IL-21 has an important role in driving Th17 differentiation and expansion. The Th17 cell subset is generated under the influence of TGF-β and IL-6. One of the genes and proteins most potently induced by IL-6 signalling is IL-21 (63,65,68). IL-21 expression creates an autocrine loop, since it further enhances IL-21 production and IL-21R expression in Th17 cells (68). Furthermore, IL-21 signalling induced the expression of IL-23R, which can also facilitate the expansion of already differentiated Th17 cells (but not naïve $CD4^+$ T cells) (63,65).

The NK T cell subset was also found to be a potent source of IL-21, which implicates its role in B cell responses (discussed later in section 'NK T_{FH}', p. 35, (63)).

Even though IL-21 is considered a hallmark cytokine of the T_{FH} cell subset, only a portion of T_{FH} cells ($CXCR5^+$ $PD\text{-}1^+$ $Bcl6^+$ $CD4^+$ T cells) expresses IL-21 (30-40% of T_{FH} cells) and this population seems to be stable in IL-21 expression (69). It has not been determined whether IL-21 is restricted to the T_{FH} residing in the GC, which actively support B cell selection, although that seems to be a plausible explanation for the selective IL-21 expression. However, there is no difference of the GC-associated marker GL-7 between IL-21^+ and IL-21^- T_{FH} cells (69). Interestingly, IL-21^+ and IL-21^- T_{FH} showed equally high levels of the TFs Bcl-6 and Interferon Response Factor 4 (IRF4), and low levels of Blimp-1 (69). The optimal IL-21 secretion requires ICOS expression on $CD4^+$ T cells (70), since $ICOSL^{-/-}$ mice show an impaired production of IL-21 (when compared to WT mice) due to the disrupted ICOS/ICOSL interaction between T cells and B cells (55). Similarly to Th17 cells, IL-21 signalling in T_{FH} was shown to have an autocrine character, since this population expresses also IL-21R which is further up-regulated upon IL-21 signalling (70).

IL-21 impacts B cells in various ways. Firstly, it leads to caspase-dependent (and Bcl-2 independent) apoptosis of naïve B cells in the absence of BCR or CD-40 signalling and in the presence of TLR signals (63). IL-21 increases levels of pro-apoptotic Bim and decreases levels of pro-survival gene Bcl-$_{xL}$ (63). The reason for this might be to inhibit the non-specific, polyclonal responses when cognate antigen-specific interaction is taking place at the same time, since IL-21 can be produced by T_{FH} cells and NK T_{FH} cells engaged with antigen-specific B cells. Secondly, IL-21 induces the differentiation of activated B cells and human memory cells into plasma cells via induction of TFs Blimp-1 and c-Maf (63,65,66,71,72). Thirdly, IL-21 plays a crucial role in the immunoglobulin production. IL-21R$^{-/-}$ animals show a severe impairment in the total and antigen-specific IgG1 production as well as elevated levels of IgE antibodies after immunisation with OVA, KLH or NP-KLH (64). This was shown to be a B-cell intrinsic effect (64). Finally, IL-21 was found to induce AID and consequently support CSR (but not SHM) (71). Therefore, via broad expression of IL-21R, IL-21 impacts various cell types and displays both an activatory and inhibitory character. Crucial role of IL-21 in GC formation is further discussed in details in the section on T_{FH} function (p. 29) and the role of IL-21 in extra follicular responses in the section on T_{FH} heterogeneity (p. 34).

1.7.2 IL-4 and IFN-γ

Alongside IL-21, T_{FH} cells secrete other cytokines to ensure that B cells undergo the class-switch appropriate for the invading pathogen. Tracking IL-4 mRNA and protein expression in CD4$^+$ T cells after immunisation with *S. mansoni* revealed that the majority of IL-4 is derived from T cells expressing T_{FH} markers, such as CXCR5, ICOS and PD-1 (73). These IL-4-producing cells expressed the T_{FH}-specific TF Bcl-6, alongside the Th2-specific GATA 3 TF (73). Similarly, the IL-4 production was identified in cells with T_{FH} hallmark markers (expressing CXCR5, ICOS, PD-1, IL-21 and Bcl-6) after *Heligmosomoides polygyrus* infection (74). Finally, experiments with IL-21 reporter mice revealed that IL-21$^+$ CD4$^+$ T cells (exhibiting other T_{FH} markers, such as CXCR5, PD-1 and Bcl-6) also expressed significant amounts of mRNA for T-bet, Gata3, IL-4 and IFN-γ, as well as mRNA for IL-10 (69). Additionally, the non-antigen specific stimulation with PMA and ionomycin showed that these IL-21$^+$ T_{FH} can also secrete IL-2 (69), although no other *in vivo*

studies have reported a biologically significant IL-2 production by T_{FH}. In contrast to that, T_{FH} cells were shown to have a low expression of CD25 (IL-2Rα, (75)). Role of IL-4 and IFN-γ in shaping humoral responses is described in section 'T_{FH} function', p. 29.

1.8 Development of T_{FH} cells

1.8.1 The role of APCs (APCs)

The induction of the T_{FH} programme occurs, similarly to other $CD4^+$ effector T cell populations, during the interaction with activated DC, which present cognate peptide in the context of the MHC class II molecules. The interaction between the co-stimulatory molecule CD28 (constitutively expressed on the surface of naïve T cells) and CD80/86 (expressed on DC) is essential for the T_{FH} formation, since $CD28^{-/-}$ mice fail to generate T_{FH} (76). CD28 signalling was found to be important for the initial up regulation of Bcl-6 (58,76). Moreover, CD28 plays also an important role in the later stages of T_{FH} cell differentiation and survival by maintaining the expression of CXCR5 and Bcl6 (76). These effects are attributed to molecules acting down stream of CD28 signalling, such as pro-survival protein $Bcl\text{-}_{XL}$ and ICOS signalling (76).

Early studies, with B cell-deficient and BCR transgenic animals showed that the T_{FH} population is absent or vastly impaired in the absence of cognate B cells after protein immunisation (22), viral infection (77) or parasite infection (73). Additionally, physical contact in the form of stable T-B cell conjugates was also found indispensible for T_{FH} survival (25,75). Therefore, B cells were found to be essential for the development of functional T_{FH} cells. However, soon it became clear that despite the absence of T_{FH} at the peak of the immune response, T cell priming by DCs is sufficient to induce T_{FH} population at earlier stages. Firstly, the entry of T cells to the B cell follicles was found to be dependent on the T cell activation by DC and not antigen presentation by B cells (21). Secondly, $CD4^+$ $CXCR5^+$ $Bcl6^+$ T cells were found abundantly at day 3 after protein immunisation or infection, and thus prior to the activation of cognate B cells (57,75,78). Moreover, in the absence of antigen-specific B cells, $CD4^+$ $CXCR5^+$ $PD\text{-}1^+$ $Bcl6^+$ T cells are still found in the B cell follicle (57,78-80). Finally, the T_{FH} genesis might be accelerated by

immunisation with Ag-pulsed DCs (75,80,81). However, it is very important to bear in mind that even though the presence of DC seems to be sufficient for the T_{FH} cell genesis, these cells have a phenotype that differs from fully developed T_{FH} found in the GC and their functional capacity for helping B cells is also questionable.

Upon contact with activated DC, cognate T cells can further differentiate into effector T cells or T_{FH}. The exact signals influencing this choice remain elusive. Asymmetrical cell division of the activated T cell (after interaction with DC) has been described as one of the possible models explaining commitment to the effector T cell pool of T_{FH} population (75). That bi-modal choice depends on the quantity of IL-2 signalling (75). IL-2Rα^{HI} T cells show the preferential commitment to the effector T cell pool (via induction of Blimp-1), while IL-2Rα^{LOW} T cells favour T_{FH} cell differentiation (mediated by Bcl6) (75). The described process of asymmetrical division was completed within 72h and depended strictly on the priming mediated by DC (75). B cells were shown to be dispensable for T_{FH} priming but to be playing an essential role in T_{FH} maintenance at later stages (75). The role of B cells in T_{FH} biology is described in details in the introduction to Chapter 4, on p. 111.

The commitment to the T_{FH} lineage is a matter of discussion and no clear developmental pathway has yet been established. Fascinatingly, the T_{FH} subset displays a unique characteristic by depending on two different APCs for its differentiation: DCs at the priming stage for induction of T_{FH} precursor cells and B cells at later stages for their survival and full development. Possible models of T_{FH} differentiation are discussed in detail in the synoptic discussion of this thesis (Chapter 6, p. 176).

1.8.2 TCR signalling in T_{FH} development

The strength of T cell receptor (TCR) signaling has a profound influence on the differentiation of effector T cell subsets. However, the role of TCR signaling in the T_{FH} development has not been fully investigated. So far only a handful of studies have directly addressed the impact of TCR signaling on the T_{FH} cell population (82,83). T cells that display more restricted TCR and TCR with high affinity for the antigen were shown to be preferentially recruited to the T_{FH} pool (82). On the other hand, another group reported that Ag avidity does not play any role in the

commitment to the T_{FH} pool (83). Details of these studies and TCR specificity within the T_{FH} population are discussed in detail in Chapter 5 (see p. 174).

1.9 TFs

1.9.1 B-cell lymphoma 6 (Bcl6)

The B-cell lymphoma 6 (Bcl6) protein was identified as a master TF involved in T_{FH} differentiation independently by three research groups nearly a decade after the first recognition of T_{FH} cells (77,84,85). Early *in vivo* and *in vitro* studies provided clear evidence that Bcl-6 over expression leads to an increased expression of many T_{FH} markers, such as CXCR5, PD-1, CD200, CXCR4 and B and T lymphocyte attenuator (BTLA), and results in the down regulation of CCR7, Blimp-1 and SLAM (signalling lymphocytic activation molecule, Fig. 1.5, (77,84,85)). Additionally, Bcl6 was shown to inhibit directly the differentiation into Th1 or Th17 cells by controlling T-bet and ROR-γt, which results in the downstream inhibition of the IFN-γ and IL-17 cytokines production (Fig. 1.5, (84,85)), although T_{FH} cells were still found to express low levels of IFN-γ as well as IL-4 (77,84). On the other hand, Blimp-1 was identified as an antagonistic TF inhibiting the commitment to the T_{FH} lineage and promoting the differentiation into other effector T cell subsets (77). Furthermore, Bcl-6-expressing T_{FH} cells were functionally competent to drive GC reactions and enhance humoral responses (77). Adoptive cell transfers into RAG-$1^{-/-}$ mice (Recombination Activating Gene 1 deficient mice, which lack mature T and B lymphocytes, (86)) and experiments utilising BM chimeras showed clearly that the expression of Bcl-6 in B cells as well as T cells is essential for GC formation and Ag-specific antibody responses (77,84).

1.9.2 c-Maf

Interestingly, none of the initial reports (77,84,85) nor further *in vivo* studies (87) linked Bcl-6 expression to IL-21 production. Although the lack of a coordinated expression of two proteins that play a pivotal role in the T_{FH} function might seem to be surprising, there is a very reasonable explanation for this phenomenon. As discussed earlier, IL-21 is produced by other cell types (alongside T_{FH} the most important source of IL-21 are Th17 cells). Therefore, linking the IL-21 expression to the expression of the Bcl6 TF, which governs the differentiation into a certain cell

subset (by inducing global gene expression changes), might be highly disadvantageous for other cell populations. Importantly, two other TFs have been found to regulate the IL-21 production.

c-Maf was shown to drive the IL-21 production in $CD4^+$ T cells both *in vitro* (88,89) and *in vivo* (Fig. 1.5, (90)). c-Maf expression was shown to be dependent on ICOS signalling (90) and the presence of the cytokines IL-6 (88) or IL-21 and IL-27 (91). Additionally, c-Maf was also found to regulate positively the expression of IL-4, but not IL-5 or IL-13 (92), which is also relevant since IL-4 is one of the important cytokines secreted by T_{FH}. c-Maf was also found to be important for the CXCR5 expression and, together with Bcl6, c-Maf was shown to play a role in the induction of optimal levels of CXCR4, PD-1 and ICOS (89).

1.9.3 Interferon response factor 4 (IRF4)

The interferon response factor 4 (IRF4) was found to be crucial for the T_{FH} development after protein immunisation or infection with *L. major* (93). *Irf4*$^{-/-}$ mice lack GC and do not form T_{FH} cells (the $CXCR5^+$ $ICOS^+$ $BCL\text{-}6^+$ population is missing) (93). Importantly, the IL-21 production is also abolished in *Irf4*$^{-/-}$ mice (93,94). Moreover, IRF4 plays an important role in the IL-21 induction in Th17 cells (95). IRF4 was found to cooperate with the STAT3 TF in the regulation of IL-21-controlled genes in $CD4^+$ T cells, including *Prdm1* (encoding the Blimp-1 protein, Fig. 1.5, (94)).

1.9.4 Basic leucine zipper TF, ATF-like (Batf)

Batf (Basic leucine zipper TF, ATF-like) was found to be essential for T_{FH} development by two lab groups (96,97). Batf was shown to control expression of Bcl-6 and c-Maf, therefore providing an important signal upstream of Bcl6 in the T_{FH} generation (Fig. 1.5, (97)). Restoring the T_{FH} activity in Batf$^{-/-}$ T cells could only be achieved in the presence of both c-Maf and Bcl-6 (c-Maf alone was not sufficient) (96,97). The signals influencing the Batf expression and other Batf target genes still remain to be identified, although Batf was shown to bind directly to the *Il21* locus (98). Other $CD4^+$ T cells subsets that were reduced in the absence of the Batf protein included the Th2 and, most prominently, Th17 cells (97).

Furthermore, Batf-deficient mice do not generate GC and show a severe impairment in class-switch recombination (CSR) (96). Impaired humoral responses to T cell-dependent Ag were manifested by almost a complete absence of IgG1, IgG2c, IgA and IgE antibodies after SRBC administration, while they showed a mild reduction in IgM antibody titres (96). Although this can be viewed as a secondary effect of the absent T_{FH} population, the B cell-intrinsic requirement for Batf was demonstrated by *in vitro* re-stimulation assays and immunisation with a T-cell independent antigen (96). Additionally, Batf was found to regulate the expression of AID and germline transcripts, encoding the intervening heavy-chain locus and constant heavy-chain locus in B cells (97).

1.9.5 Achaete-scute homologue 2 (Ascl2)

Early observations of the T_{FH} phenotype reported a correlation of the Bcl-6 and CXCR5 expression (77,84,85). The analysis of Bcl-6-deficient T cells showed that $Bcl6^{-/-}$ T cells did not differentiate into $CXCR5^{+}$ T cells (77,84,85). Furthermore, Bcl-6 expression tracked by flow cytometry staining in activated $CD4^{+}$ T cells was shown to precede the expression of CXCR5 (80). These observations lead to the hypothesis that Bcl-6 might directly drive the CXCR5 expression. Additional supporting evidence came from the analysis of the microRNA cluster 17-92, which showed that 3 microRNAs (miR-17, miR-18a, mi-20a) were repressed by Bcl-6, leading to the up regulation of CXCR5 (85). Importantly, in the experiments described above the expression of CXCR5 was assessed at later stages of the response, such as day 6 or 7. However, the analysis of the Bcl-6 expression with red fluorescent protein (RFP) reporter mice showed that CXCR5 expression precedes the Bcl-6 expression by around 3 days (87), which questions the role of Bcl-6 in the induction of the CXCR5 expression. Indeed, a recent study by Liu *et al.* has identified another TF, namely Achaete-scute homologue 2 (Ascl2), as acting early in the T_{FH} differentiation and as driving the CXCR5 expression (99). Ascl2 was shown to be selectively expressed in mouse and human T_{FH} cells and not in other T helper cell lineages (99). In fact, Ascl2 was found to repress the Th1, Th2 and Th17 differentiation (99). A very elegant experiment with transferred WT OT.II cells, $Ascl2^{fl/fl}$ OT.II cells and $Bcl6^{-/-}$ OT.II cells transduced with the CRE-expressing GFP vector showed that the early generation of $CXCR5^{+}$ $CD4^{+}$ T cells (day 3 after protein

immunisation) is fully dependent on the expression of Ascl2 (99). Bcl6 was shown to be dispensable in the induction of CXCR5 on $CD4^+$ T cells but to be required at later stages of the response (99).

Moreover, Ascl2 seems to act independently of the Bcl6, Blimp1 and Batf TFs, since Ascl2 over expression did not influence the levels of *Bcl6, Prdm1* and *Batf* mRNA (99). Intriguingly, other genes unaffected by the manipulation of Ascl2 include *Icos, Sh2d1a (SAP), Pd1, Btla, Cd40lg* and *Il21*(99). Targeted transcripts of Ascl2 include the genes involved in T cell migration (*Cxcr5, Ccr7* and *Selplg* (Psgl1), Fig. 1.5) as well as the IL-2 signaling pathway (*Cd25* and *Cd22*- encoding proteins IL2-Rα and IL2-Rβ, respectively, (99)).

Summing up, this study has established the crucial role of Ascl2 in the T_{FH} induction and of Bcl6 in the maintenance of the T_{FH} phenotype. The important question remaining to be answered concerns the nature of the signal leading to the induction of the Ascl2 expression. 'Classic' T cell and T_{FH} cell stimulation protocols, including the combination of anti-CD3, anti-CD28, anti-ICOS and IL-6 and/or IL-21, did not lead to the Ascl2 up regulation (99). Agonists of the Wnt pathway, including TWS119, have been shown to induce the Ascl2 expression in $CD4^+$ T cells (99) but so far the role of the Wnt signaling pathway in the T_{FH} differentiation has not been fully investigated.

T-bet is expressed in low amounts by T_{FH} and even though it plays an important role in the $CD4^+$ T cell activation, it was show to be dispensable for the T_{FH} development as $Tbx^{-/-}$ mice developed a T_{FH} population equivalent to WT mice, in terms of frequency and functional capacity, after protein immunisation (69).

1.10 The roles of cytokines in the T_{FH} development

1.10.1 IL-21 and IL-6

Th1, Th2 or Th17 cells can be generated *in vitro* from purified naïve $CD4^+$ T cells by stimulation with IL-12, IL-4 or IL-6/TGF-b, respectively. The situation is more complicated in the case of the T_{FH} cell subset. Although numerous *in vitro* studies showed that the exposure of naïve $CD4^+$ T cells to IL-6 or IL-21 induces the expression of IL-21 and some characteristics of T_{FH} cells (the expression of mRNA

encoding CXCR5, PD-1 and Bcl-6 (55,84,100-103)) other experiments failed to show up regulation of these genes after culturing naïve T cells with IL-6 and IL-21, despite showing high IL-21 production (104,105). This raised concerns about the insufficient replication of the *in vivo* environment by *in vitro* studies and the subsequent lack of reliable results. Therefore, it became crucial to assess the impact of cytokines on the T_{FH} development in completely physiological conditions by using the *in vivo* system.

Numerous *in vivo* studies addressed the requirement of IL-6 and IL-21 for T_{FH} generation, providing important evidence about the roles of these cytokines in T cell biology. The analysis of IL-$6^{-/-}$ mice showed a normal (79,102) or only mild decrease (55,70) in the T_{FH} development when compared to WT mice after viral infection (79,102) and protein immunisation (79). Similarly, the dispensable role of IL-21 in T_{FH} formation was illustrated by the normal T_{FH} development in IL-$21^{-/-}$ or Il-$21R^{-/-}$ mice after protein immunisation (72,79,106) or viral infection (102,107). Although neither IL-6 nor IL-21 alone seems to have a great impact on the T_{FH} differentiation, the absence of both IL-6 and IL-21 blunts the T_{FH} genesis significantly (by around 25%) (102). This can be explained by the fact that both IL-21 and IL-6 signal via STAT3 (63,108) and therefore can compensate for each other's absence. Indeed, STAT3 deficiency in $CD4^+$ T cells results in an impaired (although not fully abrogated) T_{FH} development (55,103). Even though $CD4^+$ T cells with intrinsic STAT3 deficiency ($STAT3^{flox/flox}$ CD4-CRE mice) can become $CXCR5^+$ T cells, these cells were not competent to deliver help to B cells, neither *in vitro* nor *in vivo* (104). The lack of B cell help was tied to impaired IL-21 production (104).

1.10.2 IL-27

Interestingly, one study has also implicated another STAT3 signalling cytokine, IL-27, in the T_{FH} development (101). IL-27 was shown to induce the IL-21 expression (101). IL-27R$\alpha^{-/-}$ mice had significantly reduced T_{FH} numbers, impaired GC formation, and humoral responses after protein immunisation (101). This explains the presence of a significant T_{FH} population (although lower than in WT mice) in IL-$21^{-/-}$ mice treated with anit-IL6 antibodies after protein immunisation

(102), since IL-27 could provide STAT3 signalling and rescue the T_{FH} development in the absence of IL-6 and IL-21.

Summing up, *in vitro* studies with purified naïve T cells failed to provide a reliable answer to the question of the cytokines essential to T_{FH} differentiation. Even though IL-21-producing cells can be generated *in vitro*, they show overall much lower expression of many T_{FH}-attributed molecules than T_{FH} found *in vivo*, and these IL-21 producers might represent a precursor stage in the T_{FH} development. The inability to generate T_{FH} *in vitro* suggests that multiple environmental cues, such as T cell positioning and interactions with numerous APC, are especially important in the T_{FH} development. Consequently, the T_{FH} differentiation is not a one-step process with a single signal received at the stage of priming (which seems to be the case for other effector cell populations). Thanks to the effort of many groups, a clearer picture has emerged from numerous *in vivo* studies, which overall provided evidence for the compensating roles of IL-6, IL-21 and IL-27, and for the requirement of the STAT3 signalling pathway in the T_{FH} development (101,102).

1.10.3 IL-2 and STAT5 signalling

The IL-2 and STAT5 signalling axis has been implicated as negative regulator of the T_{FH} development (Fig. 1.5, (75,109,110)). This effect is mediated by the induction of the Blimp-1 TF (111), which acts reciprocally to Bcl-6 (77,84).

Choi *et al.* showed that antigen-specific cells undergo asymmetric cell division within the first 48 h of priming, resulting in the generation of IL-2Rα $(CD25)^{HIGH}$ and IL-2Rα^{LOW} $CD4^+$ T cell populations (75). Furthermore, IL-2Rα^{HIGH} cells activate STAT5 signalling and Blimp-1 expression, which leads to the suppression of Bcl-6 and to the preferential commitment to the effector T cell pool (75). The reciprocal situation was observed in IL-25Rα^{LOW} $CD4^+$ T cells, which started expressing Bcl-6 TF, repressed the Blimp-1 expression and, as a consequence, differentiated further into T_{FH} cells (75). This bi-furcation process was completed within the first 72 h of the immune response (75).

Further evidence for the role played by IL-2 and STAT5 in the T_{FH} genesis came from studies carried out by Johnston *et al.* and Nurieva *et al.* Both groups have

shown that the targeted deletion of STAT5 in $CD4^+$ T cells ($STAT5^{flox/flox}$ $CD4^+$ T cells transduced with the CRE vector (109) and $STAT5^{flox/flox}$ CD4-CRE mice (110)) or IL-2 inhibition facilitates the T_{FH} formation *in vivo* by inducing the expression of Bcl-6. Additionally, the over expression of the constitutively active form of STAT5 limits the T_{FH} formation (109,110). Finally, the STAT5-mediated inhibition of the T_{FH} population depends on Blimp-1, since the effect of STAT5 is lost in the absence of Blimp-1 (109) and, conversely, the over expression of Blimp-1 in STAT5 deficient cells inhibits the T_{FH} formation (110).

Collectively, there is clear evidence that IL-2 signalling via STAT5 induces Blimp-1 expression and consequently inhibits Bcl-6 expression and T_{FH} development. Therefore, IL-2 has been identified as a negative regulator of the T_{FH} differentiation program.

1.11 Function of T_{FH} cells

The main function of T_{FH} subset is GC support. T_{FH} cells fulfil their role by employing various cell surface receptors as well as by secreting soluble mediators.

1.11.1 Surface molecules

ICOS

ICOS signalling has profound effect on the development of T_{FH} cells (Introduction p. 13). Surprisingly little is known about the effects of ICOSL signalling in GC B cells (Fig. 1.5). The absence of GC and humoral responses in $ICOS^{-/-}$ mice is viewed as a secondary consequence of the missing T_{FH} population (53). The extent and function of a cell intrinsic ICOSL signalling in B cells and GC reactions remains unknown (Fig. 1.4).

PD-1

The effect of PD-1 signalling on GC B cells was revealed by work of Good-Jacobson *et al*. (112). In this study interactions between PD-1 expressed by T_{FH} and PD-L2 on B cells were shown to be crucial for rescuing GC B cells from apoptosis (Fig. 1.4). Furthermore, PD-1 signalling was found to be essential for IL-21 expression by T_{FH} cells, which enhances the formation of long-lived plasma cells

(113). Alternatively, it was suggested that a high expression of PD-1 on T_{FH} cells localised within GC might reflect an ongoing cell activation by continuous TCR stimulation due to repeated interactions with cognate B cells (114).

B and T lymphocyte attenuator (BTLA)

BTLA is a co-inhibitory receptor and a member of the CD28 superfamily of surface receptors expressed by B and T cells (49,59,115). The co-inhibitory character of this receptor is illustrated by the fact that $BTLA^{-/-}$ mice have enhanced antibody titres and expanded GC B cell population after protein immunisation (116). Interestingly, BTLA deficiency has no impact on numbers of T_{FH} (116). Instead, BTLA regulates T_{FH} function by limiting IL-21 production (116). Additionally, BTLA might directly regulate numbers of GC B cells by engaging its ligands, HVEM (herpesvirus-entry mediator) or LIGHT (tumor necrosis factor superfamily member 14, *Tnfsf14*, (59,115). Any molecular mechanisms involved in BTLA signalling in T_{FH} cells are unknown. Summing up, BTLA acts as a co-inhibitory receptor to hinder T_{FH} function in order to regulate the magnitude of a humoral response.

CD40L

CD40L is the only binding partner of CD40 (114). Lack of either CD40 or CD40L completely abrogates GC formation (117,118) as well as plasma cell response (119-121). CD40 signalling in GC B cell provides crucial survival signals by rescuing B cells from apoptosis (122), possibly by induction of Bcl6 (123), (Fig. 1.4). Together with IL-21 or IL-4, CD40-CD40L interaction is an important proliferation factor for GC B cells (124). CD40 signalling is also involved in the memory B cell differentiation (125), although the molecular mechanisms governing CD40 signalling and fate decisions of B cells need further investigation. The exact nature of CD40-CD40L signalling and its effects on T_{FH} cells are also not fully understood.

SLAM family proteins

SLAM family includes several surface proteins involved in T-B cell interactions, such as CD84, SLAM (*Slamf1*, CD150), Ly108 (*Slamf6*) and Ly9 (*Slamf3*, CD229)

(126,127). There is a significant functional redundancy in the SLAM family of proteins, illustrated by the fact that mice deficient in only one of the SLAM proteins exhibit mild or no decrease in GC formation and T_{FH} differentiation (as discussed in (114). SLAM-associated protein (SAP) is an intracellular adaptor of SLAM (CD150, (126,127)). Indispensible role of SAP in GC formation is illustrated by the fact that SAP-deficient mice do not form GC and have completely abrogated humoral responses (25,128). This defect is attributed to lack of stable conjugates between T and B cells. Importantly, SAP-deficient mice have unaltered interactions with DC (25,128), which illustrates the significance of prolonged physical contact between T_{FH} and B cells. Additionally, signalling via SAP is required for IL-4 production by T_{FH} cells within GC (Fig. 1.4, (129)).

1.11.2 Cytokines

T_{FH} secrete cytokines, which are essential for shaping humoral responses. IL-21 has a profound impact on GC, as well as extra-follicular responses. IL-4 and IFN-γ play indispensible role in driving appropriate class-switch tailored to the ongoing immune response.

IL-21

The crucial role of IL-21 in TD responses and GC formation was demonstrated by the complete ablation of GC in IL-$21^{-/-}$ mice (72) and IL-$21R^{-/-}$ (64,72). This was accompanied by a vast reduction of the IgG1 antibody levels. The reason for this phenotype could be B- or T- cell intrinsic, since both B cells as well as T_{FH} cells express IL-21R (70,130). The transfer of IL-21-sufficient $CD4^+$ T cells into IL-$21^{-/-}$ mice showed that, after antigen challenge, donor cells could differentiate into T_{FH} cells, and GC responses as well as antibody responses were restored (70). The GC could not be rescued by transferring WT (IL-21 sufficient) B cells. However, IL-21 deficiency in B cells has also a profound impact on GC responses, since the lack of IL-21 secretion or IL-21R expression by B cells led to the cessation of GC and to the premature formation of memory B cells, which additionally showed impaired SHM (72). Importantly, IL-21R signalling in B cells was required for the optimal induction of Bcl-6 in B cells, as well as SHM in response to TD antigens (SRBC, Fig. 1.4,

(106)). Therefore, IL-21 signalling is essential in T cells as well as B cells in order to generate optimal GC responses.

Additionally, IL-21 became implicated in the extra-follicular response, although its exact role remains elusive. IL-21 seems to be dispensable for the extra follicular responses (such as early response to *Salmonella enterica*, (106)). On the other hand, another study showed that IL-21 is essential in supporting extra follicular B cells (131). These studies are discussed in details in section 'Heterogeneity within T_{FH} cells on p. 34.

IL-4 and IFN-γ

The question of the local cytokine secretion by T_{FH} within GC was very elegantly addressed in a study with IL-4/IFN-γ double-reporter mice that were infected with *Leishmania major* (*L. major*) (132). The analysis of the isolated conjugates of T and B cells showed that IFN-γ-secreting T cells were paired with B cells that were undergoing a switch to IgG2a, whereas IL-4-secreting T cells were paired with B cells switching to IgG1 (132). These conjugates were found within the same GC, which demonstrates that the cytokine production by T_{FH} cells acts locally rather than globally, and therefore even modest amounts of cytokine are sufficient to drive the appropriate class switch. This can also explain why microarray analysis results indicate a lack of IFN-γ or IL-4 production in T_{FH} cells (55), which may express only low amount of transcripts for these cytokines. Production of IL-4 and IFN-γ by T_{FH} was discussed in section 'cytokines secreted by T_{FH}' on p. 18.

1.12 Regulation of T_{FH} responses

The T_{FH} population supports GC formation and production of high-affinity, class-switched antibodies. These processes need to be tightly regulated in order to maintain self-tolerance and avoid the generation of auto-antibodies. So far, two populations of T cells have been identified as controlling the T_{FH} population: a subset of $CD8^+$ T cells and $CD4^+$ T follicular regulatory cells (T_{FR}).

1.12.1 T_{FH} regulation by $CD8^+$ T cells

$CD8^+$ T cells expressing the non-classical MHC I molecule Qa1 were shown to inhibit autoimmunity by controlling T_{FH} numbers in the steady state as well as during

viral infection (133). Qa1 mutant mice (with D227K mutation disrupting Qa-1 binding to the TCR/CD8 co-receptor) were found to develop spontaneous autoimmunity, characterised by elevated levels of the IgG antibody in the blood, increased deposition of IgG in renal glomeruli and autoantibodies directed against nuclear antigens (133). This phenotype was associated with T_{FH} expansion and enhanced GC formation (133). The suppressive capacity of regulatory $CD8^+$ T cells required the expression of perforin and the presence of IL-15 (133).

1.12.2 T_{FH} regulation by $CD4^+$ T follicular regulatory cells (T_{FR})

In 2011, a special population of $CD4^+$ dedicated to control humoral responses was identified and termed T follicular regulatory cells (T_{FR}) (134). The T_{FR} population shares phenotypical traits with both the T_{FH} and Treg subset. T_{FR} express a set of genes linked to the effector and suppressive function associated with the Treg phenotype, namely glucocorticoid-induced tumor necrosis factor receptor (GITR), Cytotoxic T-lymphocyte protein 4 (CTLA4), BTLA, killer cell lectin like receptor G1 (KLRG1), CD25, ICOS, Blimp-1, Granzyme A (Gzma) and IL-10, as well as features characteristic of T_{FH} cells, such as CXCR5, Bcl6, CXCL13 and ICOS (134,135). Interestingly, the T_{FR} formation is dependent on CD28 and SAP-mediated interactions with B cells, which is also the case for the T_{FH} but not the Treg subset (134). Importantly, T_{FR} did not express CD40L or transcripts for IL-21 or IL-4, which indicates that their capacity to provide help to B cells is limited and suggests a functional divergence from the T_{FH} population (134).

Microarray analysis revealed that in terms of global changes in the gene expression T_{FR} more closely resemble Tregs than T_{FH} cells (134). Moreover, adoptive transfer experiments showed that T_{FR} cells are generated from thymus-derived natural T regs (nTregs) and not from T_{FH} cells that have switched on Foxp3 expression (134,135).

T_{FR} were found to express Blimp-1 as well as Bcl-6 (134,135), which is fascinating as these TFs are known to be mutual repressors in B cells (136,137). mRNA analysis showed that the levels of Blimp-1 found in T_{FR} are higher than in any other effector cell subset, whereas Bcl-6 is expressed in lower amounts than in T_{FH} cells (134). The Bcl-6 expression enables T_{FR} to acquire a migratory profile

similar to T_{FH} cells, which enables T_{FR} to locate to GC, where they perform their function. Indeed, Tregs were found to express TFs specific to other suppressed T cell lineages: T-bet for the Th1, IRF-4 for the Th2 and Ror-γt for the Th17 populations (ref. (138-140), respectively).

T_{FR} function includes limiting the expansion of T_{FH} cells, controlling non-antigen specific B cells within the GC (134), as well as class switch and plasma cell differentiation (135). *In vitro* assays revealed that T_{FR} cells showed a suppressive potential equivalent to classic Tregs (134,135). Interestingly, the $CXCR5^+$ $Bcl6^+$ Treg population was also identified in human tonsils (135). The exact mechanism by which T_{FR} perform their functions has not been identified and clearly more work is needed to understand fully the role of this subset in humoral responses. Importantly, the suppressive potential of T_{FR} makes this subset an attractive target for designing treatments for autoimmune diseases..

1.12.3 Plasma cells

A study by Pelletier *et al.* described the previously unknown phenomenon of T_{FH} regulation by plasma cells (141). Antigen-specific plasma cells were shown to express the co-stimulatory molecules CD80/86 and MHC II as well as to present antigen in *vivo* (141). *In vitro* co-culture experiments showed a diminished *IL-21* and *Bcl6* mRNA expression when *in-vitro*- or *in-vivo*-derived T_{FH} were cultured with plasma cells (141). Additionally, plasma-cell-deficient mice had increased T_{FH} numbers (141).

However, these results should be treated with some caution, as many aspects involving spatial and temporal interactions between T_{FH} and plasma cells were not addressed. Furthermore, multiple *in vitro* studies failed to replace the complexity of the follicular environment essential for studying T_{FH} development and function. Finally, so far, there are no other reports supporting the hypothesis that plasma cells negatively regulate the T_{FH} differentiation. Whether this phenomenon plays a significant biological role remains to be established.

1.13 Heterogeneity within the T_{FH} population

The heterogeneity within $CD4^+$ T_{FH} cells is increasingly appreciated since the phenotypically similar $CXCR5^+$ $PD\text{-}1^+$ $Bcl6^+$ T cells were shown to have a distinct localisation within the SLO and different capacity to provide help to B cells (114,142).

1.13.1 Pre-T_{FH} (T_{FH})

Several studies have described the presence of $CXCR5^+$ $PD\text{-}1^+$ $Bcl6^+$ T cells in the interfollicular zone shortly after immunisation (within 2-3 days p.i.) (57,78,143). Pre-T_{FH} (also called 'T_{FH}' in some nomenclatures) show lower expression of CXCR5, ICOS, PD-1 and Bcl-6 than T_{FH} found at the peak of the GC response (57,78,143). These cells are considered to be precursors of GC T_{FH}, although the exact cues guiding the transition from pre-T_{FH} to GC T_{FH} have not been elucidated. Additionally, these pre-T_{FH} cells were found to play a role in supporting extra follicular responses (described below).

1.13.2 GC T_{FH}

Initially all T_{FH} cells were thought to localise within the GC in order to support GC B cells. However, it soon became clear that there are also T_{FH} populations performing a function outside the GC, and hence the term "GC T_{FH}" has been coined to describe GC-resident T_{FH}.

GC T_{FH} were found to express the highest amount of PD-1, CXCR5 and Bcl6 among $CD4^+$ T cells,(22,131). BTLA, CD200 and SAP have also been described to be expressed on higher levels in GC T_{FH} than in the T_{FH} localised in the apposition to the follicles (22,79,114,129). Moreover, GL7 was identified as a marker exclusively expressed by GC T_{FH} (129), although another study reported the expression of GL7 in extra-follicular T_{FH} cells at day 2 p.i. (and prior to the establishment of GC (57)). On the other hand, GC T_{FH} were found to express low levels of CCR7 and PSGL1, which facilitate the deep penetration of B cell follicles and the location to the GC (114). Interestingly, a low expression of IL-7R (CD127) was also reported for GC T_{FH} in mice (78) and GC T_{FH} in human tonsillar tissue (144), although the physiological role of IL-7 signalling in the T_{FH} differentiation remains unexplained. Finally, GC T_{FH} were found to express exclusively IL-4 (22,129), and so far there

has been no description of IL-4 expression in T_{FH} populations residing outside the GC. The IL-4 expression in GC T_{FH} is mediated by SLAM (*Slamf1*, CD150) and its adaptor SAP (129).

1.13.3 Extra-follicular T_{FH}

The role T_{FH} play in supporting extra-follicular responses became clear after published studies that showed that the presence of $Bcl6^{+}$ $CXCR5^{LO}$ $PD\text{-}1^{LO}$ T_{FH} is essential for B cell help, prior to the establishment of GC in response to TD antigen (SRBC, (131)), and in early extra follicular response to *S. enterica* (106,131). The subset of T_{FH} supporting extra follicular responses was found to be dependent on Bcl6 expression, and was localised in the inter-follicular zone (131).

The role of IL-21 in the extra-follicular zone remains unclear. Initially, IL-21 was shown to be dispensable for extra-follicular responses to *S. enterica* (106). In this study, $IL\text{-}21^{-/-}$ mice infected with *S. enterica* showed a humoral response equivalent to WT mice (106). However, a study by Lee *et al*. was performed by transferring $IL\text{-}21R^{-/-}$ and $IL21R^{+/+}$ SW_{HEL} B cells (B cells specific for HEL antigen capable of switching to all isotypes) to congenic hosts followed by immunising with SRBC coupled to HEL (131), thus directly addressing the requirement of IL-21 signalling in B cells. The results showed impaired (although not completely absent) extra-follicular plasmablast formation as well as a reduced GC B cell population (131). This suggests that IL-21 plays an important, although not absolutely necessary role, in extra follicular B cell responses.

The unimpaired extra-follicular responses in $IL\text{-}21^{-/-}$ mice (106) can be explained with redundancy in STAT3 signalling and the compensatory roles of other cytokines in the process (such as IL-6 and IL-27, as discussed in section 'The role of cytokines in T_{FH} development' on p. 25). Supporting observations of IL-21 expression in both extra follicular T_{FH} and GC T_{FH} come from IL-21 reporter mice, which showed an equal expression of PD-1, GATA3, IL-4 and Bcl6 between $IL\text{-}21^{+}$ and $IL\text{-}21^{-}$ T_{FH} cells (69). This suggests that IL-21 production is not limited to $Bcl\text{-}6^{HI}$ T_{FH}, which are thought to reside within the GC.

Additionally, the population of T_{FH} residing outside the B cell follicles in the human tonsils was found to secrete IL-21 and IL-10 in even higher amounts than GC T_{FH}, thus showing a higher capacity for helping naïve and memory B cells than GC T_{FH} (145). However, these extra-follicular T_{FH} were unable to help GC B cells due to the FAS/FASL-mediated apoptosis triggered in GC B cells upon contact with extra-follicular T_{FH} (145). Interestingly, this suggests that the distinct function of T_{FH} subsets is at least partially explained by cell-intrinsic differences and not only by the distinct location of each subset. In keeping with mice studies, human extra-follicular T_{FH} were found to express higher levels of IL-7R and lower levels of the Bcl6 protein than GC T_{FH} (145).

1.13.4 NK T_{FH}

Natural killer (NK) T cells are a heterogeneous population of cells, consisting of Type I and Type II NK T cells. Type I NK T cells express invariant TCRα V and J segments (Vα14 Jα18 in mice and Vα24 Jα18 in humans) and highly restricted, but not invariant, TCRβ (most common chains are $V_{\beta}8.2$, $V_{\beta}7$ and $V_{\beta}2$ in mice and $V_{\beta}11$ in humans) (146). This combination of V and J chains generates TCR which recognises glycolipids in the context of the non-classical MHC molecule CD1d (146). The most characterised antigen recognised by Type I NK T cells is α-galactosylceramide (α-GalCer) found on the surface of many bacterial species, including *Borrelia burgdorferi* and *Sphingomonas* (147). A synthetic mimic of α-GalCer is often used to investigate NK T cell functions *in vitro* and *in vivo*. Type II NK T cells also express invariant TCR and recognise hydrophobic antigens, such as sulfatide or lysophosphatidylcholine, as well as small aromatic (non-lipid) molecules (146).

Type I NK T cells (described below as simply 'NK T cells') interact with B cells, which have internalized lipid particles via BCR and displayed the lipid antigen via CD1d MHC molecule. This cognate engagement results in enhanced extra-follicular antibody production (148). Thus, NK T cells became implicated in supporting B cell responses.

A recent study describes a population of follicular helper NK T cells (NK T_{FH} cells) (147). It is a small subset of NK T cells (~3% of NK T cells generated after

lipid administration) expressing CXCR5 and PD-1, which are surface receptors also expressed by the T_{FH} population. NK T_{FH} cells were found to form stable and motile conjugates with antigen-specific B cells, which resulted in an enhanced B cell proliferation (147). Immunisation with lipids forming low-, intermediate- or high-affinity complexes with MHC CD1d molecules revealed that the NK T_{FH} cell formation is greater when high-affinity p:MHC interactions are present (147). Other factors required for the NK T_{FH} formation and survival (shared with T_{FH} population) are the presence of TF Bcl6 and of co-stimulatory receptor CD28 (147). B cells expressing the CD1d molecule and SAP-mediated interactions are also indispensable for NK T_{FH} generation (147). NK T_{FH} cells were found within the GC and shown to be important for the early induction of the GC in response to lipid antigens (147). Successful B cell help from NK T_{FH} cells requires IL-21 signalling in a B cell-intrinsic manner (147).

Therefore, NK T_{FH} cells provide help to B cells in response to glycolipid antigens, which are unable to generate protein-dependent 'classic' B cell helper populations (T_{FH}). Simultaneous help from both NK T_{FH} cells as well as from the T_{FH} population is also possible in the situation when a B cell internalised lipid-containing antigen via BCR and (after antigen processing) displays a protein part of this antigen on the MHC class II molecule (147).

1.14 Concluding remarks on heterogeneity

One of the main issues in investigating T_{FH} heterogeneity is the lack of specific cell surface markers that distinguish various T_{FH} subsets. In many cases differences between T_{FH} subsets are reflected in the amount of the proteins expressed rather than their presence or absence. The prevalent view in the field describes the presence of pre-T_{FH} (or early T_{FH}) cells with low to intermediate levels of Bcl6 in T cell follicles, which move to the T-B cell border and stabilises Bcl6 to show maximum Bcl6 levels in GC (114,142). This supports the model of continuous T_{FH} differentiation, in which precursors of T_{FH} cells reinforce Bcl6 expression upon multiple encounters with cognate APCs. This is further discussed in final synoptic discussion on p. 176.

1.15 T_{FH} memory

One of the important questions in the T_{FH} field concerns the ultimate fate of T_{FH} cells and their ability to persist in the system as memory T_{FH} cells without exposure to the antigen. Interestingly, there are striking parallels in the survival requirements of memory $CD4^+$ T cells and T_{FH} cells. Neither of the populations can exist in the absence of B cells ((119,149,150) for memory T cells and (75) for T_{FH} cells) and both populations require the expression of Bcl6 ((151) for memory T cells and (77,84,85) for T_{FH} cells). Therefore T_{FH} cells are likely to contribute to memory T cell responses.

Several studies have addressed the issue of T_{FH} persistence and their phenotype after recall response. The transfer of IL-21-producing, transgenic T_{FH} cells (from IL-21 reporter mice) generated after protein immunisation revealed that after recall response most of $CXCR5^+$ $IL\text{-}21^+$ T_{FH} cells have retained the original phenotype (69). Interestingly, a significant proportion of $IL\text{-}21^-$ T_{FH} cells became $IL\text{-}21^+$ cells. Finally, $CXCR5^-$ effector cells could also give rise to $CXCR5^+$ T cells (69). $IL\text{-}21^+$ T_{FH} cells were also shown to persist for 32 days after protein immunisation or viral challenge in the absence of antigen and they showed the ability to expand upon re-challenge (69). The magnitude of recall response was similar between $CXCR5^+$ and $CXCR5^-$ cells, showing that the T_{FH} population is equally efficient to form memory-like cells as effector T cells (69). In keeping with these findings, Pepper *et al.* have reported that $CXCR5^+$ memory T cells specific for *Listeria monocytogenes* can give rise to both $CXCR5^+$ and $CXCR5^-$ T cells after rechallenge (151). Importantly, the plasticity of memory $CXCR5^+$ T cells in studies described above can be partially explained by the use of a polyclonal $CD4^+$ T cell population, heterogenic in terms of their TCR expression.

In slight contrast to results described above, studies with monoclonal $CD4^+$ $CXCR5^+$ T cell populations reported a preferential retaining of the T_{FH}-like phenotype by $CXCR5^+$ T cells and a low conversion to $CXCR^-$ T cells. Weber *et al*. reported that antigen-experienced $CD4^+$ $CXCR5^-$ T cells transferred to congenic hosts and rested for several weeks in the absence of antigen, during recall response have an enhanced capacity for B cell follicle homing and B cell help due to a higher

expression of CXCR5 and IL-21 than effector cell populations or primary T cells (152). Interestingly, resting T_{FH} cells down regulated CXCR5, PD-1, Bcl6 and ICOS and rapidly re-acquired their high expression after rechallenge (152). Furthermore, studies with Bcl6 reporter mice showed that transgenic $Bcl6^+$ $CXCR5^+$ T_{FH} cells persisted in the absence of antigen after protein immunisation for nearly 3 weeks and preferentially acquired the T_{FH}-phenotype after the transfer (87). Experiments with LCMV-specific $CD4^+$ T cells rested for even longer periods of time (60-150 days) without the antigen stimulation also reported preferential acquisition of T_{FH}–like profile by $CXCR5^+$ transgenic $CD4^+$ T cells after re-challenge with the antigen (153). Authors compare the recall response of T_{FH} cells and Th1 cells, concluding that each lineage shows considerable stability during the resting period, which is illustrated by the acquisition of the original phenotype after the recall response (153).

Summing up, T_{FH} cells can persist in the absence of antigen, become re-activated during a recall response and give rise to functional T_{FH} cells. However, it seems that memory-like T_{FH} do not convert to other subsets of memory cells, such as T central memory cells (Tcm), Th1 or Th2 memory cells. This is in contrast to Tcm, which exhibit a significant level of plasticity and can differentiate into Th1 or Th2 subsets upon re-activation.

Even though the definition of memory T cells describes T cells which have undergone Ag-specific proliferation, have persisted in the organism after Ag clearance for a long time and can respond to the same Ag upon subsequent encounter, whether the organism really becomes Ag-free after terminating the GC response is a matter of debate. Depots of antigens can be held on the surface of the FDCs for extended periods of time; some pathogens (especially viruses) also show low level of persistence after an acute infection has been resolved (114,154). The presence of the antigen could therefore be an important signal for the sustenance of T_{FH} and T_{FH}-like cells and a continuous support of this memory pool. Nevertheless, several adoptive transfer studies have clearly showed that Ag exposure is dispensable for the survival of functional T_{FH} memory-like cells, which provides an important insight into the maintenance of the population that plays a pivotal role in the generation of efficient humoral response.

1.16 T_{FH} cells in autoimmunity in mice and humans

T_{FH} cells need to be tightly controlled in order to avoid a harmful humoral response. The expansion of the T_{FH} population was linked to several models of autoimmune conditions characterised by the presence of anti-dsDNA antiobodies. Increased T_{FH} numbers were found in mice over expressing OX40L or the TLR7 ligand (33), as well as in mice carrying a mutation in the Roquin gene[3] (*sanroque* mice, (155)), all of which develop a Systemic Lupus Erythromatosus (SLE)-like disease. The autoimmunity and aberrant GC reactions in *sanroque* mice were further linked to the expansion of T_{FH} (156). Increased frequencies of circulating $CXCR5^+$ T_{FH}-like cells were found in human patients with autoantibody-mediated autoimmune diseases, such as SLE, Sjörgen's syndrome and juvenile dermatomyositis (142). Moreover, $CXCR5^+$ CD45RO $ICOS^+$ $PD\text{-}1^+$ cells were found in the blood of some SLE patients (114).

An excessive production of IL-21 was also found to contribute significantly to autoimmune conditions. Single nucleotide polymporphism (SNP) within the IL-21 locus was found to be associated with SLE disease in human patients (65). SLE patients also showed higher plasma levels of IL-21 than healthy controls and increased IL-21 mRNA was found in biopsies of SLE patients (65). Although many cell types can secrete IL-21, the fact that autoimmune disorders are tied to a dysregulated GC formation and antibody production implicates T_{FH} as most likely source of this cytokine. Indeed, in *sanroque* mice developing severe autoimmunity, the uncontrolled T_{FH} population also produces an excess of IL-21 (155).

In contrast to the excessive T_{FH} formation and function in autoimmune diseases, a reduction in the T_{FH} population has been reported for several models of immundeficiencies. Reduced T_{FH} numbers have been described in human patients with mutations in STAT3, CD40Lg and ICOSL and in their corresponding mice models (53,114,142,157). In these cases a severe impairment in humoral diseases is observed to various bacterial, viral and fungal pathogens (114,142). Therefore, an

[3] Roquin is a RING-type ubiquitin ligase involved in repressing mRNA of ICOS and possibly mRNA of IL-21 and SAP (155). Sanroque mice with dysfunctional roquin protein have elevated levels of ICOS, great increase in T_{FH} and GC B cells as well as severe autoimmune phenotype (155).

excessive T_{FH} genesis as well as impairment in the T_{FH} generation may have detrimental effects on humoral responses.

1.17 Models used for *in vivo* studies

Early observations from our lab indicated that the phenotype of T_{FH} cells (measured by the expression of the surface marker PD-1) found after infection with *Salmonella enterica* was different from the phenotype of T_{FH} found after immunisation with ovine erythrocytes (SRBC, acting as a simple antigen). This sparked our interest and led to the hypothesis that observed heterogeneity within T_{FH} population might have functional consequences. I have therefore used two models of infection and immunisation to further investigate the phenotype, function and the development of these phenotypically distinct T_{FH} populations.

1.17.1 Immunology of *Salmonella* infection

In this project infection with the attenuated aro-A^- strain of *Salmonella enterica* serovar *Typhimurium* (SL3261, termed hereafter *S. enterica,* (158)) was used to study the heterogeneity within the T_{FH} subsets. This strain is commonly used as a live-attenuated vaccine since it provides protection against a more virulent strain (158). *S. enterica* is a gram-negative intracellular bacterium which infects humans via oral route. It enters Peyer's Patches via M cells and epithelial cells in the gut (159,160). *S. enterica* spreads via the mesenteric lymph nodes and lymphatic vessels to blood, spleen and liver (160,161). The systemic phase of the infection is characterised by splenomegaly caused by increased cell numbers of leukocytes ($CD11b^+$, $NK1.1^+$ and $GR1^+$ cells) and, more prominently, red blood cells (162).

S. enterica resides mainly within macrophages (163,164) and employs several mechanisms of evasion of the immune system. The bacterium can impede its uptake by DCs, evades lysosomal degradation and interferes with antigen presentation on MHC class I and class II molecules (165). The bacterial spread is controlled by activated macrophages and inflammatory cytokines, such as IL-12, IFN-γ and TNF-α (166,167). IL-12, IFN-γ, TNF-α, IL-15 and IL-18 are essential for initiating the adaptive responses to *S. enterica* (167-170). The final clearance of the bacteria depends on $CD4^+$ T cells (166).

The humoral response to *S. enterica* consists of an early wave of IgM (directed against LPS and flagellin) and the IgG2c antibody (directed against outer membrane proteins, OMP) (171). It is produced by extra-follicular plasma cells and its main role is to impede the spread of the bacteria (171). Additionally, T cell independent B-1b cells are the source of IgG2c antibodies generated against OMP C, D and F (18). Protection against subsequent infection is provided by antibodies derived from GC in much later stages of the infection (around 5-7 weeks p.i) (171,172). The appearance of GCs is related to a lower bacterial burden observed in the late stages of the infection, since the GC formation can be accelerated by treatment with antibiotics (171). B cell-intrinsic TLR signalling is absolutely essential for the switch to IgG2c, as the response to *S. enterica* in MyD88 KO mice is dominated by IgG1 (172).

The role of B cells in the response to *S. enterica* infection extends beyond antibody production. Although B cells are not necessary for the primary responses to *S. enterica* (149,173,174), they are required in the early phases of the infection to mount optimal Th1 responses by enhancing the IFN-γ production in T cells (172). This process is dependent on TLR signalling in B cells and is mediated by the cytokine secretion from B cells (IL-6 and IFN-γ, (149)). More importantly, T cell memory formation[4] is dependent on antigen presentation by B cells (149). Therefore, the significant role of B cells in the response to *S. enterica* involves early, non-cognate interactions with T cells required for an optimal effector response and late, cognate signals, providing T cell memory and protection against future infections.

In all of the experiments presented in this thesis *S. enterica* was administered intra venously (i.v.) and not orally. There were several reasons for not using the natural entry route of the pathogen. Firstly, the aim of the project was not to develop a vaccine or treatment for typhoid fever but rather to use *S. enterica* as an example of a bacterial infection eliciting a strong Th1 immune response. Secondly, the i.v. route allows for a better control of the infectious dose (which shows wider spread in oral delivery). Finally, the natural infection quickly becomes systemic (160), therefore we

[4] $CD4^+$ memory T cells in mice and humans recognise mainly epitopes derived from flagellar filament protein (228).

would hope that any effects observed after i.v. administration would also recapitulate events elicited after the oral infection.

In *S. enterica* infection model T_{FH} expressing low levels of PD-1 are found within the first week of infection. GCs are not found until much later stages of the infection.

1.17.2 Sheep red blood cells (SRBC)

SRBC immunisation is used as a model for studying TD responses, as it generates a strong early extrafollicular response (175,176). Additionally, GC induction is observed within the first week after immunisation ((177), observations from our lab). The character of the immune response to SRBC is dose dependent, as it was shown that injection of $4x10^6$ SRBC elicits mostly a Th1 response (measured by the quantity of IFN-γ producing cells) while administration of $4x10^8$ SRBC generates predominantly IL-4 producing cells (alongside IFN-γ producing cells, (178)). Consistent with this and other published studies (70) as well as unpublished observations from our lab (T. Slocombe, personal communication), standard SRBC dose used in our lab ($2x10^9$ SRBC) generates mostly IgG1 antibodies.

In SRBC immunisation T_{FH} expressing high and low levels of PD-1 are present and GC are found abundantly during the first week of the response.

1.18 Aims of this PhD thesis

The aim of this PhD work was to investigate the heterogeneity of T_{FH} populations in two different immunisation/infection models (SRBC immunisation and *S. enterica* infection), which give rise to phenotypically distinct T_{FH} populations, and to test whether there are functional consequences of this heterogeneity. In Chapter 3 I performed an extensive profiling of the T_{FH} populations with the markers known from literature to be connected to T_{FH}, showing that there is indeed a considerable level of heterogeneity within the T_{FH} populations. I also took a more global approach to characterising T_{FH} by subjecting different T_{FH} subsets to microarray analysis. Differential gene expression of general cellular pathways and immune pathways (including T_{FH} related genes) confirmed that isolated populations are indeed discreet cell subsets. In the following chapter (Chapter 4) I investigated the interactions of different T_{FH} populations with cognate B cells, which ultimately led to important conclusions about the T_{FH} development pathway. In the final chapter (Chapter 5) I studied the potential for interaction between these T_{FH} subsets by performing co-immunisation experiments with *S. enterica* and SRBC and, following an unexpected result of T_{FH} expansion, I try to broadly address the question regarding specificity of those T_{FH} cells.

The broad aims of the thesis were:

1. To investigate and characterise heterogeneity within T_{FH} populations
2. To improve our understanding of T_{FH} differentiation and role of cognate B cells in this process
3. To investigate the relationship and potential for interaction between different T_{FH} populations.

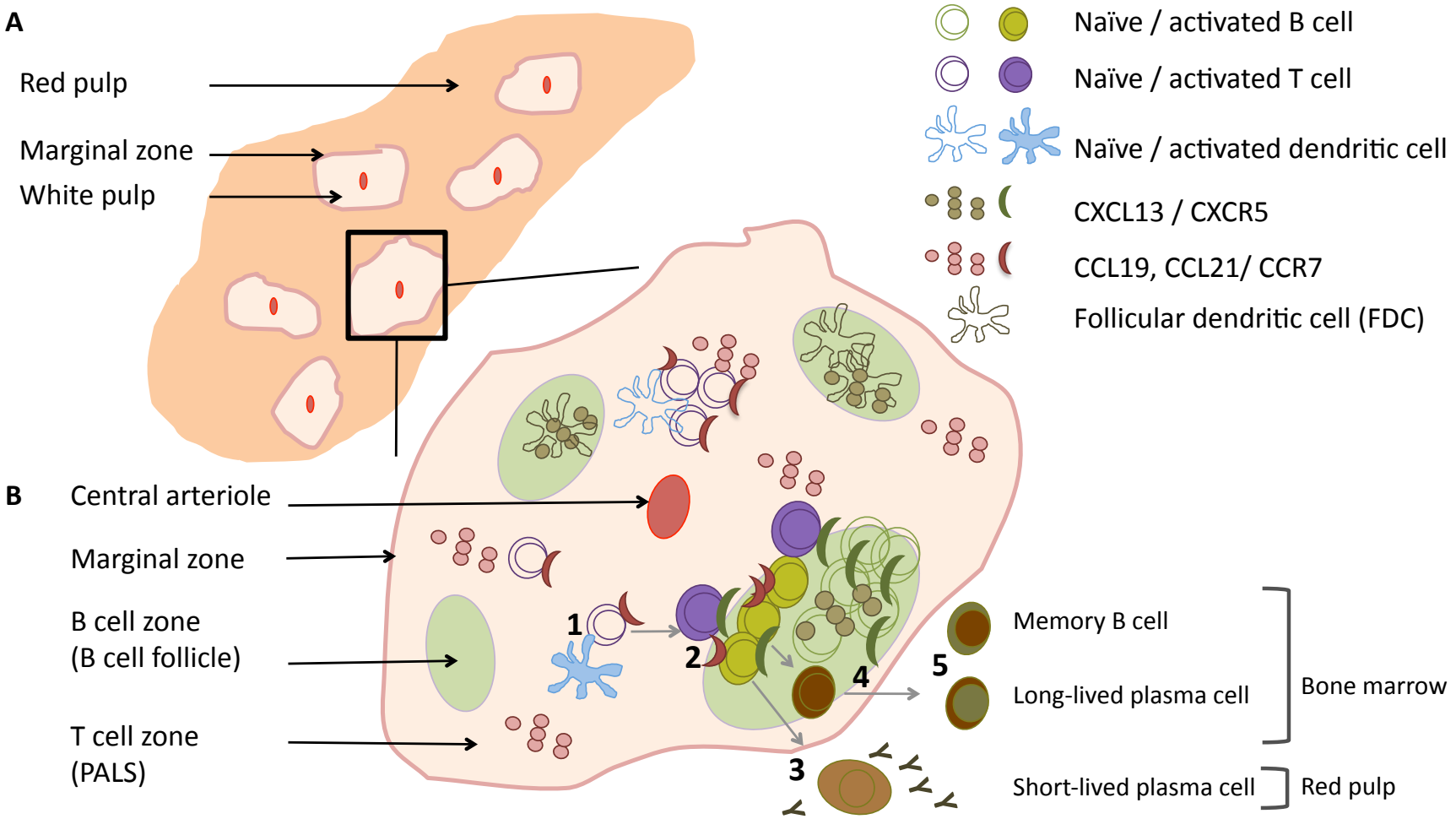

Fig 1.1 Structure of the spleen and T cell dependent responses.

(A) Structure of the spleen. White pulp of the spleen is located around central arterioles and separated from the red pulp of the spleen by the marginal zone.
(B) Structure of the white pulp and T cell dependent responses. Naïve T cells express chemokine receptor CCR7, which binds CCl19 and CCL21 chemokines secreted in T cell zones by reticular fibroblast cells. Upon cognate interaction with activated dendritic cell **(1)** T cells become activated, down regulate CCR7, up regulate CXCR5 chemokine receptor (which binds CXCL13 made by follicular dendritic cells) and migrate toward T-B cell zone border **(2).** Activated, cognate B cells (which have down regulated CXCR5 and up regulated CCR7 receptor) after receiving help from T cells can differentiate into short-lived plasma cells **(3)** or initiate GC reaction **(4)** to become long-lived plasma cells or memory B cells **(5).**

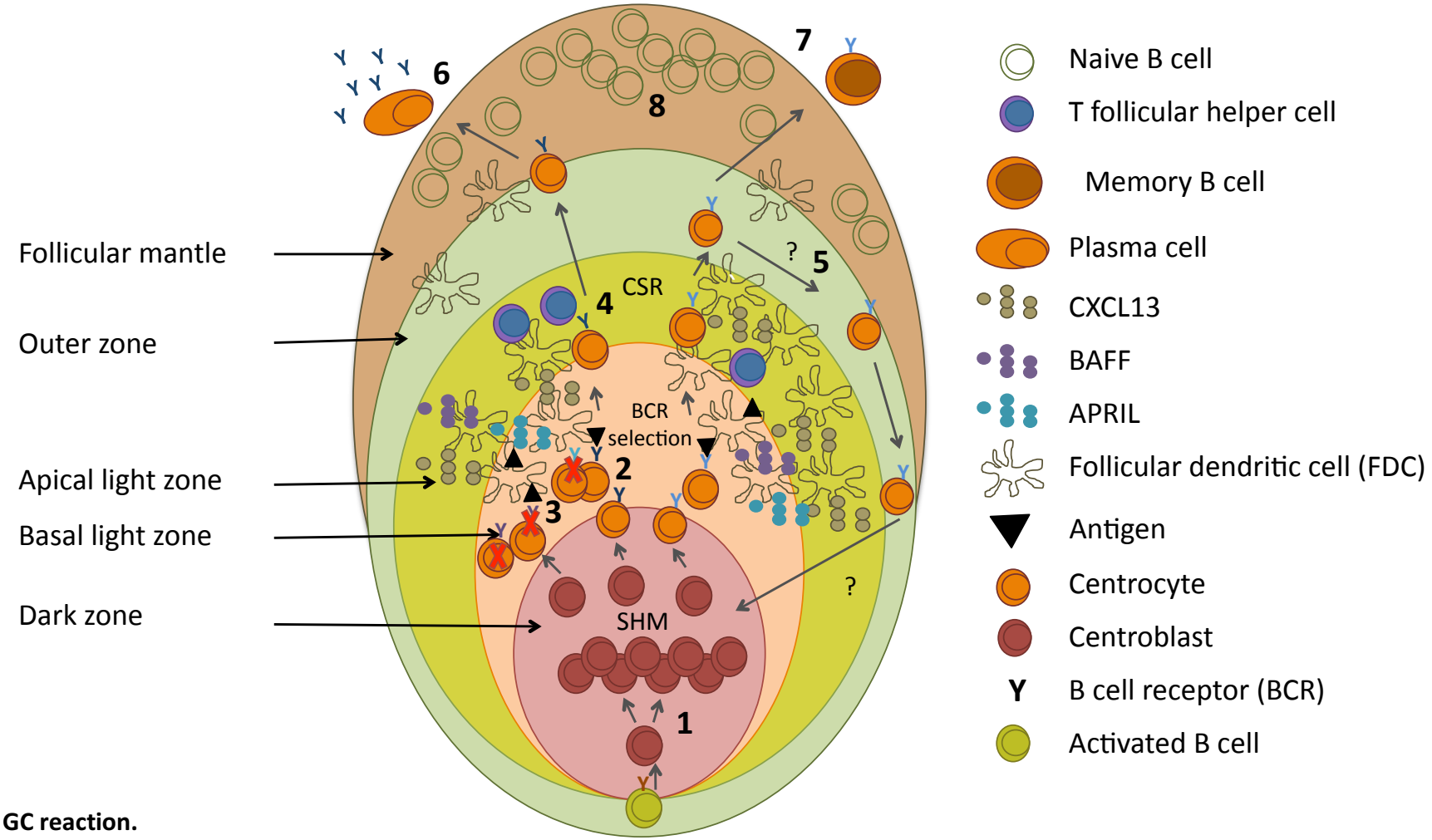

Fig 1.2 GC reaction.

Activated B cell starts to divide rapidly and is called centroblast **(1)**. Centroblasts form the dark zone of GC, undergo somatic hypermutation (SHM) and do not express B cell receptor (BCR) on the surface. After successful BCR rearrangement centroblasts, now called centrocytes, stop dividing and progress to the basal light zone of GC **(2)**, where they are tested for successful interaction with antigen held by FDC. B cells with self-reactive or low-affinity BCRs die by apoptosis **(3)**. Centrocytes with high-affinity BCRs progress to the apical light zone, undergo class switch recombination (CSR) and receive further survival signals from FDCs and T cells **(4)**. Outer zone consist of mature centrocytes and is a path for re-entry to the dark zone **(5)**. Finally, centrocytes become long-lived plasma cells **(6)** or memory B cells **(7)**. Naïve, circulating B cells, pushed out by the proliferating cells, form follicular mantle at the very edge of GC **(8)**.

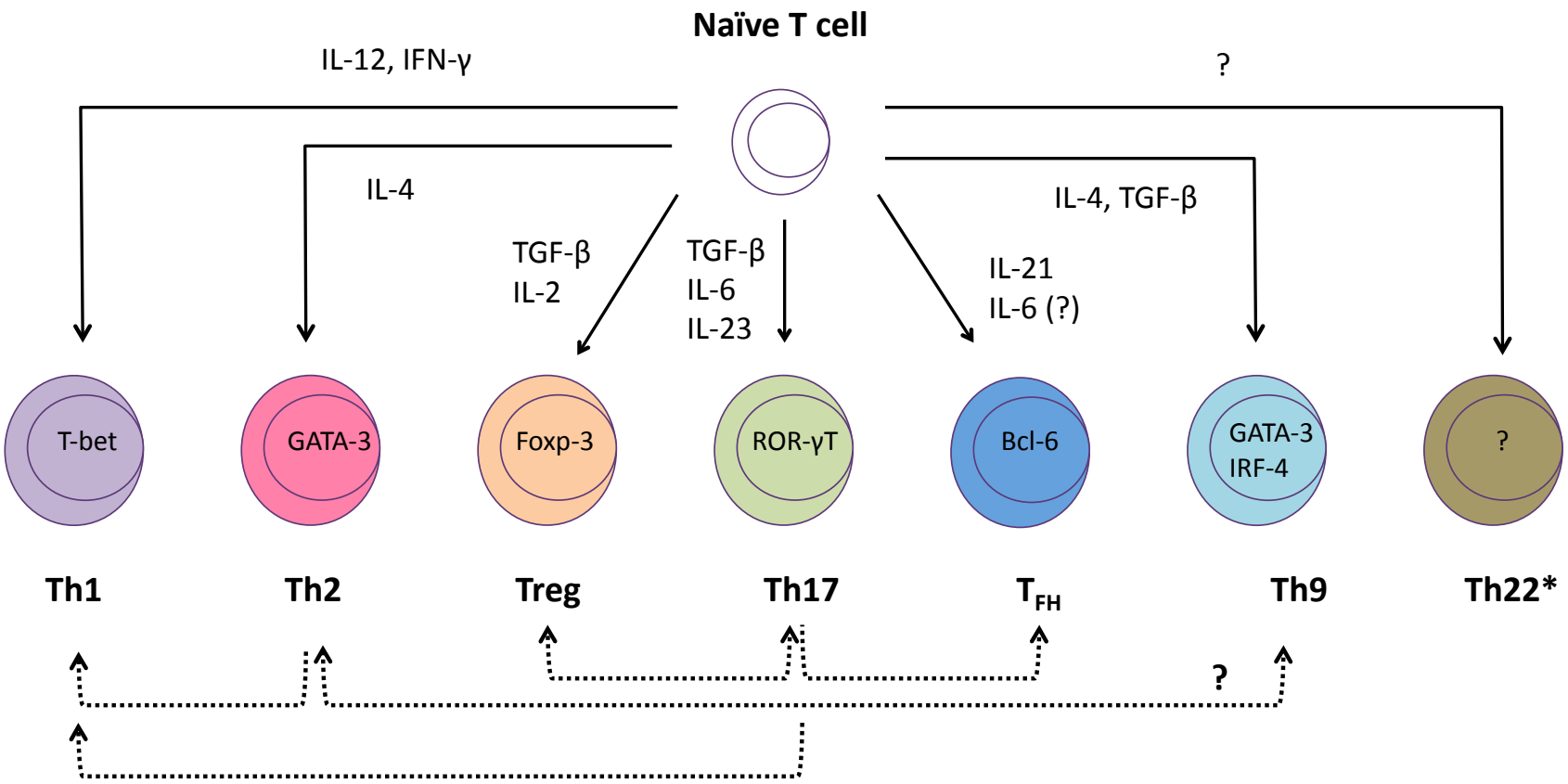

Fig 1.3 CD4$^+$ T cell differentiation and plasticity.

Naïve CD4$^+$ T cell can differentiate into effector T cell depending on cytokines present during T cell activation (derived from APC or the environment). Master TF involved in the differentiation are shown for each subset. There is a considerable plasticity in the T cell subsets, indicated by the dashed arrows. *Th22 cells have been described only in human as Th subset secreting high amounts of IL-22. No master TF or cytokine influencing differentiation have been yet indentified in the differentiation of Th22 cells.

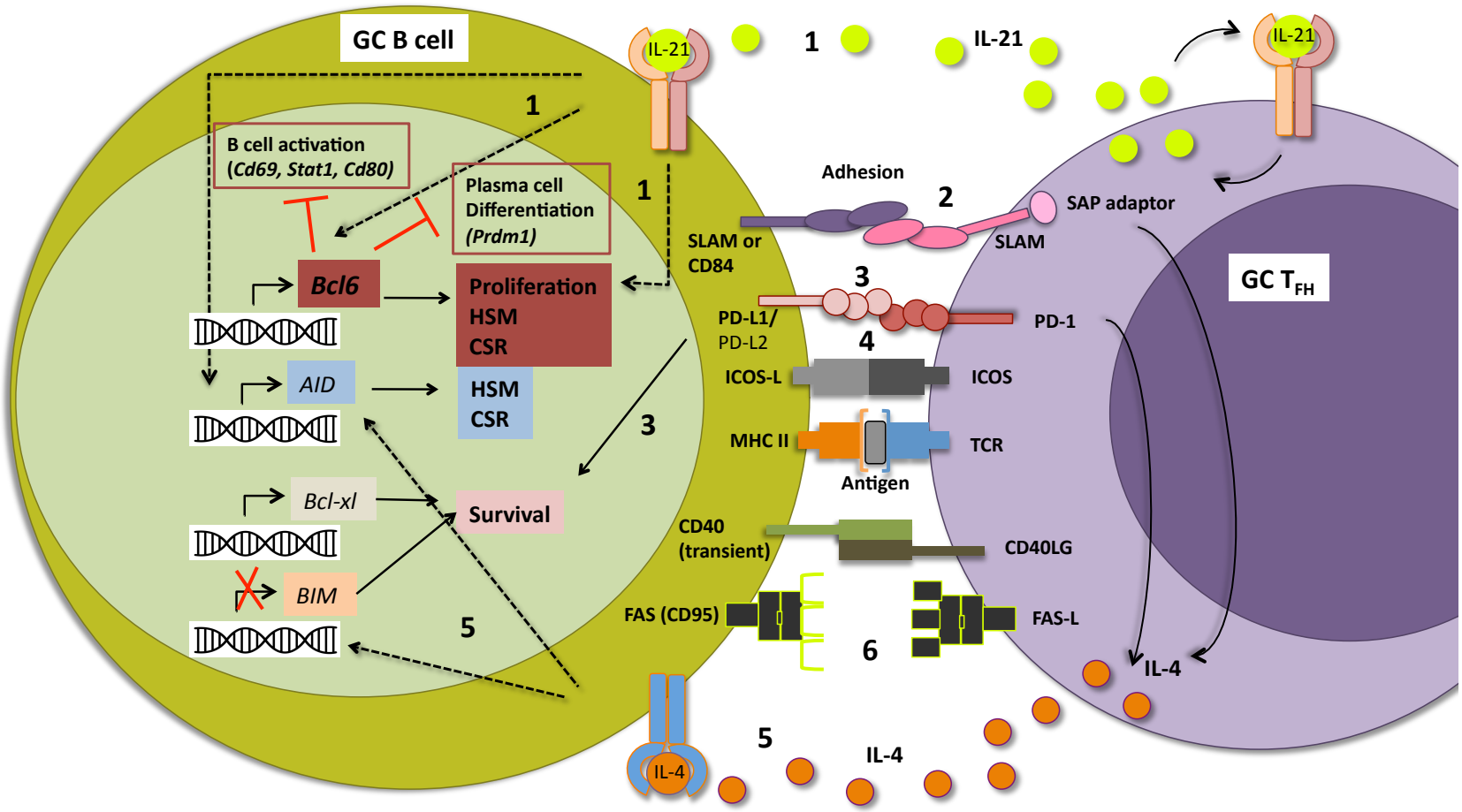

Fig. 1.4 Interaction between GC B cells and GC T_{FH}.

IL-21 provides pro-survival signals and can induce expression of both Bcl-6 in GC B cells **(1)** as well as Blimp-1 in plasma cells (not shown). Additionally, IL-21 induces expression of AID and enhances GC B cell proliferation **(1)**. SLAM/CD84 on B cells with SLAM on T cells **(2)** provides firm adhesion essential for receiving bi-directional signals. PD-L1/L2 signaling provides pro-survival signals to B cells **(3)** via an unidentified mechanism. Function of ICOS-L signaling in B cells **(4)** remains unknown. IL-4 signaling in GC B cell enhances survival by inducing expression of anti-apoptotic protein Bcl-xl **(5)**, as well as increasing glucose uptake (not shown). IL-4 is also a class-switch factor for IgG1 and IgE. In the absence of pro-survival signal GC T_{FH} trigger apoptosis in GC B cell via FAS-FASL interaction **(6).**

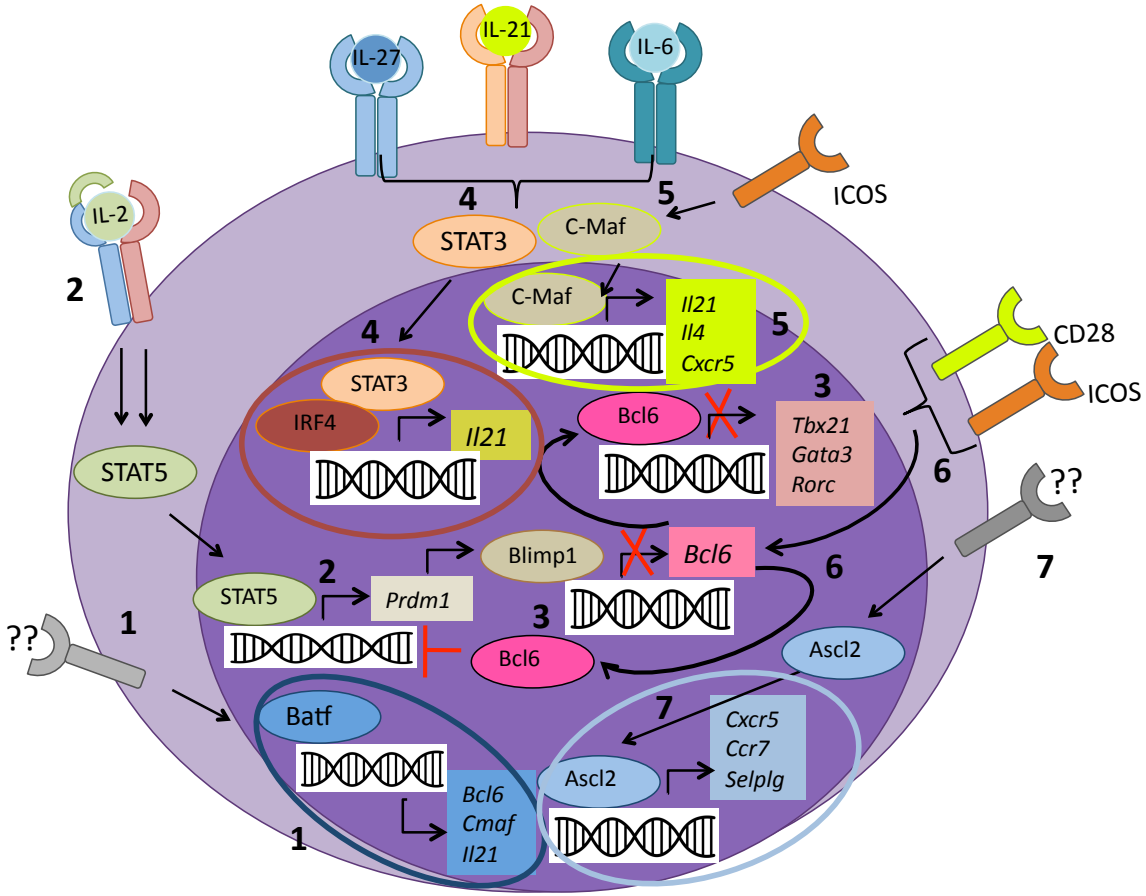

Fig 1.5 Cytokine signaling and transcription factor network in T_{FH} development.

(1) Unknown receptor induces expression of Batf TF, which positively regulates TFs Bcl6 and c-Maf as well as IL-21. **(2)** Strong IL-2 signaling via STAT5 induces expression of Blimp1 (from *Prdm1* locus), which represses transcription of Bcl6. **(3)** Weak IL-2 signaling induces expression of Bcl-6, which represses Blimp1 and TF driving commitment to Th1, Th2 and Th17 lineages. **(4)** IL-6, IL-21 and IL-27 signal via STAT3 to induce, together with IRF4, expression of IL-21. **(5)** IL-6, IL-21 and IL-27 together with ICOS induce expression of c-Maf, which positively regulates expression of IL-21, IL-4 and CXCR5. **(6)** CD28 and ICOS signaling induces Bcl6 expression upon T cell activation. **(7)** Unknown receptor induces TF Ascl2 to drive transcription of *CXCR5, CCR7* and *Selplg* and inhibit expression of *Cd25a* and *Cd25b* (IL-2Rα and IL-2Rβ, not shown.)

2 Materials and Methods

2.1 Medium and FACS buffer

Medium used in all experiments was Iscove's Modified Dulbecco's Media (IMDM, Gibco, UK) supplemented with 1% penicillin/streptomycin (Gibco, UK), 0.1% β-mercapthothanol (Gibco, UK) and 2% heat inactivated foetal calf serum (FCS, Biosera, UK).

FACS buffer (FB) was prepared by supplementing PBS (Sigma-Aldrich, UK) with 3% FCS. For cell sorting FB with 1.5% FCS was used.

2.2 Animals

C57BL/6 female mice used for all experiments were bred and kept in specific pathogen-free conditions in School of Biological Sciences animal facilities at the University of Edinburgh. Animals were 6 to 10 weeks old unless stated otherwise.

Genetically modified (GM) strains were used: MyD88$^{-/-}$mice (179), B cell deficient mice (μMT, (180)) and MHC II deficient mice (I-A$^{b-/-}$, (181)). These GM animals have C57Bl/6 background and all were females over 8 weeks old.

All experiments were carried out in agreement with Animal (Scientific Procedures) Act 1986 under the project licence and personal licence granted by Home Office and approved by the University of Edinburgh Ethical Review Committee.

2.3 BM chimeras generation

Chimeric mice with deficient MHC II expression in the B cell compartment (termed B$^{MHCII-/-}$ chimeras) were used in experiments presented in Chapter 4. B$^{MHCII-/-}$ chimeras were generated by sub-lethal irradiation (8 Gy of γ-irradiation) of B cell deficient (μMT) recipient animals, which were reconstituted with 2 to 4 million BM cells on the same day. The injected BM cell mix was depleted of CD90^{+} mature T cells (by labelling with CD90.2 microbeads and passing over LD column, Miltenyi Biotech, according to manufacturers instructions). Injected BM cell mix in experimental chimeric group consisted of μMT-derived cells (B cell-deficient) and

I-$A^{b-/-}$ cells (MHC II-deficient) cells in a 4:1 ratio. As a result B cells were derived exclusively from MHC II deficient cells whereas other haematopoietic cells were derived from both compartments (hence showing overall 20% MHC II deficiency). Control chimeras received 80% of μMT-derived BM and 20% of WT BM, therefore displaying 100% MHC II expression in all cells of hematopoietic origin. Injection mix was delivered in 200 μL intra venously (i.v.). Mice were left to reconstitute for at least 6 weeks before the start of the experiment and during this time were housed in filter cages with baytril- supplemented water.

2.4 Immunisations

2.4.1 Sheep red blood cells (SRBC)

Sheep red blood cells (SRBC) were purchased from the Mordun Research Institute (University of Edinburgh). SRBC were stored in heparin and thoroughly washed with Dulbeccos PBS (Sigma-Aldrich, UK) prior to injection. Mice received 2 x 10^9 SRBC in 200 μL PBS via intra peritoneal (i.p.) route in all experiments.

2.4.2 Salmonella typhimurium

The attenuated *Salmonella enterica* serovar *typhimurium* (SL3261, (158)) was grown in Luria-Bertani (LB) broth (DIFCO laboratories, UK) at 37 °C for 16 h without shaking. Approximately 1 x 10^6 colony forming units (CFU), unless otherwise stated, from the stationary phase were delivered in 200 μL sterile Dulbeccos PBS (Sigma) i.v. Exact infectious dose per experiment was determined by growing bacterial colonies on LB agar plates overnight at 37 °C, counting number of CFU and then calculating number of viable bacteria per mouse by taking into account dilution factor and injected volume.

Splenic bacterial load was determined by making a single cell suspension in PBS from a piece of the organ of a known weight and plating various dilutions on agar plates. The number of CFU was determined by counting colonies formed per spleen or per gram of spleen after an overnight culture at 37 °C.

In some experiment heat killed (HK) *S. enterica* was used. HK bacteria were prepared by incubating a stationary culture of *S. enterica* at 80 °C for 10 min. The remaining suspension was plated on the agar plates and incubated over night at 37

°C. No growth was observed, which confirmed that no viable bacteria were present in the injection mix.

2.5 Cell isolation

Single cell suspensions of splenocytes were obtained by manually disrupting the spleen through gauze squares in complete medium. BM was isolated by flushing the bones with complete medium using 25G needle (BD Pharmingen).

Red blood cell (RBC) lysis was done by adding 2 to 3 mL of RBC lysis buffer (Sigma Aldrich, UK) for 2 min at room temperature (RT). Viable cell count was determined after staining with trypan blue dye (0.1%, Sigma Aldrich, UK).

2.6 Flow cytometry

2.6.1 Surface staining

Single cell suspensions, containing 4 to 5 million cells, were washed with PBS. Cell viability was evaluated in some experiments by staining with amine-reactive fluorescent viability dye (1:700, LIVE/DEAD® fixable dead cell stain, Invitrogen). After 15 min incubation at 4 ˚C, cells were washed with FACS Buffer (FB) and primary antibodies applied for 25 min at 4 ˚C. Cells were then washed and secondary antibodies applied if needed (incubation for 15 min at 4 ˚C). Samples were washed prior to acquisition. All centrifugations were done at 4 °C for 2 min at 400 G.

2.6.2 Intracellular staining

For intracellular staining eBioscience Foxp3 intracellular staining kit was used according to manufacturer's instructions. Following surface staining, samples were fixed in Fix/Perm solution. After 15 min incubation at RT cells were washed with Perm Buffer. Blocking solution (2% rat serum and 1% anti-CD132) was applied for 5 min at RT and then intracellular antibodies were added for further incubation of 60 min at RT. A final wash step with Perm Buffer was performed prior to re-suspension in FB.

Samples were acquired using the LSR II flow cytometer (BD, UK) and data were analysed using FlowJo software (TreeStar). Antibodies used for flow cytometry are presented in Table 2.1.

2.7 T cell sorts and adoptive transfers

For isolation of individual T_{FH} populations flow cytometry associated sorting was used. T_{FH} populations were isolated at D6 post SRBC immunisation from WT C57Bl/6 mice, MHC II deficient mice ($MHCII^{-/-}$) or mixed BM chimeras.

CD4 T cell fraction was enriched by depletion of other cell populations prior to sorting. The depletion based on magnetic separation was done using Dynabeads (Invitrogen). Briefly, splenocytes ($1x10^8$ / mL) were labeled with anti-MHCII (clone M5114, home grown) and anti-CD8 antibodies (clone 53.6.72, home grown) for 25min at 4 ˚C in complete medium. After washing step, cells were incubated with anti-rat IgG Dynabeads (bead:cell ratio 1:2) for 30 min at 4 ˚C with the rotation. MHC II^+ and $CD8^+$ cells were bound to the beads and separated from the unlabelled cell fraction (containing $CD4^+$ T cell) by using a Dynabead magnet. The frequency of CD4 T cells after enrichment process was around 65%. T_{FH} cell staining for flow cytometry was done as described in section 2.6. Cells were sorted into PBS containing 1.5 - 2% FCS with FACS ARIA (BD) and quality control confirmed high sorting purity. The sorting strategy and purity is presented on Figure 2.1.

In adoptive transfer experiments, sorted T cell populations were washed with sterile PBS (Sigma), counted and 0.4 million cells in 200 µL of sterile PBS (Sigma) per mouse were injected i.v.

T_{FH} cells sorted for RNA isolation were stored as cell pellets or in TRIzol reagent (Invitrogen) at -80 ˚C until extraction process.

2.8 RNA extractions and quality control

RNA was extracted from T_{FH} population stored either in TRIzol (Invitrogen) or as cell pellets. RNeasy kit (Qiagen) was used in both cases.

When extracting RNA from cells stored in TRIzol, the RNA cleanup procedure was followed (p.56 of Qiagen handbook). After 5 min incubation at RT, 200 µL chloroform per 1 mL of Trizol were added, the sample was vigorously shaken and further incubated for 3 min at RT. After spinning step (15 min at 12000 G at 4 °C) the upper aqueous phase was transferred to a new collection tube, 350 µL of cold RLT buffer were added followed by 250 µL of cold 100% ethanol (both volumes per

100 µL of the aqueous phase). Tube was vortexed and liquid loaded on the RNeasy Mini column in 730 µL fractions. From then standard manufacturers' instructions were followed.

In RNA extraction performed from the cell pellets, 750 µL of RLT buffer were added to the pellet which was passed via a syringe (21G, BD Pharmingen). 750 µL of cold 75% ethanol was then added, the sample was vortexed and liquid loaded on the RNeasy Mini column. Standard manufacturers' instructions were followed as above. RNAse inhibitor (Roche) was added at the end of the extraction process and clean RNA was stored in DEPC-treated RNAse-free water (Ambion). RNA quantity was determined by Nanodrop (Thermoscientific) and RNA integrity was assessed by Bioanalyzer (Agilent Technologies). In the latter case RNA-Nano chips (Agilent Technologies) were used strictly as per manufacturers' instructions. RNA integrity number (RIN) confirmed that isolated RNA was of very high quality and no significant degradation was detected (RIN values were between 8-10, out of 10 possible, Table 2.2).

2.9 cDNA synthesis and quantitive real-time PCR

RNA was converted into cDNA using Superscript First Strand Synthesis System (Invitrogen) according to manufacturers' instructions with 50-200 ng of RNA input used per 10 µL reaction volume.

Real time qPCR was performed using probe-based assays enabling sequence-specific detection of target genes. TaqMan Gene expression master mix (Applied Biosystems, 10 µL per reaction), 55 ng of cDNA of interest, 1 µL of probe-labeled primers and water was mixed to give a total volume of 20 µL per reaction. Primer sequences or assay numbers (IDT technologies) are shown in Table 2.3 and Table 2.4. mRNA levels were normalized to reference genes UBC and 18s from GeNorm kit (Primer Design). Differences in the samples were calculated using delta delta method.

2.10 Microarray analysis of T cell populations

RNA extracts from sorted T cell populations were subjected to quality control by Nanodrop and Bioanalyzer, as described above. Extracted mRNA was stored at -70

°C until analysis. Hybridisation of mRNA to the microarray chips was performed in ARK Genomic Technologies (The Roslin Institute, University of Edinburgh). Files were fully analysed by Dr. Al Ivens (Centre for Immunity, Infection and Evolution, Edinburgh). Data were subjected to quality control (Appendix Fig. 7.1-7.4), normalisation and correction for multiple testing. As a result, tables containing lists of differentially expressed genes alongside P values and fold changes in expression were generated.

2.11 mRNA isolation, cDNA synthesis and library preparation for TCR sequencing

Sample preparation for TCR sequencing was carried out by Dr. Graeme Cowan, who kindly provided the protocols described below.

2.11.1 mRNA isolation

Dynabeads mRNA DIRECT Kit (ThermoFisher Scientific) was used for mRNA isolation. The cell pellet (containing up to 1 x 10^6 cells) was resuspended in 300 µL of lysis buffer in order to release the genomic DNA. The lysate was passed through a 21G needle (BD Pharmingen) to shear the genomic DNA. 100 µL of Dynabeads were prepared for the reaction by washing in 50 µL of lysis/binding buffer. The sample lysate was added to the dynabeads and the sample was thoroughly mixed by repeated pipetting and incubation with continuous mixing for 3 to 5 min at RT. Microcentrifuge tube was then placed on a magnet for 2 min and supernatant was removed. Beads were washed twice with 600 µL of wash buffer A and twice with 300 µL of wash buffer B. These washing steps were performed at RT and the magnet was used to separate beads from the solution. Samples with mRNA bound to the beads was stored in -80 °C until cDNA synthesis was performed.

2.11.2 First strand cDNA synthesis

First strand cDNA synthesis was carried out with the SmartScribe polymerase kit (Clontech). Washed magnetic beads (9 µL) with bound mRNA were incubated with First Strand Buffer (4 µL), DTT (0.5 µL), mix of dNTPs (2 µL of 10mM solution), SMARTer IIA PTO oligo (2 µL of 12 µM solution), SMARTScribe RTase (2 µL) and RNase inhibitor (0.5 µL, Clontech). The solution was incubated for 50 min at 42

°C with repeated mixing to resuspend the beads. Reactions were terminated by 10 min incubation at 70 °C. Samples were stored again at -80 °C until further processing.

2.11.3 Library preparation – amplification of variable regions

PCR reactions were carried out on a LightcCycler® 480 System qPCR machine (Roche) with suitable qPCR multiwell plates (Roche).

Primers used (also showed in Fig. 5.2):

Reverse primer fused to P5 Illumina adapter:

AATGATACGGCGACCACCGAGATCTACACCTTGGGTGGAGTCACATTTCT

Forward primer fused to P7 Illumina adapter with SMART indexed sequence:

CAAGCAGAAGACGGCATACGAGATTCTCGAAAGCAGTGGTATCAACGCAGAGT

PCR mix (total volume of 20 µL) contained Phusion flash (10 µL, PCR master mix, Thermo Fisher Scientific), forward and reverse primers (2 µL of 12 mM solution each), cDNA (2 µL) and dH_20 containing diluted SYBR green (4 µL, 1:2000 dilution, Invitrogen). PCR cycles were set up as follows:

98°C	2min	(cDNA denaturation)
98°C	10s }	
60°C	15s } x 5 cycles	(elongation)
72°C	25s }	
98°C	10s }	
65°C	15s } x 25 cycles	(elongation)
72°C	25s }	
72°C	2min	(termination of the reaction)

PCR products, containing amplicons of variable TCR regions, were then run on a 2% agarose gel to remove residual primers and truncated products. Bands of appropriate size were excised and purified using the Gel Extraction Kit (Qiagen) according to manufacturers' instructions.

2.12 Statistical analysis

Statistical analyses were carried out with Prism 6 software (GraphPad Software Inc., USA). Student's t-test or one-way ANOVA analyses were used to determine significance between the groups. For two-way ANOVA Tukey's correction for multiple testing was used. Significance was depicted in the graphs as follows: * for P= 0.01 to 0.05, ** for P = 0.001 to 0.01, *** for P < 0.001. P> 0.05 was considered as not significant (ns).

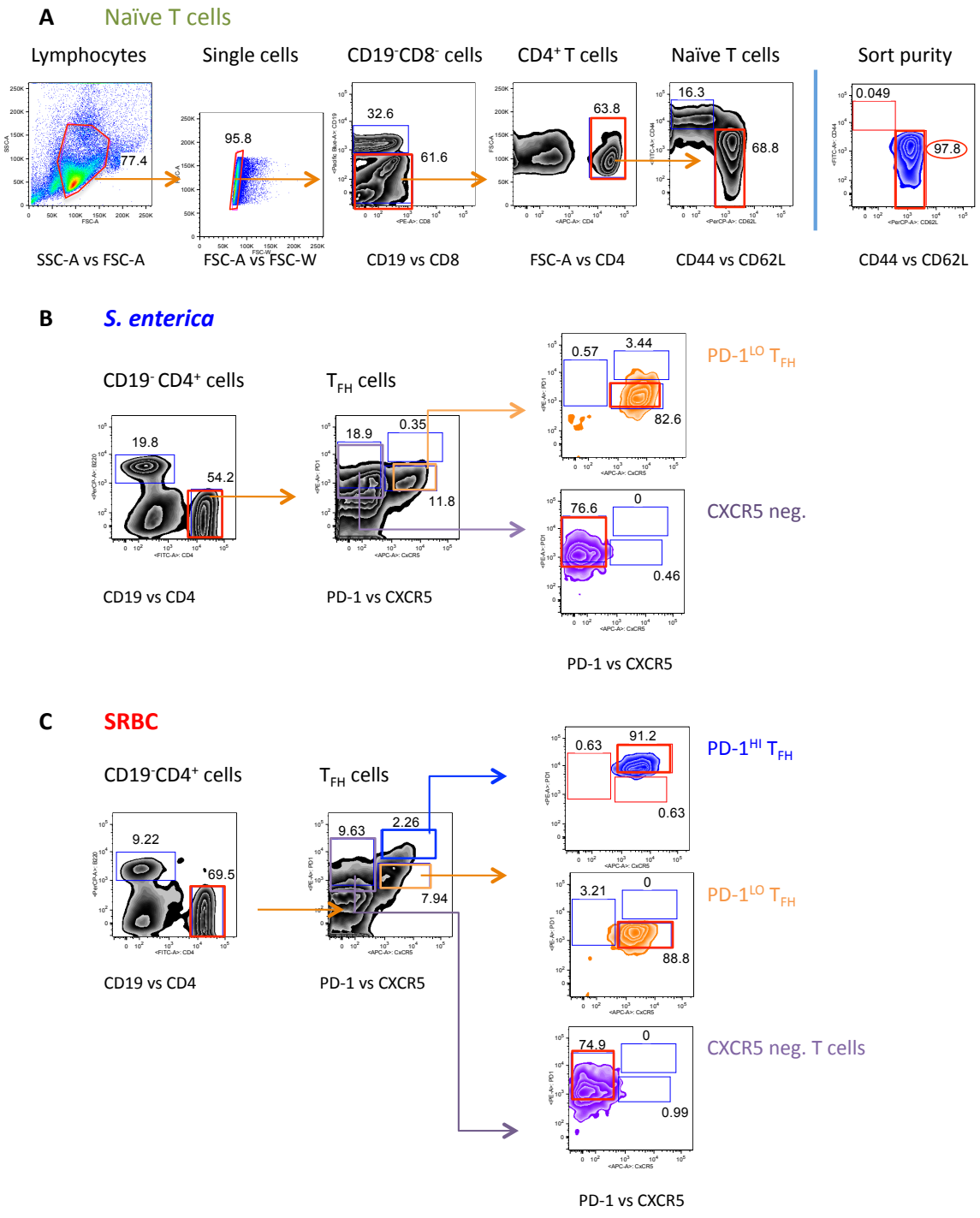

Fig 2. Sorting strategy used for T cell isolation for the microarray and next generation sequencing (WT mice).

(A) Sorting strategy for naive T cells. Lymphocytes were selected on the basis on site scatter (SSC-A) and forward scatter (FSC-A). Single cells were then positively selected based on the width of the cell (FSC-A vs FSC-W). B cells and $CD8^+$ T cells were further excluded (CD19 vs CD8). $CD4^+$ T cells were selected (FSC-A vs CD4) and naïve T cells were sorted based on the expression of CD44 and CD62L. **(B)** Sorting strategy for T_{FH} populations from WT mice 6 days after *S. enterica* infection or **(C)** SRBC immunisation**. (B)** and **(C):** lymphocytes and singles cells were gated as in **(A).** $CD19^+$ B cells were excluded and $CD4^+$ T cells were selected (CD19 vs CD4). T cell subsets were sorted based on the expression of CXCR5 and PD-1 into PD-1^{HI} T_{FH}, PD-1^{LO} T_{FH} and $CXCR5^-$ T cells.

Table 2.1. Antibodies used for flow cytometry staining.

Antibody/ reagent	Conjugate	Clone	Dilution	Provider
Anti-CD3ε	PE	145-2C11	1:200	eBiosciences
Anti-CD4	FITC	GK1.5	1:200	Southern Biotech
Anti-CD4	APC—eFluor780	RM4-5	1:200	eBiosciences
Anti-CD8α	PE	53-6.7	1:200	BD Pharmingen
Anti-CD8α	BV 650	53-6.7	1:200	Biolegend
Anti-CD11b	APC-Cy7	M1/70	1:200	Biolegend
Anti-CD11c	FITC	N418	1:100	home grown
Abti-CD16/CD32	unlabelled	2.4G2	1:100	home grown
Anti-CD19	PE	1D3	1:200	BD Pharmingen
Anti-CD19	PercP	6D5	1:200	Biolegend
Anti-CD19	BV 421	6D5	1:200	Biolegend
Anti-CD25	Pe-Cy7	PC61.5	1:200	eBioscience
Anti-CD44	FITC	polyclonal	1:200	home grown
Anti-CD45.1	FITC	A20	1:200	Biolegend
Anti-CD45.1	PE	A20	1:200	BD Pharmingen
Anti-CD45.1	BV650	A20	1:100	Biolegend
Anti-CD45.2	FITC	104	1:200	BD Pharmingen
Anti-CD45.2	PE	104	1:200	Biolegend
Anti-B220 (CD45R)	PerCP	RA3-6B2	1:200	BD Pharmigen
Anti-CD62L	PerCP/Cy5.5	MEL-14	1:200	Biolegend
Anti-CD62L	BV 605	MEL-14	1:200	Biolegend
Anti-CD127	BV421	A7R34	1:200	Biolegend
Anti-CD162	PE	2PH1	1:100	BD Pharmingen
Anti-ICOS (CD278)	PE	7E.17G9	1:100	eBiosciences
Anti-PD-1 (CD279)	PE	RMP1-30	1:100	Biolegend
Anti-PD-1 (CD279)	Pe-Cy7	RMP1-30	1:100	Biolegend
Anti-Bcl6	PE	K112-91	1:100	BD Pharmingen
Anti-CXCR5	Biotin	2G8	1:100	BD Pharmingen
Anti-F4/80	APC	BM8	1:100	eBiosciences
Anti-IgD	Pacific Blue	11-26c.2a	1:200	Biolegend
Anti-Foxp3	FITC	FJK-16s	1:100	eBioscience
Anti-Ki67	PE	B56	1:100	BD Pharmingen
Anti-KLRG1	Pe-Cy7	2F1	1:200	eBioscience

Anti-MHC II	FITC	M5114	1:200	home grown
Anti-MHC II	Pacific Blue	M5114.5.2	1:200	Biolegend
PNA	FITC	N/A	1:1600	Vector Laboratories
Streptavidin	APC	x	1:200	BD Pharmingen

Table 2.2. RNA Integrity Numbes (RIN) of the samples subjected to microarray analysis.

Sample code for the microarray	**Experimental group**	**Isolated cells**	**Isolated cells**	**RNA Integrity Number (RIN)**
1	**Naïve**	$CD44^{LO}CD62L^{HI}$	Naive T cells	9.3
2	**Naïve**	$CD44^{LO}CD62L^{HI}$	Naive T cells	9.1
3	**Naïve**	$CD44^{LO}CD62L^{HI}$	Naive T cells	8.5
4	***S. enterica***	$CXCR5^{+}PD\text{-}1^{+}$	T_{FH} $(PD\text{-}1^{LO})$	8.5
5	***S. enterica***	$CXCR5^{+}PD\text{-}1^{+}$	T_{FH} $(PD\text{-}1^{LO})$	8.1
6	***S. enterica***	$CXCR5^{+}PD\text{-}1^{+}$	T_{FH} $(PD\text{-}1^{LO})$	8.5
7	***S. enterica***	$CXCR5^{-}PD\text{-}1^{+}$	CXCR5 neg. T cells	9.9
8	***S. enterica***	$CXCR5^{-}PD\text{-}1^{+}$	CXCR5 neg. T cells	9.8
9	***S. enterica***	$CXCR5^{-}PD\text{-}1^{+}$	CXCR5 neg. T cells	10.0
10	**SRBC**	$CXCR5^{+}PD\text{-}1^{HI}$	T_{FH} $(PD\text{-}1^{HI})$	9.4
11	**SRBC**	$CXCR5^{+}PD\text{-}1^{HI}$	T_{FH} $(PD\text{-}1^{HI})$	8.6
12	**SRBC**	$CXCR5^{+}PD\text{-}1^{HI}$	T_{FH} $(PD\text{-}1^{HI})$	9.2
13	**SRBC**	$CXCR5^{+}PD\text{-}1^{LO}$	T_{FH} $(PD\text{-}1^{LO})$	9.8
14	**SRBC**	$CXCR5^{+}PD\text{-}1^{LO}$	T_{FH} $(PD\text{-}1^{LO})$	9.0
15	**SRBC**	$CXCR5^{+}PD\text{-}1^{LO}$	T_{FH} $(PD\text{-}1^{LO})$	9.1
16	**SRBC**	$CXCR5^{-}$ $PD\text{-}1^{+}$	CXCR5 neg. T cells	9.5
17	**SRBC**	$CXCR5^{-}$ $PD\text{-}1^{+}$	CXCR5 neg. T cells	9.3
18	**SRBC**	$CXCR5^{-}$ $PD\text{-}1^{+}$	CXCR5 neg. T cells	9.6

Table 2.3. qPCR primer sequences (Integrated DNA Technologies, Iowa, USA).

Gene symbol	**Gene name**	**Forward primer 5'-3'**	**Reverse primer 5'-3'**
Bcl6	B cell lymphoma-6	AGTCACATTCGTTGCAGAAGA	CAGAGATGTGCCTCCATACTG
Tox2	TOX High Mobility Group Box Family Member -2	GATTGGGAGGCGTTATAGGAG	GAAGTTTGATGGTGACAGTGC

Table 2.4. PrimeTime® qPCR assay numbers (Integrated DNA Technologies, Iowa, USA)

Gene symbol	**Gene name**	**PrimeTime qPCR assay number**
Ascl2	Achaete-scute complex homolog 2, Drosophila	Mm.PT.58.11676006.gs
Ccr7	Chemokine (C-C motif) receptor 7	Mm.PT.58.31257202
Il7r	IL-7 Receptor	Mm.PT.56a.14297778
Il21	IL-21	Mm.PT.56a.7853071
Klrg1	Killer cell lectin like receptor G1	Mm.PT.56a.30803964
Prdm1	PR domain zinc finger protein 1	Mm.PT.56a.10253822

3 Characterisation of T_{FH} cell populations in SRBC immunisation and *S. enterica* infection

3.1 Introduction

In the current literature the existence of more than one type of T_{FH} population is a matter of debate. Clearly, there is some heterogeneity among $CXCR5^+$ $CD4^+$ T cells revealed by the existence of T_{FR} (134) and NK T_{FH} ((147), discussed in main introduction on p. 33), but whether other $CXCR5^+$ $PD\text{-}1^+$ $Bcl6^+$ cells contain specialized subsets that perform different functions is unknown.

In the early days after the discovery of T_{FH}, all $CD4^+$ cells expressing CXCR5 and ICOS were termed T_{FH}. Since many cell types up-regulate ICOS after the cell activation, it became clear that there is the need for another marker for T_{FH} population. PD-1 protein was shown to be highly expressed by $CXCR5^+$ $ICOS^+$ cells (182). PD-1 plays a pivotal role in the GC (GC) and long-lived plasma cell formation and B cell proliferation (113,134). The discovery of Bcl6 as a T_{FH} specific TF (77,84,147) changed the standards of identifying $T_{FH,}$ by now linking the presence of this subset to its function in supporting B cells and antibody production. Therefore, when doing research on T_{FH}, one cannot simply look at the surface phenotype but must also consider the functional output of the population.

The aim of this PhD work was to investigate the heterogeneity of T_{FH} populations in two different immunisation/infection models (SRBC immunisation and *S. enterica* infection), which give rise to phenotypically distinct T_{FH} populations, and to test whether there are functional consequences of this heterogeneity. In Chapter 3 I performed an extensive profiling of the T_{FH} populations with the markers known from literature to be connected to T_{FH}, showing that there is indeed a considerable level of heterogeneity within the T_{FH} populations. I also took a more global approach to characterising T_{FH} by subjecting different subsets to microarray analysis. Differential gene expression of general cellular pathways and immune pathways (including T_{FH} related genes) confirmed that isolated populations are indeed discreet cell subsets. In the following chapter (Chapter 4) I investigated the interactions of

different T_{FH} with cognate B cells, which ultimately led to important conclusions about the T_{FH} development pathway. In the final chapter (Chapter 5) I studied the potential for interaction between these T_{FH} subsets by performing co-immunisation experiments and, following an unexpected result of T_{FH} expansion, I try to broadly address the question regarding specificity of those T_{FH} cells.

3.2 Results

3.2.1 SRBC response generates PD-1^{HI} and PD-1^{LO} T_{FH}, with the former population missing after *S. enterica* infection.

T_{FH} population was first identified by flow cytometry as $CXCR5^+$ $ICOS^+$ subset within $CD4^+$ T cells (183,184). PD-1 protein has soon become recognized as another relevant surface marker (22,129). Currently CXCR5 and PD-1 are the most commonly used cell surface markers used for defining the T_{FH} subset. Additionally, the Bcl6 TF is used as an intracellular marker for *bona fide* T_{FH} (77,84,85). Therefore, in my work I have identified different T_{FH} subsets by using these three commonly accepted markers: PD-1, CXCR5 and Bcl6.

In all of the experiments presented the spleen was used as the source of T_{FH} isolation. The gating strategy for T_{FH} identification (Fig. 3.1A, upper panel) involved selecting the lymphocytes based on their side and forward scatter appearance (SSC-A vs FSC-A) and then excluding doublets (SSC-A vs SSC-W) and $CD8^+$ T cells (SSC-A vs CD8). B cells were identified alongside $CD4^+$ T cells (CD19 vs CD4). As an important technical control, surface expression of CXCR5 on B cells was graphed (Fig. 3.1A, lower panel, first and second graph to the left). Since B cells are uniformly CXCR5 positive (4,5), this was an important quality control for CXCR5 staining (which proved to be technically challenging at times). Finally, PD-1 and CXCR5 double positive cells were selected within the $CD4^+$ T cells (Fig. 3.1A, lower panel, second graph to the right). Relevant isotype controls were used to determine PD-1 and CXCR5 positive cut-off gates on $CD4^+$ T cells (Fig. 3.1A, lower panel, first graph to the right). Live/dead stain, often used to gate out dead or apoptotic cells, was not commonly used since staining of the fresh *ex-vivo* splenocytes resulted in around 90% or 98% viability (for *S. enterica* and SRBC model, respectively) and, most importantly, early experiments showed that gating out dying cells did not have any impact on downstream T_{FH} analysis.

The T_{FH} analysis of early stages of the immune response to the immunisation with SRBC or *S. enterica* infection provided clear results indicating that T_{FH} observed in

the early stages of *S. enterica* infection displayed much lower levels of PD-1 on the cell surface than corresponding CXCR5 positive population generated during the SRBC response. This phenomenon raised curiosity in our lab and, therefore a time course analysis of the T_{FH} populations was carried out to investigate the kinetics of the CXCR5, PD-1 and Bcl-6 expression in the two models.

In the SRBC immunisation, T_{FH} populations (expressing high and low levels of PD-1, therefore termed 'PD-1^{HI}' and 'PD-1^{LO}' T_{FH}) became visible around day 5 and peak in frequency around day 7 (Fig. 3.1 B and D). However, in the *S. enterica* model, T_{FH} cells appear earlier (around day 3), express predominantly low levels of PD-1 (hence 'PD-1^{LO} T_{FH}') and their frequency peaks around day 9 p.i. (Fig. 3.1C and D). In both models PD-1^{HI} and PD-1^{LO} T_{FH} populations decline from day 9 onwards (Fig. 3.1 B-E) and by day 15 are contracted almost to the levels observed in non-immunised animals (graphed as day 0).

In striking contrast to the SRBC model, in *S. enterica* infection the PD-1^{HI} T_{FH} population is present at a very low frequency (0.36% ± 0.05, of $CD4^+$ T cells at day 6, Fig. 3.1 C and D). Furthermore, even the few $T_{FH,}$ which fall into the PD-1^{HI} gate in the *S. enterica* model express less PD-1 protein on the surface than the PD-1^{HI} T_{FH} arising after SRBC immunisation (MFI of PD-1: 5404±1273 for the PD-1^{HI} T_{FH} in *S. enterica* infection vs. 7437±235 for the PD-1^{HI} T_{FH} in SRBC model, $p<0.05$). This shows that the distinction between PD-1^{HI} and PD-1^{LO} T_{FH} in terms of PD-1 expression is consistent during the first week of the response (Fig. 3.1E). Interestingly, PD-1^{HI} T_{FH} from both models express more CXCR5 protein than PD-1^{LO} T_{FH} (Fig. 3.1F), which suggests potential differences in the positioning of these cell subsets (MFI of CXCR5: PD-1^{HI} T_{FH} vs PD-1^{LO} T_{FH}: 2526±195 vs 1818±36 for the *S. enterica* infection and 2162±43 vs 1597±42 in SRBC model, $p<0.001$ for both models).

One might argue that classifying T_{FH} into PD-1^{HI} and PD-1^{LO} subsets depends on arbitrary positioning of the PD-1^{HI} and PD-1^{LO} gates. However, the gates are consistent for all samples and the results from multiple experiments are highly reproducible, which illustrates the validity of distinguishing the T_{FH} subsets based on their PD-1 expression. Additionally, high and low expression of PD-1 is observed

already from day 3 of the response to both SRBC and *S. enterica*, and the T_{FH} phenotype remains stable over time (Fig 3.1E).

Summing up, within the first two weeks of the response to SRBC, the T_{FH} population peaks around day 7 and there is a clear distinction between PD-1^{HI} and PD-1^{LO} T_{FH} cell subsets. This is in contrast to the *S. enterica* model, where the vast majority of T_{FH} cells express low to intermediate levels of PD-1 and the PD-1^{HI} T_{FH} population is scarce in terms of frequency. Therefore, clear phenotypical heterogeneity within CXCR5 positive cells has been recognised in two different models of the immune response. Whether this phenomenon carries also functional consequences remains to be established.

3.2.2 GC B cells are found abundantly after SRBC immunisation but not after *S. enterica* infection.

The T_{FH} population is linked to GC support (discussed in the Introduction, p. 27) and therefore the presence of these structures in SRBC and *S. enterica* immunisations was assessed to establish the functional capacity of different T_{FH} subsets.

GC B cells can be identified and quantified by means of flow cytometry as a subset of $CD19^+$ lymphocytes expressing high levels of TF Bcl6 (185). The gating strategy for identifying GC B cells (Fig. 3.2A) involved the positive selection of lymphocytes, single cells and CD19 B cells while excluding $CD4^+$ T cells at the same time (as some of $CD4^+$ cells, namely T_{FH}, will be Bcl-6 positive). GC B cells were finally identified as cells expressing both CD19 and Bcl6 (Fig. 3.2A, second graph from the right). The relevant isotype control was used to confirm the specificity of the staining (Fig. 3.2A, far right).

In keeping with other published findings (171) and previous observations from our lab, GC B cells were absent during the first 2 weeks of the response to *S. enterica* (Fig 3.2C, D), since, as discussed before (Introduction, p. 40), GC formation in this model is delayed until around week 7 p.i. In striking contrast to this, GC B cells were abundantly found in animals immunised with SRBC as early as day 5 p.i.

with the peak of the expansion around day 9 and a decline in frequency by day 15 (Fig. 3.2B, D). The summary of GC B cell frequencies and numbers (Fig. 3.2D and E, respectively) illustrated clearly that while the SRBC model gives a robust GC response within the first two weeks p.i., these structures are completely absent in the *S. enterica* infection (GC B cells as % of B cells at day 6 p.i.: 0.58±0.06 in *S. enterica* model vs 3.49±0.58 in SRBC model, $p<0.01$). These results were confirmed by flow cytometry analysis using alternative surface markers (with GC B cells identified as $CD19^+$ cells positive for peanut agglutinin (PNA) and negative for IgD, Appendix Fig. 7.5).

In conclusion, the clear presence of GC in SRBC model and their absence in *S. enterica* infection raised questions about the function of PD-1^{LO} T_{FH} cells found in the latter model. Considering that the PD-1^{HI} T_{FH} subset is present in the model generating GC response (SRBC) suggests that this subset is a GC supporting T_{FH} population

3.2.3 Altered splenic structures do not hamper PD-1^{HI} T_{FH} formation after *S. enterica* immunisation.

The reasons for the absence of the PD-1^{HI} T_{FH} subset in *S. enterica* are unknown. One of the most noticeable differences between SRBC and S. *enterica* immunisations is splenomegaly found in the latter model. This is in contrast to SRBC response, where spleen architecture is intact and B cell follicles and T cell zones are easily distinguished. I therefore decided to address the question whether altered splenic structures found in the early stages of *S. enterica* infection hamper the formation of PD-1^{HI} T_{FH} by, for example, disrupting the niche required for this subset to develop or survive.

The standard infectious dose of *S. enterica* in our lab is 10^6 CFU/mouse and this dose causes, as mentioned, severe splenomegaly. However, increase in the spleen size can be limited by using a lower infectious dose (10^4 CFU/mouse) or heat killed (HK) bacteria. Previous work of an honours student in our lab, Lewis Cawkwell, showed that at a lower infectious dose ($1x10^4$ CFU) there is a significant immune response in terms of $CD4^+$ and $CD8^+$ T cell activation and cytokine secretion by T cells (unpublished data). At the same time, with respect to the FDC network and

B cell follicles, the splenic structure appears comparable to the undisrupted spleen of naïve animals. To test the hypothesis that distorted splenic structures impede the formation of PD-1^{HI} T_{FH} in *S. enterica* infection, I infected animals with the standard dose of live *S. enterica* ($1x10^6$ CFU/mouse), a low dose of live bacteria ($1x10^4$ CFU/mouse) and also HK bacteria. T_{FH} and GC formation were assessed 6 days p.i. by flow cytometry. In agreement with previous studies from our lab, animals immunised with $1x10^6$ CFU had on average 5 times larger spleens than naïve animals (Fig 3.3A). Importantly, splenomegaly was not observed in infection with the lower dose of live bacteria and HK bacteria (Fig 3.3A). The difference in the immunisation dose was reflected in bacterial burden measured on day 6 p.i. (Fig. 3.3B). Animals immunised with the $1x10^6$ CFU dose of live bacteria displayed higher CFU count per spleen and per gram of spleen than animals with the lower dose immunisation (Fig. 3.3B).

As shown previously (Fig.3.1C and D), immunisation with the standard dose of $1x10^6$ CFU of *S. enterica* did not generate many PD-1^{HI} T_{FH} but PD-1^{LO} T_{FH} were found abundantly (Fig. 3.3C-E). Fascinatingly, this was also the case for the lower dose and HK bacteria immunisation (Fig. 3.3C-E). In all three immunisation models the frequency and numbers of PD-1^{HI} T_{FH} were comparable to unimmunised animals (Fig. 3.3D and E, left). PD-1^{LO} T_{FH} cells were found at the highest frequency and numbers in the high-dose immunisation model (Fig. 3.3D and E, right. PD-1^{LO} T_{FH} as % of $CD4^+$ T cell: 7.05±0.17 for high dose *S. enterica* vs. 2.35±0.22% for low dose and 2.83±0.33 for HK bacteria). A detectable increase in PD-1^{LO} T_{FH} frequency (although of lower magnitude) above the levels observed in naïve animals was also found in the lower dose infection and HK bacteria immunisation. However, these parameters were not always statistically significant, partly due to the fact that naïve animals used for this experiment showed higher background levels of PD-1^{LO} T_{FH} than usually observed.

The induction of GC B cells was further assessed as a functional readout of T_{FH} presence. As expected, in the light of the missing PD-1^{HI} T_{FH} population, GC B cells ($CD19^+$ $Bcl6^+$, Fig. 3.3F) were also absent in all immunised groups in terms of frequency and numbers (Fig. 3.3G).

Summing up, altered splenic structures do not prevent formation of PD-1^{HI} T_{FH} and GC populations in *S. enterica* infection as these lymphocyte populations are not found in the infection/immunisation models when the splenic architecture is intact. The expansion of PD-1^{HI} T_{FH} seems to be proportional to the infectious dose, since infection with higher dose of *S. enterica* leads to greater PD-1^{LO} T_{FH} expansion than in the low dose or HK bacteria immunisation. Concluding further, the PD-1^{LO} T_{FH} population found in the early stages of immune response to *S. enterica* is not able to support GC formation in this model.

3.2.4 PD-1^{HI} and PD-$1^{LO}$$T_{FH}$ populations display different levels of TFs Bcl6, Blimp1, Ascl2 and Foxp3.

So far the presence of T_{FH} populations expressing high or low levels of the PD-1 protein on the cell surface has been established in *S. enterica* and SRBC models. It was further important to establish whether other proteins associated with the T_{FH} function were differentially expressed between the PD-1^{HI} T_{FH} and PD-1^{LO} T_{FH} populations. To investigate the levels of the relevant cell surface and intracellular markers T_{FH} profiling by flow cytometry and qPCR based on the published T_{FH} studies was carried out.

Firstly, the levels of TFs important for the T_{FH} lineage were measured by qPCR on sorted T_{FH} populations isolated on day 6 p.i. with SRBC or *S. enterica* (sorting strategy is described in Material and Methods chapter on p. 52.) In the SRBC model, message levels of the Bcl6 TF, recognised as a master regulator of the T_{FH} lineage (Introduction p. 21), has been found highly expressed in PD-1^{HI} T_{FH} (Fig. 3.4A, left) and to a lesser extent in the PD-1^{LO} T_{FH} subset. In *S. enterica* infection PD-1^{LO} T_{FH} expressed significantly more Bcl6 mRNA than $CXCR5^{-}$ T cells (Fig. 3.4A, left). The frequency of PD-1^{HI} T_{FH} cells found in the *S. enterica* model was too low to allow for cell isolation and RNA extraction.

Taking advantage of the fact that the flow cytometry enables analysis of protein levels in cells found also at very low frequencies, a time course analysis of Bcl6 protein expression was carried out in the first two weeks of the response to SRBC

and *S. enterica* (Fig. 3.4B). In both models PD-1^{HI} T_{FH} showed much higher Bcl6 expression than PD-1^{LO} T_{FH} and, interestingly, these differences in expression levels were clear already at the early stage of the response (day 3 p.i.). Intriguingly, at day 3 p.i. PD-1^{HI} T_{FH} from *S. enterica* infection express just as much Bcl6 protein as PD-1^{HI} T_{FH} from SRBC. However, on day 5-6 p.i. there is no difference in protein levels between PD-1^{HI} T_{FH} and PD-1^{LO} T_{FH} in the *S. enterica* model (Fig. 3.4B, right). In contrast to that finding, PD-1^{HI} T_{FH} from the SRBC model further increased their expression of Bcl6 from day 3 p.i. and at day 6 p.i. have around twice as much protein as PD-1^{LO} T_{FH} from the same model (Fig. 3.4B, right). The peak of the Bcl6 expression for all analysed populations was observed around day 7 p.i. Importantly, both T_{FH} populations (PD-1^{HI} T_{FH} and PD-1^{LO} T_{FH}) expressed more Bcl6 protein than CXCR5$^-$ T cells and naive T cells (CD62L$^+$ CD44$^-$, graphed as day 0), and this is true for both investigated models. CXCR5$^-$ cells from both models show consistently low levels of Bcl6 throughout the response, comparable to the levels of naïve T cells (day 0).

Blimp1 (B lymphocyte-induced maturation protein 1), the antagonist TF of Bcl6, was described to have a reciprocal expression pattern in the T_{FH} population and the effector cell populations, with T_{FR} being the only T cell subset expressing significant levels of both proteins at the same time (134). Since reliable flow cytometry staining for Blimp1 protein was not available at the time the experiment was carried out, qPCR analysis of sorted populations isolated at day 6 p.i. was used to asses the level of the transcript *Prdm1*, encoding for the protein Blimp1. In keeping with other studies, the population with the highest expression of Bcl6 mRNA and protein (PD-1^{HI} T_{FH} from SRBC) had the lowest expression of *Prdm1* mRNA (Fig. 3.4A, centre) and vice versa. CXCR5$^-$ cells from both models, being poor in Bcl6 expression, show abundant message for the Blimp1 protein (Fig. 3.4A, centre).

The Ascl2 (Achaete-scute complex homolog 2, Drosophila) TF has recently been identified in T_{FH} as an important protein in driving CXCR5 expression (Introduction p. 23, (99)) and therefore it was expected to be found most abundantly in CXCR5 positive populations. Levels of Ascl2 mRNA were assessed by qPCR on day 6 p.i. due to lack of reagents for flow cytometry. Indeed, the PD-1^{HI} T_{FH} from SRBC

model showed by far the highest expression of *Ascl2* mRNA. Interestingly, PD-1^{LO} T_{FH} populations (which are CXCR5 positive) from both the SRBC and *S. enterica* model expressed comparable levels of *Ascl2* mRNA to $CXCR5^-$ T cells isolated from both models (Fig. 3.4A, right).

One possible functional difference between the PD-1^{HI} T_{FH} and PD-1^{LO} T_{FH} subsets from both models could be that one of the populations consists of T_{FR} cells (discussed on p. 31), which express significant amounts of both Bcl6 and Foxp3 TFs. The expression of the latter protein was assessed by flow cytometry. Since there is a clear dichotomy in Foxp3 expression ($Foxp3^+$ and $Foxp3^-$ cells can be clearly identified on the histogram), the frequency of Foxp3 positive cells was calculated for each T_{FH} subset to address the question about the quantity of T_{FR} in each T_{FH} population. In the SRBC model, the highest frequency of $Fopx3^+$ cells was found among $CXCR5^-$ cells from day 5 onwards (Fig. 3.5 C, % of $Foxp3^+$ cells within $CD4^+$ T cells at day 6: 26.23±0.85). These are most likely 'classical' regulatory T cells, since they express Blimp1 transcript (*Prdm1*, Fig. 3.4A, centre) and neither Bcl6 transcript nor protein (Fig. 3.4A, left and 3.4B). PD-1^{HI} T_{FH} and PD-1^{LO} T_{FH} populations from SRBC show a comparable, lower frequency of $Foxp3^+$ cells (Fig. 3.5C.; % of $Foxp3^+$ cells within $CD4^+$ T cells at day 6: 5.81±0.74 for PD-1^{HI} T_{FH} and 5.34±0.58 for PD-1^{LO} T_{FH}). This frequency is not significantly higher than the incidence observed for the naïve T cells ($CD62L^+$ $CD44^-$, graphed as day 0, % of $Foxp3^+$ cells within $CD4^+$ T cells 5.26±0.45).

Importantly, the analysis of the Foxp3 expression in the populations raised in the *S. enterica* model revealed that the highest frequency of $Foxp^+$ cells (42.8±7.1%) is found among PD-1^{HI} T_{FH}, suggesting their role as T_{FR} subset (Fig. 3.4C). PD-1^{LO} T_{FH} from *S. enterica* showed much lower frequency of Foxp3 epositive cells (comparable to T_{FH} populations from SRBC model and naïve T cells, Fig. 3.4C; 6.4 ± 0.52% of $CD4^+$ T cells). $CXCR5^-$ T cells showed slightly higher proportion of $Foxp3^+$ T cells than PD-1^{LO} T_{FH} and naïve T cells (14.87 ± 1.00%), although this differences was not statistically significant. Since the Foxp3 function depends not only on the frequency of $Foxp3^+$ cells but also on the levels of the Foxp3

protein expressed in the cells (quantity versus quality), the geometrical MFI of the Foxp3 protein was analysed for all $Foxp3^+$ populations.

Summing up the TF expression analysis, PD-1^{HI} T_{FH} from SRBC resemble the classic, GC associated T_{FH} population as described in the literature in terms of their high expression of Bcl6 and Ascl2 and low expression of Blimp1 mRNA levels (77,84,99). In the SRBC model T_{FR} cells are restricted neither to the PD-1^{HI} T_{FH} nor the PD-1^{LO} T_{FH} population and are found most abundantly among $CXCR5^-$ T cells. In contrast to that, PD-1^{HI} T_{FH} from the *S. enterica* model seem to represent the T_{FR} population, since they express high levels of Bcl6 and 40% of cells express also the Foxp3 TF. PD-1^{LO} T_{FH} from both models seem to be intermediate populations in terms of their Bcl6 protein and *Prdm1* mRNA expression. This analysis further enforces the idea of heterogeneity within the T_{FH} population beyond the surface expression of the PD-1 protein.

3.2.5 The analysis of IL-7Rα expressed by T_{FH} subsets points to PD-1^{HI} T_{FH} as GC associated population.

Certain cytokine receptors are important for T_{FH} development and their surface expression distinguishes T_{FH} from other effector cell subsets. I have, therefore, investigated the expression of relevant cytokine receptors markers by flow cytometry and qPCR.

IL-7Rα (CD127) is a member of a common γ-chain family of cytokine receptors. It is highly expressed on the naïve T cells and becomes subsequently down regulated upon T cell activation (186,187). IL-7 signalling was also shown to drive homeostatic T cell expansion in lymphopenic conditions (188). Most importantly, low IL-7Rα expression was associated with GC-associated populations of T_{FH} (78,144). To determine further whether any of the PD-1^{HI} T_{FH} or PD-1^{LO} T_{FH} subsets resemble the reported GC supporting population I have investigated the expression of IL-7Rα by analysis of *Il7r* mRNA by qPCR and the cell surface protein by flow cytometry. Two methods were chosen to assess the IL-7Rα expression since all of the investigated populations (T_{FH} cells and $CXCR5^-$ T cells from both model) are activated T cells and the levels of IL-7Rα are consequently expected to be very low.

PD-1^{HI} T_{FH}, PD-1^{LO} T_{FH} and $CXCR5^-$ T cells were isolated by fluorescence activated cell sorting at day 6 p.i. with SRBC or *S. enterica*. The qPCR analysis of mRNA levels for *Il7r* gene showed that PD-1^{HI} T_{FH} from SRBC model express the lowest amounts of *Il7r* mRNA (significantly less than $CXCR5^-$ T cells from the same model, Fig. 3.5A, left), while PD-1^{LO} T_{FH} populations from both *S. enterica* infection and SRBC immunization show comparable levels of mRNA to the $CXCR5^-$ T cell populations from the same models (Fig3.5A, left).

The flow cytometry analysis confirmed that PD-1^{HI} T_{FH} at day 6 p.i. with SRBC or *S. enterica* infection have the lowest amount of IL-7Rα on the cell surface (Fig. 3.5A, right), which is in agreement with detected mRNA levels for *Il7r*. $CXCR5^-$ T cells from both models expressed the highest amounts of the IL-7Rα protein and PD-1^{LO} T_{FH} were found to be intermediate in IL-7Rα (Fig.3.5A, right).

Another cytokine receptor implicated in T_{FH} development and function is IL-2Rα (CD25, Introduction p. 26). It has been found to be expressed preferentially by non-T_{FH} populations and only in low amounts on the T_{FH} cell surface (75). STAT5, the downstream signalling pathway of IL-2Rα, was shown to inhibit the commitment to the T_{FH} pool (109,110). Therefore it was important to determine whether there is a differential expression of IL-2Rα between PD-1^{HI} T_{FH} and PD-1^{LO} T_{FH}, as this could provide an insight into developmental pathways taken by each subset.

In agreement with other studies (109,110), IL-2Rα expression was the highest for $CXCR5^-$ T populations in both *S. enterica* and SRBC model at day 6 p.i. (Fig. 3.5B, right). Furthermore, all of the T_{FH} populations had lower IL-2Rα expression than the $CXCR5^-$ T cells from their models (Fig. 3.5B, right). However, no significant differences between PD-1^{HI} T_{FH} and PD-1^{LO} T_{FH} were found in either the SRBC or *S. enterica* model at day 6 p.i. (Fig. 3.5B, right). The time course analysis of the cell surface IL-2Rα levels (Fig. 3.5B, left) revealed similar expression kinetics in both models. Slight initial up regulation of IL-2Rα (with respect to naïve T cells, graphed as day 0) was observed on day 3 p.i. in all populations. Interestingly, a clear distinction between IL-2Rα high and low populations in both models was visible by

day 5-6 p.i. From day 7 onwards the levels of IL-2Rα expression seem to be stabilised (Fig.3.5B, left).

The results obtained from the analysis of IL-7Rα and IL-2Rα cytokine receptors suggested that: 1) PD-1^{HI} T_{FH} are indeed a GC-associated population (low IL-7Rα expression, as reported in the literature); 2) PD-1^{HI} T_{FH} and PD-1^{LO} T_{FH} might follow similar developmental pathways, which are different from the one of $CXCR5^-$ T cells (no differences in IL-2Rα expression between PD-1^{HI} T_{FH} and PD-1^{LO} T_{FH}, with both populations expressing less IL-2Rα than $CXCR5^-$ T cells). Thus, further important phenotypical differences between PD-1^{HI} T_{FH} and PD-1^{LO} T_{FH}, and first clues about the development pathways of the subsets were established.

3.2.6 Expression of *Ccr7*, PSGL-1 and CD62L suggests differences in positioning and homing potential between PD-1^{HI} and PD-1^{LO} T_{FH} subsets.

Spleen and lymph nodes are highly organised structures with a clear segregation of T cells and B cells into discrete zones (Introduction p. 2). Since the movement of T cells and subsequent T-B cell interaction are important for differentiating into T_{FH} or T effector cells, several proteins that play a role in lymphocyte positioning in SLO were investigated.

CCR7 is recognised as a T cell retention signal (189). It binds CCL19 and CCL21, produced by fibroblastic reticular cells (190). The pattern of expression is reciprocal with CXCR5, with B cell areas high in CXCR5 and low in CCR7, and naïve T cells showing the opposite expression pattern (Introduction p. 2). Expression of *Ccr7* mRNA was carried out by qPCR on FACS sorted T_{FH} populations since protein staining for the protein proved to be technically difficult despite several attempts.

In agreement with published studies (183,184,191) in the SRBC model PD-1^{HI} T_{FH} express significantly less *Ccr7* mRNA than PD-1^{LO} T_{FH} and $CXCR5^-$ T cells (Fig. 3.6A). Interestingly, PD-1^{LO} T_{FH} were found to be equally rich in the message for *Ccr7* as $CXCR5^-$ T cells, suggesting that PD-1^{LO} T_{FH} co-express CCR7 and CXCR5 at the same time.

In the *S. enterica* model PD-1^{LO} T_{FH} and $CXCR5^-$ T cells express similar, low amounts of *Ccr7* mRNA (no statistically significant difference, Fig. 3.6A). Therefore, similarly to the situation observed in the SRBC model, the PD-1^{LO} T_{FH} seem to co-express CXCR5 and CCR7. Of note, naïve T cells show the highest *Ccr7* mRNA levels (scale of relative mRNA levels is below 1 as it was normalised to naïve T cells levels using delta delta method.).

Another T cell retention signal binding CCL21 and CCL19 is CD162 (P selectin glycoprotein ligand 1 [PSGL-1], (192)). Down regulation of PSGL-1 on T_{FH} cells was reported to be essential for T_{FH} migration to the follicles as well as GC (58,79). Analysing the expression of PSGL-1 was, therefore, important to obtain information about the positioning of the investigated T_{FH} subsets. In agreement with the literature, the highest expression of PSGL-1 was found on the naïve T cells (Fig. 3.6.B, left, graphed as day 0). By day 3 down regulation of PSGL-1 was observed on PD-1^{HI} T_{FH}, PD-1^{LO} T_{FH} and $CXCR5^-$ T cells from both the SRBC and *S. enterica* model (Fig. 3.6.B, left). Interestingly, $CXCR5^-$ T cells formed in *S. enterica* infection are the only population which regained and stabilised high PSGL-1 expression from day 5 onwards, comparable to the levels found on the naïve T cells. Around day 6 (Fig. 3.6 B, left) levels of PSGL-1 seem to stabilise for all populations. Importantly, PD-1^{HI} T_{FH} show significantly less surface levels of PSGL-1 than PD-1^{LO} T_{FH} and $CXCR5^-$ T cells at day 6 p.i. and this is true for both models (Fig. 3.6.B,right). Low PSGL-1 expression on PD-1^{HI} T_{FH} is in agreement with other studies characterising GC T_{FH} populations (58,79,87).

As well as considering the positioning within the SLO, entry to or exit from these structures is important in T cell migration. CD62L is a key protein involved in homing to lymph nodes as it mediates the lymphocytes' entry via HEV (193,194). The highest expression is confined to naïve T cells and T cell activation results in CD62L down regulation by active shedding of CD62L from the cell surface (195).

Analysis of the CD62L protein expression by flow cytometry showed that in the SRBC model, the PD-1^{HI} T_{FH} population expressed very low amounts of CD62L at day 6 p.i. (Fig. 3.6.C, right) and this is in striking contrast to PD-1^{LO} T_{FH} and $CXCR5^-$ T cells, which have high cell surface levels of CD62L (Fig. 3.6.C, right).

PD-1^{LO} T_{FH} from the SRBC immunisation can be described as CD62L intermediate population, showing at day 6 p.i. significantly less CD62L than $CXCR5^-$ T cells and more than PD-1^{HI} T_{FH} (Fig. 3.6.C, right). In the *S. enterica* model the expression of CD62L seems to be generally much weaker than in the SRBC model (Fig. 3.6.C). This might reflect a higher T cell activation status in the immunization with an actively replicating pathogen. Importantly, also in the *S. enterica* model at day 6 p.i. PD-1^{HI} T_{FH} had significantly less CD62L on their surface than $CXCR5^-$T cells (Fig. 3.6.C, right). PD-1^{LO} T_{FH} cells, similarly to the SRBC model, show intermediate levels of CD62L expression (Fig. 3.6.C, right).

The time course analysis of the CD62L expression in the SRBC system (Fig. 3.6.C, left) revealed that PD-1^{HI} T_{FH} become a CD62L low population already on day 3 and then further steadily down regulate CD62L over time. PD-1^{LO} T_{FH} and $CXCR5^-$ T cells from the same model showed consistently higher CD62L levels than PD-1^{HI} T_{FH}. In the *S. enterica* model PD-1^{HI} T_{FH}, PD-1^{LO} T_{FH} and $CXCR5^-$ T cells consistently express low levels of CD62L.

Overall, the expression pattern of CD62L indicates that whereas $CXCR5^-$ T cells and PD-1^{LO} T_{FH} cells generated after SRBC immunisation can easily enter the lymph node from the circulation (due to high levels of CD62L on the cell surface), PD-1^{HI} T_{FH} cells are far less likely to access the lymph nodes due to strong down regulation of CD62L. This is also true in the *S. enterica* model, albeit the differences between the $CXCR5^-$ T cells, PD-1^{LO} T_{FH} cells and PD-1^{HI} T_{FH} cells are of lower magnitude.

Summing up the results of analysis of the proteins involved in T cell migration, PD-1^{HI} T_{FH}, PD-1^{LO} T_{FH} subsets and $CXCR5^-$ T cell from both models of immunization displayed different expression patterns of *Ccr7* mRNA and CD62L and PSGL-1 protein. This analysis indicated that PD-1^{HI} T_{FH} cells from the SRBC model have unique positioning properties within the B cell follicle and are the GC-associated population, as described previously in literature (due to low expression of *Ccr7* mRNA and PSGL-1 protein). Furthermore, PD-1^{LO} T_{FH} and PD-1^{HI} T_{FH} populations showed different homing potential to the lymph nodes (measured by CD62L expression). Overall, the results further confirm the discrete natures of PD-

1^{HI} T_{FH} and PD-1^{LO} T_{FH} cells in terms of their localisation in the spleen and homing properties.

3.2.7 PD-1^{HI} and PD-1^{LO} T_{FH} populations show an early burst of proliferation with a further equal potential towards the terminal differentiation stage.

Investigating T_{FH} populations in terms of their phenotype by analysing expression of TFs, cytokine receptors and molecules involved in positioning provided an important insight into the T_{FH} heterogeneity. One of the main questions that still remained to be answered is whether any of the T_{FH} subsets has reached the stage of terminal differentiation, characterized by a decreased potential to proliferate. This property of the cell can be assessed with flow cytometry by staining for the Ki67 protein. Ki67 is a nuclear protein essential for rRNA synthesis (196). It is expressed in the cells that undergo active proliferation in the cell cycle (late G1, S, G2 and M phase of the cell cycle) and is absent in the stationary (G0) phase of the cycle (197,198). I, therefore, investigated Ki67 expression in T_{FH} populations to determine whether there are differences in the proliferative activity in each of the cell subsets, which would indicate their developmental stage in terms of terminal differentiation.

In the SRBC model (Fig. 3.7A) an early proliferative burst can be observed at day 3 p.i. for all of the investigated populations (PD-1^{HI} T_{FH}, PD-1^{LO} T_{FH} and $CXCR5^-$ T cells), with PD-1^{HI} T_{FH} being the brightest in the Ki67 staining (Fig. 3.7C). On day 5 p.i. all of the groups slow down in the proliferation cycle and by day 6 there are no significant differences between the investigated T_{FH} and $CXCR5^-$ T cell groups (Fig. 3.7C, right). From day 7 p.i. in all populations analysed in the SRBC model the potential for proliferation decreases and remains stable until day 15 p.i. (Fig. 3.7A).

In *S. enterica* infection (Fig. 3.7.B) PD-1^{LO} T_{FH} show a significant increase in proliferation compared to PD-1^{HI} T_{FH} and $CXCR5^-$ T cells at day 3 p.i. (Fig. 3.7D, left). All three populations (PD-1^{HI} T_{FH}, PD-1^{LO} T_{FH} and $CXCR5^-$ T cells) display their peak of proliferation around day 5-6 p.i. Similarly to the SRBC model, there are no significant differences between the groups at day 6 p.i. (Fig. 3.7D, right). From day 9 p.i. onwards proliferation was stabilised in all analysed subsets, with PD-1^{HI} T_{FH} expressing slightly more Ki67 than PD-1^{LO} T_{FH} and $CXCR5^-$ T cells (Fig. 3.7B).

Summing up, in both models there is an initial peak of T cell proliferation, followed by a contraction phase and a stable Ki67 expression from around day 7 onwards. Interestingly, at day 3 p.i. with SRBC PD-1^{HI} T_{FH} were the only population displaying a significant proliferative burst in contrast to PD-1^{LO} T_{FH} and $CXCR5^-$ T cells, whereas in the *S. enterica* model PD-1^{LO} T_{FH} proliferated the most. Additionally, the proliferation peak is observed at day 3 p.i with SRBC, and is slightly delayed in the *S. enterica* model, where it occurs at day 5. This data shows that although there is an early peak of expansion in certain T_{FH} populations (PD-1^{HI} T_{FH} for SRBC and PD-1^{LO} T_{FH} for *S. enterica* model) at later time points there are no significant differences in proliferation (as measured by Ki67 staining) and, therefore, no strong conclusions can be drawn with respect to the differentiation stage of any of the populations.

3.2.8 Principal component analysis of the T_{FH} populations reveals the discreet nature of isolated cell subsets.

So far the investigation of the T_{FH} populations involved the analysis of individual proteins based on current knowledge. This approach, although very useful, is biased (by focusing mainly on the known candidate proteins only) and limited by the availability of reagents, funds and time. One of the approaches that offer an unbiased and unlimited insight into the transcriptional activity of the cell are microarrays. This technology provides information about all genes that are actively transcribed in the cell. Combining it with bioinformatics and statistical analysis enables to build a general overview of the relationship between the cell populations as well as to identify uniquely expressed transcripts for further investigation.

In order to perform the microarray analysis of T_{FH} subsets extensive fluorescence activated cell sorting was carried out on spleen cell suspensions 6 days p.i. with SRBC or *S. enterica*. RNA was further extracted from the sorted cell populations and subjected to microarray analysis (described in Materials and Methods chapter on p.54). Various types of data analysis and representation were performed to illustrate the relationship between the T_{FH} subsets. The overview of the cell sorting, RNA processing and microarray analysis is illustrated in Fig. 3.8.

Principal component analysis (PCA) was used to investigate the relationship between the samples based on differential gene expression. It works by employing a mathematical algorithm to remove the redundancy within the data (199). Plotted on a 2d or 3d axis, the artificial dimension (called principal component), which represents maximal variation of the data, is graphed on each axis (199). In other words, PCA reduces dimensionality of the dataset by re-aligning the dimensions of the dataset to maximise the variability that can be plotted on a minimal set of axes. This is a very powerful, unbiased approach, which allows very quickly an assessment and visualization of the general relationship between the samples and the experimental groups. Samples with the most similar gene expression pattern are positioned closely together. PCA therefore serves as an important quality control, since replicates form the same group should always cluster close to each other.

PCA was performed on the T_{FH} microarray data by selecting all 3726 differentially expressed genes (regardless of fold change and with adj. P value < 0.001). Importantly, all the samples isolated from the same experimental group (biological replicates) form tight clusters (Fig. 3.9), which confirms the high technical quality of the array. The analysis of the positioning of discrete experimental groups shows clearly that naïve T cells sorted from non-immunised mice are the most isolated cluster with the greatest distance to all other groups, which are activated T cells (Fig. 3.9). Fascinatingly, PD-1^{LO} T_{FH} from the *S. enterica* model are positioned most closely to PD-1^{HI} T_{FH} from SRBC model, which suggest general similarities in gene expression. It would be interesting to see the positioning of PD-1^{HI} T_{FH} from *S. enterica* on this diagram. Unfortunately, this was not possible due to the very low frequency of these cells. Intriguingly, PD-1^{HI} T_{FH} and PD-1^{LO} T_{FH} from SRBC model, even though positioned closely to each other, form discrete clusters, indicating that these cell subsets are indeed separate populations.

It is important to bear in mind that the PCA discussed above was performed on all the differentially expressed transcripts, which would include genes involved in metabolism, proliferation, apoptosis, biogenesis etc. It is therefore essential to assess whether the observed patterns of relationships could also be applied to immunologically relevant pathways.

3.2.9 The T_{FH} character of the isolated populations is reflected on the transcriptional level

The next step in the microarray analysis was to confirm the character of the isolated populations based on current knowledge. That is, to confirm that T cells with surface expression of CXCR5 and PD-1 express the transcripts assigned to previously isolated and analysed T_{FH} populations described in literature.

The expression of 30 genes previously analysed in T_{FH} populations is presented in the form of a heatmap (Fig. 3.10). Yellow to red colour indicates up regulation of the gene and blue colour depicts down-regulation of the transcript (with respect to various house keeping genes). The dendrogram presented at the top of the heatmap shows the relationship between isolated groups. This graphical form of hierarchical clustering works by finding and placing next to each other the most similar pairs of samples, then adding the second similar one and so on until all the features are bound together (200). Once again, biological replicates cluster together, which confirms the high quality and relevance of the microarray (Fig. 3.10). Starting from the right-hand side, $CXCR5^-$ T cells from the SRBC model are most closely related to $PD\text{-}1^{LO}$ T_{FH} from SRBC. Then, surprisingly, $PD\text{-}1^{LO}$ T_{FH} and $CXCR5^-$ cells from *S. enterica* infection come out as the ones with most similar gene expression patterns. Strikingly, $PD\text{-}1^{HI}$ T_{FH} are positioned the furthest to the left and, therefore, are the group with the most unique gene expression pattern. Unexpectedly, even naïve T cells cluster first with other activated groups rather than with $PD\text{-}1^{HI}$ T_{FH}. This further confirms that $PD\text{-}1^{HI}$ T_{FH} are the most discrete subset.

The surface phenotype of the isolated T_{FH} populations (expression of CXCR5 and PD-1 proteins) is clearly reflected in the amount of the transcript present in the cells (Fig. 3.10). CXCR5 positive populations from the SRBC and the *S. enterica* model show higher expression of CXCR5 mRNA than $CXCR5^-$ T cells. The same pattern of expression is observed in PD-1: $PD\text{-}1^{HI}$ T_{FH} from SRBC have the highest PD-1 transcript levels *(Pdcd1)*. $PD\text{-}1^{LO}$ T_{FH} from both the SRBC and the *S. enterica* model show the same PD-1 message expression as $CXCR5^-$ and are comparable to each other. Importantly, levels of mRNA of both PD-1 and CXCR5 are higher than in naïve T cells. Notably, high levels of expression of the master T_{FH} TF, Bcl-6, in PD-

1^{HI} T_{FH} and PD-1^{LO} T_{FH} from both models confirms the T_{FH} 'identity' of these subsets (since they express more mRNA than $CXCR5^-$ T cells from the same models). With regard to IL-21, a 'signature' cytokine of T_{FH}, PD-1^{HI} T_{FH} from SRBC model produce the highest amount of the transcript, although all of the activated T cell groups (PD-1^{LO} T_{FH} and $CXCR5^-$ T cell populations) seem to express more *Il21* mRNA than naïve T cells. Moreover, a brief look at expression of the transcripts associated with Th1 and Th2 response (*Ifng* and *Tbx* for Th1 response and *Il4* and *Gata3* for Th2 response) confirms the expected character of the response for *S. enterica* and SRBC models (Th1 and Th2, respectively). Overall, this gives confidence in the nature of the isolated material and confirms that the surface phenotype selected for the separation of the cells is reflected on the transcriptional level.

Finally, PD-1^{HI} T_{FH} are the only population which shows the hallmark T_{FH} profile (as described in literature) by low expression of *Ccr7, Il7r, Il2ra, Cd160, Slamf1* and high levels of transcripts *Bcl6, Il21, Ascl2, Btla, Cd81* and *Sh2d1a* (Fig. 3.10). This raises the intriguing question of the function and identity of isolated PD-1^{LO} T_{FH} cell populations.

Summing up, both graphs (Fig. 3.9 and 3.10) provide an interesting insight into the heterogeneity within isolated T_{FH} populations. Importantly, the two pieces of analysis presented (PCA of all differentially expressed genes and heatmap presenting expression of T_{FH}-related transcripts) suggest that PD-1^{HI} T_{FH} and PD-1^{LO} T_{FH} from SRBC model are indeed separate cell subsets.

Overall, PCA of immunologically relevant pathways emphasises discreet nature of the isolated cell subsets. Thus, combining an unbiased, global approach and literature-based selection of the relevant pathways provided more information on the relationship between the T_{FH} populations from the SRBC and *S. enterica* models.

3.2.10 Unique gene expression in T_{FH} populations points towards PD-1^{HI} T_{FH} as the most specialized cell subset.

One of the easiest ways of comparing differential gene expression between populations is by creating Venn diagrams. Venn diagrams are a simple graphical

output, illustrating shared and unique genes of the investigated cell subsets. The analysis of the genes that are differentially expressed by T_{FH} and CXCR5$^-$ cell populations from SRBC and *S. enterica* was carried out by selecting transcripts which fold change in expression are larger than two and for which the P value is lower than 0.001. Full lists of the differentially expressed genes can be found in an excel file on the CD.

In the *S. enterica* model (Fig. 3.11A) PD-1^{LO} T_{FH} have 1703 genes differentially expressed (up or down regulated) with respect to naïve T cells, whereas CXCR5$^-$ T cells have 2403 differentially expressed transcripts compared to naïve T cells. Both populations share changes in the expression of 1307 genes (Fig. 3.11A, full lists the differentially expressed genes can be found in an excel file on the CD). and this most likely reflects cell activation.

In the SRBC model PD-1^{HI} T_{FH}, PD-1^{LO} T_{FH} and CXCR5$^-$ T cells have an altered expression of 1296, 653 and 685 genes with respect to naïve T cells, respectively. The highest number of uniquely expressed genes was observed for PD-1^{HI} T_{FH} (599 genes) and the lowest for PD-1^{LO} T_{FH} (18 genes). There were 92 unique transcripts for CXCR5$^-$ T cells. A significant proportion of altered genes was shared between all populations (437 transcripts), comprising 33% of all differentially expressed genes in PD-1^{HI} T_{FH}, 67% for PD-1^{LO} T_{FH} and 64% for CXCR5$^-$ T cells, which reflects the activation status of all cell populations. In striking contrast to the very high number of unique genes for PD-1^{HI} T_{FH} (nearly 600 genes), PD-1^{LO} T_{FH} altered exclusively expression of very few transcripts (less than 20 genes). This could be explained by the fact that PD-1^{HI} T_{FH} are the most specialised cell subset while PD-1^{LO} T_{FH} cells are at an earlier stage of the differentiation, or that there are few PD-1^{HI} T_{FH} precursors embedded in the PD-1^{LO} T_{FH} population. The fact that PD-1^{LO} T_{FH} share more of the differentially expressed genes with PD-1^{HI} T_{FH} than with CXCR5$^-$ T cells (151 versus 109 genes, respectively) suggests a closer relationship to the former population (Fig. 3.11B). A full list of the differentially expressed genes can be found in an excel file on the CD.

The comparison of differential gene expression with respect to naïve T cells gives an idea of the overall changes in T cells due to cell activation and this is very useful

as a first line of analysis. However, it does not allow for a direct comparison of the T_{FH} populations. In order to do that another Venn diagram was created (Fig. 3.11C), where the number of unique genes in each of the T_{FH} population was determined by comparison to the CXCR5$^-$ T cells from the same model. This analysis removed genes that were commonly altered genes due to the cell activation and allowed for the extraction of the genes characteristic for each T_{FH} population. Surprisingly, there are very few genes (5) whose expression pattern is shared between all T_{FH} populations (PD-1^{HI} T_{FH} and PD-1^{LO} T_{FH} from the SRBC model and PD-1^{LO} T_{FH} from the *S. enterica* model). However, this can be attributed to the exceedingly different nature of the models. Interestingly, PD-1^{LO} T_{FH} generated during *S. enterica* infection share more transcripts with PD-1^{HI} T_{FH} from SRBC than PD-1^{LO} T_{FH} from SRBC model (Fig. 3.11C), despite being phenotypically more similar to the latter population (based on the surface expression of CXCR5 and PD-1). The vast majority of genes differentially expressed between each of the T_{FH} populations and CXCR5$^-$ T cells are unique for each T_{FH} cell subset (213 genes for PD-1^{HI} T_{FH} from SRBC model and 157 for PD-1^{LO} T_{FH} from *S. enterica* model). PD-1^{LO} T_{FH} raised in SRBC model showed very low numbers of genes differentially expressed with respect to CXCR5$^-$ T cells (only 9 genes). This supports the idea that PD-1^{LO} T_{FH} are a relatively 'young' cell subset that undergoing a process of differentiation, where switching on CXCR5 expression is a possible first step towards further specialisation. Therefore, most of the transcripts remain as yet unchanged with respect to CXCR5$^-$ population. Since sorted populations showed very high purity (Materials and Methods chapter, Fig. 2.1), the contamination of the sorted CXCR5$^+$ cells with the CXCR5$^-$ subset is a highly unlikely reason for the similar gene expression between these populations. Full lists of the differentially expressed genes can be found in an excel file on the CD.

3.2.11 PD-1^{HI} T_{FH} have an enhanced potential to interact with B cells

The main function of the T_{FH} population is associated with the formation and support of GC after physical interaction with B cells. Since the initial analysis of T_{FH}-related transcripts revealed that PD-1^{HI} T_{FH} are the subset resembling 'classical' T_{FH}, it is reasonable to speculate that PD-1^{HI} T_{FH} might also show higher expression of other molecules involved in T-B cell interactions. To investigate this aspect

microarray analysis was employed and the transcriptome of isolated T_{FH} populations was probed for the genes encoding proteins known to be important in T-B cell contacts.

For many proteins involved in direct T-B cell interaction increased message levels with respect to naïve $CD4^+$ T cells were detected in all experimental SRBC groups (PD-1^{HI} T_{FH}, PD-1^{LO} T_{FH} and $CXCR5^-$ cells, Fig. 3.12), such as most of the SLAM family members or SAP proteins (*Slamf1, 3-7* and *9*, *Sh2d1a*) and co-stimulatory or co-inhibitory receptors of the CD28 superfamily of molecules (*Icos*, *Cd28* and *Ctla4*). However, there was no significant change between T_{FH} populations and $CXCR5^-$ T cells in the expression of those transcripts, which suggests that none of the above proteins has a selective and exclusive role for the PD-1^{HI} T_{FH} population. On the other hand, genes encoding BTLA and CD81 proteins showed the same expression pattern as PD-1 (they cluster together on the heat map), with expression levels highest for PD-1^{HI} T_{FH} and lowest for $CXCR5^-$ T cells in SRBC (Fig. 3.12, framed fragments of the heat map). Similarly, CD30L transcript (*Tnfsf8)* showed also significantly higher expression for PD-1^{HI} T_{FH} than 2 other experimental SRBC groups (Fig. 3.12, framed fragments of the heat map). Fold changes and P values for the transcripts of interests are presented in Table 3.1. The functional importance of these molecules in the context of the T_{FH}-B cell dialogue is described in the Discussion part of this chapter.

In conclusion, the microarray analysis of the T_{FH} populations, PCA of significant differences in the gene expression between PD-1^{HI} $T_{FH,}$ PD-1^{LO} T_{FH} and $CXCR5^-$ T cells (including all altered genes as well as immunologically relevant pathways) further confirmed the discrete nature of the T_{FH} subsets with PD-1^{HI} T_{FH} resembling the most commonly studied T_{FH} population in the literature. Furthermore, the analysis of proteins involved in the T-B cell interaction identified three potential protein candidates whose mRNA is significantly increased in PD-1^{HI} T_{FH} with respect to PD-1^{LO} T_{FH} and $CXCR5^-$ T cells from the SRBC model.

3.2.12 Results summary

- SRBC response generates PD-1^{HI} and PD-1^{LO} T_{FH}, while the former population is missing after *S. enterica* infection (Fig. 3.1B, C and D).
- GC B cells are found abundantly after SRBC immunisation but not after *S. enterica* infection (Fig. 3.2B, C and D).
- Altered splenic structures do not hamper PD-1^{HI} T_{FH} and GC formation after *S. enterica* immunisation (Fig. 3.3D,E and G)
- PD-1^{HI} and PD-1^{LO} T_{FH} populations display different levels of the TFs Bcl6, Blimp1, Ascl2 and Foxp3 (Fig. 3.4A, B and C).
- Analysis of IL-7Rα expressed by T_{FH} subsets points to PD-1^{HI} T_{FH} as the GC-associated population (Fig. 3.5 A).
- Expression of Ccr7, PSGL-1 and CD62L suggests differences in positioning and homing potential between PD-1^{HI} and PD-1^{LO} T_{FH} subsets (Fig. 3.6).
- PD-1^{HI} and PD-1^{LO} T_{FH} populations show early bursts of proliferation with equal potential towards the terminal differentiation stage (Fig. 3.7).
- The T_{FH} phenotype of the isolated populations is reflected on the transcriptional level (Fig. 3.10 and 3.11A)
- Principal component analysis of all differentially expressed genes (Fig. 3.9) confirms the discreet nature of isolated T_{FH} populations.
- The PD-1^{HI} T_{FH} subset expresses the highest number of unique genes (Fig. 3.11C) and this points towards PD-1^{HI} T_{FH} as the most specialized cell subset.
- The PD-1^{HI} T_{FH} population has an enhanced potential for interacting with B cells by expressing BTLA, CD30L and CD81 (Fig. 3.12).

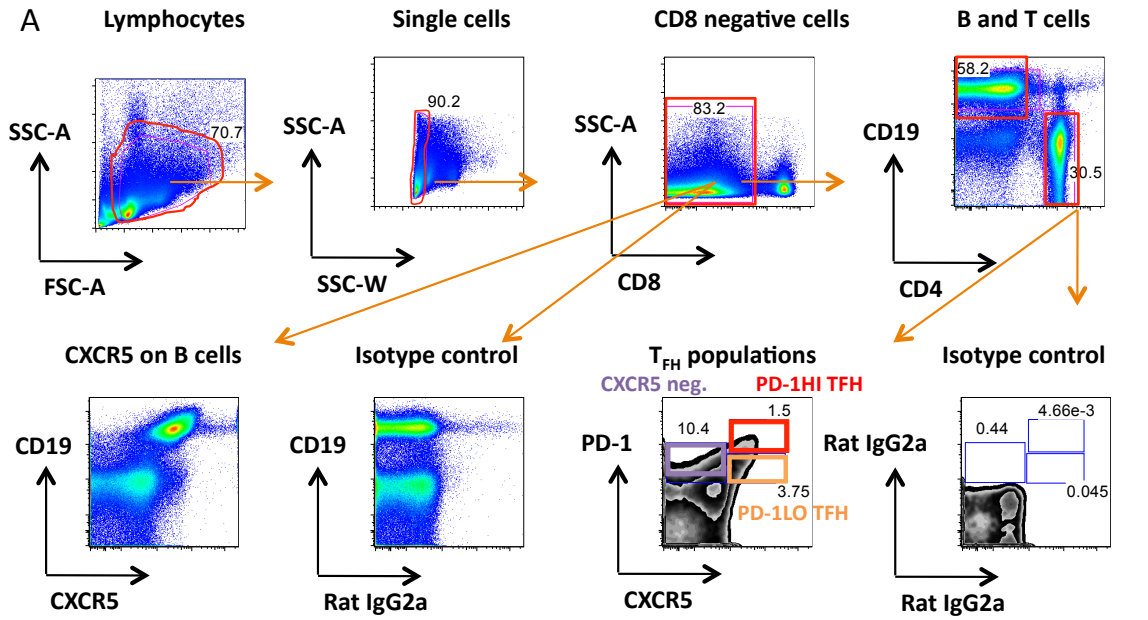

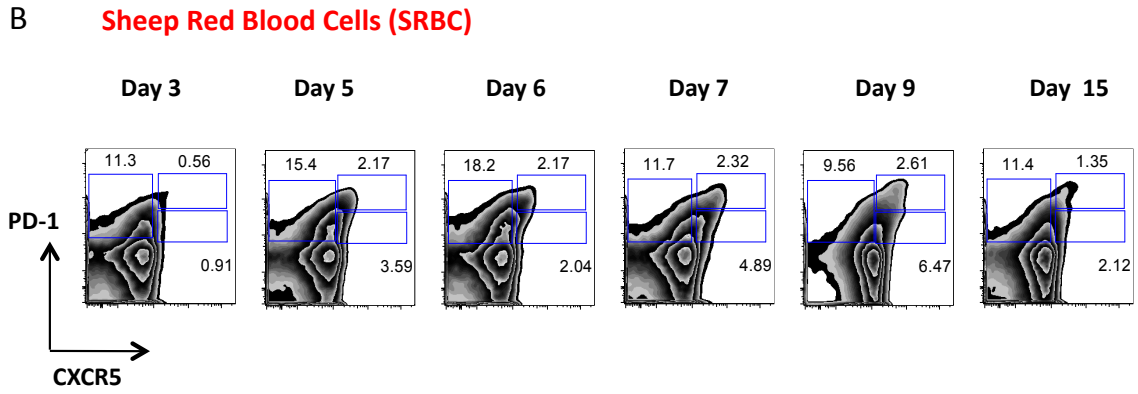

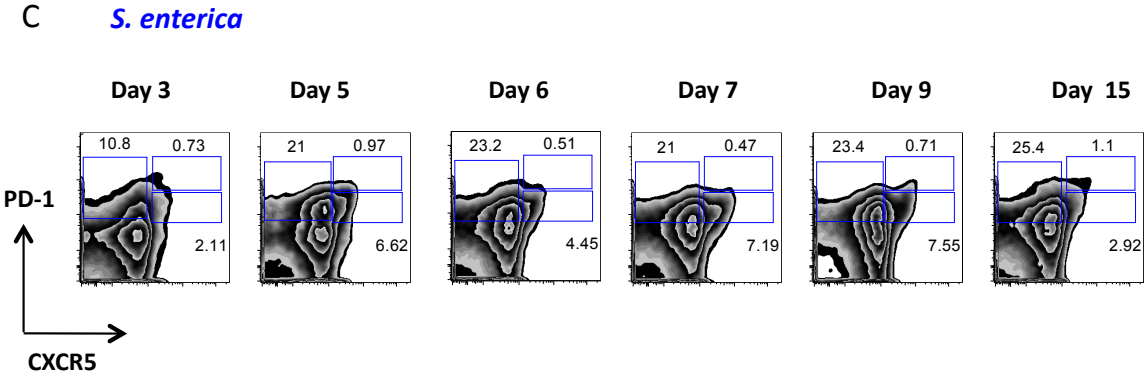

Fig 3.1. Continued overleaf.

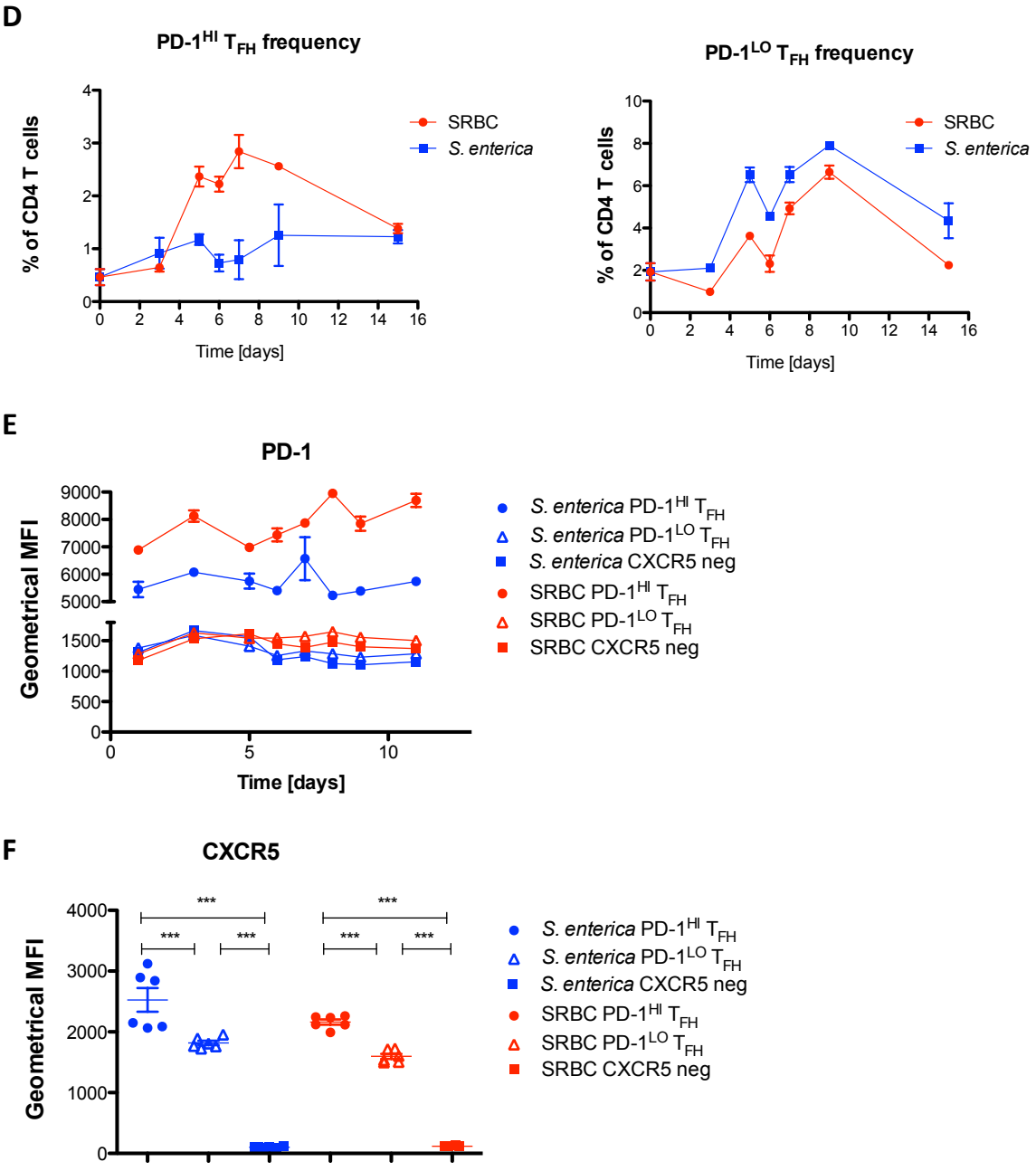

Fig 3.1. Induction of T_{FH} populations after immunisation with SRBC or *S. enterica* infection over time.

(A) Gating strategy for T_{FH} populations and positive control for CXCR5 staining alongside isotype controls (WT mouse on day 6 p.i with SRBC). **(B)** Representative flow cytometry plots of PD-1^{HI} T_{FH} and PD-1^{LO} T_{FH} $CD4^+$ T cell populations after SRBC immunisation (upper panel) or *S. enterica* infection (lower panel) over time. Summary of T_{FH} frequencies **(C)** or cell numbers **(D)** after SRBC immunisation (red) or *S. enterica* infection (blue) over time. Geometrical MFI of PD-1 **(E)** and CXCR5 proteins **(F)** measured by flow cytometry at day 6. p.i with SRBC or *S. enterica*.

Data arerepresentative of two independent experiments with similar results (A-E, n=3) or pulled results from two experiments (F, n=6). Three animals were used per each time point.

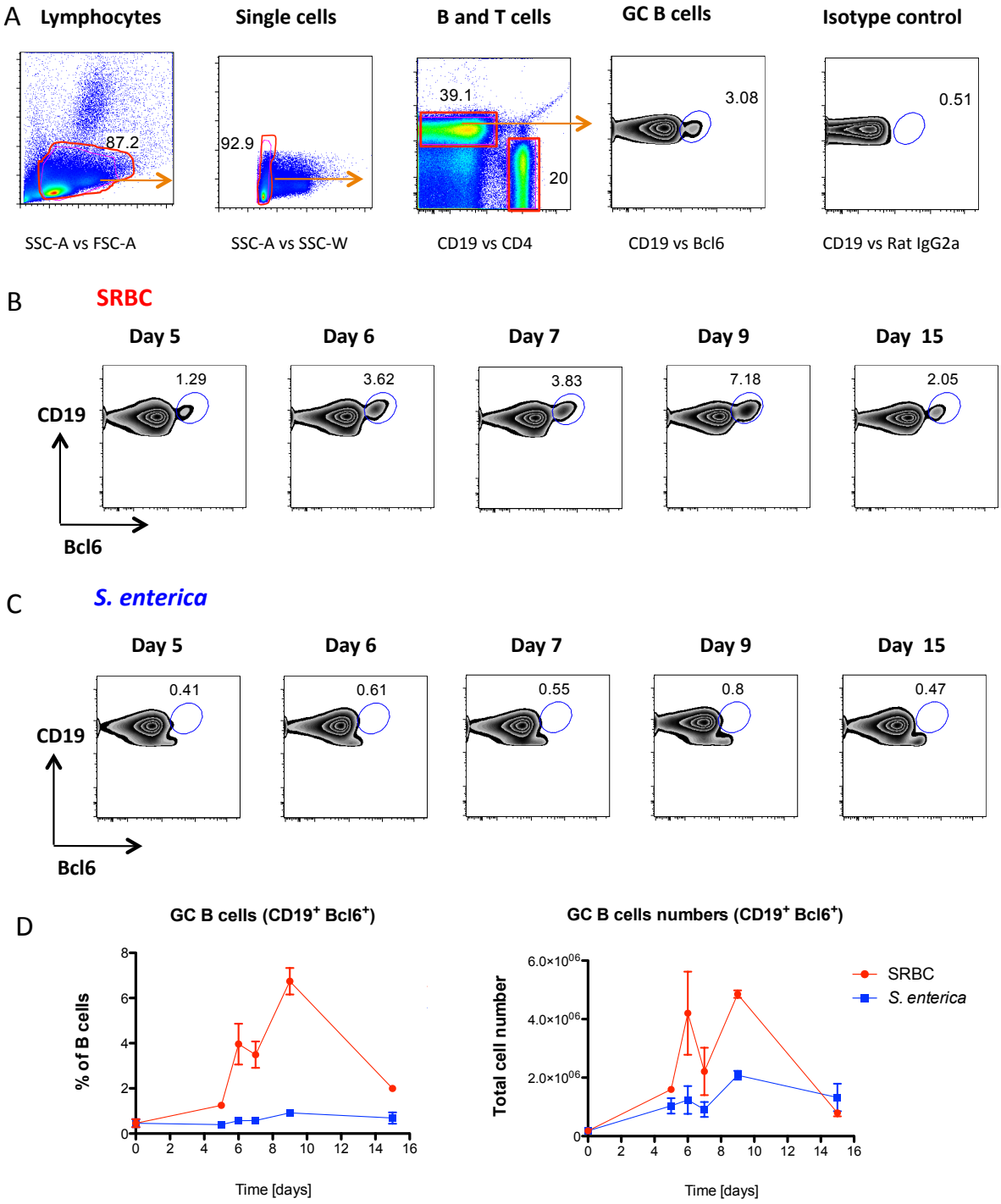

Fig 3.2. Induction of GC B cell population ($CD19^+$ $Bcl6^+$) after immunisation with SRBC or *S. enterica* infection over time.

(A) Gating strategy for GC B cells at day 6 p.i with SRBC. Representative flow cytometry plots of GC B cell populations after SRBC immunisation **(B)** or *S. enterica* infection **(C)** over time. **(D)** Summary of GC B cell frequencies (left) or cell numbers (right) after SRBC immunisation (red) or *S. enterica* infection (blue) over time.

(D) Data representative of one experiment with three animals (n=3) used per each time point.

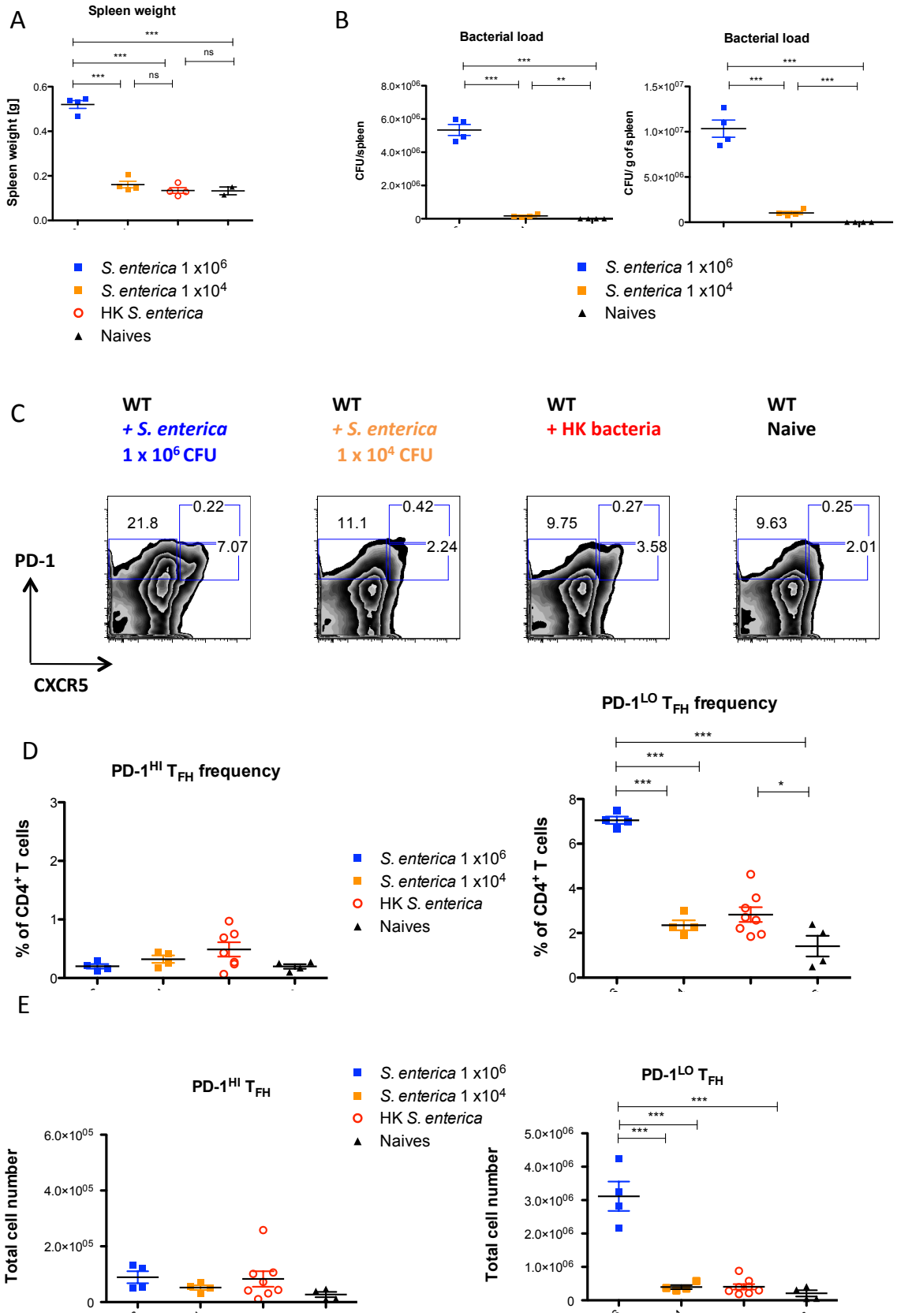

Fig 3.3. Continued overleaf.

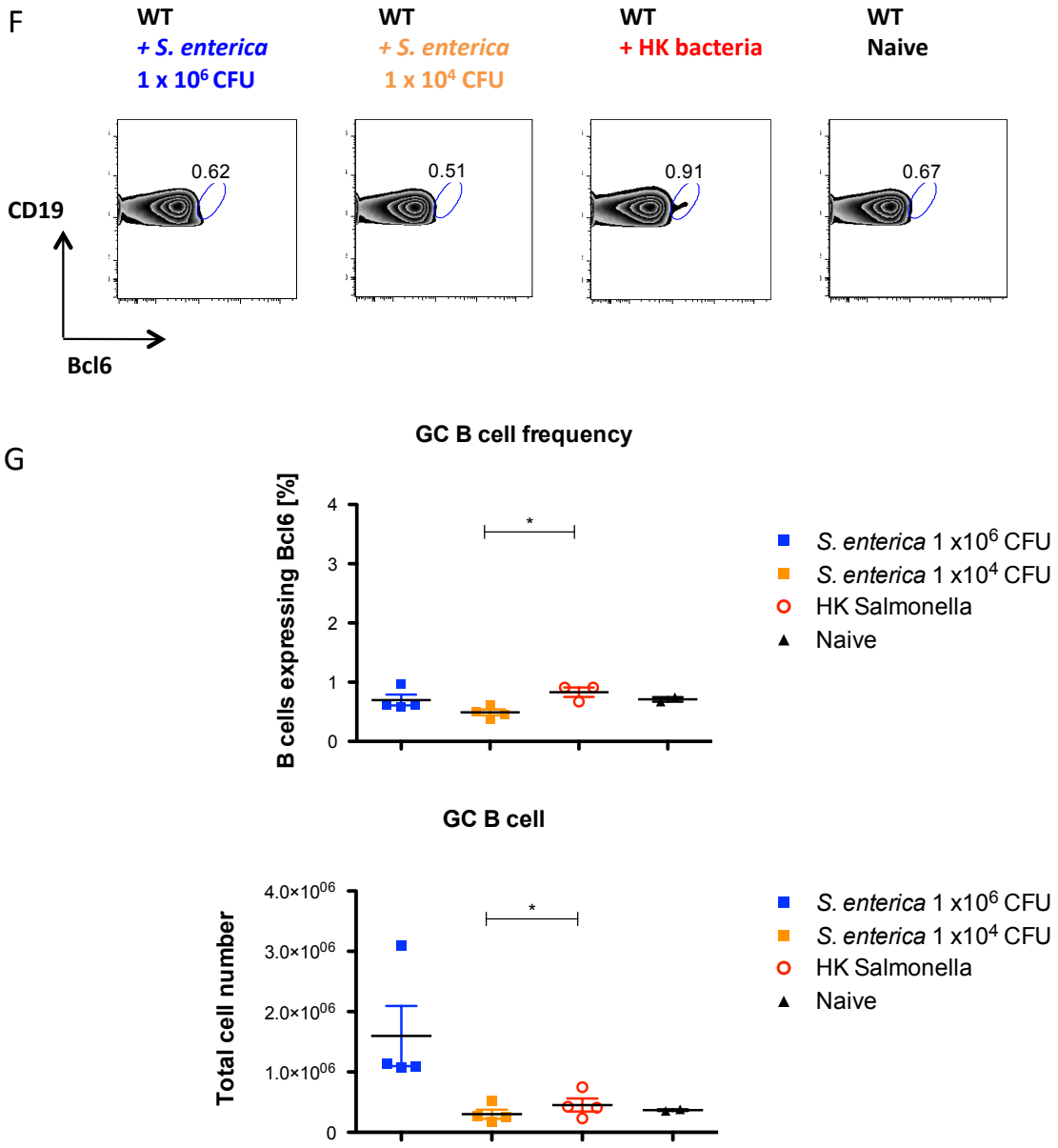

Fig 3.3. Influence of splenic architecture on PD-1^{HI} T_{FH} formation.

(A) Spleen weight of immunised animals as indicated on day 6 p.i **(B)** Bacterial load quantification expressed as number of colony forming units (CFU) per spleen (left side) or per gram of spleen (right side). **(C)** Representative flow cytometry plots of PD-1^{HI} T_{FH} and PD-1^{LO} T_{FH} CD4^{+} T cell populations in each immunisation model. **(D)** Summary of PD-1^{HI} T_{FH} (left) and PD-1^{LO} T_{FH} (right) frequencies and **(E)** cell numbers. **(F)** Representative flow cytometry plots of GC B cells staining in each experimental group. **(G)** GC B cell quantification showed as a frequency of total CD19^{+} B cells.

(A, B) Data represents one experiment with n=4 for *S. enterica* 10^6 and *S. enterica* 10^4 and 2 experiments for HK bacteria group (n=4) and for naive animals (n=2). (D,E, F, G) Data represents one experiment with n=4 for for *S. enterica* 10^6, *S. enterica* 10^4 and HK bacteria and n=2 for naïve; each dot represents one mouse.

Statistical significance was determined by One-way ANOVA with post-ANOVA Tukey's test for multiple comparisons (Fig. 3.8 A, C-F) or by two-tailed Student's *t*-test with 95% confidence (Fig. 3.8 B).

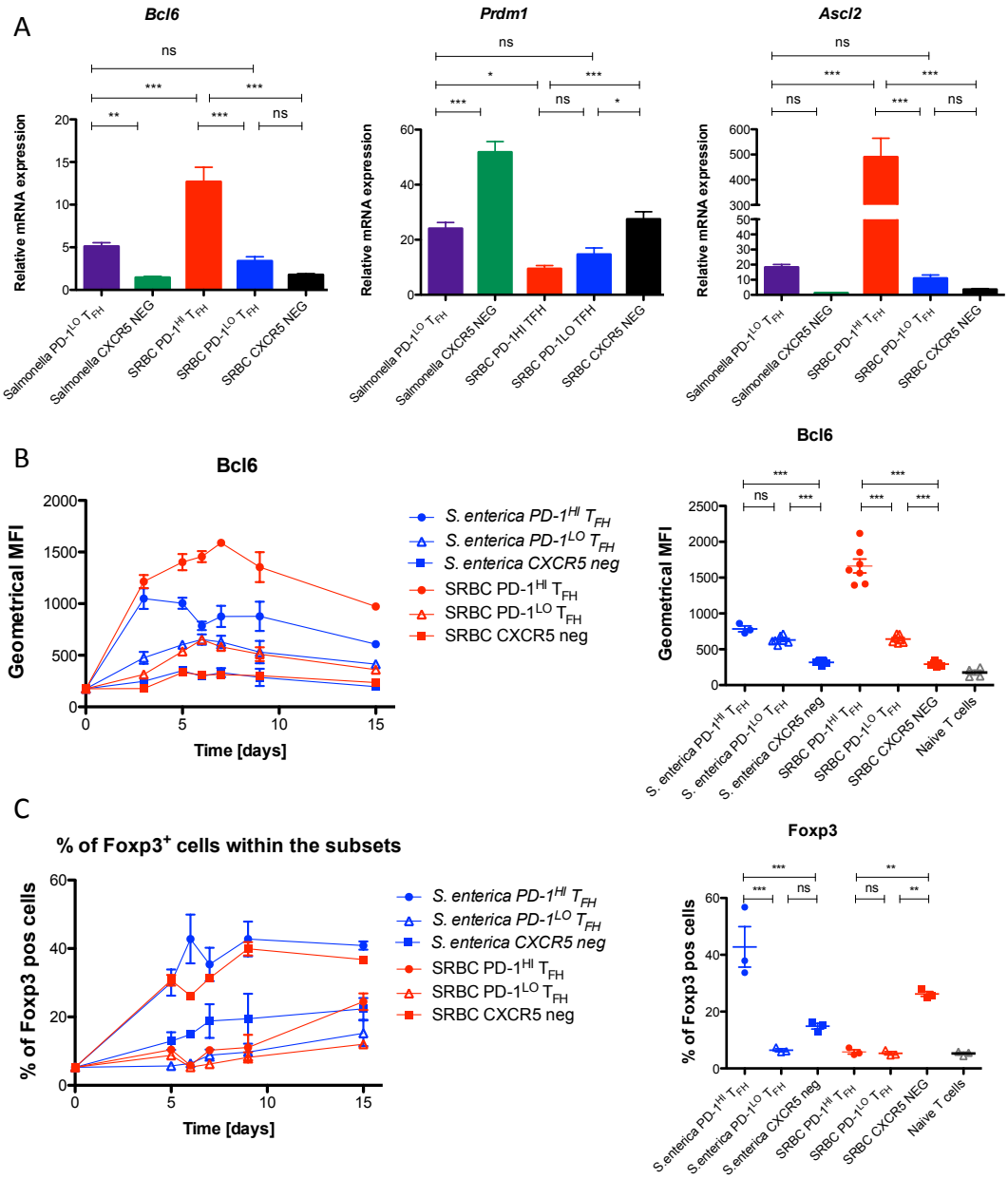

Fig 3.4. Analysis of transcription factor expression in T_{FH} populations.

(A) Analysis of mRNA levels of *Bcl6, Prdm1* (Blimp1) and *Ascl2* by qPCR on day 6 p.i with SRBC or *S. enterica* in isolated T cell populations. Analysis of protein levels for Bcl6 **(B)** and Foxp3 **(C)** over time (left) or on day 6 p.i (right) with with SRBC *or S. enterica* by flow cytometry.

Fig. 3.4.A: Each group consists of 3 biological replicates. Data are representative of 2 independent experiments with similar results. Fig. 3.4 B and C (left): data representative of a single experiment, n=3. Fig. 3.4 B and C (right): data representative of 2 independent experiments with similar results, n=3. Each dot symbolises one mouse.

Statistical significance was determined by One-way ANOVA with post-ANOVA Tukey's test for multiple comparisons.

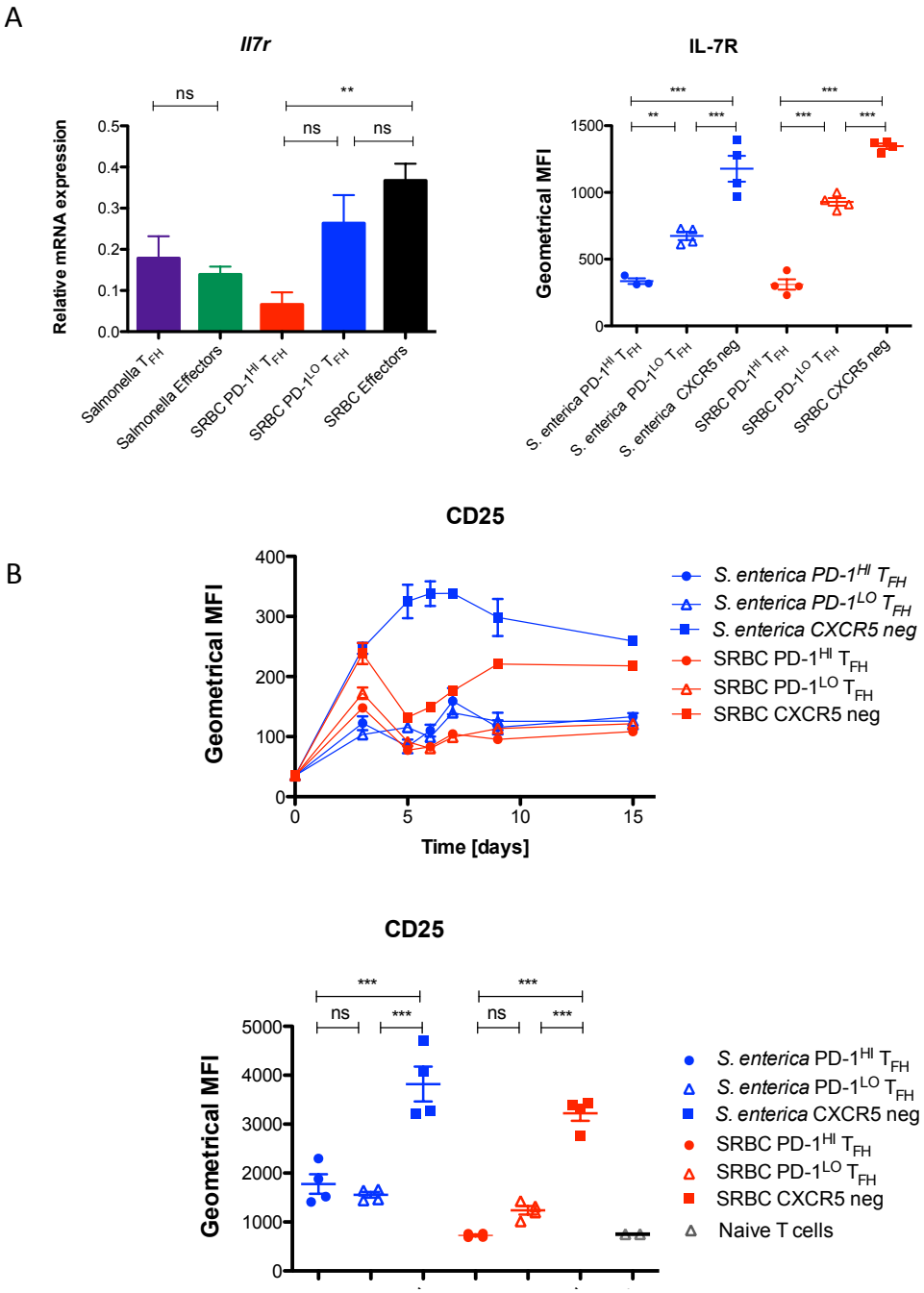

Fig 3.5. Analysis of selected cytokine receptors expressed by T_{FH} populations.

(A) Analysis of *Il7r* mRNA levels by qPCR (left side graph) or IL-7R protein by flow cytometry (right side graph) at day 6 p.i with SRBC or *S. enterica.*

(B) Flow cytometry analysis of IL-2Rα (CD25) protein levels expressed in isolated T cell populations over time (left side graph) or at day 6 p.i (right side graph) with SRBC or *S. enterica.*

Fig. 3.5 A, left: data representative of 2 independent experiments with similar results, each group consists of 3 replicates. Fig. 3.5 A right and 3.5 B: data representative of one experiment with n=3.

Statistical significance was determined by One-way ANOVA with post-ANOVA Tukey's test for multiple comparisons.

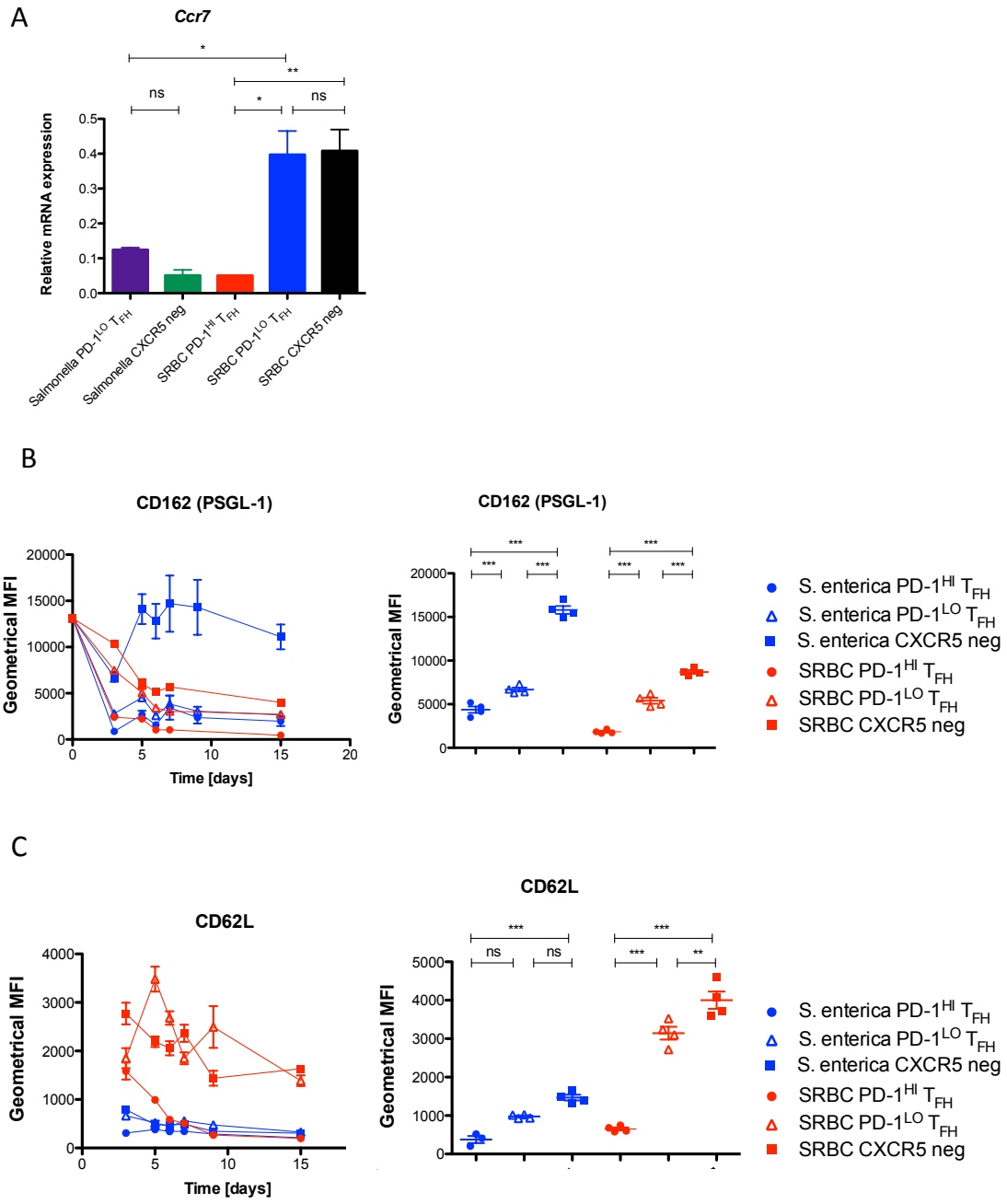

Fig 3.6. Analysis of proteins involved in positioning expressed by T_{FH} populations.

(A) Analysis of *Ccr7* mRNA levels by qPCR on day 6 p.i with SRBC *or S. enterica* in isolated T cell populations. Analysis of protein levels for CD162 (PSGL-1, **B)** and CD62L **(C)** over time (left) or on day 6 p.i with with SRBC *or S. enterica* in isolated T cell populations.

Statistical significance was determined by One-way ANOVA with post-ANOVA Tukey's test for multiple comparisons. Data representative of 2 independent experiments with 3 replicates per group (Fig. 3.6A) or a single experiment (Fig. 3.6B and C), each dot symbolises 1 mouse.

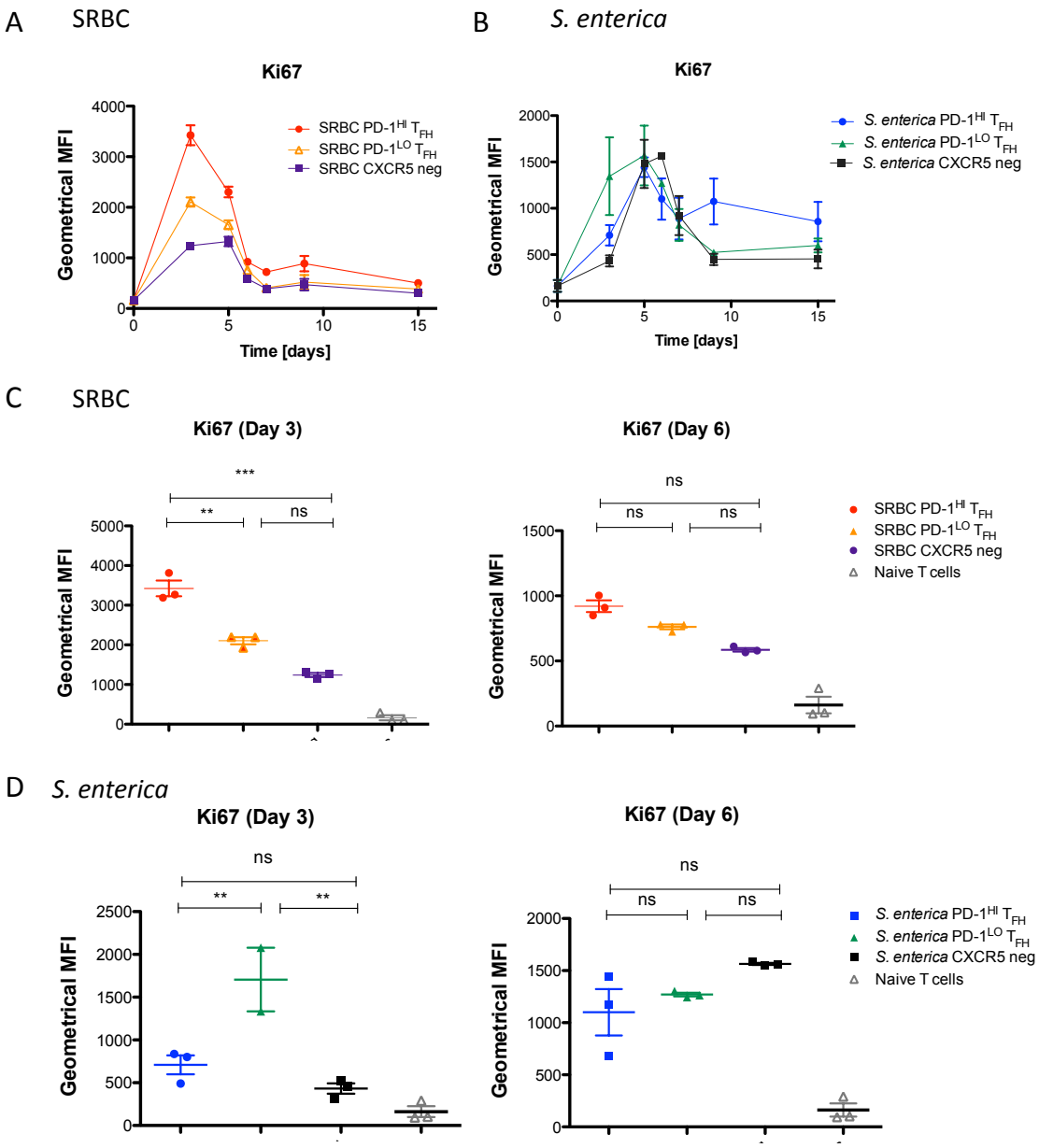

Fig 3.7. Analysis of proliferative potential of T_{FH} populations.

Flow cytometry analysis of Ki67 protein expression after SRBC immunisation over time **(A)** and on day 3 and 6 p.i. **(C)** and after *S. enterica* infection over time **(B)** and on day 3 or day 6 **(D)**.

Data representative of a single experiment with 3 animals per time point. Each dot symbolises 1 mouse. Statistical significance was determined by One-way ANOVA with post-ANOVA Tukey's test for multiple comparisons (Fig. 3.7 C and D).

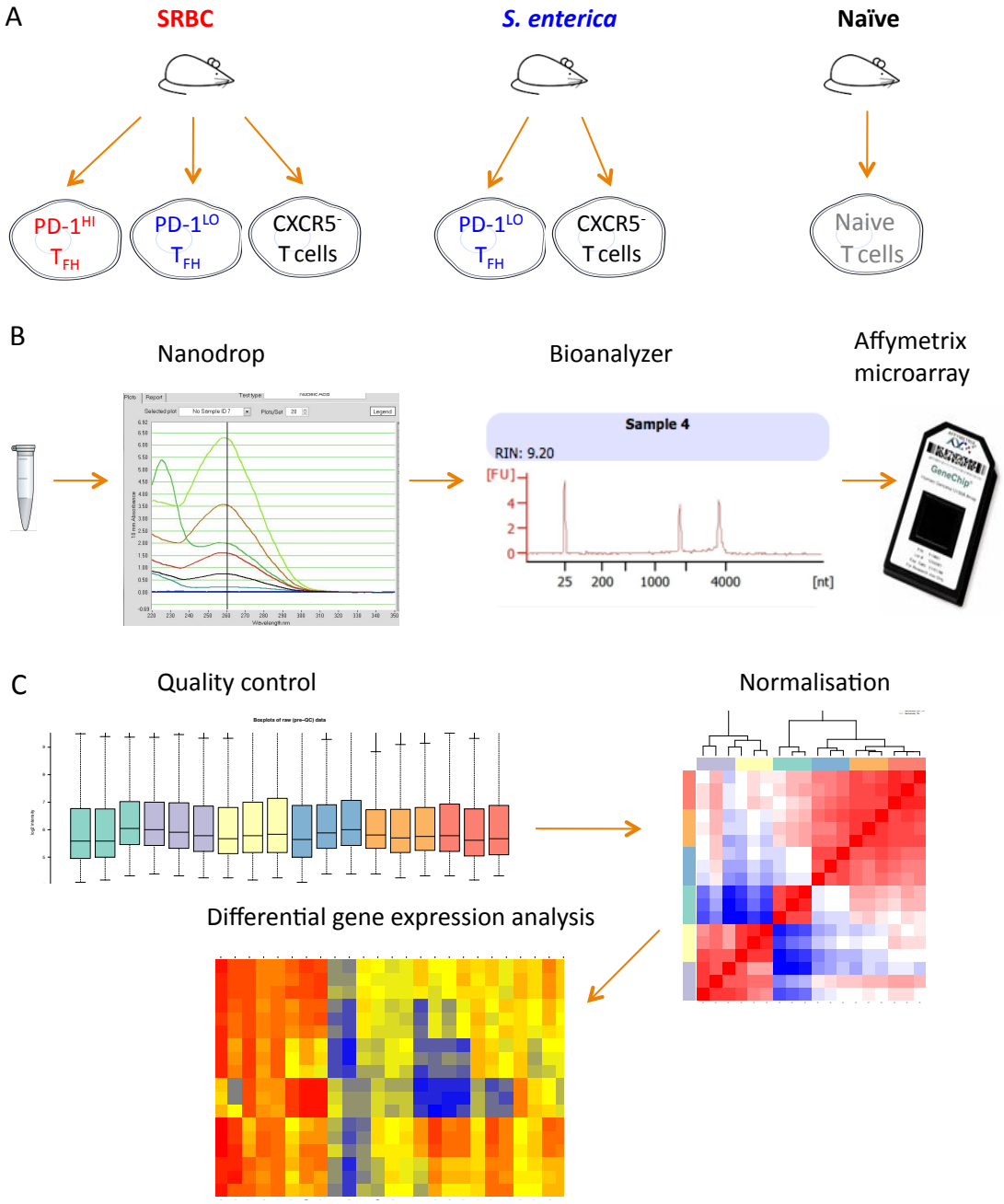

Fig 3.8. Microarray analysis of T_{FH} populations

(A) Overview of isolated T cell populations at day 6 p.i. with SRBC (left) or *S. enterica* (centre) and naïve mice (right). Cells were stored in TRIzol at -80°C until further processing.

(B) RNA isolation was carried out with RNeasy kit (Qiagen; left). RNA was then quantified by Nanodrop (centre left) and quality was confirmed by Bioanalyser (centre right). Isolated RNA was hybridised to Affymetrix mouse microarrays (MoGene).

(C) Raw data obtained from microarray were subjected to quality control (boxplots, left). Data were further normalised (heatmap, right). Heatmaps were used as a graphic representation of the results (bottom).

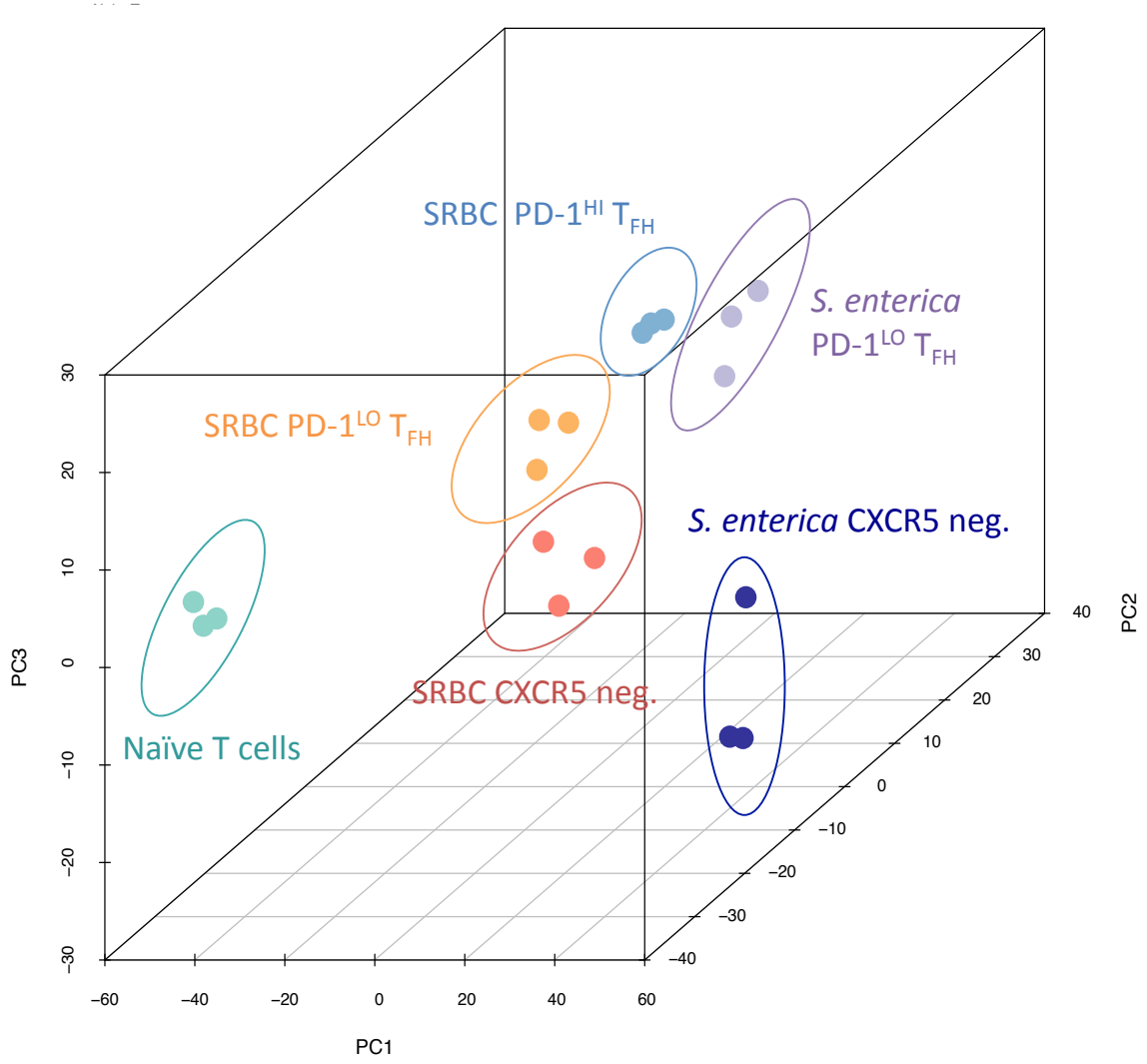

Fig 3.9. Principal component analysis of all significantly differentially expressed genes in isolated T_{FH} populations.

3726 loci with adj. P value <0.0001 were subjected to principal component analysis.

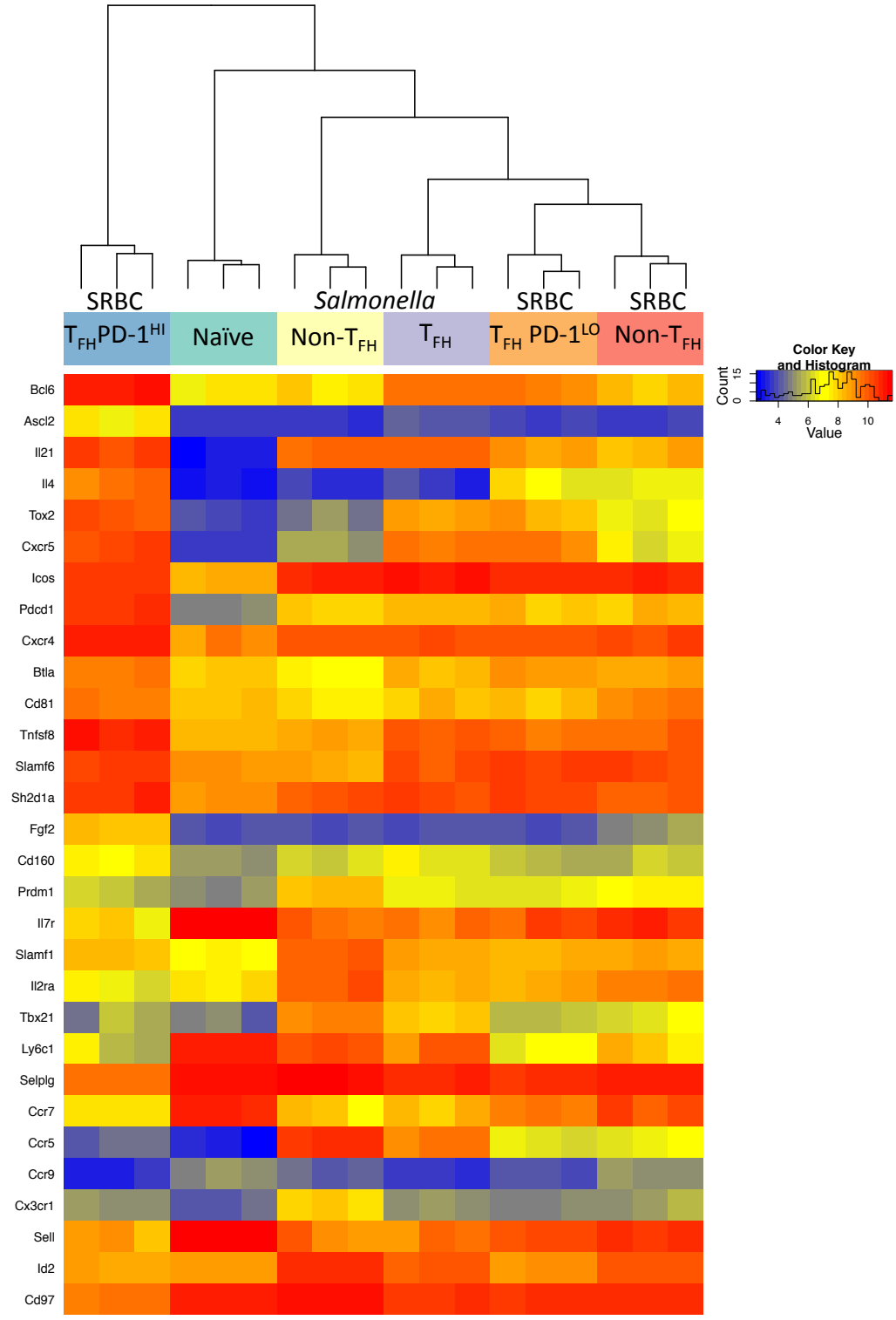

Fig. 3.10. Heat map illustarting expression of genes associated with T_{FH} phenotype in isolated T cell populations 6 days p.i. with SRBC or *S. enterica.*

Red colour indicates up regulation of the transcript (while blue depicts down regulation) with respect to houskeeping genes. T_{FH} and CXCR5 negative T cells were isolated 6 days p.i. with SRBC or *S. enterica.* Naïve T cells ($CD62L^{HI}$ $CD44^{LO}$) were isolated from the unimmunised animals. Each group is represented in biological triplicates.

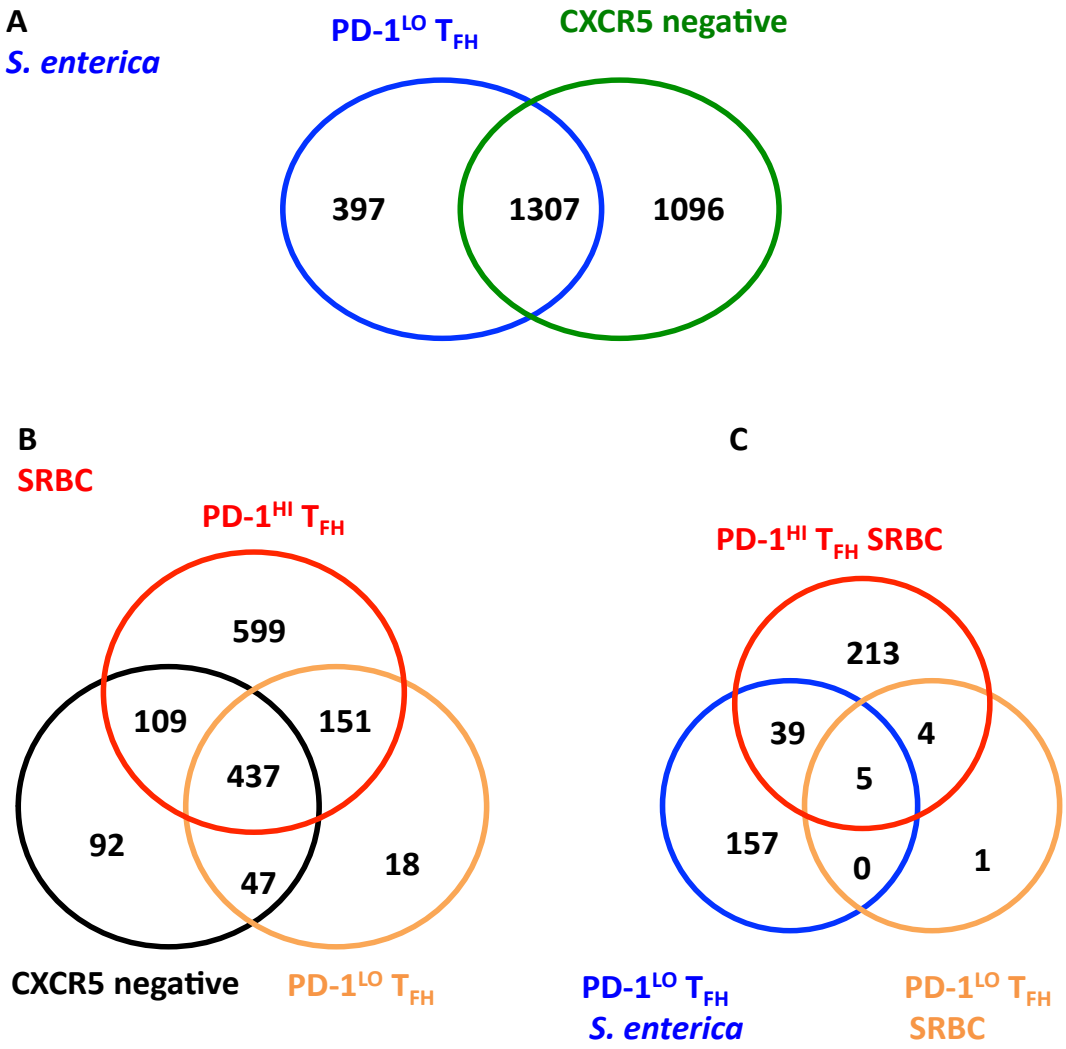

Fig 3.11. Venn diagrams representing numbers of differentially expressed genes between isolated T cell populations.

(A) Genes differentially expressed in PD-1^{LO} T_{FH} and $CXCR5^-$ T cells isolated after *S. enterica* infection with respect to naïve T cells.

(B) Genes differentially expressed in PD-1^{HI} T_{FH}, PD-1^{LO} T_{FH} and $CXCR5^-$ T cells isolated after SRBC immunisation with respect to naïve T cells.

(C) Genes differentially expressed in PD-1^{HI} T_{FH} and PD-1^{LO} T_{FH} from SRBC immunisation and PD-1^{LO} T_{FH} from *S. enterica* infection with respect to $CXCR5^-$ T cells from the corresponding model.

Naïve CD4 T cells ($CD62L^{HI}CD44^{LO}$) were isolated from unimmunised animals. T_{FH} and $CXCR5^-$ T cells were isolated 6 days post SRBC immunisation or *S. enterica* infection. Each group is represented in biological triplicates.

A

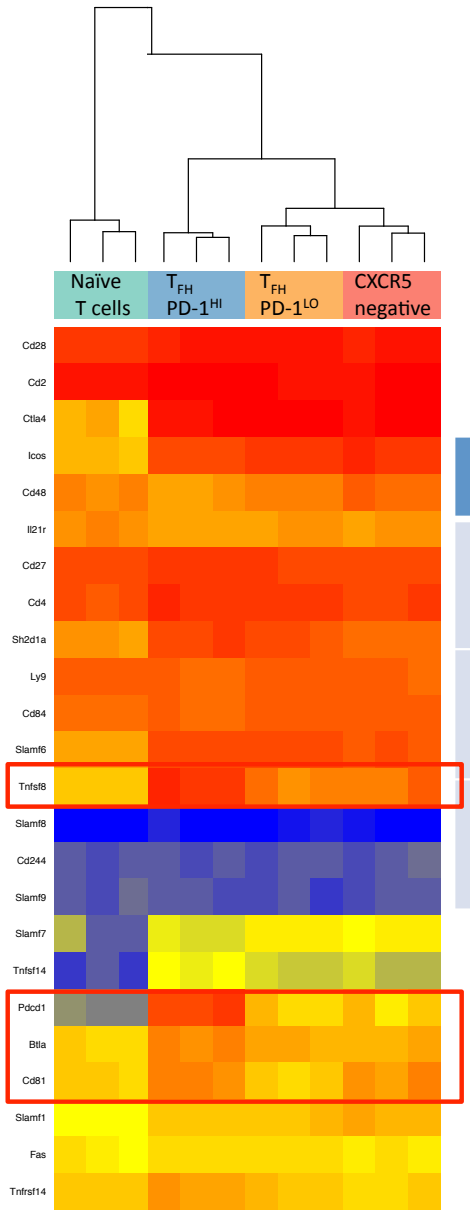

B

	vs. Naïve T cells			PD-1^{HI} T_{FH} vs.		PD-1^{LO} T_{FH} vs.
	PD-1^{HI} T_{FH}	PD-1^{LO} T_{FH}	CXCR5 neg T cells	PD-1^{LO} T_{FH}	CXCR5 neg T cells	CXCR5 neg T cells
Btla	2.3	1.7	1.5	1.3	1.6	1.2
	***	**	*	ns	*	ns
Cd81	2.2	1.0	2.0	2.2	1.1	0.5
	**	ns	*	*	ns	ns
Tnsfs8 (CD30l)	5.1	2.2	2.4	2.3	2.1	0.9
	***	***	***	**	**	ns

*** P < 0.0001
** P < 0.001
* P < 0.01

Fig 3.12. Microarray analysis of transcripts encoding proteins involved in T-B cell interactions.

(A) Heat map showing mRNA expression of transcripts encoding proteins with known roles in T-B cell interactions. T_{FH} and CXCR5- T cells were isolated 6 days post SRBC immunisation from C57Bl/6 mice. Naïve T cells (CD62L^{HI} CD44^{LO}) were isolated from the unimmunised C57Bl/6 animals. Each group is represented in biological triplicates.

(B) Table describing fold changes observed between the groups and P values.

3.3 Discussion

3.3.1 PD-1^{HI} T_{FH} from SRBC display a set of markers characteristic for GC associated population.

After SRBC immunization, the sub-specialisation of T_{FH} populations based on the surface levels of PD-1 have resulted in the identification of two discreet subsets of T_{FH} that exhibit further differences in expression of many markers, including Bcl6, Ascl2, Blipm1, Foxp3, IL-7R, CD62L, CCR7 and PSGL-1. PD-1^{HI} T_{FH}, found abundantly in the SRBC model, but at a very low frequency after *S. enterica* infection, displayed a set of features associated with a GC supporting population (114): elevated levels of CXCR5 (Fig. 3.1F), Bcl-6 and Ascl-2 (Fig. 3.4A and B), low expression of IL-7R (Fig. 3.5A), low mRNA levels of CCR7 (Fig. 3.6A) and Blimp-1 (Fig. 3.4A) and high mRNA levels of IL-21, IL-4, CXCR4, BTLA and CD81 (Fig. 3.10). Therefore, even though PD-1 expression on $CXCR5^{+}$ T cells displays a continuous rather than discreet character, the phenotypic analysis between PD-1^{HI} T_{FH} and PD-1^{LO} T_{FH} resulted in a discrimination of two populations with many significant differences in the expression of cell surface and intracellular markers.

The general separation between T_{FH} populations was very elegantly further illustrated by the analysis of global gene expression changes (Fig. 3.9) as well as immunologically relevant transcripts (Fig. 3.11). In all the cases of PCA, including genes known to be important for T_{FH} identity (Fig. 3.10 and 3.11A), PD-1^{HI} T_{FH}, PD-1^{LO} T_{FH} and $CXCR5^{-}$ T cells formed very discreet subsets with strikingly different gene expression pattern with respect to naïve T cells (Fig. 3.11). PD-1^{HI} T_{FH} elicited in SRBC immunisation showed the highest number of unique transcripts when compared to naïve T cells (Fig. 3.12B) and $CXCR5^{-}$ T cells from SRBC model (Fig. 3.12C). Interestingly, PD-1^{LO} T_{FH} from the SRBC model seem to share more similarities in gene expression with the PD-1^{HI} T_{FH} population than with $CXCR5^{-}$ T cells (Fig. 3.12B), which suggests a potential differentiation of PD-1^{LO} T_{FH} to PD-1^{HI} T_{FH}.

3.3.2 Positioning and migratory potential of T_{FH} populations.

T cell positioning within SLO is absolutely crucial in eliciting and sustaining an optimal immune response. Naïve T cells, held in the T cell zone, express high levels of CCR7 and PSGL-1, which are considered to be a 'T cell zone retention signal'. Up regulation of CXCR5 on T cells and movement towards the T-B cell border, followed by the penetration of B cell follicles is generally considered a first step towards acquiring the T_{FH} phenotype and function. The up-regulation of CXCR5 occurs at the same time as the down-regulation of CCR7 and this reciprocal change in chemokine expression is thought to be essential for the entry to the B cell zone. However, results from our lab (unpublished data) show that CXCR5-deficient T cells are equally capable of homing to the B cell follicle as CXCR5-sufficient T cells and this is in keeping with other studies (22). However, interestingly, CXCR5 is essential for accessing the GC rather than the B cell follicle (unpublished data). Therefore, with regard to T cell positioning down-regulation of CCR7 seems to playing a crucial role in providing entry to the B cell follicle (22) and eventually into the GC as it is finally lost. The balanced expressed of both CXCR5 and CCR7 seems to be critical for maintaining the PD-1^{LO} T_{FH} population in the follicular mantle.

Remarkably, only the PD-1^{HI} T_{FH} subset from SRBC immunisation actively down regulates *Ccr7* mRNA (Fig. 3.6A) or the PSGL-1 protein (Fig. 3.6B). The fact that PD-1^{LO} T_{FH} from the *S. enterica* and SRBC models, expressing intermediate levels of CXCR5 (Fig. 3.1F), do not down regulate CCR7 message or the PSGL-1 protein to the same extent as PD-1^{HI} T_{FH} (Fig. 3.6B) further supports the idea of a differential positioning and consequently of different functions of these cell subsets. This is in agreement with other published studies, which described that GC-associated T_{FH} express low amounts of PSGL-1 and CCR7. However, it is important to stress that location of T_{FH} cells in *S. enterica* immunisation has not been directly assessed with microscopy and so one cannot conlude whether these T cells reside in the B cell follicles, in their close apposition or in the T cell zones.

A recent study by Weber *et al.* provided insight into the coordinated regulation of CXCR5, CCR7 and PSGL-1 expression by the TF Krüppel-like factor 2, Klf2 (58). Klf2, which is repressed by ICOS, directly binds to DNA encoding CXCR5, CCR7

and PSGL-1 (58). Interestingly, this phenomenon results in the repression of CXCR5 but has an opposite, activatory effect on the expression of CCR7 and PSGL-1(58).

Furthermore, the PD-1^{HI} T_{FH} population was found to express the lowest amounts of the CD62L protein (Fig. 3.6C) and transcript (*Sell*, Fig. 3.10). Intermediate levels of CD62L were found on PD-1^{LO} T_{FH} and the highest for $CXCR5^-$ T cells, with the same expression pattern in *S. enterica* and SRBC models. These results further indicate that PD-1^{HI} T_{FH} have the weakest migratory potential and are the subset least capable to move via HEV of SLO. CD62L expression, therefore, logically reflects the differences in the positioning of the T_{FH} subsets. PD-1^{HI} T_{FH}, buried within the GC of B cell follicles, are the furthest away from exit and entry points of the lymphocytes (HEV), whereas PD-1^{LO} T_{FH} and $CXCR5^-$ T cells, positioned within the T cell zone or closer to the B-T cell border, still retain the possibility to move in and out of the SLO.

3.3.3 PD-1^{HI} T_{FH} from the SRBC model perform different function than PD-1^{HI} T_{FH} from the *S. enterica* model

The PD-1^{LO} T_{FH} population is the dominant T_{FH} subset elicited during the *S. enterica* response but some T_{FH} cells with PD-1^{HI} phonotype can still be found. Although the PD-1^{HI} T_{FH} population is present in the *S. enterica* model at a very low frequency (0.36% ± 0.05, of $CD4^+$ T cells at day 6, Fig.3.1C and D) this result is highly reproducible and consistent. Interestingly, the analysis of the TFs expressed by the PD-1^{HI} T_{FH} subset in *S. enterica* infection revealed that a significant proportion of this population (42.8% ± 7.1, Fig. 3.4C) expresses also the Foxp3 TF, which makes them *bona fide* T_{FR} (134). A possible function of the T_{FR} population at this stage of the response could be to limit the ongoing extra-follicular antibody production, which also requires T cell help (171). Also, the fact that the proliferation peak of the PD-1^{HI} T_{FH} population in *S. enterica* is observed later than the one of PD-1^{HI} T_{FH} from the SRBC model (day 5 as opposed to day 3, Fig. 3.7) further indicates that the former population might be linked to the early extra-follicular response. Meanwhile, the proliferation peak at day 3 for PD-1^{HI} T_{FH} in SRBC immunisation is in agreement with the time frame of the expansion of the GC-supporting population, since GC B cells are clearly visible at day 5 (Fig. 3.2B and D) and productive T-B

cell interaction, therefore, needs to happen earlier. Additionally, the proliferative delay of PD-1^{HI} T_{FH} in the *S. enterica* model (day 5) as opposed to SRBC (day 3) may also reflect the complexity of the response to multiplying and simple antigen.

Fascinatingly, when comparing the expression of Bcl6 in the PD-1^{HI} T_{FH} subset from *S. enterica* infection and PD-1^{HI} T_{FH} from the SRBC model, it becomes clear that both populations express equivalent levels of the Bcl6 protein at day 3 (which are significantly higher than observed in PD-1^{LO} T_{FH} and $CXCR5^-$ T cells from both models). However, around day 6 PD-1^{HI} T_{FH} from *S. enterica* have dropped Bcl6 to levels lower than the ones observed in PD-1^{LO} T_{FH} from the same model, whereas PD-1^{HI} T_{FH} from SRBC immunisation have a further reinforced Bcl6 expression (Fig. 3.4B). This could be explained by the fact that there is a window (between days 3 and 5) in which a certain signal needs to be received by T_{FH} cells in order to further increase Bcl6 levels. Alternatively, the highest levels of Bcl6 might only be expressed when GC structures are formed due to the dialogue between T_{FH} and early GC B cells, and therefore the *S. enterica* model will not express such high amounts of Bcl6 in T cells until GC structures can be established (around week 7 post infection).

3.3.4 Microarray analysis of genes involved in T-B cell interactions identifies PD-1^{HI} T_{FH} –specific protein candidates for further investigation

The analysis of the molecules known to be involved in the interactions between T and B cells revealed transcripts for few proteins (BTLA, CD30L and CD81) that are exclusively up-regulated in PD-1^{HI} T_{FH} (Fig. 3.11). As PD-1^{HI} T_{FH} are possibly a GC-associated population, one could expect more transcripts of proteins involved in T and B cell contact to be selectively altered in this subset. Low number of differentially expressed transcripts could be explained by the fact that, firstly, some of the genes involved in the interaction are not regulated on the transcriptional level, and, therefore, would not be identified by the microarray study. Secondly, the microarray technology works on mRNA extracted from many individual cells and it represents an 'average' gene expression profile of the isolated subset. Although it is a very reliable means to obtain general information about large-scale changes between the populations, it is not possible to extract changes in the expression of a

very small cell subset. Therefore, if there is a more specialized T_{FH} population within PD-1^{HI} T_{FH} subsets (e.g. the cells with the highest levels PD-1 and CXCR5) it would not be possible to identify those cells with microarray, as this utterly selective gene expression would be 'blurred' or 'dominated' by the profile of other, more numerous cells. Thirdly, the effects of the interaction of T_{FH} with B cells within GC might be mediated by the close and selective positioning of the cells, rather than by altering the surface expression of the proteins involved in the interaction. Consequently, all three subsets (PD-1^{HI} $T_{FH,}$ PD-1^{LO} T_{FH} and CXCR5^{-} T cells) may express equivalent levels of a certain protein but the functional consequences of this would be different in each case due to the distinct space occupied by each population within the SLO. Nevertheless, three transcripts involved in the contact between T and B cells were identified by microarray analysis as exclusively up regulated (*Btla, Tnfsf8* and *Cd81*) in PD-1^{HI} T_{FH} (Fig. 3.13)

B and T lymphocyte attenuator (BTLA) is a co-inhibitory receptor, member of the same family as CTLA4 and CD28 (115). CXCR5^{+} T cells were found to express higher levels of BTLA than CXCR5^{-} T cells (116) and our results are in keeping with this finding. Moreover, it has been shown that BTLA4 has a role in limiting the production of both antigen-specific antibodies as well as autoantibodies by limiting the IL-21 derived by T_{FH} (116). However, effects of T-cell intrinsic BTLA expression have not been investigated and since BTLA is also expressed on GC B cells it would be important to elucidate its function in each of the cell types (116). Higher expression of BTLA in PD-1^{HI} T_{FH} within the GC might be essential to prevent excessive antibody production at a later stage of the immune response and therefore represents a negative feedback loop in the T-B cell dialogue.

CD81, another protein of interest, is a co-stimulatory receptor, physically associated with the CD4 and CD8 co-receptor in T cells (201). It is also expressed on B cells, where it forms part of the complex with CD21, CD19 and Leu13 (201). Importantly, CD81 has been shown to have a role in the physical T-B cell interaction by up regulating LFA expression on T cells (202) and activating integrin α4β1 in B cells, as well as increasing IL-4 synthesis in T cells responding to antigen presented by B cells but not by monocytes (203). Therefore, a higher expression of

CD81 by PD-1^{HI} T_{FH} supports the idea of enhanced physical interaction between PD-1^{HI} T_{FH} and B cells. In further agreement with the role of CD81 as published in the literature, IL4 mRNA was one of the most highly up regulated genes in the PD-1^{HI} T_{FH} population (represented on the heat map in Fig. 3.10).

Tnfsf8 is a transcript encoding for the CD30L (CD153) protein, a member of a TNF superfamily. It is a ligand for CD30 (204). CD30L is expressed on many cell types upon activation, including T and B lymphocytes, granulocytes, macrophages and eosinophils (204). The role of CD30L in generation of humoral response does not seem to be fully elucidated. The engagement of CD30L on T cells with CD30 on B cells has an inhibitory effect on the antibody production (205). However, there are also reports that describe opposite consequences of the CD30-CD30L interaction with effects on B cells, including enhanced proliferation, cytokine secretion and antibody production (204). CD30L was also reported to play a role in maintaining the balance between Th1 and Th2 type of an immune response (206).

The results of the T_{FH} microarray show the highest expression of CD30L mRNA (*Tnfsf8*, Fig. 3.13) in PD-1^{HI} T_{FH} from SRBC model with a moderate expression in other activated cell types (PD-1^{LO} T_{FH} and $CXCR5^-$ T cells from both models) and this is in agreement with previously published studies (182). This could illustrate another negative feedback mechanism, alongside BTLA, involved in controlling the quantity and quality of the antibodies produced. Alternatively, since the role of CD30L is still controversial, it might also be one of the selective interactions between PD-1^{HI} T_{FH} and B cells involved in sustaining GC reaction.

Interestingly, the specific up regulation of co-inhibitory molecules (BTLA, CD30L?) and co-stimulatory proteins (CD81, CD30L?) in PD-1^{HI} T_{FH} underlines the importance of a controlled T-B cell interaction as part of a balanced immune response.

Overall, the microarray results suggest that although many transcripts encoding proteins important in the T-B cell interaction are commonly altered in PD-1^{HI} $T_{FH,}$ PD-1^{LO} T_{FH} and $CXCR5^-$ T cells from SRBC model, there are some changes that are exclusive to PD-1^{HI} T_{FH} (BTLA, CD81 and CD30L). The role of these proteins could

be further investigated, in a first step, by confirming the expression pattern on the protein level by flow cytometry. Again, the fact that a certain T_{FH} population expresses a set of molecules also found in GC B cells reinforces the idea that a reciprocal dialogue between these cells is an essential process for providing fully functional T_{FH} and GC B cells.

3.3.5 Kinetics of the SRBC and *S. enterica* models

The important aspect of the microarrays is that this technology gives an overview of the transcriptional profile of the cell or population at a particular time point only. T_{FH} populations from SRBC and *S. enterica* models display different kinetics of activation as measured by incorporation of the proliferative marker Ki67 (Fig. 3.7A), with PD-1^{HI} T_{FH} peaking in proliferation at day 3 while PD-1^{LO} T_{FH} proliferate the most at day 5. Microarray analysis was carried out at day 6 p.i. with either SRBC or *S. enterica*, which means that the T_{FH} populations were at different proliferative stages. This could result in differential expression of many transcripts, for instance proteins associated with metabolism, ribosome synthesis or translation. However, although it is important to keep this issue in mind, the microarray approach is still valid when assessing potential for the B cell help and the expression of the proteins associated with *bone fide* GC T_{FH}.

In subsequent chapters I investigated further some of the questions raised in this chapter, such as the potential of the PD-1^{LO} T_{FH} under appropriate conditions to become PD-1^{HI} T_{FH} (Chapter 4). I was also interested to know how the two populations of T_{FH} would develop in a situation where a response to *S. enterica* and SRBC is happening concurrently (Chapter 5).

4 The role of cognate T-B cell interactions in T follicular helper cell (T_{FH}) formation in SRBC immunisation

4.1 Introduction

The contributions of the T_{FH} cell population to successful generation of GC responses are widely recognized and have already been discussed in detail elsewhere in this thesis (Introduction p. 27- 'Function of T_{FH} cells'). Interestingly, however, there is a growing interest in investigating the reciprocal nature of T-B cell interactions and in disentangling the signals by which B cells influence the T_{FH} population.

The essential role of B cells in the T_{FH} development in various experimental models is demonstrated by the fact that the T_{FH} population is not formed in B cell deficient mice in response to SRBC immunisation (134), viral infection (75,77) or parasite infection (73). Furthermore, depleting B cells at day 2, 6 or 10 post *S. enterica* infection with anti-CD20 beads leads to the loss of both early stage T_{FH} and the already established T_{FH} population within 24 hours of the treatment (unpublished data from our lab). Therefore, the anti-CD20 depletion study indicates that B cells play a crucial role in T_{FH} survival. Furthermore, it may suggest that T_{FH} cells require continuous contact with cognate B cells as a survival signal rather than a single interaction at a certain time point.

As professional APCs the nature of the B cell interaction with T cells can be either cognate or non-cognate. While the cognate interactions necessarily require physical contact between T and B cells to allow the pairing of MHC-peptide complex with TCR, the non-cognate interactions can involve either delivery of soluble mediators (e.g. cytokines) or the engagement of surface bound receptors, such as ICOS-L, CD80/86, CD28 and CD84. Experiments conducted with MD 4 mice, where all B cells carry BCR specific for hen egg lysozyme (HEL) antigen, showed only transient T_{FH} development after SRBC immunisation or viral infection (57,75,77). However, the T_{FH} frequency in the early stages of the response is still significantly higher than in B cell deficient mice, which suggests that some T_{FH}-B cell interactions can be of non-cognate character and later on antigen

presentation by B cells might be crucial for sustaining the T_{FH} population. It is important to keep in mind, though, that induction of T_{FH} depends on the DCs, as discussed in the Introduction on p. 19.

Furthermore, the need for physical, non-cognate interactions between T and B cells was elegantly demonstrated in a recent study that establishes that engagement of ICOS-ICOSL receptors from T cells and non-cognate B cells, respectively, is crucial for recruiting T_{FH} to the B cell follicle (56). ICOS-ICOSL engagement between T cells and cognate B cells, respectively, was also found to be important for T_{FH} development in environments with low amounts of antigen (207).

The opinion that B cells deliver a unique, cell-specific signal to $T_{FH,}$ optimizing their development and functional character, seems to be prevalent in the scientific field. However, one study reported that the need for an encounter between T_{FH} and B cells is only due to the fact that at the later stages of the immune response B cells take over antigen presentation from DCs (208). Therefore, the requirement for cognate T-B cell contact can be overcome by an extra dose of antigen. This suggests that there is no qualitative difference between, for example, DCs and B cells, and that their differing roles in the induction and maintenance of the T_{FH} population is purely due to the fact that as immune response progresses B cells become the main APC, while DCs play a more important role in the priming stages. This notion has been challenged in subsequent publications, which show that priming by DC and B cells has different outcomes for the generation of T_{FH} populations *in vitro* (81) and *in vivo* in the viral infection model (83,209). Furthermore, an elegant study by Qi *et al.* demonstrated that disrupting physical interactions between T_{FH} and B cells (transgenic SAP-deficient[5] OT.II $CD4^+$ T cells and peptide immunisation) impairs T_{FH} survival and GC formation (25). Importantly, in this model interactions between T cells and DCs are not affected, which further suggests a special character of physical T-B cell interactions (25).

Overall, it is clear that T_{FH} cells need the presence of B cells to fully develop and to survive. T-B cell interactions require physical contact between T_{FH} and B cells and

[5] SAP (SLAM-associated protein) is a cellular adaptor providing signaling for the SLAM family members, such as CD84, 2b4, Ly9 and Ly108 (142).

the character of the interaction can be both cognate and non-cognate. However, there are some inconsistencies in the reports investigating the need for and timing of antigen presentation by B cells in influencing T_{FH} population development. It is also possible that multiple types of T_{FH}-B cell interactions are required at different stages or for different types of immune response.

4.2 Aims of the chapter

In the previous chapter I have shown that there is heterogeneity within the T_{FH} population and that PD-1^{HI} T_{FH} and PD-1^{LO} T_{FH} subsets differ in their expression of the surface and intracellular markers. The aim of this chapter is to determine whether both of the T_{FH} subsets (PD-1^{HI} T_{FH} and PD-1^{LO} T_{FH}) are dependent on antigen presentation by B cells. This aspect has been addressed by using mixed BM chimeras with the B cell compartment exclusively deficient in MHC II expression (Materials and Methods chapter, p. 49) in a SRBC immunisation model, since, in contrast to *S. enterica* infection, SRBC immunisation gives rise to both PD-1^{HI} T_{FH} and PD-1^{LO} T_{FH} cell subsets. I characterize PD-1^{HI} T_{FH}, PD-1^{LO} T_{FH} and GC B cell populations in $B^{MHCII-/-}$ chimeras by flow cytometry, using both surface and intracellular markers and show that there is a striking difference in their dependency on cognate B cells.

The second question addressed in this chapter concerns T_{FH} plasticity and differentiation pathway. I investigated two possible models of T_{FH} development in the context of the interactions with cognate B cells (Fig.4.1). In the first, the linear model (Fig. 4.1A), the commitment to the T_{FH} pool is made early during the course of the immune response (at the stage of the naïve T cell) and the pool of T_{FH}-precursor cells is consequently established alongside other effector T cell lineages. In this linear model the T_{FH} differentiation pathway is separate from the effector $CD4^+$ T cell pathway and there is no conversion between the two cell types (activated T cells do not become T_{FH} cells). In the second one, the continuous differentiation model (Fig. 4.1B), there is a similar stepwise progression from a naïve T cell to pre-T_{FH} and then T_{FH} cell with possible recruitment of the activated effector cells to the T_{FH} pool. A final aspect of the T_{FH} differentiation process is the ultimate fate of T_{FH} cells and the question whether they can revert back to become non-T_{FH} effector

T cells (and, for instance, lose CXCR5 expression). By using an adoptive transfer approach and mixed BM chimeras I demonstrate that activated PD-1^{+} T cells (both $CXCR5^{+}$ and $CXCR5^{-}$) can enter T_{FH} pool. Furthermore, I show that there is a significant plasticity observed within the PD-1^{LO} T_{FH} cell subset. In contrast to that, the PD-1^{HI} T_{FH} population seem to be much more restricted in their ability to convert to other cell subsets. My overall aim in this chapter is to investigate how B cells (by presenting an antigen) influence the plasticity and differentiation of T_{FH} population.

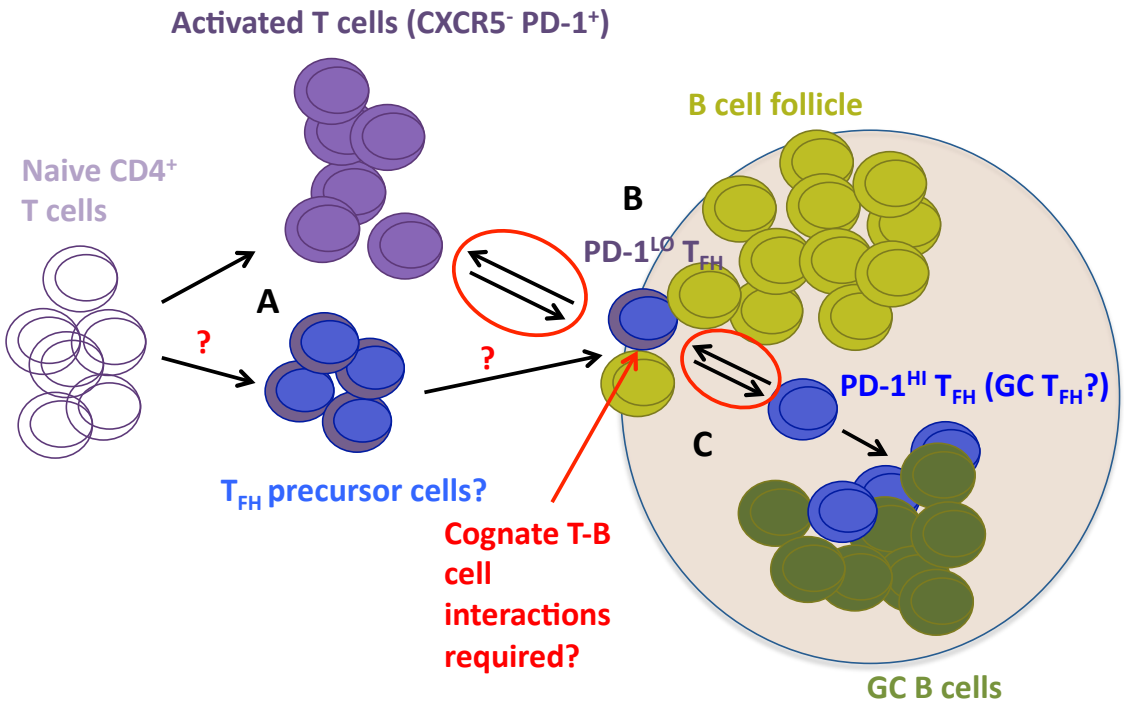

Fig 4.1. Plasticity within PD-1^{LO} and PD-1^{HI} T_{FH} subsets.

(A) Naïve $CD4^+$ T cells become activated by interaction with cognate dendritic cells (not shown) and pool of putative pre-T_{FH} cells is established alongside activated CXCR5- T cells. **(B)** pre-T_{FH} cells and/or activated T cells become PD-1^{LO} T_{FH} **(C)** Upon interaction with cognate B cells (?) PD-1^{LO} T_{FH} cells differentiate into PD-1^{HI} T_{FH} cells, which support GC B cell formation. Red circles indicate areas of T_{FH} plasticity and conversion (between activated T cells, PD-1^{LO} T_{FH} and PD-1^{HI} T_{FH}) investigated in this chapter.

4.3 Results

4.3.1 Formation of PD-1^{HI} T_{FH} after SRBC immunisation depends on cognate interactions with B cells.

In order to investigate the requirements for cognate interactions with B cells, $B^{MHCII-/-}$ chimeras were immunised with SRBC and T_{FH} formation was assessed 6 days later by flow cytometry (Fig. 4.2A). In these BM chimeras all of the B cells are deficient in MHC II expression whereas other APCs show 20% reduction in the MHC II expression. As controls, WT chimeras were used, which have undergone BM reconstitution but were supplemented with WT, and not MHC II deficient, BM and hence all the cellular compartments have normal MHC II expression. The phenotype of B cells in each type of the chimeric mice was confirmed by analysing MHC II expression levels on B cells (Fig. 4.2B)[6]. As a positive control for the induction of the PD-1^{HI} T_{FH} population WT mice were also immunised with SRBC. Representative flow cytometry plots and T_{FH} gating is showed in Fig. 4.2C.

The results show that after SRBC immunisation $B^{MHCII-/-}$ chimeras generate PD-1^{LO} T_{FH} cells in comparable frequency and numbers to WT chimeras (Fig. 4.2D and E, respectively, right panel). In a striking contrast to that, the PD-1^{HI} T_{FH} population is virtually absent in $B^{MHCII-/-}$ chimeras when compared to either WT chimeras or WT mice (Fig. 4.2D and E, respectively, left panel) immunised with SRBC.

This experiment demonstrates that there are differential requirements for cognate interactions with B cells between PD-1^{HI} T_{FH} and PD-1^{LO} $T_{FH,}$ and while antigen presentation is necessary for the formation of the PD-1^{HI} T_{FH} population it seems to be dispensable for the generation of PD-1^{LO} T_{FH} cells.

4.3.2 PD-1^{LO} T_{FH} present in $B^{MHCII-/-}$ chimeras express intermediate levels of Bcl6

Results from chapter 3 (Fig. 3.4A and B) show that PD-1^{LO} T_{FH} generated in WT mice express lower levels of Bcl6 than PD-1^{HI} T_{FH}, hence PD-1 and Bcl6 expression

[6] The slight shift in MHC II expression between two MHC II positive groups (B cells from WT mice and WT chimeras) was also observed in the isotype control and thus it does not reflect true differences in the protein expression.

correlate in immunised WT mice. It is therefore important to determine the levels of Bcl6 expression in the PD-1^{LO} T_{FH} population in $B^{MHCII-/-}$ chimeras to confirm that the observed surface phenotype (lack of high PD-1 expression) is reflected in the level of intracellular master TF.

Flow cytometry analysis showed that PD-1^{LO} T_{FH} raised in $B^{MHCII-/-}$ chimeras express comparable levels of Bcl6 to PD-1^{LO} T_{FH} from WT chimeras or WT mice 6 days post SRBC immunisation (Fig. 4.3 A and B). All PD-1^{LO} T_{FH} populations express lower levels of Bcl6 than the PD-1^{HI} T_{FH} populations from either WT chimeras or WT mice. Nevertheless, Bcl6 expression in PD-1^{LO} T_{FH} is higher than in $CXCR5^{-}$ $CD4^{+}$ T cells from all immunised groups (Fig. 4.3 A and B).

4.3.3 $B^{MHCII-/-}$ chimeras lack GC response

As T_{FH} cells are essential supporters of GC response it is important to investigate the presence of these structures in WT and $B^{MHCII-/-}$ chimeras 6 days post SRBC immunisation (as in Fig. 4.2A). As a positive control for GC induction WT mice immunised with SRBC were included. GC B cells were identified by flow cytometry by expression of Bcl6 in $CD19^{+}$ B cells (representative plots are shown in Fig. 4.4A).

While WT chimeras show a clear induction of the GC B cell population (around 8% ± 0.84 of B cell population) after SRBC immunisation, in $B^{MHCII-/-}$ chimeras GC B cells were virtually undetectable and comparable to levels observed in naïve WT mice or naïve $B^{MHCII-/-}$ chimeras (around 0.35% ± 0.29, of B cells Fig. 4.4B and C). There was no statistical difference in GC B cell frequencies and numbers between immunised WT mice and WT chimeras. The absence of GCs in immunised $B^{MHCII-/-}$ chimeras was further confirmed by histology (Trüb *et. al.,* manuscript in submission).

This result demonstrates that in $B^{MHCII-/-}$ chimeras after SRBC immunisation GCs are not formed despite the presence of the PD-1^{LO} T_{FH} subset. Additionally, this confirms that the PD-1^{HI} T_{FH} subset is the main population supporting GC B cells. Therefore, deficient MHC II expression by B cells can impede the GC formation by halting the generation of PD-1^{HI} T_{FH} cells.

4.3.4 B cell transfer rescues PD-1^{HI} T_{FH} differentiation and GC formation in $B^{MHCII-/-}$ chimeras.

In $B^{MHCII-/-}$ chimeras all B cells lack MHC II expression but there is also a 20% deficiency in MHC II expression in other cell types (e.g. DCs, macrophages, basophils, mast cells and plasmacytoid DC). Therefore, one could argue that the decreased capacity of antigen presentation in other cells could also influence PD-1^{HI} T_{FH} formation. To control for this effect an additional group of chimeras with 20% deficiency in MHC II expression on all cell types (including B cells) was created. Data from our lab (Barr *et al.,* manuscript under revision) show that in these control chimeras immunised with SRBC, PD-1^{HI} T_{FH} are formed in comparable frequency and numbers to immunised WT chimeras, which excludes the possibility that impaired antigen presentation in other cell types recapitulates the phenotype observed in the experimental $B^{MHCII-/-}$ chimeras.

B cell transfer experiments were carried out to further confirm the role of the B cells as main APCs in PD-1^{HI} T_{FH} formation in $B^{MHCII-/-}$ chimeras after SRBC immunisation. $B^{MHCII-/-}$ chimeras have received either WT or MHC $II^{-/-}$ B cells (10 million B cells per mouse) of syngeneic background alongside SRBC immunisation (Fig. 4.5A). T_{FH} formation and Bcl6 expression were assessed 6 days later by flow cytometry. The phenotype and purity of transferred B cells (more than 92%) was confirmed prior to the transfer (Fig. 4.5B). The following groups were used as control groups: 1) naïve $B^{MHCII-/-}$ chimeras and 2) immunised $B^{MHCII-/-}$ chimeras with no B cells transferred

As expected, naïve $B^{MHCII-/-}$ chimeras showed very low levels of T_{FH} present (as previously in Fig. 4.2C) and upon immunisation with SRBC only the PD-1^{LO} T_{FH} population was observed to develop (Fig. 4.5C, upper panel). Interestingly, this was also the case in $B^{MHCII-/-}$ chimeras, which received MHC $II^{-/-}$ B cells. Importantly, the transfer of WT B cells into $B^{MHCII-/-}$ chimeras induced the development of both PD-1^{LO} T_{FH} and PD-1^{HI} T_{FH} cells (Fig. 4.5C). The summary of T_{FH} frequencies and cell numbers is shown in Fig. 4.5D and E, respectively.

In experimental $B^{MHCII-/-}$ chimeras that received MHC II sufficient $CD19^{+}$ B cells these cells made up only 5-15% of the B cell populations at day 6 p.i. (this

population was not detectable in the $B^{MHCII-/-}$ chimeras, which received MHC $II^{-/-}$ B cells, Fig. 4.5C, lower panel). This suggests that only a small fraction of B cells expressing MHC II (around 10%) is sufficient to fully restore PD-1^{HI} T_{FH} frequency.

It was also important to confirm that PD-1^{HI} T_{FH} in $B^{MHCII-/-}$ chimeras supplemented with WT B cells had recovered high expression of Bcl6. The results graphed in Fig. 4.5F and G show that the PD-1^{HI} T_{FH} population from WT B cell transfer group expressed high levels of Bcl6. Furthermore, the PD-1^{LO} T_{FH} populations from both $B^{MHCII-/-}$ chimeras and WT mice expressed significantly less Bcl6.

Summarising, the B cell transfer experiment confirms that B cells are crucial for the development of a T_{FH} subset characterized by high expression of PD-1 and Bcl6 by presenting antigen via MHC II. On the other hand, cognate B cell interactions seem to be dispensable to induce a T_{FH} subset that expresses PD-1 and Bcl6 on a low level as this latter population was not affected in any of the B cell transferred groups in terms of frequency, cell numbers and Bcl6 expression.

4.3.5 Transfer of MHC II-sufficient B cells rescues GC formation in $B^{MHCII-/-}$ chimeras immunised with SRBC

The restoration of the PD-1^{HI} T_{FH} population in $B^{MHCII-/-}$ chimeras with the transfer of WT B cells leads on to the question whether GC formation is also rescued in this setting. Indeed, providing WT B cells expressing MHC II, but not MHC $II^{-/-}$ B cells, fully restored the GC B cell population (Fig. 4.6A and B) as assessed by flow cytometry 6 days post SRBC immunisation. Interestingly, in $B^{MHCII-/-}$ chimeras which received WT B cells only around 10% of total B cell population expresses MHC class II but this is enough to fully restore GC B cells.

4.3.6 PD-1^{LO} T_{FH} cells in $B^{MHCII-/-}$ chimeras are stalled in the differentiation to PD-1^{HI} T_{FH}.

As previous experiments have shown, the presence of PD-1^{LO} T_{FH} per se is not enough to drive the GC reaction in SRBC immunisation in $B^{MHCII-/-}$ chimeras (Fig. 4.4A) but the transfer of WT B cells rescues the formation of both PD-1^{HI} T_{FH} and GC populations (Fig. 4.5D, E and 4.6B). Newly-formed PD-1^{HI} T_{FH} cells in $B^{MHCII-/-}$

chimeras receiving WT B cells could be derived directly from the naïve $CD4^+$ T cells. Alternatively, the $PD1^{LO}$ T_{FH} that are present in the $B^{MHCII-/-}$ chimeras could be stalled in this differentiation state and so might continue their progression to the PD-1^{HI} T_{FH} pool after experiencing cognate interactions with MHC II^+ B cells. Whether these pre-PD-1^{HI} T_{FH} cells, embedded in the PD-1^{LO} T_{FH} pool, survive for some time in the absence of cognate B cells (or, in contrast, undergo apoptosis if required signals are not received at a certain point) is also an intriguing question, as it raises the subject of T_{FH} plasticity and of the reciprocal conversion between PD-1^{HI} T_{FH} and PD-1^{LO} T_{FH} populations.

To address the issue of T_{FH} ontogeny described above, adoptive transfer experiments were performed in which the PD-1^{LO} T_{FH} population (carrying the CD45.2 allelic marker) isolated from $B^{MHCII-/-}$ chimeras 6 days post SRBC immunisation was subsequently transferred into lightly irradiated (300Gy) congenic WT hosts (expressing CD45.1 allele). These mice were then challenged with SRBC approximately 36h post transfer and analysed 3 days later (Fig. 4.7A). I sought to answer the question whether PD-1^{LO} T_{FH} from $B^{MHCII-/-}$ chimeras could give rise to PD-1^{HI} T_{FH} after encountering B cells expressing MHC II and receiving fresh antigen supply.

As a control, PD-$1^+$$CXCR5^-$ T cells were also isolated from $B^{MHCII-/-}$ chimeras (activated extra follicular T cells, termed $CXCR5^-$ cells). Alongside $B^{MHCII-/-}$ chimeras, SRBC immunised WT chimeras were used for the isolation of PD-1^{LO} T_{FH}, PD-1^{HI} T_{FH} and $CXCR5^-$ cells. The sorting strategy was identical to that used in the T_{FH} cell isolation for the microarray (Fig. 2 on p. 57) and the purity of the sorted populations was similar (80-90%). However, the possibility of contamination between different populations cannot be fully excluded.

Analysis of the T_{FH} phenotype 5 days post adoptive transfer (as showed in Fig. 4.7) shows that, firstly, most of the PD-1^{LO} T_{FH} lose CXCR5 expression and acquire $CXCR5^-$ PD-1^+ T cell phenotype (46.38±1.69% of all transferred cells for WT chimera and 42.54±6.21% for $B^{MHCII-/-}$ chimeras, Fig. 4.7B and C). Secondly, a proportion of PD-1^{LO} T_{FH} cells retains their original CXCR5 and low PD-1 expression levels (Fig. 4.7B and C, 9.86±1.27% of all transferred cells for WT

chimera and 6.26±1.5% for $B^{MHCII-/-}$ chimeras). Thirdly, and most importantly, the PD-1^{LO} T_{FH} population from $B^{MHCII-/-}$ chimeras can give rise to PD-1^{HI} T_{FH} (Fig. 4.7B and C), and the frequency of conversion is similar to the PD-1^{LO} T_{FH} isolated from WT chimeras (Fig. 4.7D, % of all transferred cells with PD-1^{HI} T_{FH} phenotype derived from transferred PD-1^{LO} T_{FH} populations: 10.88±0.76% for WT chimera and 6.98±0.88% for $B^{MHCII-/-}$ chimeras). Notably, there is an equal division of transferred PD-1^{LO} T_{FH} into PD-1^{LO} T_{FH} or PD-1^{HI} T_{FH} cells: out of around 20% of $CXCR5^{+}$ cells half of them acquired high PD-1 expression and half has retained low PD-1 expression (Fig. 4.7D).

Interestingly, the $CXCR5^{-}$ population seems to be the most conservative in the retention of their phenotype (Fig. 4.7E). Most of the cells show $CXCR5^{-}$ phenotype after the transfer (58.53±0.99% of all transferred cells for WT chimeras and 50.46±2.26% for $B^{MHCII-/-}$ chimeras). Only a small proportion acquires CXCR5 expression and becomes PD-1^{LO} T_{FH} or PD-1^{HI} T_{FH}.

Overall the above results demonstrate that PD-1^{LO} T_{FH} from $B^{MHCII-/-}$ chimeras and PD-1^{LO} T_{FH} from WT chimeras are equivalent in their abilities to convert to PD-1^{HI} T_{FH} and to $CXCR5^{-}$ cells in the SRBC immunisation model.

In the next step, I have addressed the question whether PD-1^{HI} T_{FH} generated from PD-1^{LO} T_{FH} isolated from WT or $B^{MHCII-/-}$ chimeras show high Bcl6 expression levels, as observed in the de-novo induced PD-1^{HI} T_{FH} population in WT mice. Indeed, the analysis of Bcl6 MFI at day 5 post adoptive transfer clearly showed that PD-1^{LO} T_{FH} populations converted to PD-1^{HI} T_{FH} up regulate their Bcl6 expression (Fig. 4.7F and G). Furthermore, there are no differences, again, between PD-1^{LO} T_{FH} isolated from $B^{MHCII-/-}$ chimeras and WT chimeras (Fig. 4.7F and G).

Collectively, the T_{FH} adoptive transfer experiments showed that PD-1^{LO} T_{FH} from $B^{MHCII-/-}$ chimeras are equivalent to PD-1^{LO} T_{FH} from WT chimeras in their capacity to acquire PD-1^{HI} T_{FH} phenotype and up regulate Bcl6 levels, further suggesting that PD-1^{LO} T_{FH} are not in a terminally differentiated state and still exhibit considerable plasticity.

4.3.7 PD-1^{HI} T_{FH} convert at low frequency to PD-1^{LO} T_{FH}.

The results from section 3.6 have illustrated that PD-1^{LO} T_{FH} can convert to PD-1^{HI} T_{FH} upon adoptive transfer. Whether the opposite phenomenon is possible (PD-1^{HI} T_{FH} acquiring PD-1^{LO} T_{FH} phenotype) is also an intriguing question.

To address this issue PD-1^{HI} T_{FH} from WT chimera immunised with SRBC were analysed at day 5 post-adoptive transfer (as in Fig. 4.7A). Similarly to the PD-1^{LO} T_{FH} population, most of the transferred cells (51.0 ± 2.8% of transferred CD45.2 population) have lost CXCR5 expression and acquired the CXCR5$^-$ T cell phenotype (Fig. 4.8A and B). However, out of the remaining CXCR5 positive cells the vast majority retained high PD-1 expression: PD-1^{HI} T_{FH} phenotype was 4 to 5 times more abundant than PD-1^{LO} T_{FH} phenotype after the transfer (% of all transferred PD-1^{HI} T_{FH}-derived cells with PD-1^{HI} T_{FH} phenotype vs. PD-1^{LO} T_{FH} phenotype: 20.13 ± 2.65% vs. 4.62 ± 0.87%). Therefore, it is worth noting that while CXCR5 positive PD-1^{LO} T_{FH} cells split equally after transfer and antigen re-challenge into PD-1^{LO} T_{FH} and PD-1^{HI} T_{FH}, PD-1^{HI} T_{FH} preferentially keep their original phenotype. Overall, PD-1^{HI} T_{FH} show less plasticity than the PD-1^{LO} T_{FH} subset. (However, it is important to keep in mind that around 50% of both populations lose CXCR5 expression after adoptive transfer).

4.3.8 Results summary

- The development of PD-1^{HI} T_{FH} cells in response to SRBC immunisation requires antigen presentation by B cells, while PD-1^{LO} T_{FH} cells are formed independently of cognate B cell interactions (Fig. 4.2C, D and E).
- Despite prevalence of PD-1^{LO} T_{FH} cells expressing intermediate levels of Bcl6 GCs are not found after SRBC immunisation in the $B^{MHCII-/-}$ chimera (Fig. 4.4).
- The PD-1^{HI} T_{FH} population and GC formation are restored in $B^{MHCII-/-}$ chimeras by transfer of WT B cells, but not MHC $II^{-/-}$ B cells, in SRBC immunisation (Fig.4.5C, D and E; Fig.4.6).
- The adoptive transfer of PD-1^{LO} T_{FH}, isolated from $B^{MHCII-/-}$ chimera, to WT host and re-challenge with antigen demonstrates plasticity of this cell subset and its potential to differentiate into PD-1^{HI} T_{FH} population, which expresses high levels of Bcl6 (Fig.4.7B, C and D).
- PD-1^{HI} T_{FH} cells preferentially retain their phenotype after adoptive transfer and antigen re-challenge and convert at low levels to PD-1^{LO} T_{FH} cells, showing overall less plasticity than PD-1^{LO} T_{FH} subset (Fig. 4.8).

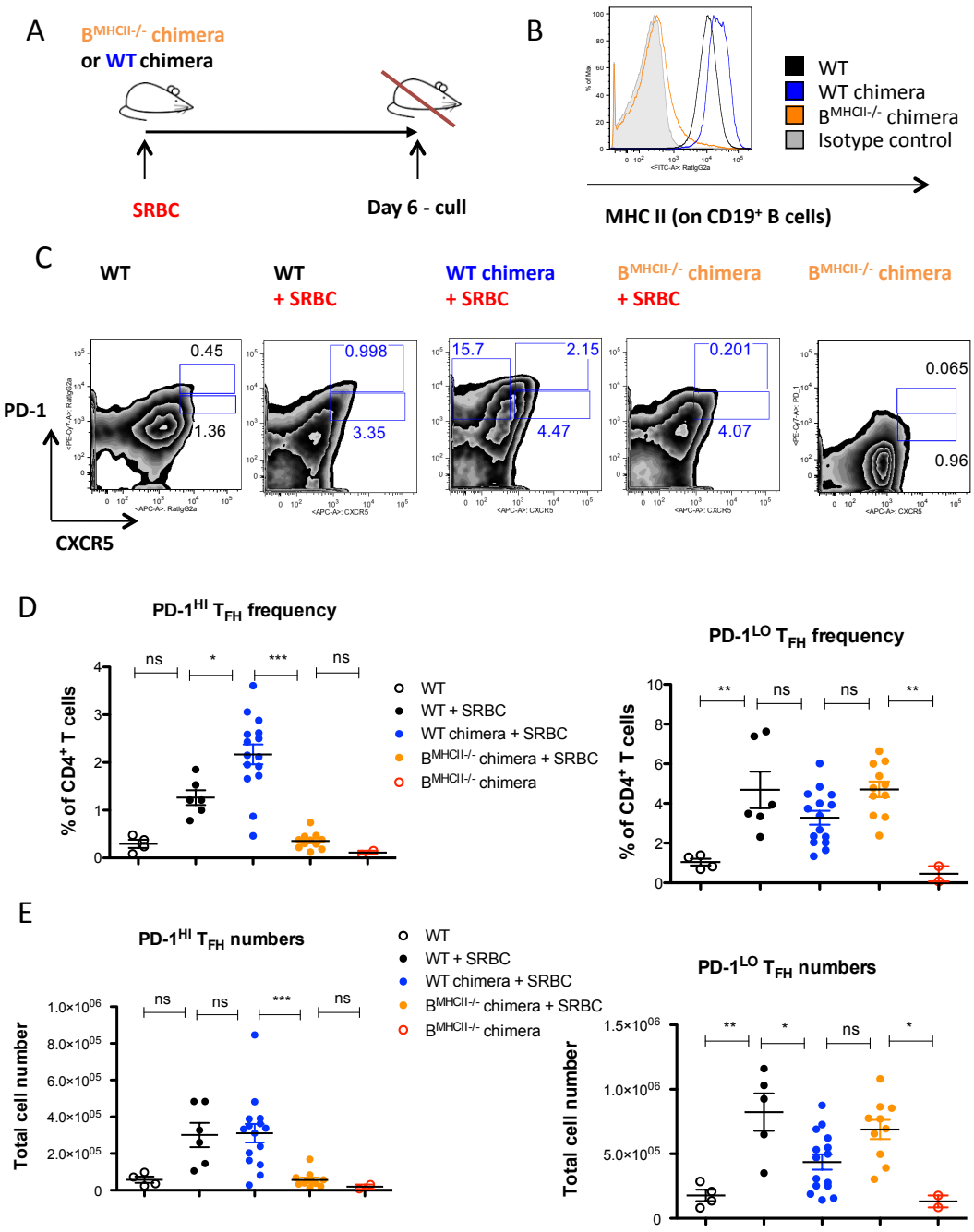

Fig 4.2. Formation of PD-1^{HI} T_{FH} depends on cognate interactions with B cells.

(A) Experimental outline of SRBC immunisation in WT or B$^{MHCII-/-}$ chimeras. **(B)** MHC II expression by B cells. **(C)** Representative flow cytometry plots of PD-1^{HI} T_{FH} and PD-1^{LO} T_{FH} CD4^{+} T cell populations in each mouse type. **(D)** Summary of PD-1^{HI} T_{FH} (left) and PD-1^{LO} T_{FH} (right) frequencies and **(E)** cell numbers.

Data pulled from 5 independent experiments (n=3-5, B$^{MHCII-/-}$ chimeras + SRBC), 4 independent experiments (n=3-5, WT+ SRBC), 6 independent experiments (n=1, WT + SRBC), 2 independent experiments (n=1, B$^{MHCII-/-}$ chimeras) and 4 independent experiments (n=1, WT), each dot represents one mouse.

Statistical significance was determined by One-way ANOVA with post-ANOVA Tukey's test for multiple comparisons.

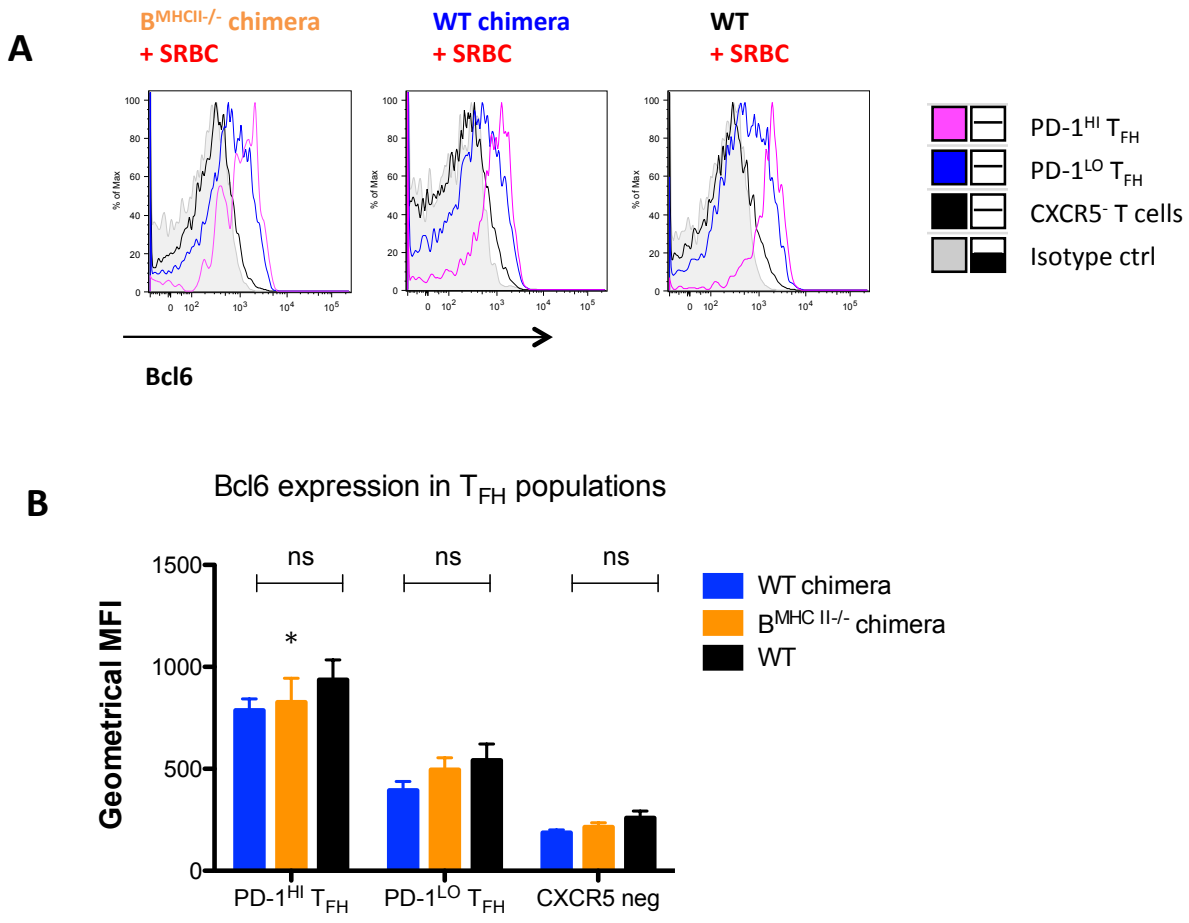

Fig 4.3. PD-1^{LO} T_{FH} present in B$^{MHCII-/-}$ chimeras express low levels of Bcl6.

(A) Representative flow cytometry plots of Bcl6 expression in PD-1^{HI} T_{FH} (pink line), PD-1^{LO} T_{FH} (blue line) and CXCR5^{-} CD4^{+} T cell populations (black line) in each experimental group 6 days after immunisation with SRBC. Shaded area shows isotype control. **(B)** Summary of Bcl6 expression as geometrical MFI in PD-1^{HI} T_{FH}, PD-1^{LO} T_{FH} and CXCR5^{-} T cells from WT chimeras (blue bars), B$^{MHCII-/-}$ chimeras (orange bars) or WT mice (black bars). Data pulled from multiple experiments.

* Gated on few PD-1^{HI} T_{FH} observed in B$^{MHCII-/-}$ chimeras (0.2-0.5.% of CD4^{+} T cells)

Experimental repeats as in Fig. 4.2.

Statistical significance was determined by One-way ANOVA with post-ANOVA Tukey's test for multiple comparisons.

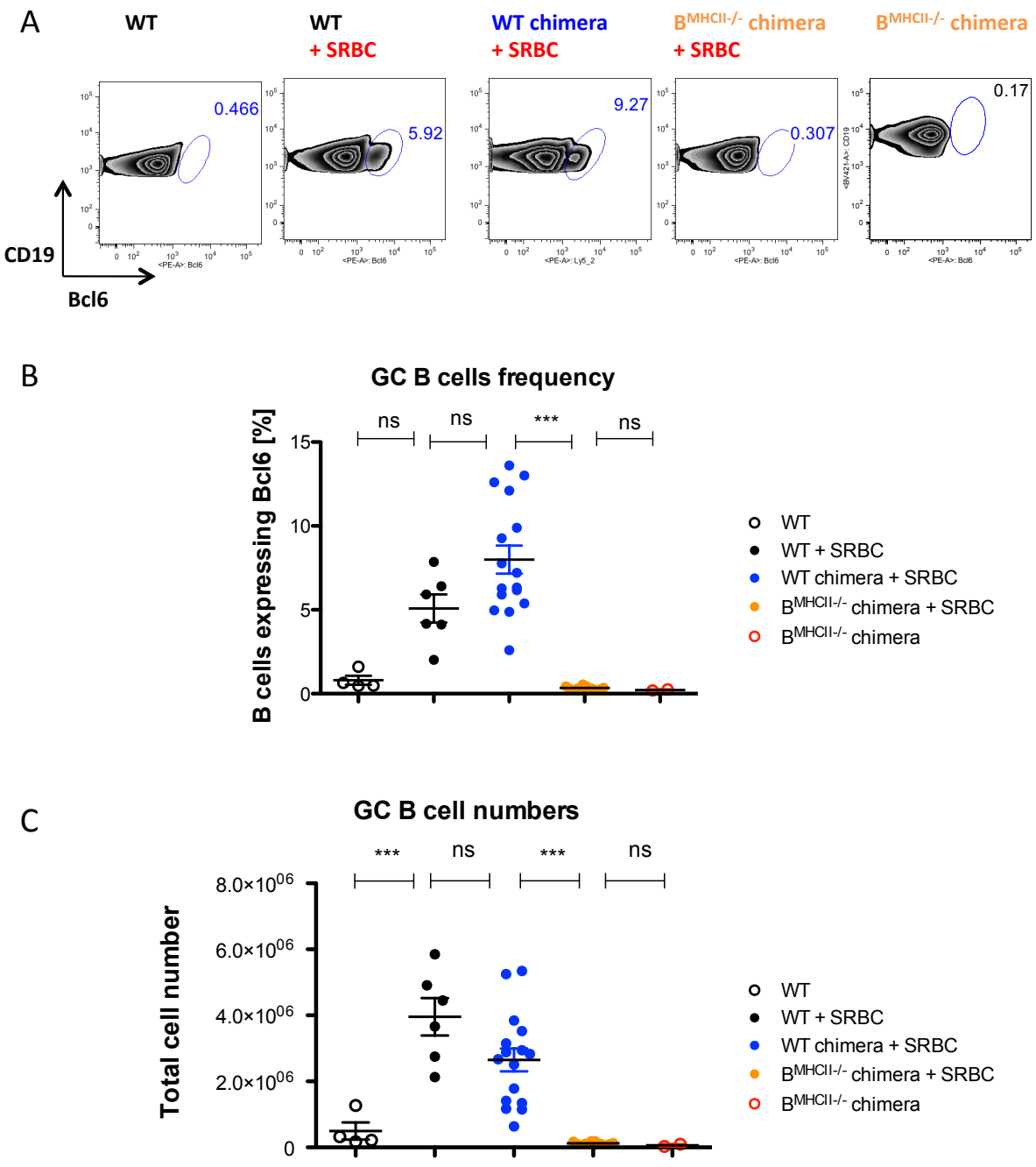

Fig 4.4. $B^{MHCII-/-}$ chimeras lack GC (GC) response.

(A) Representative flow cytometry plots of GC B cell staining in each experimental group 6 days post SRBC immunisation. GC B cell quantification showed as a frequency of total $CD19^+$ B cells **(B)** and absolute cell numbers **(C)**. Data pulled from multiple experiments, each dot represents one mouse.

Experimental repeats as in Fig. 4.2.

Statistical significance was determined by One-way ANOVA with post-ANOVA Tukey's test for multiple comparisons.

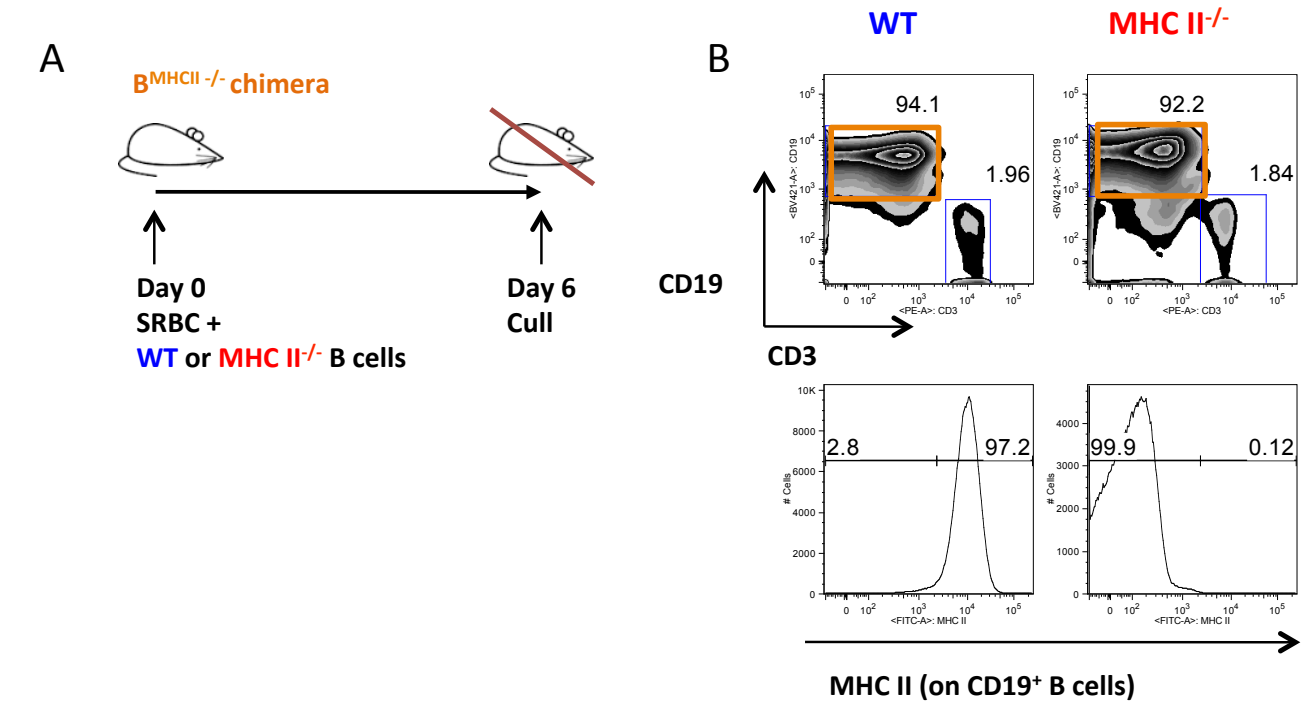

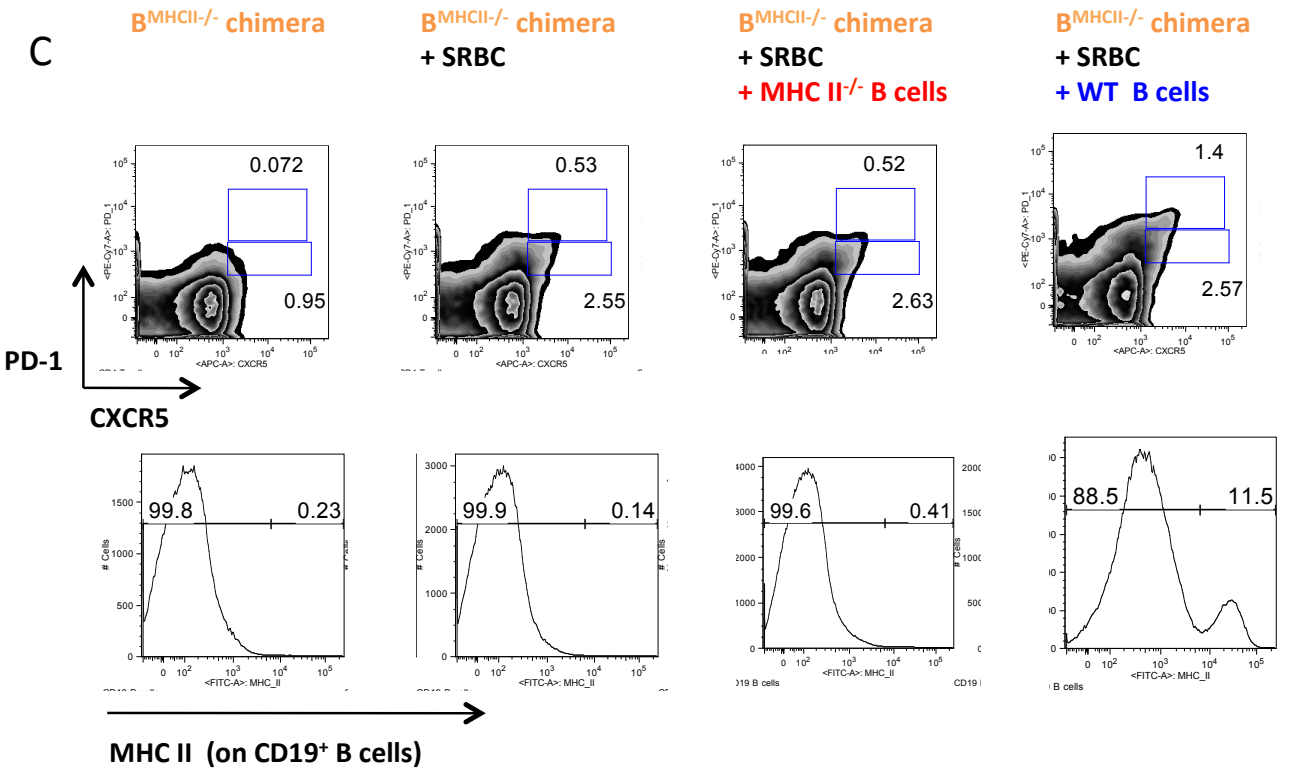

Fig 4.5. Continued overleaf.

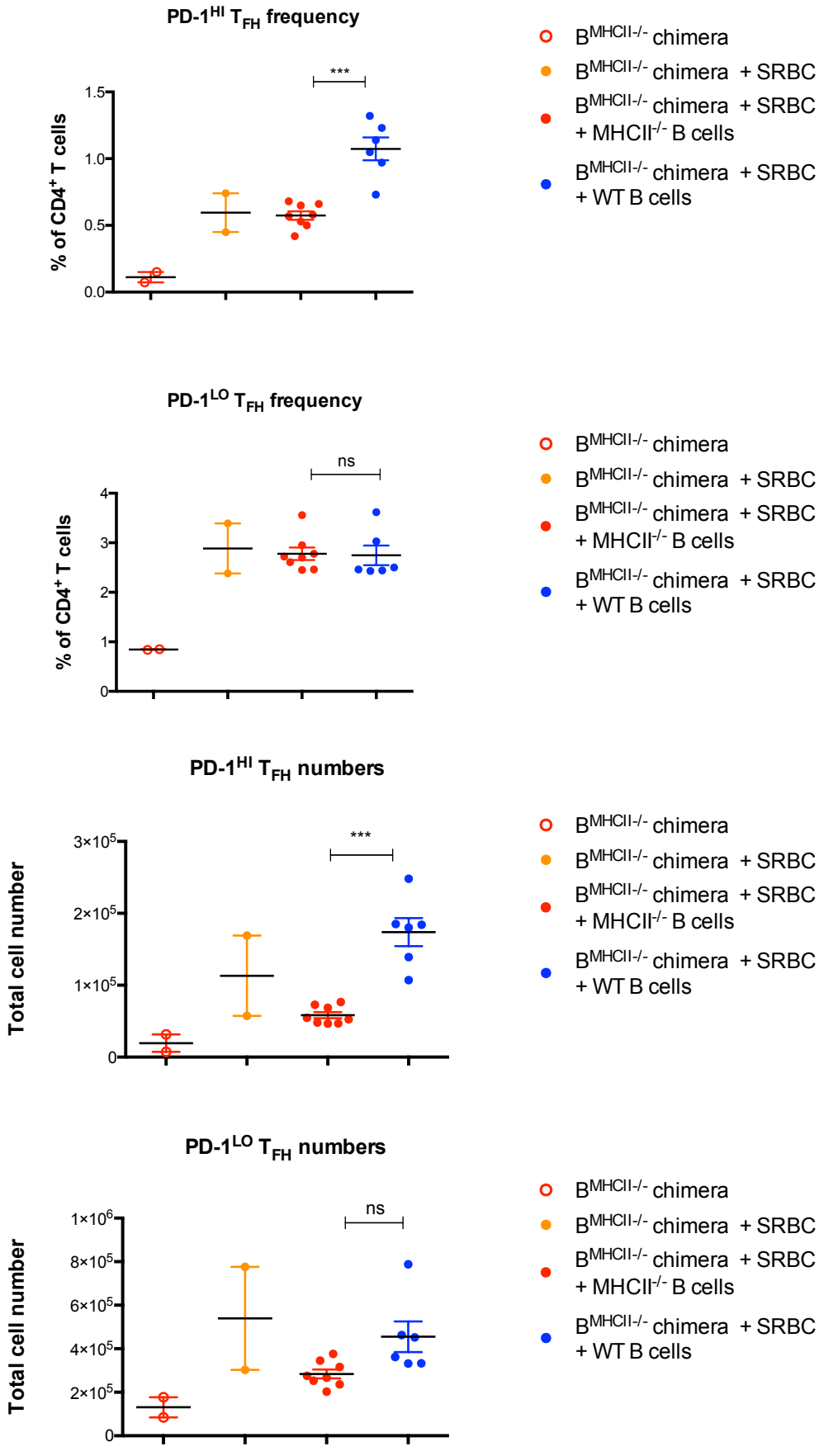

Fig 4.5. Continued overleaf.

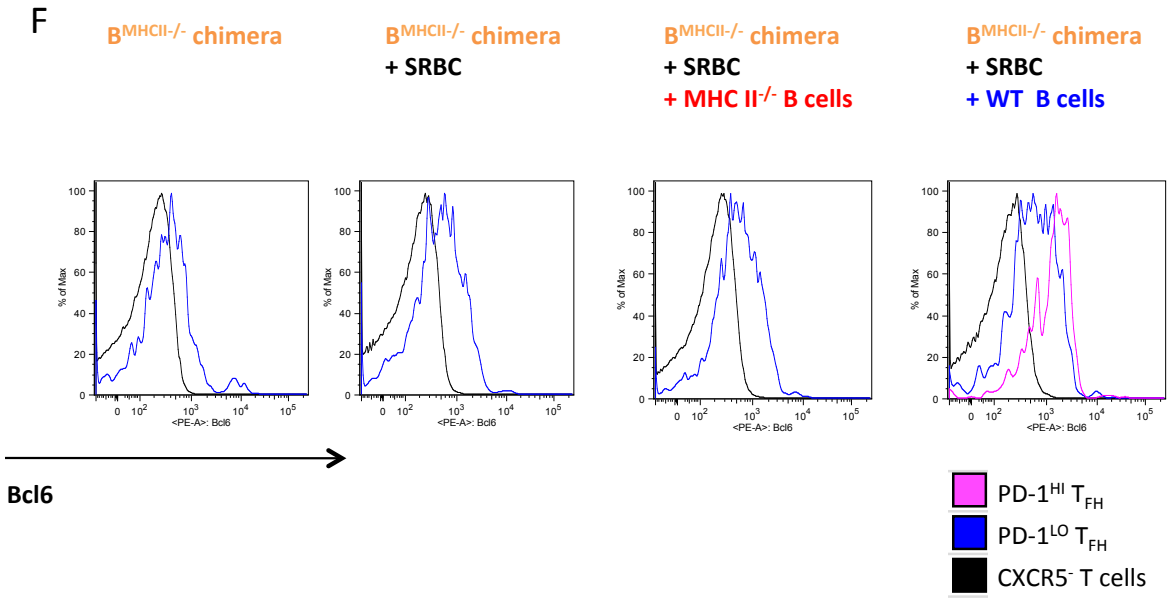

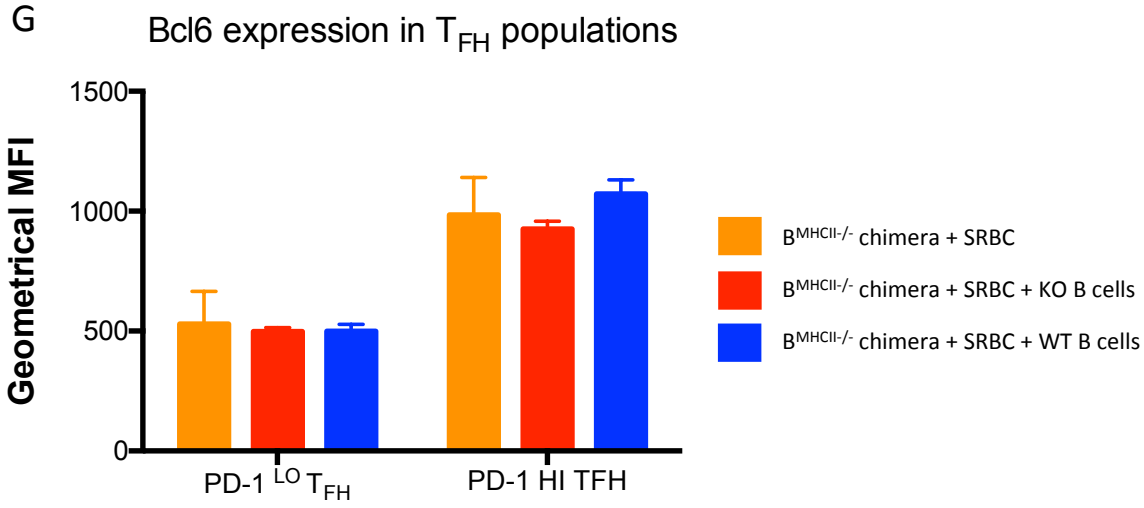

Fig 4.5. Transfer of WT, but not MHC II$^{-/-}$ B cells, rescues PD-1^{HI} T_{FH} formation in B$^{MHCII-/-}$ chimeras immunised with SRBC.

Outline of the B cell transfer experiments **(A)**. Purity of transferred CD19^{+} population (**B, upper panel**) and MHC II expression on transferred B cells (**B**, **lower panel**) assessed on day 0. Representative flow cytometry of PD-1^{HI} T_{FH}, PD-1^{LO} T_{FH} and CD4^{+} T cell populations from each of the experimental group **(C, upper panel)** and MHC II expression on CD19^{+} B cells (**C, lower panel**). **(D)** Summary of PD-1^{HI} T_{FH} and PD-1^{LO} T_{FH} frequencies and **(E)** cell numbers. Representative flow cytometry plots of Bcl6 expression in of PD-1^{HI} T_{FH}, PD-1^{LO} T_{FH} and naïve CD4^{+} T cells **(F, upper panel)** and summary of geometrical mean fluorescence intensity **(G)**.

Data pulled from two independent experiments with 2 animals per group (B$^{MHCII-/-}$ chimera, B$^{MHCII-/-}$ chimera + SRBC) or 4 animals per group (B$^{MHCII-/-}$ chimera + WT or KO B cells); each dot represents one mouse.

Statistical significance was determined by One-way ANOVA with post-ANOVA Tukey's test for multiple comparisons.

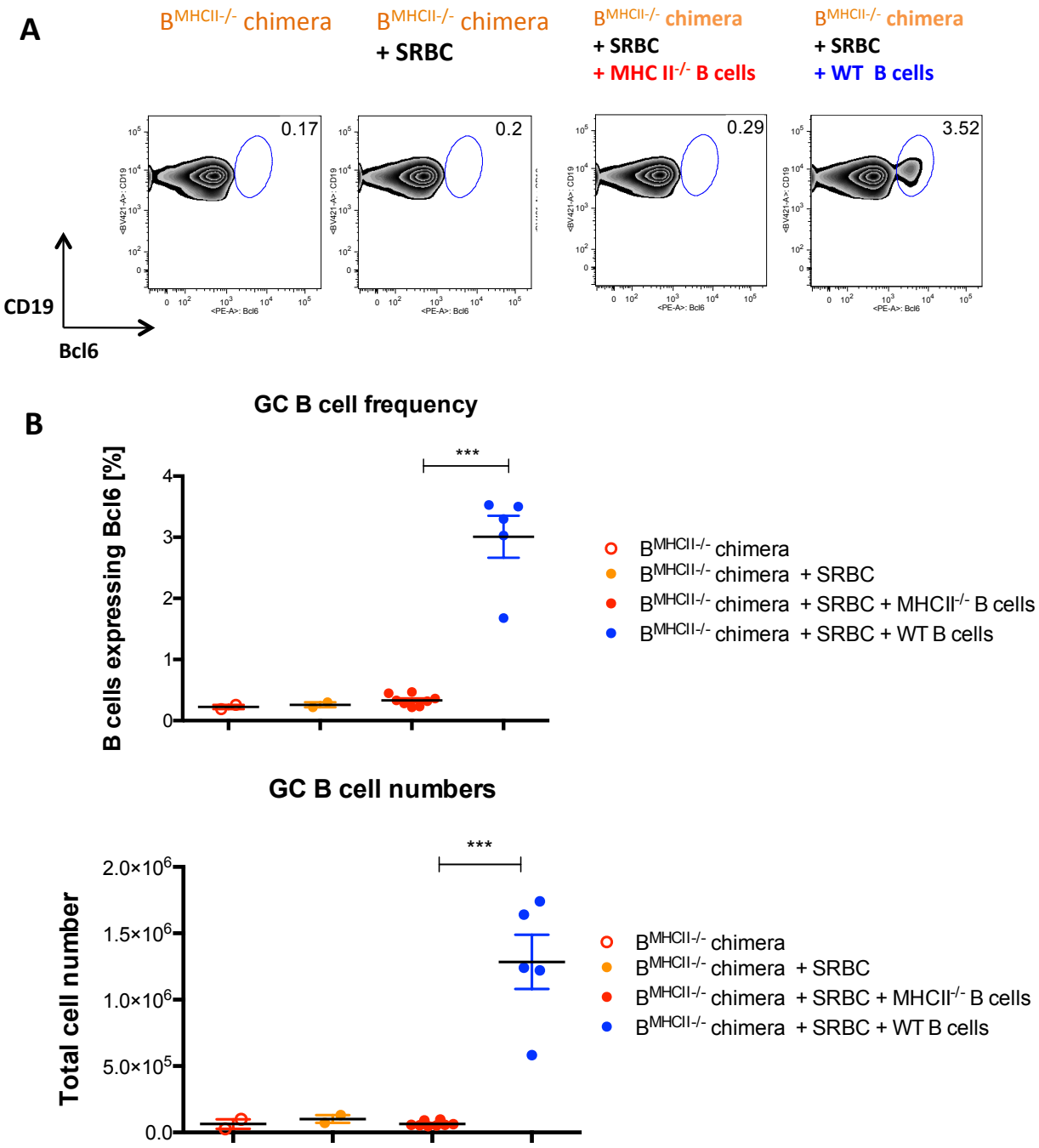

Fig 4.6. Transfer of WT, but not MHC II $^{-/-}$ B cells, rescues GC formation in B$^{MHCII-/-}$ chimeras at day 6 post SRBC immunisation.

(A) Representative flow cytometry plots of GC B cells from each of the experimental group. Gate frequencies indicate percentage of B cells. **(B)** Summary of GC B cell frequencies (left) and numbers (right). Data pulled from two independent experiments with 2 to 4 animals per group; each dot represents one mouse.

Experimental repeats as in Fig. 4.5.

Statistical significance was determined by One-way ANOVA with post-ANOVA Tukey's

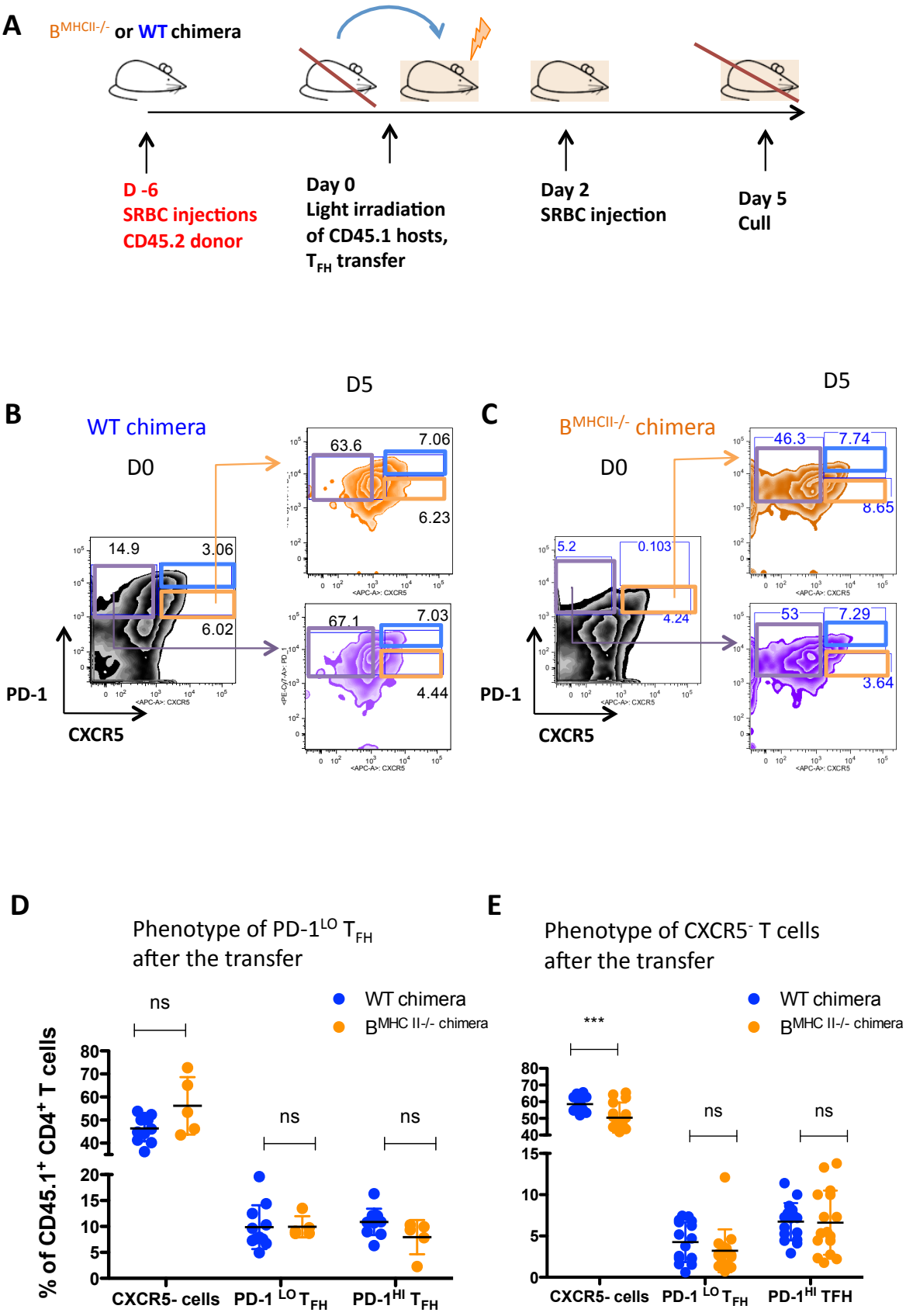

Fig 4.7. Continued overleaf.

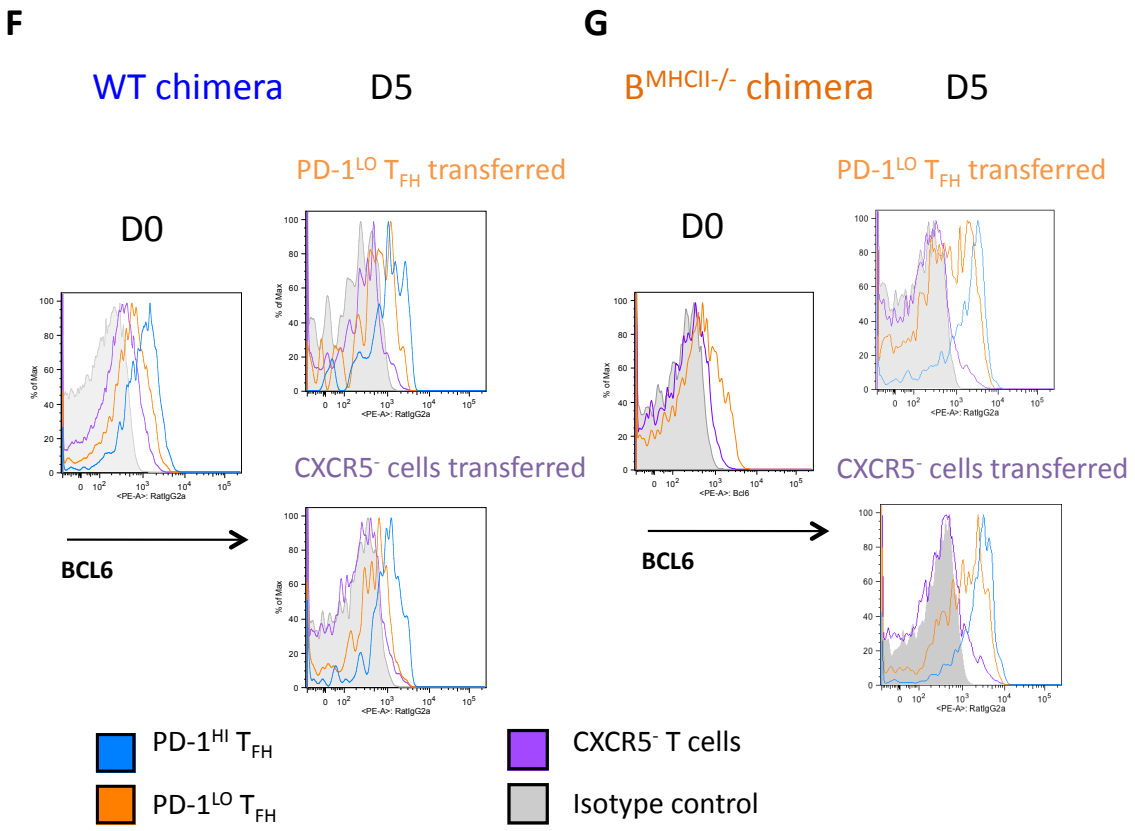

Fig 4.7. PD-1 ^{LO} T_{FH} generated in $B^{MHCII-/-}$ chimeras immunised with SRBC can convert to PD-1^{HI} T_{FH} and up regulate Bcl6 expression upon the transfer to WT host and re-challenge with SRBC.

(A) Experimental outline of T_{FH} transfer experiments. Flow cytometry plots of T_{FH} populations isolated from WT chimera **(B)** or $B^{MHCII-/-}$ chimera **(C)** on day 0 (left) or day 5 post transfer (right). Transferred PD-1^{LO} T_{FH} population is showed in orange and control CXCR5^{-} group in violet. Summary of the phenotype acquired by PD-1^{LO} T_{FH} **(D)** and CXCR5^{-} T cells **(E)** at day 5 post transfer. Bcl6-expression in T_{FH} populations (gated as in B and C) from WT chimeras **(F)** or $B^{MHCII-/-}$ chimeras **(G)** on day 0 (left) or day 5 post transfer (right).

Data pulled from 2 independent experiments (n=4-5, WT chimera) or 3 independent experiments (n=3-5, $B^{MHCII-/-}$ chimeras). Each dot represents a mouse.

Statistical significance was determined by One-way ANOVA with post-ANOVA Tukey's test for multiple comparisons.

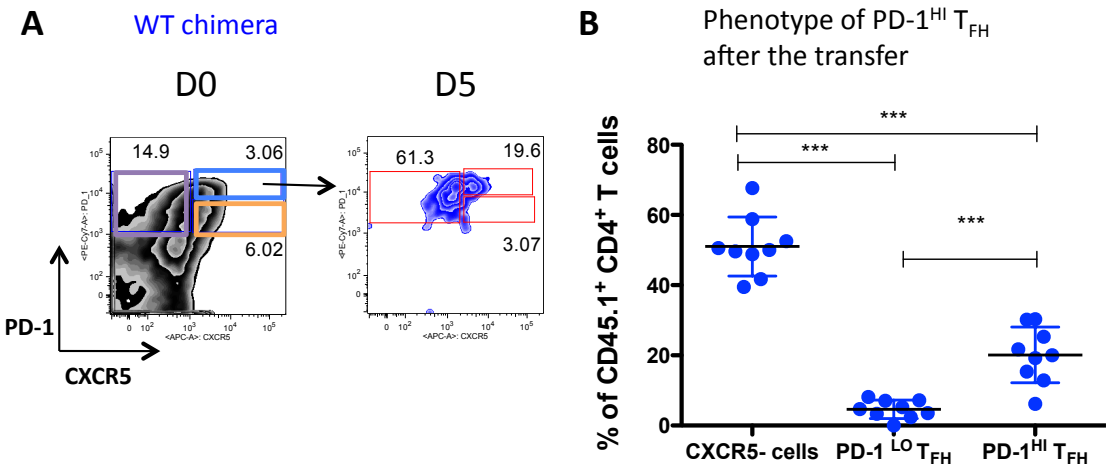

Fig 4.8. PD-1^{HI} T_{FH} from WT chimeras show less plastic phenotype and convert at low frequency to PD-1^{LO} T_{FH} upon the transfer to WT host and re-challenge with SRBC. **(**Experimental outline as in Fig. 4.6.A)

(A) Flow cytometry plots of T_{FH} populations isolated from WT chimera on day 0 (left) or day 5 post transfer (right). Transferred PD-1^{HI} T_{FH} population is showed in blue. **(B)** Summary of the phenotype acquired by PD-1^{HI} T_{FH} at day 5 post transfer. Data pulled from 2 independent experiments with 4 and 5 animals per group, each dot represents one mouse.

Statistical significance was determined by One-way ANOVA with post-ANOVA Tukey's test for multiple comparisons.

4.4 Discussion

4.4.1 Formation of PD-1^{HI} T_{FH} after SRBC immunisation depends on cognate interactions with B cells.

Using the SRBC immunisation model and $B^{MHCII-/-}$ chimeras provided an important insight into the requirement for the B cell antigen presentation in the T_{FH} development. While the generation of the PD-1^{LO} T_{FH} population 6 days post SRBC immunisation was not affected in terms of both cell frequency and numbers when compared to the control WT chimera or WT mice, PD-1^{HI} T_{FH} were virtually absent when B cells were lacking MHC class II expression. The fact that the PD-1^{HI} T_{FH} population depends so closely in its development on cognate contact with B cells further suggests potentially different locations and functions of these cells linked to B cell support and GC development. Another likely explanation for the observed phenomenon is that the PD-1^{HI} T_{FH} population requires continuous TCR stimulation as one of the survival signals (suggested by Shane Crotty (114)). In the context of the immune response this seems to be a plausible explanation since those GC-residing T_{FH} could have a constant access to the antigen from the surface of FDCs, which hold deposits of the antigen required for the B cell selection post SHM (210). Additionally, it has also been shown that the ablation of FDC leads to the disappearance of both GC B cells and T_{FH} (31). The issues of TCR specificity and diversity within T_{FH} populations are discussed in more details in Chapter 5.

PD-1^{LO} T_{FH} raised in $B^{MHCII-/-}$ chimeras in response to SRBC display lower levels of TF Bcl6 than PD-1^{HI} T_{FH} in the immunised control WT chimeras. Therefore it can be proposed that one of the mechanisms through which cognate B cells support PD-1^{HI} T_{FH} formation might be by providing high Bcl6 expression. However, it is important to point out that a small proportion of T_{FH} raised in $B^{MHCII-/-}$ chimeras after SRBC immunisation falls into the PD-1^{HI} T_{FH} gate and expresses high levels of Bcl6 that are equivalent to PD-1^{HI} T_{FH} from immunised WT mice or WT chimeras. This suggests that cognate interaction between T_{FH} and B cells is enhancing or stabilising high Bcl6 expression but may not be an absolute requirement for its induction. These results are in agreement with other studies which show that in the absence of cognate B cells $CXCR5^{+}$ PD-1^{+} T_{FH} cells are still formed and express higher levels of Bcl6

than naïve T cells (57,208,209). Furthermore, it was demonstrated that the maintenance of high CXCR5 and high PD-1 expression depends on antigen presentation by B cells (57). Finally, the T_{FH} subset expressing high levels of Bcl6 was not found when antigen presentation was limited to conventional $CD11c^{+}$ APC (209), which further highlights the need for cognate B cells in the formation of PD-1^{HI} T_{FH} cells.

Transfer experiments required separating the PD-1^{HI} T_{FH} and PD-1^{LO} T_{FH} populations. Although the purity of the sample was always assessed post sorting, possible contamination issues of PD-1^{LO} T_{FH} cells with PD-1^{HI} T_{FH} cell during sorting cannot be formally excluded. This could have the consequences for the downstream analysis of the phenotype acquired post activation, since low numbers of PD-1^{HI} T_{FH} cells transferred alongside PD-1^{LO} T_{FH} could theoretically expand in the adaptive host and restore PD-1^{HI} T_{FH} population.

4.4.2 $B^{MHCII-/-}$ chimeras lack GC response after SRBC immunisation

The development of GCs in $B^{MHCII-/-}$ chimeras in response to SRBC was completely abolished in terms of GC B cell frequency and number. At the same time, PD-1^{LO} T_{FH} cells were abundantly found in the spleens of immunised $B^{MHCII-/-}$ chimeras, indicating that the presence of this subset *per se* is not enough to drive GC structures in response to SRBC. This is in keeping with other findings, which show that despite the presence of cells with T_{FH}-like phenotype ($CXCR5^{+}$ PD-1^{+} $Bcl6^{+}$) GC formation is still impaired (208,209).

One could speculate that the lack of GC response in $B^{MHCII-/-}$ chimeras in the SRBC model is rather a direct effect of the lack of MHC II expression on B cells than a secondary consequence of the missing PD-1^{HI} T_{FH} subset. Interestingly, the study by Barnett *et al.* revealed an absence of the GC structure alongside the missing PD-1^{HI} T_{FH} population despite using the animal model in which MHC II expression is actually restricted to B cells (209). Another interesting aspect of T-B cell interaction worth considering is the possibility that GC B cells (and possibly cognate B cells) secrete a cytokine or other soluble factor, which influences T_{FH} generation in the first place. Deenick *et. al.* challenged this idea by showing that the T_{FH} population is not formed when T cells cannot physically engage with B cells despite

abundant GC structures present (208). They do so by transferring OT.II cells of WT and SAP KO background (the latter population being unable to form stable conjugates with B cells) to WT congenic recipients and immunizing with cognate antigen. T_{FH} cells were found to be exclusively derived from WT and not SAP KO OT.II cells (208), despite restored GCs. This experiment argues against the presence of a secreted germinal-centre-derived soluble factor as an exclusive means by which B cells support the T_{FH} development and further highlights the need for physical contact between T and B cells in T_{FH} generation.

The fact that B cells function as a crucial APC in the generation of the PD-1^{HI} T_{FH} is further illustrated in my results by the B cell transfer studies, where providing $B^{MHCII-/-}$ chimeras with only 5-10% of WT B cells alongside SRBC immunisation restored both PD-1^{HI} T_{FH} and GC formation. Unfortunately, from my analysis it cannot be distinguished whether GCs generated in this model were derived from a WT or MHC II deficient B cells (although that would be possible by means of flow cytometry). However, it is highly likely that they are of WT origin. To investigate the significance of co-stimulatory molecules displayed on the surface of cognate B cells, similar B cell transfer experiments, using $B^{MHCII-/-}$ chimeras and SRBC, could be carried out with ICOS-L or CD40L deficient B cells. Additionally, the transfer of *in vitro* activated non-cognate B cells (for example of MD4 background) could further help to investigate the importance of the activation status and antigen presentation by B cells in the PD-1^{HI} T_{FH} and GC formation. Also, providing WT B cells at different time points (for example at day 3 or 5 post SRBC immunisation) would help to understand the kinetics of cognate T-B cell interactions required for PD-1^{HI} T_{FH} population survival.

In summary, the presence of PD-1^{LO} T_{FH}, and the lack of both GCs and PD-1^{HI} T_{FH} in the absence of cognate B cells elegantly illustrate the functional consequences of the phenotypic differences observed in the previous results chapter.

4.4.3 PD-1^{LO} T_{FH} cells from $B^{MHCII-/-}$ can convert to PD-1^{HI} T_{FH} and express high levels of Bcl6.

The adoptive transfer of the PD-1^{LO} T_{FH} population (isolated from either WT or $B^{MHCII-/-}$ chimeras immunised with SRBC and re-challenged within 48 h post

transfer) demonstrated that this population is able to give rise to a PD-1^{HI} T_{FH} population, which expresses high levels of Bcl6. This is a very important finding. Firstly, it illustrates that T_{FH} cells need to interact with cognate B cells in order to acquire the PD-1^{HI} T_{FH} phenotype and stably express Bcl6. Secondly, it shows that activated T cells can become PD-1^{HI} T_{FH} cells after receiving the appropriate signal. One might speculate that some of the PD-1^{LO} T_{FH} cells stall in their progression (but do not undergo apoptosis) to the PD-1^{HI} T_{FH} stage until cognate interaction with B cells has occurred. Overall, the possibility of a conversion from PD-1^{LO} T_{FH} (and, to a lesser extent, also $CXCR5^-$ cells) to PD-1^{HI} T_{FH} shows that recruitment to the latter pool is a continuous process, occurring beyond the priming stage of a naïve $CD4^+$ T cell during an immune response. Importantly, the significant level of heterogeneity within the PD-1^{LO} T_{FH} population is illustrated by the fact that the split between the cells acquiring PD-1^{LO} T_{FH} or PD-1^{HI} T_{FH} phenotype is close to 50% (among $CXCR5^+$ cells).

Interestingly, adoptively transferred $CXCR5^-$ cells (isolated either from SRBC-immunised WT or $B^{MHCII-/-}$ chimeras) can also acquire a T_{FH} phenotype although their frequency of conversion is lower than the one observed for the PD-1^{LO} T_{FH} subset. Intriguingly, $CXCR5^-$ cells seem preferentially to become PD-1^{HI} T_{FH} rather than PD-1^{LO} T_{FH}. Therefore, adoptive transfer experiments suggest that neither PD-1^{LO} T_{FH} nor $CXCR5^-$ cells are terminally differentiated cell subsets, and as activated cells, both can continuously supply the PD-1^{HI} T_{FH} pool. This is important for the progression of a secondary immune response, since the possibility of drawing PD-1^{HI} T_{FH}, which support GCs, from more than one cell population creates the option to respond to newly arising antigens (for example in case of mutating viruses) or pathogens closely related, but not identical, to the ones encountered in the past.

4.4.4 The PD-1^{HI} T_{FH} population generated in WT chimera after SRBC immunisation preferentially retains its phenotype after adoptive transfer.

The adoptive transfer of the PD-1^{HI} T_{FH} population (isolated from WT chimeras immunised with SRBC and re-challenged within 48 h post transfer) provided an important insight into the differentiation state of this cell subset. Although the majority of the transferred PD-1^{HI} T_{FH} population has lost CXCR5 expression

(similarly to PD-1^{LO} T_{FH} cells), the cells that remained CXCR5 positive showed also high PD-1 and Bcl6 expression. Therefore, very few of the original PD-1^{HI} T_{FH} cells have converted to PD-1^{LO} T_{FH} cells. Importantly, whereas PD-1^{LO} T_{FH} split equally after the transfer between PD-1^{LO} T_{FH} and PD-1^{HI} T_{FH} (when taking into account CXCR5 positive cells), there were on average 5-6 times more PD-1^{HI} T_{FH} than PD-1^{LO} T_{FH} after the antigen boost than when the PD-1^{HI} T_{FH} population was transferred. This finding suggests that the PD-1^{HI} T_{FH} population is in a more terminally differentiated state than PD-1^{LO} T_{FH} since it shows very little plasticity. Moreover, when the frequency of conversion to PD-1^{HI} T_{FH} cells is compared between originally isolated PD-1^{HI} T_{FH}, PD-1^{LO} T_{FH} and CXCR5- cells (from either WT or $B^{MHCII-/-}$ chimeras), it is clear that most of the PD-1^{HI} T_{FH} cells generated after adoptive transfers come from the PD-1^{HI} T_{FH} subset. This may be advantageous for the organism during a secondary infection, since the ability to draw a GC-associated population from the pool of the cells, which has already been selected on the basis of their ability to interact with cognate B cells might shorten the time of the response.

Intriguing questions arising from the analysis of PD-1^{HI} T_{FH} transfers regards the signals, which are required by this population to retain its phenotype. After the transfer to congenic recipient cells have a possibility to interact with all APC (including B cells) post SRBC boost. It is therefore reasonable to speculate that continuous access to the antigen might be one of the requirements for retaining high CXCR5, PD-1 and Bcl6 expression, since PD-1^{HI} T_{FH} subset expresses higher levels of these proteins than PD-1^{LO} T_{FH} population. This hypothesis could be further tested by adoptive transfer of the PD-1^{HI} T_{FH} population to congenic hosts without SRBC boost and by assessing their phenotype in the steady state conditions after they have been deprived of antigen supplies.

Alongside antigen recognition and TCR signaling, the PD-1^{HI} T_{FH} phenotype can be driven by other receptors (including co-stimulatory molecules) displayed on the surface of different APCs. The contributions of cognate interactions between PD-1^{HI} T_{FH} and APCs could be investigated by adoptively transferring the PD-1^{HI} T_{FH} population to MHC II KO mice. Furthermore, the involvement of B cells specifically could be explored by transferring PD-1^{HI} T_{FH} cells into $B^{MHCII-/-}$ chimeras. Finally, to

disentangle the role of DCs in this process, depletion of $CD11c^+$ DCs could be performed prior to the PD-1^{HI} T_{FH} transfer into CD11c DTRX mice (211)[7]. Transferring the PD-1^{LO} T_{FH} population alongside would provide a more detailed insight into the different requirements for contact with cognate APCs of these two populations.

4.4.5 Loss of CXCR5 expression post adoptive transfer

One of the important observations from adoptive transfers of T_{FH} populations from the SRBC-immunised WT and $B^{MHCII-/-}$ chimeras to the WT hosts is that a majority of CXCR5 positive cells (PD-1^{LO} T_{FH} and PD-1^{HI} T_{FH}) down regulate CXCR5 expression by day 3 post transfer and re-challenge with SRBC.

In all of the adoptive transfer experiments (including 24h transfer) the recipient animals have received a light dose of irradiation, which could influence splenic structure, the positioning of transferred cells and the subsequent chemokine receptor expression. This does not explain, though, why some cells retained CXCR5 expression. Another possibility is that finding the 'right' location by transferred cell is a random process, and therefore some cells will find the right way and survive with keeping their original phenotype whereas other will loose or change their chemokine receptor expression.

In the published study with Bcl6 reporter mice, vast majority (80-90%) of $CXCR5^+$ and $CXCR5^-$ cells have retained their original phenotype after adoptive transfer and antigen challenge (87). This proportion has decreased to 50% (of $CXCR5^+$ cells keeping their phenotype) when cells were left to rest in antigen-free environment for 20-30 days (87). The important difference in the experimental set up is that T_{FH} cells were isolated in my experiments at the peak of the response to SRBC (day 6 p.i.) whereas Liu and colleagues transferred small population of cells from the draining lymph nodes 20-30 days p.i. with protein antigen. Therefore, these cells had a chance to stabilize their phenotype (and undergo contraction phase). Nevertheless,

[7] These transgenic mice have diphteria toxin receptor expressed under the CD11c promoter and efficient depletion of $CD11C^+$ DC can be achieved by administration of diphteria toxin (211).

phenotype of cells, which retained CXCR5 expression, provided important information about differentiation cues of T_{FH} population.

4.4.6 Transferred T_{FH} populations have different recovery rates.

In the T_{FH} adoptive transfer experiments with WT or $B^{MHCII-/-}$ chimeras immunised with SRBC significant differences in the frequency and numbers of the CD45.2 positive cells could be observed between transferred populations recovered from CD45.1 congenic recipients mice at day 3 post transfer. $CXCR5^{-}$ cells showed consistently the highest frequency of recovery and PD-1^{HI} population the lowest (Appendix Fig. 7.6). This could be explained, firstly, by differences in dissemination to other organs post transfer, secondly, by different proliferation rates (discussed in Chapter 3 in part 3.2.) or, thirdly, by distinct intrinsic apoptotic and survival properties of the transferred populations.

The observed differences in the recovery of transferred populations were not due to differences in the dissemination of the isolated subsets within other SLO, as CD45.2 transferred cells were virtually non-detectable in the axillary, brachial, inguinal, mesenteric, and popliteal lymph nodes in any of the transferred groups 24h post i.v. injections (data not shown). Furthermore, entry to the lymph nodes via HEV requires CD62L expression (212). The population found with the lowest frequency after the transfer (PD-1^{HI} T_{FH}, Appendix Fig. 7.6) expresses very low levels of CD62L (Fig. 3.6C), which makes PD-1^{HI} T_{FH} even less prone to lymph node homing, and this explanation is therefore not very plausible.

The second likely explanation for the observed recovery rates concerns the differences in proliferation between the populations. As shown in Fig. 3.7,_Ki67 staining points to the fact that there are no differences in proliferation between PD-1^{HI} T_{FH} and other populations.

Finally, the third possible explanation could be the differences in the survival of those populations due to their intrinsic pro-apoptotic potential. This question has not been directly addressed but one could do it by flow cytometry staining for proteins known to be involved in apoptosis, such as Bcl-2 and activated Caspase-3 and Caspase-7. Nevertheless, despite differences in the recovered numbers of the

transferred cells, the proportion of PD-1^{HI} T_{FH}, PD-1^{LO} T_{FH} and $CXCR5^-$ cells converting into other subsets was very consistent between the animals used in multiple experiments and the large group size enabled statistical testing of the hypothesis.

4.4.7 Discussion summary

The experiments presented in this chapter investigate cognate T-B cells interaction using a model in which MHC II deficiency is almost exclusive to the B cell compartment. Interestingly, the study by Barnett *et. al.* uses the opposite strategy by employing transgenic mice, where MHC II expression is restricted to the B cell compartment (B-MHC II mice, (209)). Adoptive OT.II T cell transfer and peptide immunisation demonstrated that when MHC II expression is limited to B cell lineage $CD4^+$ T cells are primed inefficiently and T_{FH} cells and GCs are not formed (209). Interestingly, when LCMV-specific Smarta T cells are transferred to the B-MHC II mice and challenged with LCMV, 90% of transgenic T cells show T_{FH} phenotype (compared to 50% in a WT control), which indicates that priming *in vivo* by B cells in the context of viral infection skews antigen specific T cells towards the T_{FH} phenotype. Intriguingly, in this adoptive transfer model GC are not formed and almost no IgG^+ antigen specific antibodies found (209). Overall, the paper demonstrates that when B cells are the only functional APC functional T_{FH} cells are not induced, despite up regulating expression of CXCR5 and PD-1 on the cell surface after viral infection. Interestingly, exclusive MHC II expression by DCs also leads to the generation of $CXCR5^+$ PD-1^+ T_{FH} cells expressing Bcl6, but, again, these cells are not functional in terms of IL-21 secretion and GC support (81). Restoring MHC II expression in DCs (alongside MHC II competent B cells) rescues both T_{FH} and GC development (209), which illustrates that cooperation between different APCs is essential to provide optimal T_{FH} and humoral responses after protein or peptide immunisation, or viral infection (209), (81).

5 TCR repertoire of T_{FH} populations generated after immunisation with SRBC and *S. enterica*

5.1 Introduction

In Chapter 3 I have investigated PD-1^{HI} T_{FH} and PD-1^{LO} T_{FH} populations formed after immunisation with SRBC and *S. enterica* by characterising their phenotype by flow cytometry and investigating their transcriptional profile using microarray analysis. In the following chapter (Chapter 4) I studied the dependency of PD-1^{HI} T_{FH} and PD-1^{LO} T_{FH} from SRBC model on cognate interactions with B cells, leading ultimately to a discussion on the development and plasticity of T_{FH} cells. In this chapter I go on to investigate the relationship and potential for interaction between PD-1^{HI} T_{FH} and PD-1^{LO} T_{FH} subsets. I was interested to know if the aborted T_{FH} differentiation I observed during *S. enterica* infection (PD1^{LO} T_{FH}) could be corrected by a concurrent immune response to SRBC, which drives strong PD1^{HI} T_{FH} response. Not only was this the case but the co-immunisation study with SRBC and *S. enterica* resulted in an unexpectedly high number of PD1^{HI} T_{FH}.

We wanted to see if the expanded PD1^{HI} T_{FH} cells after co-immunization were *Salmonella*–specific PD1^{LO} T_{FH} that were converted to PD1^{HI} T_{FH} under the influence of the SRBC response. Alternatively, the SRBC-specific PD1^{HI} T_{FH} could be expanded as a result of the concomitant response to *S. enterica* (and adjuvant effect). To address this question we needed to identify the specificity of the T cells in each of the responses. As appropriate MHC II tetramers were not readily available we sequenced TCR V genes, as we hypothesized that the two responses would exhibit different and readily distinguishable TCRα/β V gene repertoire expansions. The results of TCRβ V gene sequencing show that, indeed, *S. enterica* infection leads to the expansion of selected TCR clones while SRBC immunisation results in polyclonal T cell activation with little evident clonal selection.

Fascinatingly, T_{FH} populations expanded in the co-immunised animals seem to exhibit an expansion of both SRBC- and *Salmonella*-activated T cells demonstrating that presence of SRBC can recruit *Salmonella*-specific PD-1^{LO} T_{FH} into the PD-1^{HI} T_{FH} population. Finally, the analysis of TCR diversity showed no differences

between PD-1^{HI} T_{FH} and PD-1^{LO} T_{FH} from SRBC model, demonstrating that there is no preferential TCR combination in any of the populations. This ultimately led to the discussion of TCR repertoire diversity within the T_{FH} populations.

5.1.1 TCR structure and diversity

The specificity and binding strength of the TCR to peptide:MHC complex has a crucial impact on the selection, survival and differentiation of each T cell (213-215). Whether T cells are recruited to the T_{FH} pool on the basis of their TCR clonotypes is unclear and so far only a handful of studies (discussed later) have addressed this issue. This chapter opens the discussion on the TCR repertoire found in different T_{FH} populations by using next generation sequencing technology to interrogate TCR diversity of PD-1^{HI} and PD-1^{LO} T_{FH} cells from the SRBC and *S. enterica* models.

The T cell receptor (TCR) is a heterodimer made of two chains, α and β (Fig. 5.1A). Each chain consists of variable (V), diversity (D, only in β chain), joining (J) and constant (C) subunits ((216,217), Fig. 5.1). TCRαβ arrangement occurs in thymus where stochastic recombination of V, D and J segments takes place to ensure that a great number of diverse TCRs is generated in the T cell population (213). Adding or deleting nucleotides in a random fashion at the junctions of the segments (V-J for α chain; V-D and D-J for β chain) further enhances TCR diversity (214). Finally, random pairing of α and β chains also increases combinatorial TCR variety (213,214). Overall, the number of possible unique TCRs is estimated at $1x10^{18}$ for mouse and $1x10^{15}$ in human (218,219). However, this number is limited by the thymic selection (due to deletion of self-reacting clones and clones that have no affinity for MHC) and overall the estimated number of TCRs actually found in the periphery is a couple of magnitudes lower: $2x10^6$ clonotypes in mouse and $2.5x10^7$ in human (213), although some sources estimate human TCR clones as $3x10^6$ (218,220).

The TCR sequence diversity is focused in complementary-determining regions (CDRs), which are parts of TCR contacting peptide:MHC molecule ((213,221), Fig. 5.1 B and C). There are three CDRs (CDR1-3) within the α chain and three within the β chain. The CDR1 and CDR2 regions of TCR interact with the MHC molecule,

whereas the CDR3 region forms an antigen-binding site as it is positioned above the peptide in the p:MHC complex (Fig. 5.1C, (213)). CDR3 covers parts of the V, D and J segments (Fig. 5.1B) and the flexibility of CDR3 loops adds further promiscuity in the TCR binding by enabling the recognition of peptides with similar sequences (222).

The importance of TCR diversity is illustrated by the mouse models in which, due to genetic manipulation, the diversity of TCR has been artificially limited. For example, in NZW mice with deleted TCR segments Vβ5 and Vβ8-13 TCR diversity shows a 60% reduction and there is a severe impairment in immune responses to 11 out of 22 tested antigens (213). OT-1β transgenic mice with only 2% of normal TCR diversity ($4x10^5$ clones) fail to reject F1 BM (213). Furthermore, in humans, 99.9% reduction of TCR results in a 7 to a 100 fold reduction in responses to mitogens and antigens (213). The above examples clearly show that TCR diversity is absolutely essential for maintaining effective immune responses to foreign and self antigens.

5.1.2 Repertoire analysis by Next Generation Sequencing

So far TCR diversity was investigated and estimated by a method called PCR spectratyping or immunoscope (213,218, 219). This approach was labour, time and cost intense and was significantly limited in resolution by only providing information about the CDR3 length and not the exact nucleotide sequence (220). A breakthrough for TCR interrogation occurred when next generation sequencing (NGS) became commercially available (220). NGS enables to investigate the TCR repertoire in an unprecedented fashion by providing the TCR sequence on the level of the single cell. Moreover, the enormous diversity of TCR sequences can only be captured by collecting the data of a very large number of unique TCRs (218). We have therefore decided to employ the NGS technology to probe the TCR repertoire of T_{FH} populations and address the unappreciated issue of TCR diversity in T_{FH} subsets (Fig. 5.2).

Sorted T_{FH} populations isolated 6 days p.i. with SRBC or *S. enterica* were subjected to mRNA isolation and cDNA synthesis on magnetic beads. This was followed by creating amplicons (amplified sequences of interest) of TCR-β V-regions using PCR with indexed primers, which enabled the identification of the

TCR sequence derived from a single cell. The PCR products were then separated by gel electrophoresis and purified by extraction from the agarose bands. Concentration by ethanol precipitation was performed as a last step prior to sequencing. The overview of the whole process is presented in Fig. 5.2.

Next generation sequencing can be performed with many platforms, which differ in sequencing biochemistry. For this study, the Illumina MiSeq sequencing technology was used (223). This technology is described as sequencing by synthesis since it detects the single nucleotides as they are inserted into growing DNA strands (224). Briefly, dNTPs carry a reversible terminator with a fluorescent tag attached. dNTPs are imaged as they are incorporated in the strand (only one base is inserted at the time) and the terminator is subsequently cleaved, allowing for the insertion of the next base (224). This approach is preferable for the analysis of TCR due to its high accuracy (it is less prone to insert or delete nucleotides, so called in–del mistakes, than e.g. Roche 454 sequencing, (218)). Important advantage of Illumina MiSeq over other sequencing platforms (e.g. Illumina 2500, also commonly used in RNA sequencing) is that it provides reliable read for sequences of around 400 bp long, which means that whole V gene sequence is covered with a single read (and there is no need for re-assembling shorter forward and reverse reads). In the platforms providing shorter reads final sequences are then reassembled bioinformaticaly, which is impossible for V genes due to the high number of very similar sequences. Additionally, in this study 3' end of the V region was a first part to be sequenced, which is important as a quality of sequencing goes down as the read length progresses. Therefore, the TCR sequencing was designed to ensure that variable sequences will be a full length and a high quality sequence, without need for sequence re-assembly.

TCR sequencing focuses on the CDR3 region, since, due to its tremendous diversity, it is characteristic for only one clone of T cell (218). Moreover, it can be sequenced with shorter reads and higher throughput (218). As a result, specialised programmes tailored for the investigation of CDR3 regions of the sequencing data became available (as described below). These programmes join sequencing technology with bioinformatic analysis.

Vast amount of data generated by NGS requires a careful analysis in order to provide reliable and reproducible results. Open source software programmes emerge as a standard strategy designed for the specific analysis of the primary data (218). One such software created especially for the analysis of the sequencing results of TCR α and β chains is MiTCR (225). This platform was used for the analysis of the T_{FH} TCR repertoire described in this chapter since it is specialised in CDR3 sequence extraction (218). In addition to that, the MiTCR programme enables quality control of the raw sequence, identification of V, D and J segments, correction or deletion of low quality reads and clonotypes assembly (Fig. 5.3, (225)). It thus represents an excellent, standardised tool to investigate details of lymphocyte biology with the single cell receptor resolution.

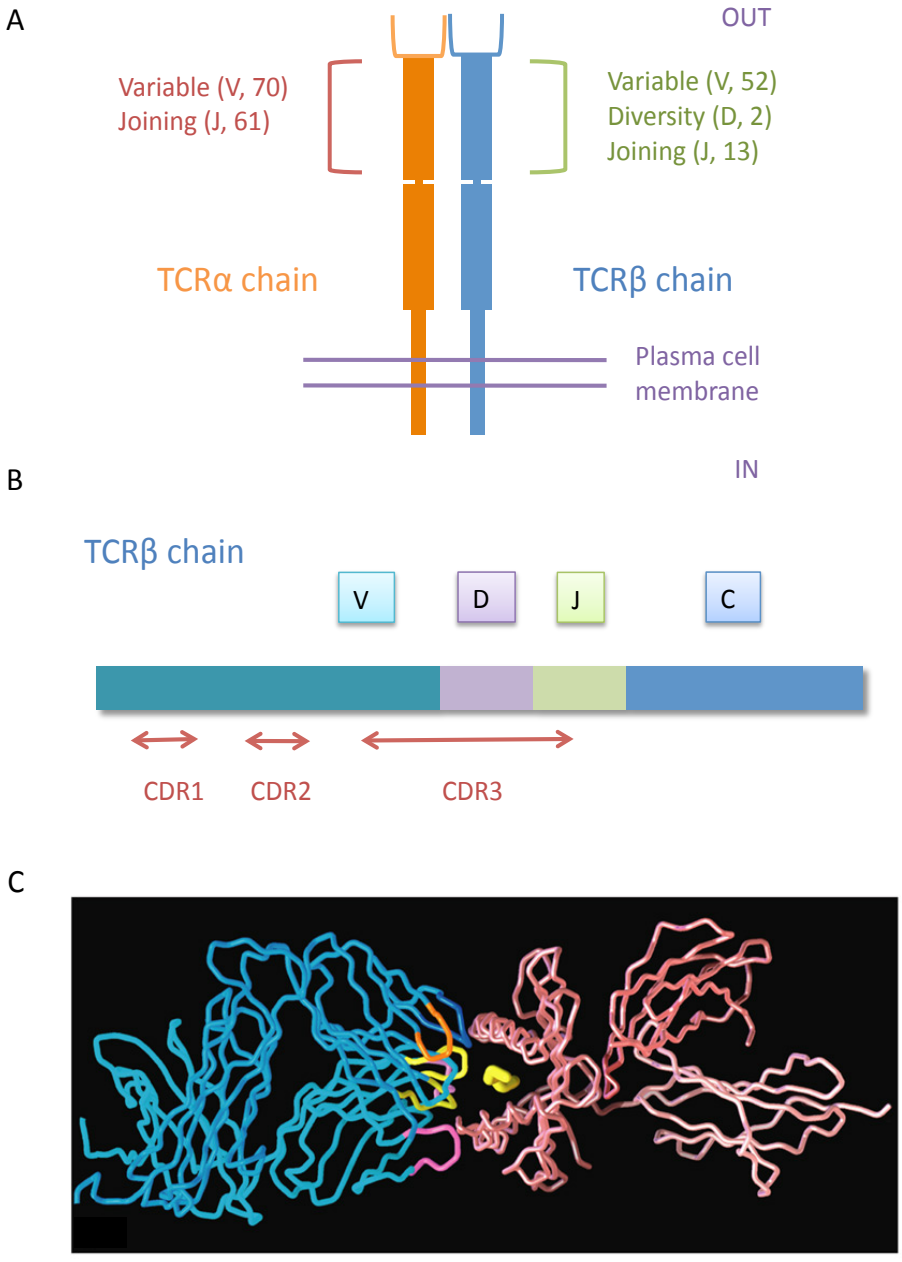

Nikolich-Žugich J *et. al*.Nat Rev Immunol. 2004 Feb;4(2):123–32.

Fig. 5.1. T cell receptor (TCR).

(A) TCR structure. TCR is composed of α and β chains, which contain variable (V), diversity (D) and joining (J) segments. Numbers in brackets indicate numbers of different segments encoded in the germline. **(B)** Location of complementarity determining regions (CDRs) within TCRβ chain. CDR3 spans through V, D and J segments. **(C)** Crystal structure depicting TCR-pMHC interaction. TCR is shown in blue, MHC molecule in red and peptide in yellow. Orange, yellow and pink fragments of TCR depict CDR loops.

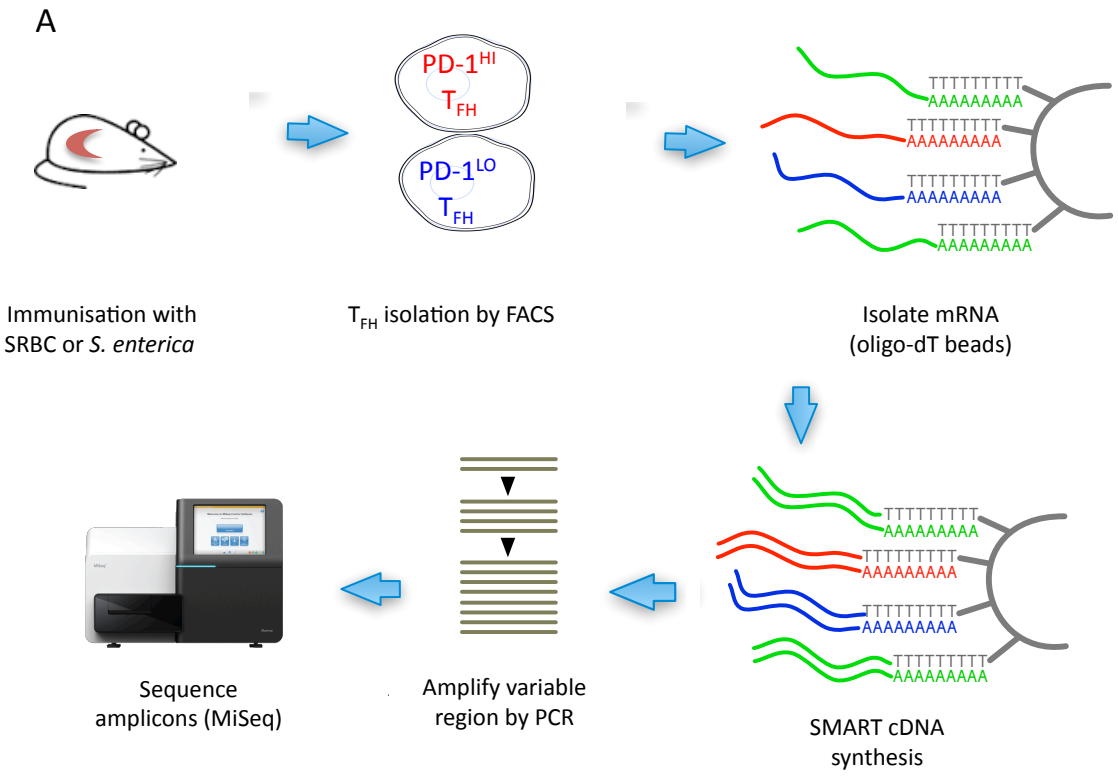

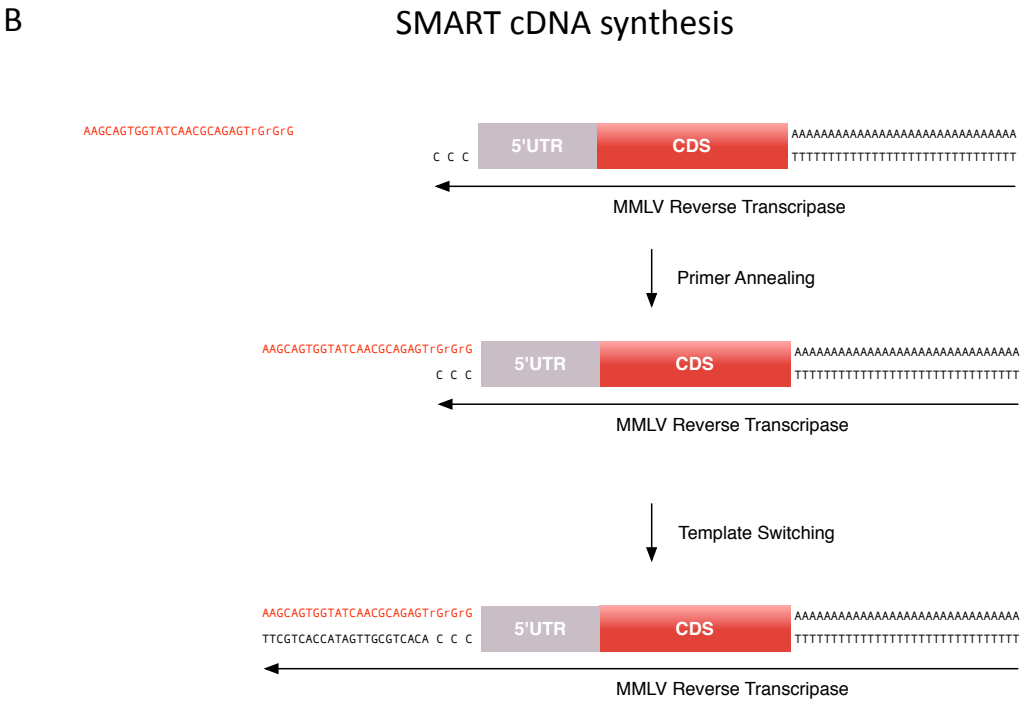

Fig 5.2 Continued overleaf.

C Primer strategy for TCR sequencing

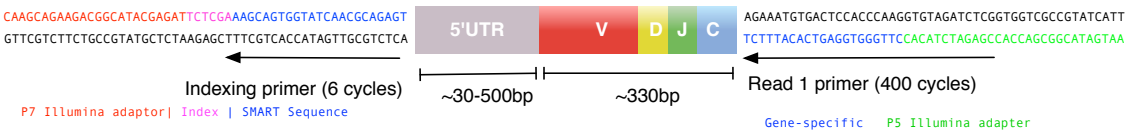

D

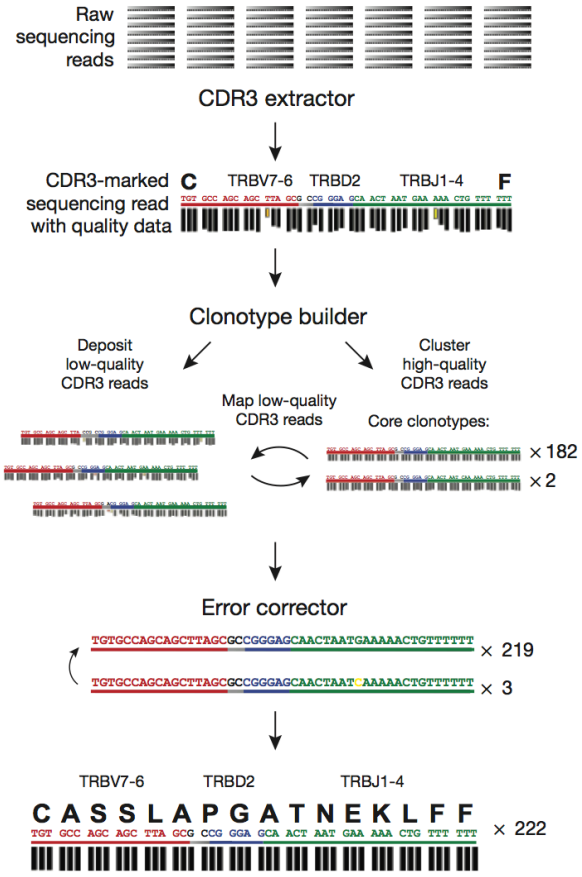

Bolotin DA, *et al*. Nature Publishing Group; 2013 Jul 28;10(9):813–4.

Fig 5.2. Overview of TCR sequencing.

(A) Spleen was used as a site of T_{FH} isolation 6 days p.i. with SRBC and /or *S. enterica*. T_{FH} subsets were sorted by FACS. mRNA and cDNA synthesis was carried out on oligo-dT beads. PCR was used to amplify CDR3 regions of TCR-β chain. Sequencing was carried out with Illumina MiSeq platform. **(B)** Details of smart cDNA synthesis with Moloney Murine Leukemia Virus (MMLV) reverse transcriptase. **(C)** Primers used for the amplifiaction of TCR-β V region prior to sequencing. **(D)** Analysis pipeline of MiTCR, platform used for sequencing data analysis. Horizontal bars show raw sequencing reads and vertical bars show sequence quality. CDR3 sequences are extracted from all reads. V, D and J segments are identified. Low quality reads are either filtered out or corrected. As a result, TCR clonotype sequence and abundance is established.

5.2 Results

5.2.1 Co-immunisation with SRBC and *S. enterica* leads to the expansion of PD-1^{HI} T_{FH} and PD-1^{LO} T_{FH} populations.

Results presented earlier showed that immunisation neither with heat-killed nor live *S. enterica* is able to generate PD-1^{HI} T_{FH} populations (Fig. 3.3C-E, p. 90). This could be attributed either to the nature of the *S. enterica* infection or the strong inflammatory conditions present during early stages of the response. Nevertheless, the question of whether the PD-1^{HI} T_{FH} subset could be generated and sustained in the environment created during early stages of the response to *S. enterica* was an intriguing issue. In order to address this question I performed a co-immunisation experiment, in which WT mice were immunised with both SRBC and HK *S. enterica* or SRBC and live, replicating *S. enterica* (at a standard dose of $1x10^6$ CFU). T_{FH} phenotype and the presence of GC were assessed on day 6 p.i.. Thus, we sought to answer the question whether the PD-1^{HI} T_{FH} population, which would most likely be raised after the immunisation with SRBC, could be present in co-immunised animals. This experiment would also provide an answer to the question whether one T_{FH} subset dominates over another, since for instance prevalence of PD-1^{LO} T_{FH} in *S. enterica* could impede the formation of PD-1^{HI} T_{FH} subsets.

Presence of SRBC alongside HK bacteria or live *S. enterica* did not have any influence on the spleen weight (Fig. 5.3A) or infectious dose (Fig. 5.3B). As expected, single immunisation with SRBC generated PD-1^{HI} T_{FH} and PD-1^{LO} T_{FH} populations and single immunisation with HK bacteria or live *S. enterica* produced only the PD-1^{LO} T_{FH} subset (Fig. 5.3C-E). Fascinatingly, in the co-immunised groups of SRBC and HK bacteria or SRBC and live bacteria the PD-1^{HI} T_{FH} population was not only present but also, surprisingly, expanded in frequency (1.18±037% for SRBC vs. 1.84±0.37 for SRBC and HK bacteria and 3.89±0.91% for SRBC and live bacteria, Fig. 5.3C and D, left) and total cell numbers (Fig. 5.3C and E, left). The expansion was more prominent when live bacteria were present alongside SRBC rather than HK bacteria. Intriguingly, the frequency and cell numbers of PD-1^{LO} T_{FH} cells were also expanded in co-immunised groups (again, with greater magnitude for live bacteria than for HK bacteria, Fig. 5.3. C-E). Importantly, the frequencies of PD-

1^{LO} T_{FH} found in co-immunised groups are greater than the additive effect of both immunisations (combined frequencies after immunisation with *S. enterica* only and SRBC only).

The analysis of the presence of GC showed, as expected, a lack of these structures in single immunisation with HK or live bacteria (Fig. 5.3F and G). Fascinatingly, GC B cells were clearly induced in terms of frequency and numbers when SRBC were present alongside HK or live bacteria (Fig. 5.3F and G). Moreover, the frequency of GC B cells in co-immunised groups was comparable to the one in the SRBC only group.

The most fascinating questions emerging from the co-immunisation study concern the nature of the expanded PD-1^{HI} T_{FH} and PD-1^{LO} T_{FH} populations. If the frequencies of PD-1^{HI} T_{FH} and PD-1^{LO} T_{FH} subsets in co-immunised groups were similar to the ones observed in the individual models, one could simply conclude that infection with *S. enterica* most likely does not prevent PD-1^{HI} T_{FH} formation in response to SRBC. However, synergistic (and not additive) results of expansion observed for both PD-1^{HI} T_{FH} and PD-1^{LO} T_{FH} questions this conclusion and raises the possibility that in some way SRBC immunisation could either facilitate *de novo* formation of PD-1^{HI} T_{FH} specific for *S. enterica* or that *S. enterica* infection provided enhanced conditions for SRBC-specific PD-1^{HI} T_{FH} expansion. Expended T_{FH} population could be also a mixture of cells specific for SRBC or *S. enterica*. To tackle the fascinating issue of the specificity of the expanded T_{FH} populations, TCR sequencing was performed on sorted T_{FH} populations.

5.2.2 Outline of TCR sequencing – technique and protocols

T cell isolation for TCR sequencing was carried out by fluorescence activated cell sorting, using the same protocol as for T cell isolation for the microarray analysis (materials and Methods chapter, p. 52 and Fig. 2, p. 57). Activated T cells were isolated 6 days p.i. with SRBC, *S. enterica* or both immunogens. Unimmunised animals were used as a source of naïve T cells (Fig. 5.2A). Frozen cell pellets (0.5 x 10^6 T cells in each sample) were subjected to high purity mRNA isolation with oligo dT beads (Fig. 5.2A). The magnetic beads are covalently coupled to multiple thymine (T) residues, which pair with the polyA tail present at the 3'end of most

mRNA molecules. Importantly, other RNA species (ribosomal RNA, micro RNA and small nucleaolar RNA) as well as DNA or proteins do not carry the polyA tail, therefore are not bound by the beads and are easily removed during the isolation process.

cDNA synthesis was carried out with SMART Moloney Murine Leukemia Virus Reverse Transcriptase (MMLV RT, Fig.5.2B). The MMLV RT is the enzyme used especially for the preparation of cDNA libraries, as its high sensitivity enables the amplification of rare mRNA copies and the preservation of the relative abundance of the original transcripts at the same time. MMLV RT has the additional property of switching the RNA template (Fig. 5.2B). Ribosylated guanine (rG)[8] was introduced as a complementary sequence to the string of cytosines (C) at the 5' of the untranslated region (UTR). As a result, MMLV RT continued the cDNA synthesis by adding the same primer for all cDNA molecules at 5' end (Fig. 5.2B). Importantly, providing the same primer at 5' end for all cDNA molecules removed the possibility of a V region bias during the PCR reaction, as there was no V-region specific primer used in the reaction.

TCR-β variable (V) regions were further amplified by PCR with the use of indexed forward primers (containing SMART synthesis oligo sequence) and a reverse primer complimentary to the TCR-β constant region (Fig. 5.2C). Forward and reverse primers were fused to a P7 or a P5 illumina tag, respectively (Fig. 5.2C). Such prepared clones (amplicones) of V regions were extracted from agarose gel bands, precipitated by ethanol and subjected to sequencing on the MiSeq Illumina sequencer (with single-end reads of 400bp length). Custom read 1 primers and indexing primers complimentary to the amplification primer sequences were used in sequencing.

The primary data obtained from sequencing were analysed by the open source software MiTCR utility (225) by using Python scripts (Fig. 5.2D).

[8] This modification is essential for the MMLV template switch.

5.2.3 T_{FH} populations isolated after SRBC immunisation show higher TCR diversity than the T_{FH} populations isolated after *S. enterica* infection

Sequencing technology provides an unparalleled opportunity to gather information about the T cell receptor repertoire at any time during the course of an immune response. One of the main issues addressed by TCR sequencing is the magnitude of the diversity observed among all TCR sequences. When few T cell clones are selected for proliferation due to carrying the advantageous CDR3 sequence (e.g. with a high affinity to the foreign antigen) clonal expansion is observed and such expanded TCRs are found at a much higher frequency than others. Alternatively, polyclonal T cell expansion takes place and many TCR sequences are found at similar frequencies, without any dominant clonotypes[9] observed. The aim of the undertaken TCR sequencing of T_{FH} populations was, firstly, to answer the question about the level of TCR diversity observed after SRBC immunisation and *S. enterica* infection and, secondly, to determine clonal expansion patterns that are likely to be characterstic of a response to a particular antigen (in this instance SRBC or *S. enterica*).

Diversity value (D50) is a mean to express the level of diversity within the TCR repertoire. Diversity value is the number of most prevalent TCR clones, which make 50% of the total TCR repertoire. It is calculated by: 1) working out the total number of CDR3 sequences, 2) sorting CDR3 sequences from the most prevalent to the least frequent, 3) adding the most frequent CDR3 sequences to reach half of all sequences in TCR repertoire. Therefore, the higher the number is, the greater is the observed diversity. Contrary to that, low D50 means a great expansion of some single clones.

The results of the T_{FH} sequencing of TCR show that, as expected, the highest diversity of TCR is observed in naïve T cells ($CD62L^{HI}$ $CD44^{LO}$), isolated from non-immunised animals (Fig. 5.4). Intriguingly, populations isolated from the SRBC immunisation model ($PD\text{-}1^{HI}$ T_{FH}, $PD\text{-}1^{LO}$ T_{FH} and $CXCR5^-$ T cells) show a degree of diversity similar to naïve T cells, with the D50 value around 15-20 (Fig. 5.4). Interestingly, experimental groups of T cells isolated from animals infected with *S. enterica* ($PD\text{-}1^{LO}$ T_{FH} and $CXCR5^-$ T cells) show a much lower D50 value (in the

[9] Clonotype is a TCR with the same D - J region and CDR3 sequence.

range of around 5, Fig. 5.4), indicating that clonal expansion of the selected CDR3 sequences has taken place. Fascinatingly, in groups co-immunised with SRBC and *S. enterica*, the diversity value is placed between the immunisations with SRBC or *S. enterica* alone for PD-1^{LO} T_{FH}, suggesting a mixed expansion of both SRBC and *S. enterica*-activated populations. On the other hand, PD-1^{HI} T_{FH}, isolated from the co-immunised animals show a D50 value within the range observed for single immunisation with *S. enterica*, which suggests that the clonal expansion of the immunodominant CDR3 sequences has taken place. $CXCR5^-$ T cells of animals co-immunised with SRBC and *S. enterica* exhibit the lowest D50 value of all populations (Fig.5.4), therefore, showing diversity closer to the one observed in *S. enterica* immunisation.

Overall, the analysis of the diversity value shows that SRBC immunisation leads to polyclonal T cell activation without expansion of single clones and the level of TCR diversity is similar to the one observed in naïve animals. *S. enterica* infection, however, results in the expansion of the few selected TCRs which dominate the repertoire. Surprisingly, the analysis of the TCR diversity (by D50 value) revealed that PD-1^{HI} T_{FH} population from co-immunised animals displays a similar range of clonal expansion to the one observed in the *S. enterica* infection alone (Fig. 5.4). Additionally, the PD-1^{LO} T_{FH} subset formed after co-immunisation exhibit diversity value placed between the ones observed in the single immunisation models. This suggests that PD-1^{LO} T_{FH} population might be a mixture of cells specific for *S. enterica* and SRBC.

5.2.4 PCA suggests mixed expansions of the T_{FH} populations isolated from co-immunised animals

Principal component analysis (PCA, employed already previously for the microarray study) explains variability within the dataset by removing redundancy of the data and bringing out strong patterns in a dataset. PCA of TCR sequencing results (Fig. 5.5) revealed that the TCR repertoires of PD-1^{HI} T_{FH}, PD-1^{LO} T_{FH} and $CXCR5^-$ T cells isolated from SRBC immunised mice are very similar to the one observed in naïve mice, since biological replicates of these populations are

interspaced and positioned very closely together. It also shows that neither of the T_{FH} populations stands out in terms of having a unique TCR repertoire, which indicates that there is no preferential CDR3 sequence that would drive the expansion of a certain TCR clone. Interestingly, $CXCR5^-$ T cells and $PD\text{-}1^{LO}$ T_{FH} from *S. enterica* are placed in a very distant part of the graph (Fig. 5.5), pointing to differences in the TCR repertoires of these groups with respect to naïve T cells and activated T cells isolated from SRBC immunised mice (Fig. 5.5). Intriguingly, populations isolated from co-immunised groups ($PD\text{-}1^{HI}$ T_{FH}, $PD\text{-}1^{LO}$ T_{FH} and $CXCR5^-$ T cells) position themselves in-between the groups isolated from the single immunisation models (Fig. 5.5 and 5.6), suggesting mixed specificity populations (with slight dominance of SRBC response) of T_{FH} cells isolated from the co-immunised animals.

5.2.5 SRBC immunisation leads to polyclonal TCR activation, whereas *S. enterica* infection results in the clonal selection of immunodominant TCR sequences

Clustering plots are very useful in assessing the degree of similarities between the sequences and visualizing the data. The algorithm used to generate clustering plots works by blasting all the sequences against each other and putting the link between the most similar sequences. A force-directed algorithm then places the sequences which are highly linked closer together[10]. The node size is proportional to the number of reads of the sequence and therefore reflects how prevalent each combination is in the isolated TCR repertoire. Each colour represents a family of J segments (since the J segment contributes more amino acids to CDR3 sequence than the V segment).

The clustering analysis of T_{FH} populations isolated after the SRBC immunisation shows, again, that the TCR repertoire is very similar to the naïve T cells (Fig. 5.7 A and 5.8), further confirming the results described for the D50 value and PCA. The clustering analysis of $PD\text{-}1^{HI}$ T_{FH}, $PD\text{-}1^{LO}$ T_{FH} and $CXCR5^-$ T cells (from SRBC model, Fig. 5.8) clearly indicates the polyclonal character of the response with a very large diversity of TCR sequences and no expansion of single clonotypes (all the

[10] Sequences, which are less than 90% similar, are considered not related, as this would create too many links between the samples and the force-directed algorithm would not be useful.

nodes are the same size, reflecting a similar frequency of multiple TCR sequences within the total TCR repertoire).

In strong contrast to the results described above, the clustering analysis of the TCR sequences of PD-1^{LO} T_{FH} and $CXCR5^-$ T cells isolated after *S. enterica* infection indicates a clear expansion of the selected TCR clones (Fig. 5.9) since nodes vary in size with some sequences clearly being found most frequently within the TCR repertoire. As a consequence, the TCR repertoire found in *S. enterica* infection shows less TCR diversity than in naïve mice or after SRBC immunisation.

Intriguingly, the clustering analysis of the T cell populations isolated from the animals co-immunised with SRBC and *S. enterica* (Fig. 5.10) shows that nodes vary in size, and that therefore clonal expansion, rather than polyclonal activation, has taken place within PD-1^{HI} T_{FH}. This result strongly indicates that at least some of the PD-1^{HI} T_{FH}, PD-1^{LO} T_{FH} and $CXCR5^-$ T cells expanded in the co-immunisation setting are, quite unexpectedly, specific to the *S. enterica* infection.

5.2.6 Concluding remarks

Overall, the results of TCR sequencing identify a polyclonal T cell activation in SRBC immunization without clonal selection of certain CDR3 sequences. In strong contrast, *S. enterica* infection presents a more immunodominant system with clonal selection and expansion of certain VDJ chains (Fig. 5.4 and 5.9). The repertoire analysis of the expanded T_{FH} populations from animals co-immunised with SRBC and *S. enterica* suggests a recruitment of T_{FH} cells specific for both antigens (Fig. 5.4 and 5.6-7), with a clear presence of immunodominant clones specific for *S. enterica* observed in the populations of PD-1^{HI} T_{FH} and PD-1^{LO} T_{FH} (Fig. 5.10).

5.2.7 Results summary

- Co-immunisation with SRBC and *S. enterica* leads to the expansion of PD-1^{HI} T_{FH} and PD-1^{LO} T_{FH} populations (Fig. 5.3).
- T_{FH} populations isolated after SRBC immunisation show higher TCR diversity than the T_{FH} populations isolated after *S. enterica* infection (Fig. 5.4).

- SRBC immunisation leads to polyclonal TCR activation, whereas *S. enterica* infection results in the clonal selection of immunodominant TCR sequences (Fig. 5.8 and 5.9).
- PCA suggests a mixed specificity of the T_{FH} populations isolated from co-immunised animals (Fig. 5.6 and 5.7).
- TCR clones specific to *S. enterica* are found in the PD-1^{HI} T_{FH} and PD-1^{LO} T_{FH} populations raised in co-immunised animals (Fig. 5.10).

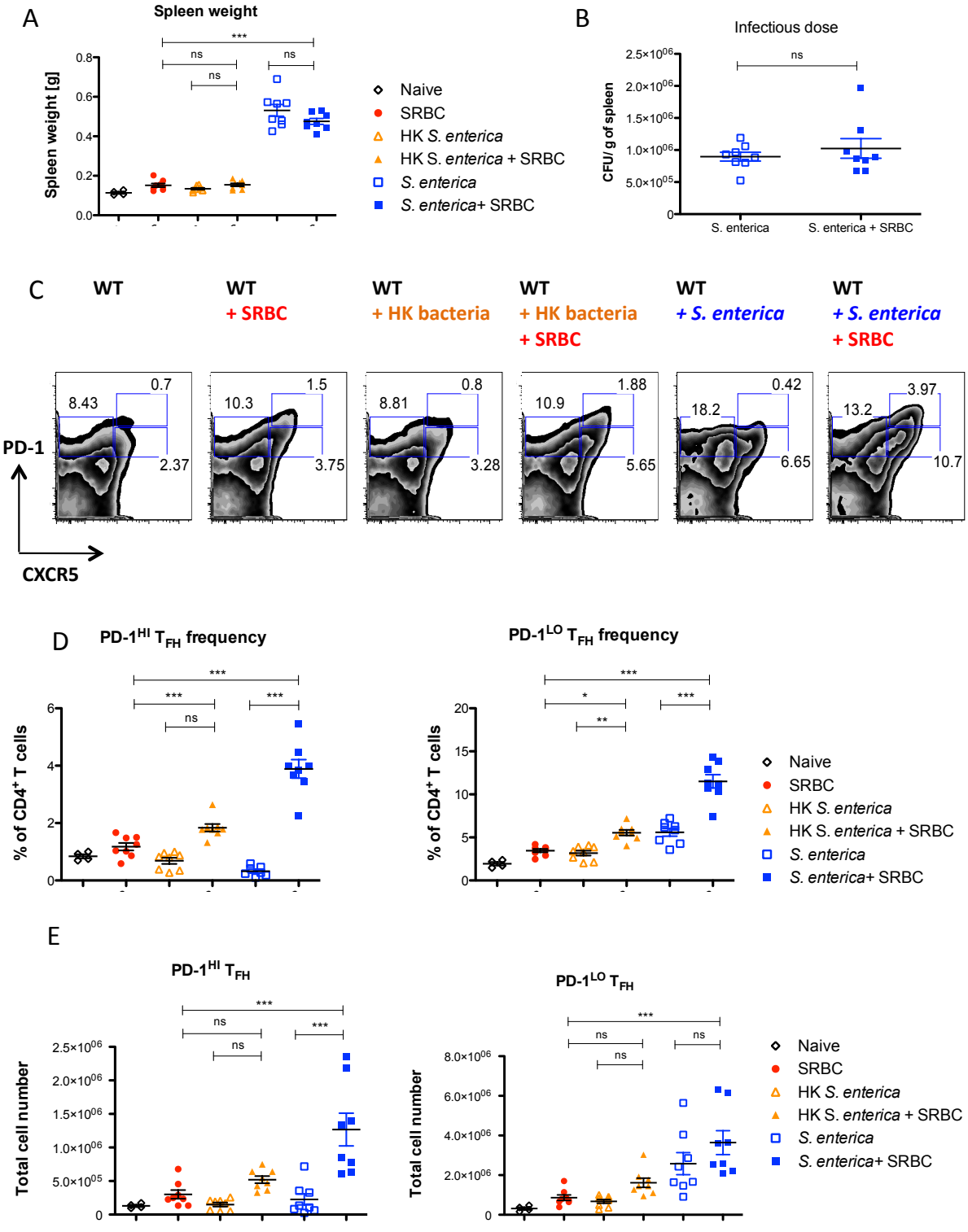

Fig 5.3. Continued overleaf.

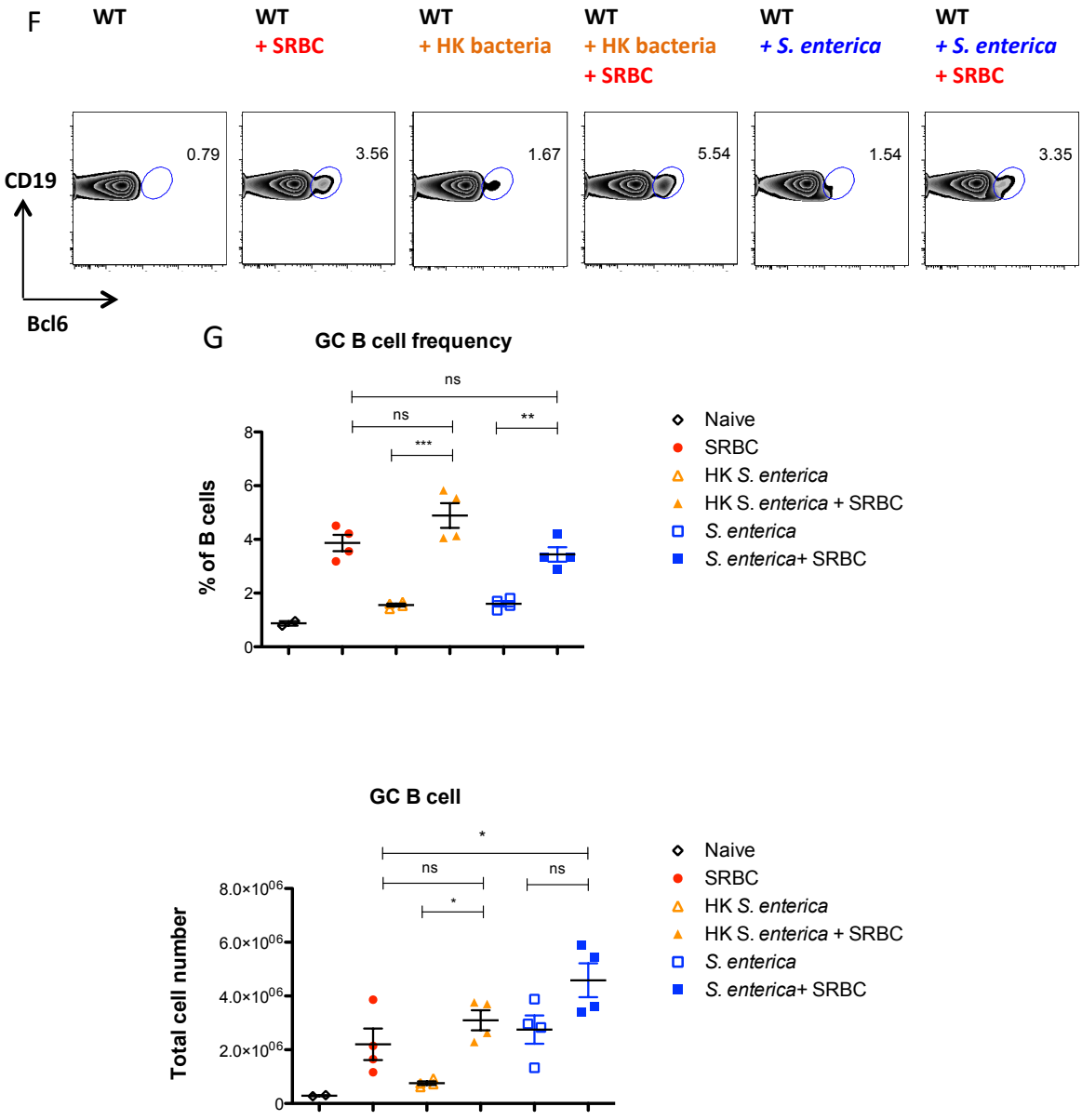

Fig 5.3. Induction of T_{FH} and GC populations after co-immunisation with SRBC and *S. enterica* (day 6 p.i.)

(A) Spleen weight of immunised animals as indicated on day 6 p.i. **(B)** Bacterial load quantification expressed as number of colony forming units (CFU) per spleen (left side) or per gram of spleen (right side). **(C)** Representative flow cytometry plots of PD-1^{HI} T_{FH} and PD-1^{LO} T_{FH} $CD4^+$ T cell populations in each immunisation model. **(D)** Summary of PD-1^{HI} T_{FH} (left) and PD-1^{LO} T_{FH} (right) frequencies and **(E)** cell numbers. **(F)** Representative flow cytometry plots of GC B cells staining in each experimental group. **(G)** GC B cell quantification showed as a frequency of total $CD19^+$ B cells.

Data are pooled from two independent experiments (A-E) or one experiment (F-G) with n=1 (naïve), n=4 (SRBC), n=8 for HK *S. enterica*, n=4 for HK *S. enterica* and SRBC, n=4 (*S. enterica),* n=4 (*S. enterica* +SRBC); each dot represents one mouse.

Statistical significance was determined by One-way ANOVA with post-ANOVA Tukey's test for multiple comparisons (Fig. 3.8 A, C-F) or by two-tailed Student's *t*-test with 95% confidence (Fig.3.9 B).

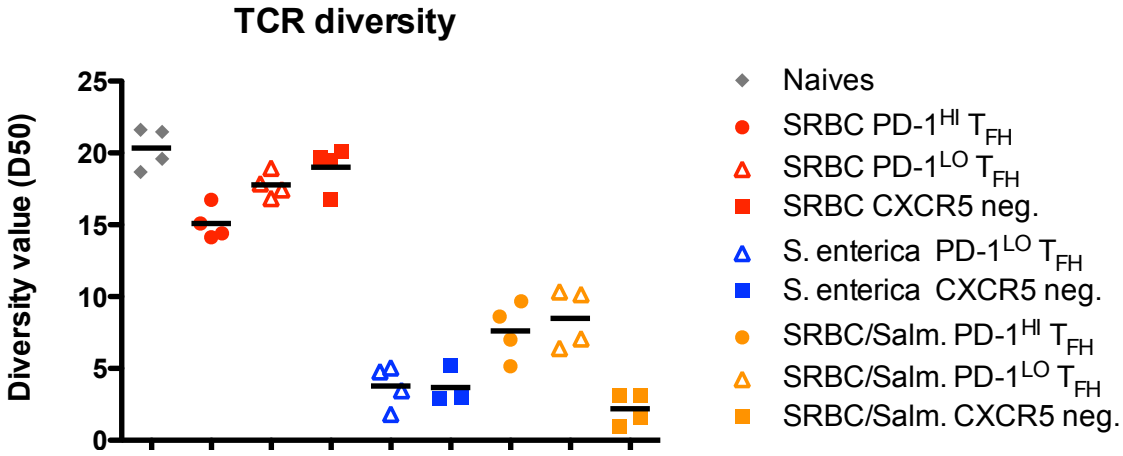

Fig 5.4. Analysis of TCR diversity within isolated T cell populations.

Diversity value (D50) represents a minimum number of unique TCR clones that can account for 50% of all reads. Higher d50 value indicates greater diversity of TCR sequences.

Experimental groups consist of mice immunised with SRBC, *S. enterica* or both SRBC and *S. enterica*. Each symbol represents a biological replicate made of pooled samples from 3 to 6 mice. Naïve T cells ($CD62L^{HI}$ $CD44^{LO}$) were isolated from unimmunised animals. N=4 for each group, each dot represents a pooled biological replicate.

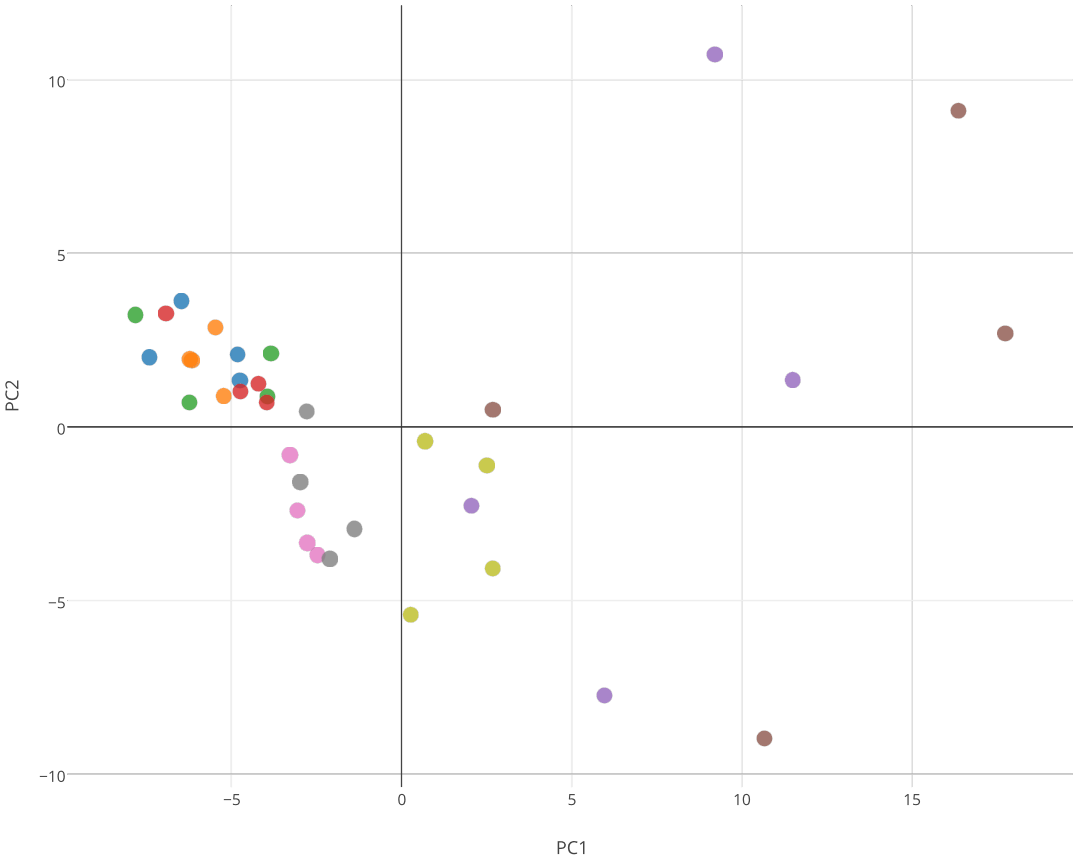

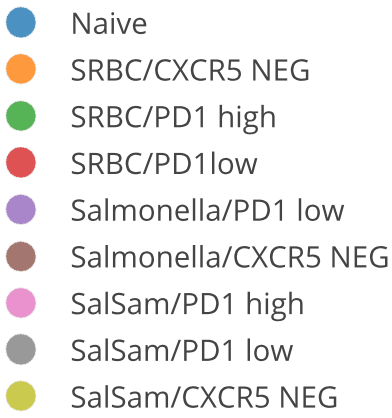

Fig 5.5. Principal component analysis (PCA) of TCR sequences from isolated T cell subsets.

Experimental groups consist of mice immunised with SRBC, *S. enterica* or both SRBC and *S. enterica*. Each symbol represents the biological replicate made of pooled samples from 3 to 6 mice. Naïve T cells ($CD62L^{HI}$ $CD44^{LO}$) were isolated from unimmunised animals.

N=4 for each group, each dot represents a pooled biological replicate.

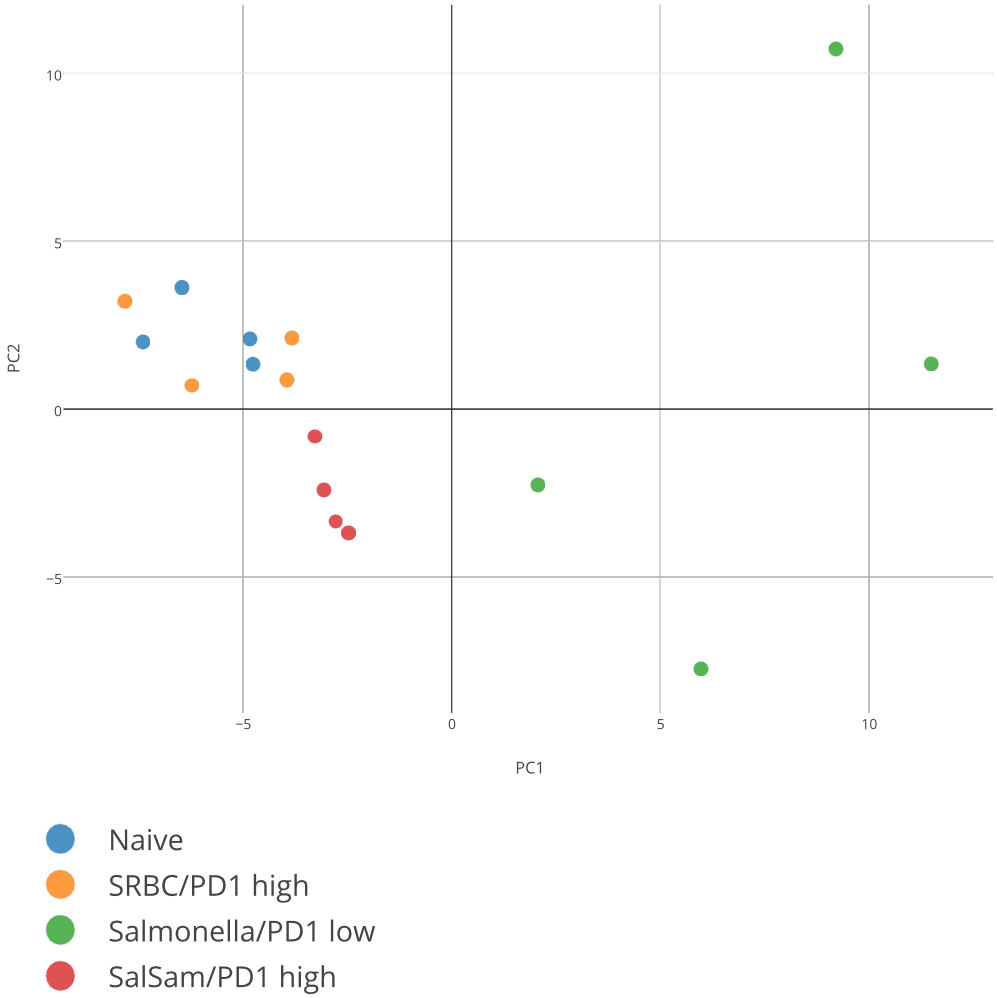

Fig 5.6. Principal component analysis (PCA) of selected T_{FH} subsets.

Please note that this graph depicts the same data as in Fig. 5.5 but with fewer experimental groups plotted for clearer overview.

Experimental groups consist of mice immunised with SRBC, *S. enterica* or both SRBC and *S. enterica*. Each symbol represents the biological replicate made of pooled samples from 3 to 6 mice. Naïve T cells ($CD62L^{HI}$ $CD44^{LO}$) were isolated from unimmunised animals.

N=4 for each group, each dot represents a pooled biological replicate.

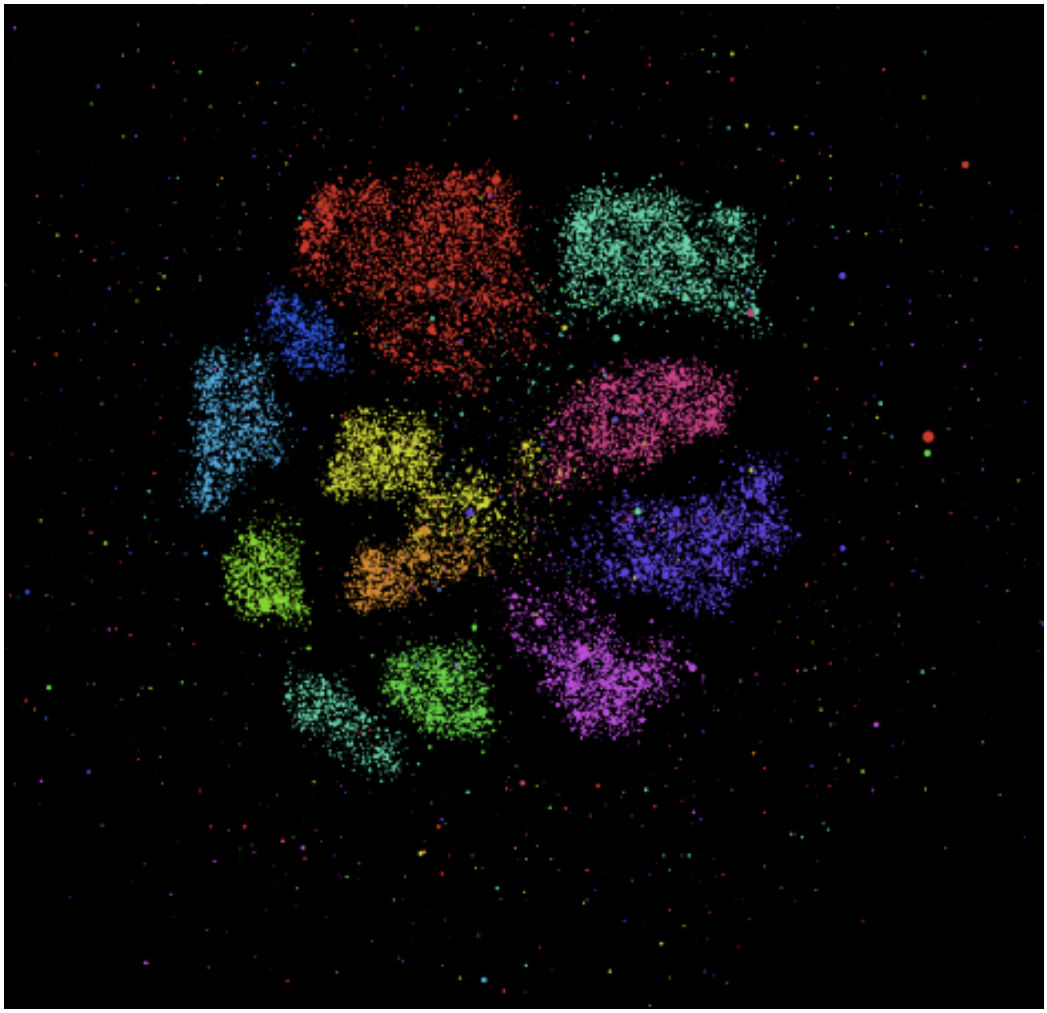

Fig 5.7. Clustering analysis of TCR repertoire of naive T cells isolated from unimmunised mice.

Clustering analysis is a force directed algorithm which links the most similar sequences. Each colour represents a family of J segments. Node size is proportional to the numbers of reads of the certain sequence within the total TCR repertoire.

N=4 for each group.

A ***S. enterica:*** **PD-1^{LO} T_{FH}**

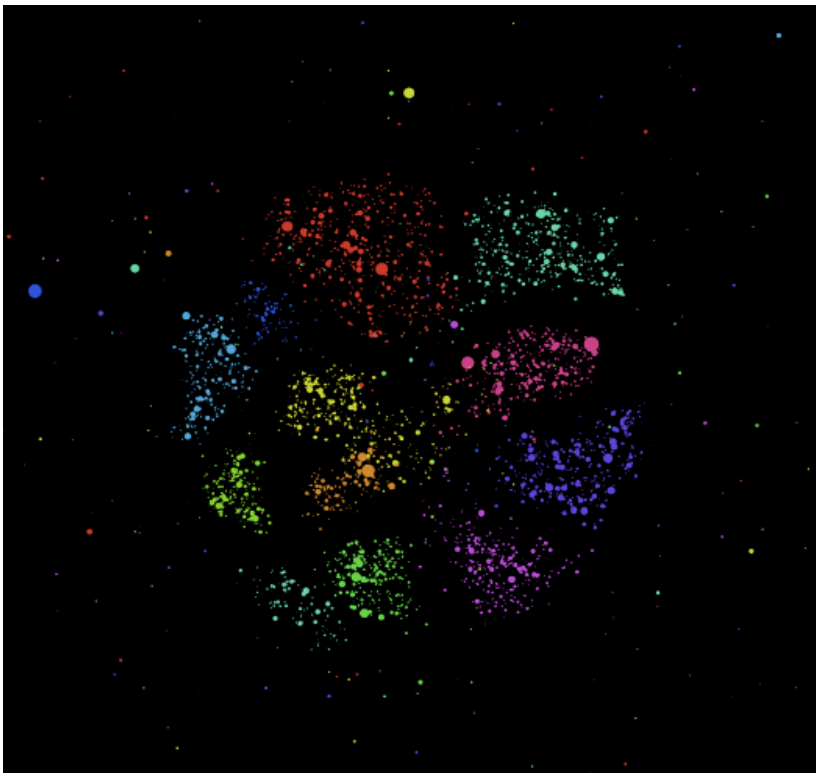

B ***S. enterica:*** **CXCR5 neg. T cells**

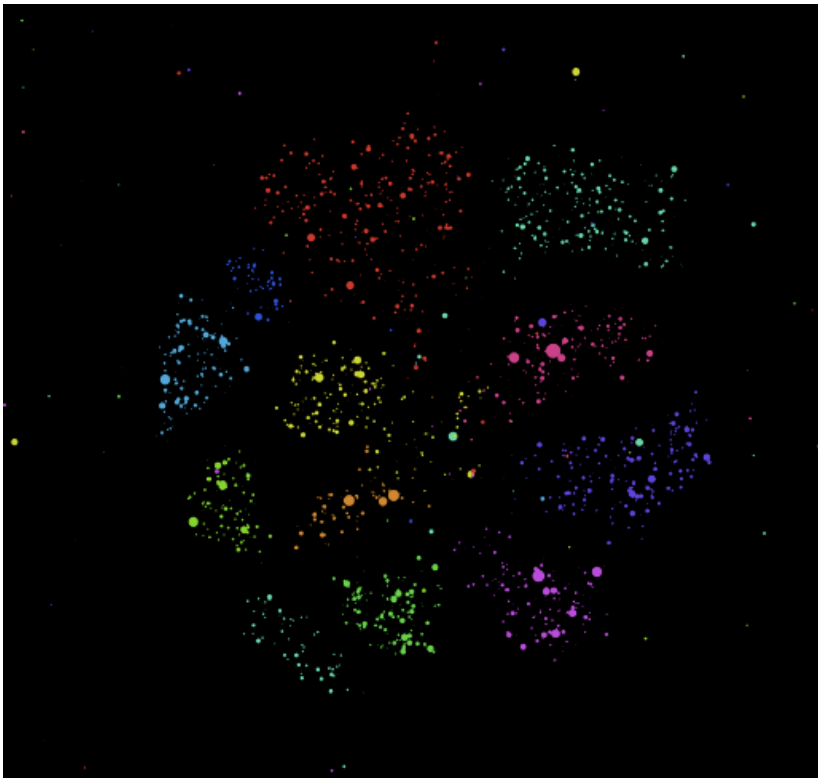

Fig 5.8. Clustering analysis of TCR repertoire of cells isolated from mice 6 days p.i. with *S. enterica*: PD-1^{LO} T_{FH} (A) and CXCR5^{-} T cells (B).

Clustering analysis as in Fig. 5.7

N=4 for all groups.

A

SRBC:
PD-1^{HI} T_{FH}

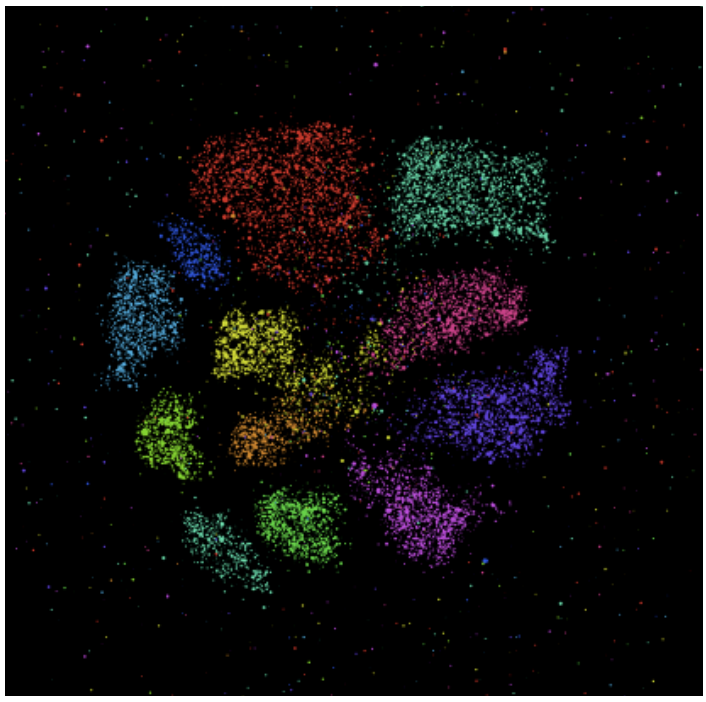

B **SRBC: PD-1^{LO} T_{FH}**

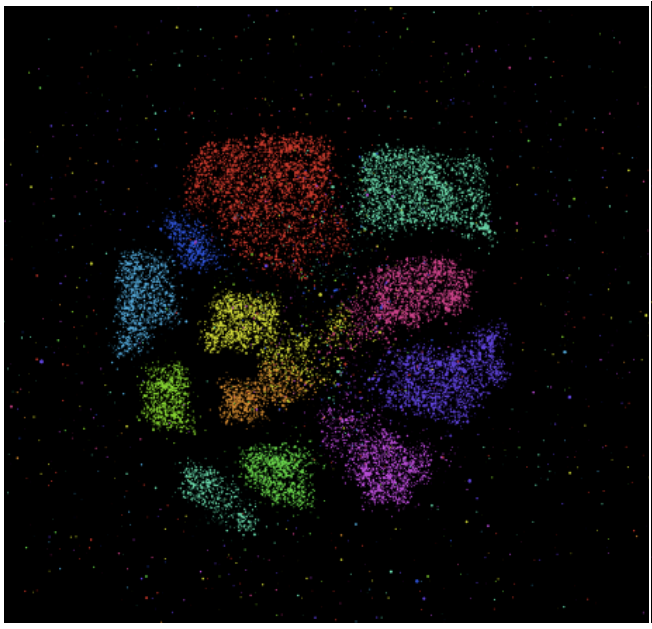

C **SRBC: CXCR5 neg. T cells**

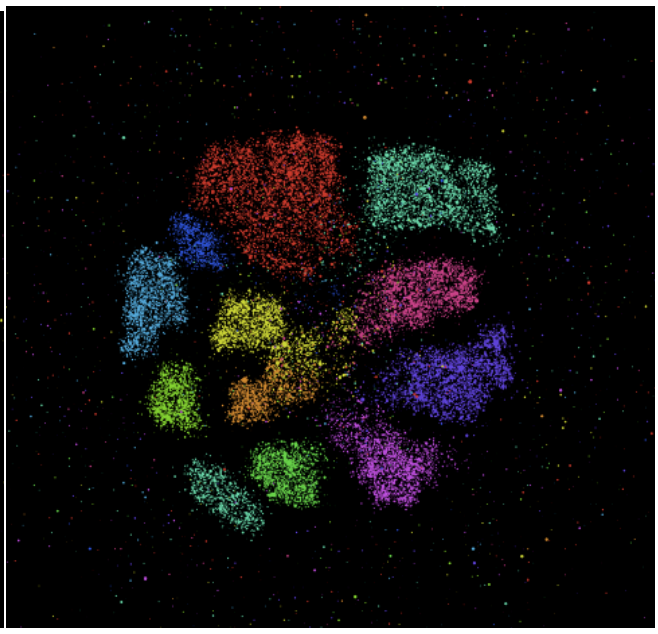

Fig 5.9. Clustering analysis of TCR repertoire of cells isolated from mice 6 days p.i. with SRBC: PD-1^{HI} T_{FH} (A), PD-1^{LO} T_{FH} (B) and CXCR5^{-} T cells (C).

Clustering analysis as in Fig. 5.7

N=4 for all groups.

A

S .enterica **+ SRBC:**
PD-1^{HI} T_{FH}

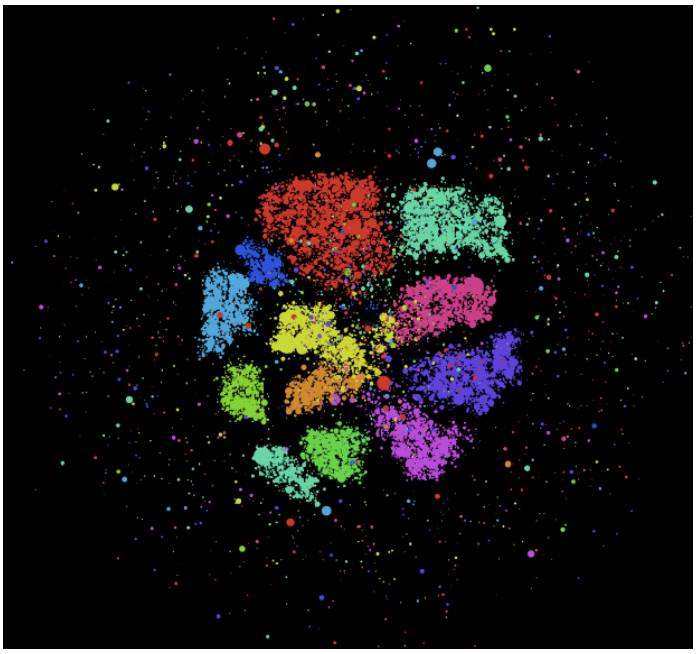

B ***S .enterica*** **+ SRBC: PD-1^{LO} T_{FH}**

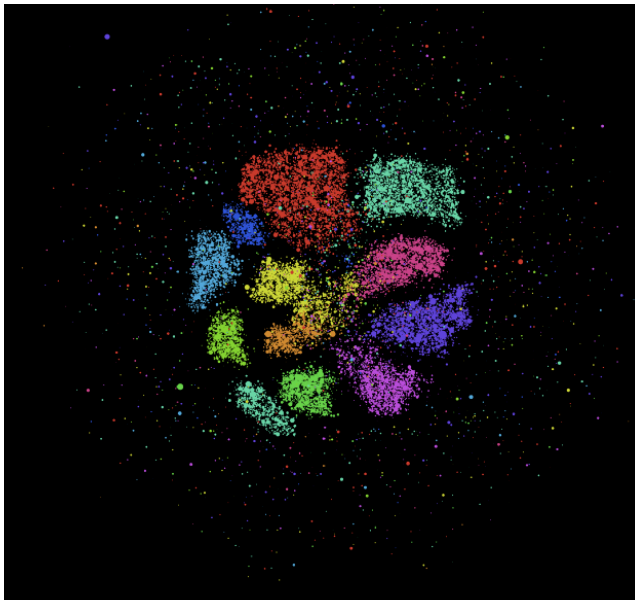

C ***S .enterica*** **+ SRBC: CXCR5 neg. T cells**

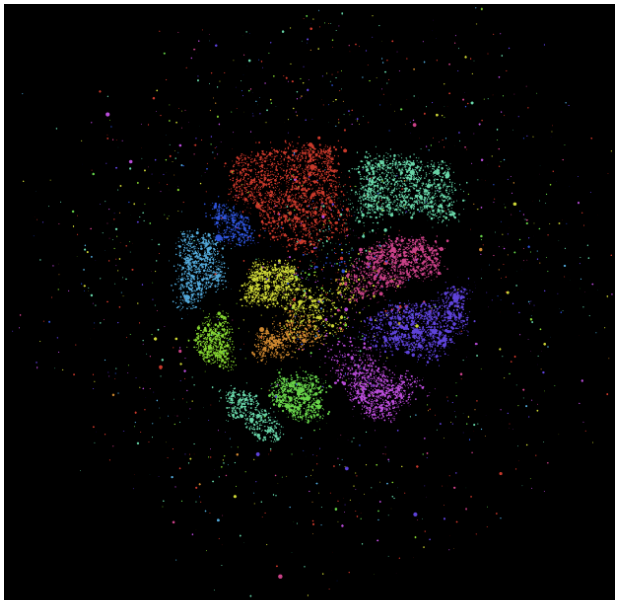

Fig 5.10. Clustering analysis of TCR repertoire of cells isolated from mice 6 days p.i. with SRBC and *S. enterica*: PD-1^{HI} T_{FH} (A), PD-1^{LO} T_{FH} (B) and CXCR5^{-} T cells (C).

Clustering analysis as in Fig. 5.7

N=4 for all groups.

5.3 Discussion

5.3.1 Expanded T_{FH} populations after co-immunisation with SRBC and *S. enterica*

The co-immunisation experiments using SRBC and *S. enterica* revealed an unexpected expansion of the PD-1^{HI} and PD-1^{LO} T_{FH} populations. The specificity of the expanded T_{FH} populations is an intriguing issue.

One of the ways to elucidate T_{FH} specificity is by investigating T cell binding to MHC II tetramers. Unfortunately, this approach was not possible due to lack of such reagents. Another option would be to perform antigen-specific *in-vitro* re-stimulation assays on the sorted T_{FH} populations. Since the protocols for the SRBC re-stimulation were not well established in the lab and optimization of the assay on the sorted populations would be too time and cost consuming, this approach was not followed. Another alternative is to perform adoptive transfers of the T_{FH} populations from co-immunised animals and provide an antigen boost in the host animals, followed by the measurement of the T cell activation, proliferation, and commitment to the memory pool and antibody responses. This approach, however elegant, is unfortunately not feasible, as sorts from single immunisations would have to be carried out in parallel as essential controls, and due to the low T_{FH} frequency in the single immunisation models this would be difficult and costly to achieve. We, therefore, decided to employ TCR sequencing of the CDR3 region to tackle the fascinating issue of T_{FH} specificity, which was already being used in the lab (Dr. Graeme Cowan). Considering the vast differences in the investigated immune responses (T-cell dependent Th-2 response to SRBC and strong inflammatory Th1 response to *S. enterica*), we were hoping to identify TCR clones characteristic for SRBC or *S. enterica* and subsequently investigate if any of them would be dominant in the expanded T_{FH} population raised in the animals co-immunised with SRBC and *S. enterica*. Alternatively, TCR diversity could be also addressed by flow cytometry, which could provide an information on the presence of selected V chains.

5.3.2 TCR repertoire of T_{FH} populations in SRBC immunisation and *S. enterica* infection

The analysis of the diversity value and clustering plots as well as principal component analysis showed that the TCR repertoire of PD-1^{HI} and PD-1^{LO} T_{FH} after SRBC immunisation is very similar to the one found in the naïve mice, where no clonal selection of any preferential CDR3 sequences takes place. Therefore, SRBC appear to stimulate a polyclonal T cell expansion. Intriguingly, there seem to be no differences in the TRC repertoire of the PD-1^{HI} T_{FH} and PD-1^{LO} T_{FH} populations in the SRBC model, even though, as discussed in the previous chapter, the PD-1^{HI} T_{FH} population requires cognate contacts with B cells for the its survival while the PD-1^{LO} T_{FH} subset does not. Together the results of this thesis indicate that there is no single CDR3 sequence that would be preferentially selected for expansion in the SRBC immunisation, even in the T_{FH} population relying on antigen provision by B cells (namely PD-1^{HI} T_{FH}).

The TCR of the T_{FH} population in the *S. enterica* infection model shows a very strong clonal selection/expansion of certain CDR3 sequences dominating in the response and therefore limiting the general diversity of the TCR repertoire. Clonal expansion indicates the presence of the immunodominant epitope preferentially recognised by T cells. Indeed, a few studies showed that the late, protective response to *S. enterica* is generated preferentially against the flagellin (226-228) and type III secretion system (229), while antibodies produced early after the infection are directed mostly against outer membrane proteins (171,230). Moreover, it was recently showed that *S. enterica* infection influences the structure and function of the thymus by altering the distribution of double negative (DN), double positive (DP) and single positive (SP) thymocytes (231). Interestingly, TCR usage in DP cells as well as $CD8^+$ and $CD4^+$ SP T cells (measured by the frequency of certain TCRVβ genes by flow cytometry) is also affected during *S. enterica* infection (231). Therefore, strong clonal expansion observed in *S. enterica* infection model can be explained by enhanced proliferation of the selected clones present in the spleen or the periphery as well as a consequence of increased TCR restriction during the thymic selection.

The differences in the activation kinetics between the SRBC and *S. enterica* models should be taken into account while considering clonal expansion of T_{FH} populations. At day 6 p.i. T_{FH} from *S. enterica* are almost at the peak of the proliferation, whereas T_{FH} from SRBC (both PD-1^{HI} and PD-1^{LO} T_{FH}) have expanded the most at day 3 and are already declining in frequency. This has a potential impact on the sequencing results, since T_{FH} cells from *S. enterica* are most likely still undergoing clonal expansion and the sequencing profile will most likely look different once this process is completed. Nevertheless, the comparison of PD-1^{HI} and PD-1^{LO} T_{FH} from SRBC model have provided an important cues on TCR repertoires in these populations.

Since SRBC and *S. enterica* immunisation have vastly different impacts on the TCR repertoire (polyclonal response vs. clonal selection, respectively), the employment of TCR sequencing for the characterisation of the T_{FH} populations in co-immunised animals was well justified. Intriguingly, the PD-1^{HI} T_{FH} and PD-1^{LO} T_{FH} populations isolated from co-immunised animals showed presence of the cells specific for SRBC and *S. enterica* at the same time. This result might not seem to be surprising for the PD-1^{LO} T_{FH} population, since this subset is present in both single immunisations models and the expansion observed upon co-immunisation seems to have an additive effect. However, the possibility of generating PD-1^{HI} T_{FH} cells specific for *S. enterica* in the co-immunised group is highly surprising, since this population is virtually absent when only *S. enterica* is used for immunisation (as discussed in Chapter 3). The next question therefore would be: what is the nature of the signal provided by SRBC, which drives the expansion of *Salmonella*-specific PD-1^{HI} T_{FH}? It could be a soluble factor (e.g. cytokine) released as part of the SRBC response, which would then drive progression of *Salmonella*-specific PD-1^{LO} T_{FH} into PD-1^{HI} T_{FH} alongside the formation of PD-1^{HI} T_{FH} specific for SRBC. Alternatively, an unknown feedback mechanism coming from SRBC-specific GC could push abundantly present *Salmonella*-specific PD-1^{LO} T_{FH} into PD-1^{HI} T_{FH} and only then GC specific for *S. enterica* would be established. However, this would have to be a non-antigen specific feedback signal, since antigens of SRBC and *S. enterica* are of vastly different natures. Nevertheless, taking into account how robust the GC response against SRBC is, both options are plausible.

5.3.3 Specificity of GC in SRBC and *S. enterica* co-immunisation.

GC of unknown specificity were abundantly present in the animals co-immunised with SRBC and *S. enterica* (Fig. 5.3F and G), and this is in keeping with the presence of PD-1^{HI} T_{FH} as a GC-associated population.

In *S. enterica* infection GC are not formed until 5 weeks post infection (171), when bacterial levels are vastly reduced. Therefore, GC formation can be brought forward by the treatment with antibiotics (171). Since the bacterial burden and spleen weight is similar in the group with single immunisation with *S. enterica* and the co-immunised group, one could, therefore, expect that SRBC will be the main antigen against which GC are elicited. However, the strong indication of the presence of *Salmonella*-specific PD-1^{HI} T_{FH} allows for the speculation that *Salmonella*-specific GC might be also present. Ideally, visualization of antigen specific B cells (for both *S. enterica* and SRBC) would provide a definitive answer to the question of the nature of GC present in co-immunised animals, but this approach is still technically challenging and I did not have time to perfect this. One of the available options would be B cell receptor (BCR) sequencing, provided that each of the single immunisation models will result in a different BCR repertoire. The indirect way to determine the specificity of GC B cells is by looking at the GC's output - the antibody. Early stages of *S. enterica* infection elicit strong IgG2c responses directed mainly against outer membrane proteins but this is of extra follicular origin (171,172). The appearance of the GC is characterized by affinity maturation of the IgG2c antibody, and different antigens (flagellin and LPS) are targeted at this stage of the response (171). It would be interesting to determine whether the presence of SRBC influences the antibody levels specific for *S. enterica* during both early and late stages of the co-immunisation study and, vice versa, whether SRBC-specific antibody levels are altered in any ways during co-infection with SRBC and *S. enterica*.

5.3.4 Tissue disruption in co-immunised animals

In Chapter 3 it was shown that tissue disruption observed during *S. enterica* infection is not a direct reason for the absence of GC in this model, since during the immunisation with low dose bacteria or HK bacteria, where splenic structures are

normal, GC are still not formed (Fig. 3.3F and G). The results presented in this chapter describe the opposite situation: GC (of unknown specificity) are formed under conditions where splenic disruption has most likely taken place, since the animals co-immunised with SRBC and *S. enterica* show the same level of splenomegaly as in *S. enterica* only immunisation. However, the histology of the spleen found after co-immunisation has to be confirmed by microscopy. Overall, the results from Chapter 3 (Results section 3.3) and this chapter (Results section 5.1) show that, quite surprisingly, the formation of the PD-1^{HI} T_{FH} population and GC is not limited by gross alternations in the spleen's anatomy.

5.3.5 Influence of co-immunisation on T cell memory responses and antibody formation

One of the most interesting and important aspects of the co-immunisation study to be considered is the potential adjuvant effect of SRBC as a polyclonal T cell activator and the SRBC influence on the formation of *Salmonella*-specific T cell memory.

Adoptive transfers of T cells derived from SRBC and *S. enterica* co-immunised animals to congenic hosts and re-challenge with *S. enterica* antigen would provide an interesting insight into T_{FH} cell memory formation and the possible impact on *Salmonella*-specific antibody levels. Whether any of the expanded T_{FH} populations (PD-1^{LO} T_{FH} or PD-1^{HI} T_{FH}) would preferentially be expanded upon secondary immunisation is also an open and fascinating question. It is worth mentioning that the CXCR5 $^{-}$ T cells (activated non-T_{FH} cells) raised in the co-immunised animals are the group with the most restricted TCR diversity and strongest clonal expansion, and this might suggests clonal selection of the cells progressing into the memory pool. Therefore, it would be interesting to assess the phenotype and behaviour of this cell population after adoptive transfer and rechallenge with the antigen. Additionally, establishing whether any of the adoptively transferred T_{FH} populations from the co-immunised animals would enhance antibody responses after secondary immunisation with live *S. enterica* would provide an insight into the function of these cell subsets.

5.3.6 TCR specificity and avidity in T_{FH} formation

So far only a handful of studies have addressed the issue of TCR selection in the T_{FH} formation. Ploquin *et al.* have followed Friend virus-specific polyclonal $CD4^+$ T cell population by investigating TCRβ transgenic T cell population with 25% of T cells showing high functional avidity for the virus and 75% showing lower functional avidity (83). The authors have concluded that the differentiation of virus-specific T_{FH} cells was not affected by the avidity for the antigen (83). In contrast to this finding, Fazilleau (82) *et. al.* suggested that T cells with more restricted and higher affinity of TCR are preferentially recruited to the T_{FH} pool. This study used pigeon cytochrome c (PCC) immunisation, which in B10.BR mice elicits an antibody response with the selection of known variable regions (Vα11 and Vβ3). The further advantage of this system is the availability of antigen-specific peptide:MHC tetramers (raised against immunodominant peptide), which enables to track antigen-specific T cell population (221).

In the study published by Fazilleau *et al.* adoptive transfer of high and low affinity T cell clones indicated that T_{FH} cells preferentially develop from high affinity clones (82). However, the differences in the T_{FH} cell numbers raised from low and high affinity clones are quite modest. Furthermore, the ratio of high to low affinity TCR mRNA in T_{FH} and non-T_{FH} populations is of a similar range. Finally, the analysis of mRNA for IL-21, Bcl-6 and Blimp-1 proteins in high and low affinity T cell clones (after 3 day *in vitro* culture with DCs and the peptide) shows basically no difference in the message levels of these proteins. Nevertheless, T_{FH} cells do bind more p:MHC complex than other effector cell subsets and TCR sequencing of single antigen-specific T_{FH} and non-T_{FH} cells showed a higher TCR repertoire restriction for the former subset (82).

The experimental setup of TCR sequencing from T_{FH} populations raised after SRBC or *S. enterica* immunisation does not allow for speculation on the TCR affinity of certain CDR3 sequences but only on the prevalence of certain clones in the total TCR repertoire, as the TCR:pMHC complex interaction cannot be predicted based solely on the CDR3 sequence (220). Our results of a lack of preferential TCR restriction among T_{FH} and non-T_{FH} populations support the study of Ploquin *et al.*

(83) but stand in contrast to the finding of Fazilleau *et al*. (82). This can be explained by the experimental models used for the investigation: simple protein PCC immunisation might have a different impact on the TCR repertoire than the much more complex *S. enterica* infection. The SRBC immunisation, eliciting a clear T-cell dependent response, is far less characterized than the PCC model in terms of clonal T and B cell selection. The fact that it was not possible to follow a SRBC-specific T cell response might also influence the results. Overall, employing a more sensitive system for antigen-specific T cell tracking would greatly benefit TCR and CDR3 characterization. Nevertheless, the fact that it was possible to detect a strong clonal expansion in the *S. enterica* infection and a lack of it in SRBC immunisation shows that even despite the antigen-tracking tool vast differences in the TCR repertoire were identified, which opens the door to further, more detailed investigations.

6 Synoptic Discussion and Further Work

6.1 T_{FH} differentiation pathways

The development of T_{FH} cells has been intensively investigated since the discovery of the T_{FH} subset (114). I would like to discuss several models of T_{FH} differentiation considering recently emerging data to support each model.

6.1.1 Linear model

The linear model of T_{FH} differentiation (Fig. 6.1A) describes the differentiation of activated $CD4^+$ T cells into T_{FH} under the influence of cytokines IL-6 and IL-21. This would represent a situation analogous to the one of the Th1, Th2 and Th17 subsets, which can be generated *in vitro* under the exposure of naïve $CD4^+$ T cells to IL-12, IL-4 or IL-6 and TGF-β, respectively. An important aspect of this model is that the T_{FH} differentiation is considered completely separated from other lineages. Some studies have shown that $CD4^+$ T cells cultured with IL-6 and IL-21, indeed, produce IL-21 and that T_{FH}-associated transcripts (CXCR5, and Bcl6) are also up-regulated (55,84,100-103). On the other hand, some studies did not confirm the induction of the T_{FH} profile in IL-21-producing cells grown *in vitro* (104,105). This finding is not really surprising, taking into account the fact that other T cell subsets, e.g. Th17 cells, also produce IL-21 (232). Moreover, the presence of IL-21 during the priming stage remains an important issue. Although DC can produce IL-6 (233), they have not been reported to produce IL-21 (actually, no APC has been shown to express IL-21 (114)). Furthermore, multiple evidence from *in vivo* studies show a limited impact of the IL-21 or IL-6 deficiency on T_{FH} populations (72,79,102,107,114). The linear model of T_{FH} differentiation also does not explain the requirement of cognate B cells in the T_{FH} cell development (55,84,100-103,114). Therefore, the simple model of T_{FH} differentiation upon exposure to certain cytokines during the activation stage is not enough to explain complexity of T_{FH} biology.

6.1.2 Pluripotent model

The pluripotent model also recognizes T_{FH} as a lineage separate from the Th1, Th2 and Th17 subsets. In this model of T_{FH} differentiation (Fig. 6.1B, (104,105,114))

$CD4^+$ T cells are primed by DCs, giving rise to the precursors of T_{FH} and for instance Th1 cells. Then some of the pre-T_{FH} move towards the T-B cell border (in response to undefined cues) and T_{FH} cells are generated after the interaction with cognate B cells, which induces expression of Bcl6 and draws T cells deeper into the follicle to initiate the differentiation into GC T_{FH} and GC B cells. However, the pluripotent model does not explain the fact that, as shown in multiple studies, Bcl-6 expression is readily detectable prior to the contact with cognate B cells (57,75,78,232). Furthermore, the signals guiding naïve T cells to become pre-T_{FH} cells also remain unexplained.

6.1.3 Secondary program model

The secondary program model (Fig. 6.1C) differs greatly in principle from the previous two models. In the secondary program model T_{FH} cells are not induced during the priming stage but are derived from already differentiated Th1, Th2 or Th17 cells (114,233). Therefore, differentiation into one of the non-T_{FH} subsets is essential prior to the acquisition of the T_{FH} phenotype, and therefore T_{FH} are viewed as a 'secondary program' and not *de facto* a separate subset. After differentiation into, for example, Th1 effector cell, the Th1-specific program is inhibited and, possibly, by switching on Bcl6, the T_{FH} phenotype is acquired. In agreement with this hypothesis, Th1 were found capable of acquiring the T_{FH} phenotype under IL-2-limiting conditions by alerting the balance of the Tbet/Bcl6 complex (114,234). Moreover, there is an overlapping gene expression pattern between T_{FH} and other cell subsets, for instance, the expression of the master TFs of the Th1 and Th2 subsets (73,77,90,129,132), and, in consequence, their characteristic cytokines. However, several facts argue against this hypothesis. For instance, the T_{FH} development is unaltered in T-bet deficient mice ($Tbx^{-/-}$ mice) upon protein immunisation (69). Additionally, $Bcl6^+$ T_{FH}-like cells are present already at very early stages (day 2-3 p.i.) after priming and therefore there is simply not enough time for cells to undergo the full differentiation into, for example, Th1 cells and then to remodel the gene expression extensively to become T_{FH} cells. Finally, the presence of master TFs of other lineages may simply be a means to express the cytokines that are controlled by this locus, which is also essential for T_{FH} cells, and not a reminiscence of a previous differentiation state.

6.1.4 Integrated model

The integrated model of T_{FH} differentiation is the most complex one and currently the most accepted in the scientific community (Fig.6.2). In principle, the integrated model recognizes T_{FH} as a separate lineage among other T cell subsets. The pre-T_{FH} state is induced during priming with APC via ICOS-ICOS ligand interactions and significant contributions from STAT3 signaling cytokines IL-6 and/or IL-21. After this commitment stage, Bcl6 is weakly expressed. The subsequent maintenance of the T_{FH} phenotype depends on interactions with activated, cognate B cells via ICOS-ICOSL interactions (114), although non-cognate by stander B cells have also been implicated in the process (56). The third and final stage of T_{FH} differentiation is the full polarization into GC T_{FH} cells, which would depend on SAP-mediated interactions with cognate B cells in order to induce maximal expression levels of Bcl6 and CXCR5, PD-1, BTLA, ICOS and possibly of GL7. The GC T_{FH} would be the only T_{FH} subset capable of driving the GC response. The GC T_{FH} could be maintained within the GC by IL-21 (acting in autocrine manner) as well as IL-6 produced by FDCs, which additionally provide continuous access to the antigen held on the surface.

The results presented in this PhD thesis strongly support the integrated model of T_{FH} differentiation. First of all, I show that in the absence of antigen presentation by B cells, T_{FH} cells expressing intermediate levels of CXCR5 and PD-1 are formed. These cells cannot support the GC formation. Secondly, MHC II expression by B cells is essential for the generation of the PD-1^{HI} T_{FH} population, which expresses high levels of Bcl6 and can drive the GC response. Most importantly, I provide evidence for a linear progression from the PD-1^{LO} T_{FH} stage to PD-1^{HI} T_{FH} differentiation. The PD-1^{LO} T_{FH} population deprived of cognate contact with B cells is stalled in its development into PD-1^{HI} T_{FH}. Importantly, PD-1^{LO} T_{FH} can continue this line of differentiation once antigen is experienced in the context of B cells. This illustrates a continuous supply to the PD-1^{HI} T_{FH} pool from PD-1^{LO} T_{FH} pool. The fact that in the absence of MHC II on B cells this final step in T_{FH} differentiation

does not happen argues for a critical role of antigen-presentation by B cells in this process.

6.2 Proliferation and terminal differentiation of T_{FH} cells.

The adoptive transfer of PD-1^{HI} T_{FH} into WT host (Chapter 4, Results section 4.7) revealed a limited plasticity of the PD-1^{HI} T_{FH} cell subset with a low conversion to PD-1^{LO} T_{FH}. This suggests that the PD-1^{HI} T_{FH} population represents a more terminally differentiated state of the T_{FH} development. Whether multiple interactions with cognate B cells are important for sustaining the PD-1^{HI} T_{FH} population (thus, beyond induction stage) is still an unresolved matter. This issue could be addressed by an adoptive transfer of PD-1^{HI} T_{FH} to MHC II KO mice (or $B^{MHCII-/-}$ chimeras) and by investigating whether the PD-1^{HI} phenotype would be lost in the absence of functional APC or, more specifically, cognate B cells.

Fascinatingly, the differentiation of $CD4^+$ T cells and B cells is governed to some extent by the same TFs. The choice between terminally differentiated plasma cells and proliferating GC B cells is mediated by Blimp-1 or Bcl-6, respectively. Similarly, the phenotype of effector T cells and T_{FH} cells is also imposed by the presence of Blimp-1 or Bcl6, respectively. Whether this pattern of expression in $CD4^+$ T cells is tied to the proliferative capacity as observed in B cells remains to be established.

I have performed intracellular staining with the Ki67 nuclear marker characteristic for dividing, and not resting cells, and found no differences between PD-1^{HI} T_{FH} and PD-1^{LO} T_{FH} present in the SRBC immunisation model (Chapter 3, p. 76). This experiment did not provide conclusive evidence about the terminal differentiation of any subset. A study with IL-21^+ reporter mice showed that IL-21^+ T_{FH} cells are not a terminally differentiated cell subset, as they are undergoing substantial cell division (measured by incorporation of thymidine analogue BrdU [bromodeoxyuridine] and propidium iodide staining) (69). Experiments with carboxyfluorescein succinimidyl ester (CFSE) are not particularly feasible in our model due to the low numbers of isolated polyclonal T_{FH} cells and the high rate of cell death during the labelling process (roughly 50% of starting population). The monoclonal population could be used, however, as the studies with monoclonal and polyclonal system might yield

different results (discussed in section 1.17 'T_{FH} memory', p.37) and therefore it is better to use a more physiological set up when possible.

6.3 Specificity of T_{FH} found in co-immunised animals

The finding that co-immunisation with SRBC and *S. enterica* leads to the expansion of the T_{FH} population is very surprising. This experiment is difficult to interpret without establishing the specificity of the expanded T_{FH} cells and GC B cells. For numerous reasons (discussed in the Introduction to Chapter 5, p. 169) we decided to employ TCR sequencing, firstly, to characterize the clonal repertoire of the T_{FH} populations in both models and, secondly, to use the observed differences to investigate the T_{FH} populations in the co-immunised animals. Interestingly, SRBC activate T cells polyclonally without expansion of any selected clonotype. The opposite situation is observed after *S. enterica* infection, where certain T cell clones expand vastly over the others. Fascinatingly, the co-immunised groups indicate the presence of both T_{FH} populations, since they carry characteristics of the T_{FH} found in single immunisation with SRBC and with *S. enterica*. If PD-1^{HI} T_{FH} specific for *S. enterica* and SRBC in co-immunised animals are truly present, then the most important question is: what is the nature of the signal provided by SRBC that is required to generate PD-1^{HI} T^{FH} specific for *S. enterica* (and, consequently, drive a *Salmonella*-specific GC response)?

One of the transcripts selectively expressed by PD-1^{HI} T_{FH} in the SRBC model is IL-4 (Fig. 3.10). IL-4 was found to play an essential role in GC formation (235,236) and therefore would be a plausible candidate protein responsible for facilitating T_{FH} expansion. However, the absence of IL-4 was actually shown to enhance the Th-1 type response (237). Therefore, the role of IL-4 in co-immunised animals would have to be addressed experimentally (by either using IL-4R KO mice or anti-IL-4 blocking antibodies).

A completely separate conclusion comes from the analysis of each population within the single immunisation model. So, PD-1^{HI} T_{FH} and PD-1^{LO} T_{FH} (as well as $CXCR5^-$ T cells) raised after SRBC immunisation do not show evidence of clonal expansion. This is a significant finding since, first of all, there are not many studies that address the issue of the TCR repertoire within the T_{FH} population. Some

published reports suggest that T cells with the highest TCR affinity are recruited to the T_{FH} pool (82, 238), while others indicate that there is no preferential TCR usage in the T_{FH} and Th1 effector cell population (83). Therefore, similar TCR usage between both of the T_{FH} cell subset and the effector T cell population might indicate (although this is not a strict evidence) that there is no preferential specificity within any of the subsets. Thus, the TCR affinity might not influence the commitment to the T_{FH} or T effector cell subset.

Importantly, TCR sequencing does not directly determine the specificity. This issue can be directly addressed by *in vitro* restimulation assays or *in vivo* transfer studies, as described above (Introduction to Chapter 5, p. 169). Instead, TCR sequencing identifies clonal expansion patterns that are likely to be characteristic of a response to a particular antigen. Important cues and conclusions are derived from this study, while also more fascinating questions arise to be tackled in the future.

6.4 T_{FH} memory – Tcm or Tem population?

$CD4^+$ T cell memory is characterized by the presence of two populations: T central memory cells (Tcm) and T effector memory cells (Tem) (239). These populations are distinguished by the expression of CD62L, CD44 and CCR7 (239). Tcm cells express high amounts of CD62L and CCR7. They are thought to be circulating within SLO and proliferate rapidly upon re-exposure to the antigen. Tem express low levels of CD62L and CCR7, and they home preferentially to inflamed tissues (239). Both Tcm and Tem express high levels of CD44 on the surface, which is a marker of cell activation. Expression of CD62L is therefore important when considering the memory potential of the T_{FH} population.

My experiments have shown that PD-1^{HI} T_{FH} found within one week p.i. with SRBC have low CD62L expression, whereas PD-1^{LO} T_{FH} and $CXCR5^-$ T cells retain high CD62L expression, which points to the latter two populations as potential sources of T_{CM} cells. Whether the same CD62L expression pattern is also found on persisting T_{FH} is an interesting question. In the adoptive transfer experiments PD-1^{HI} T_{FH} did not up regulate the CD62L upon reactivation with SRBC (when measured at 24 h post transfer or 72 h post transfer and boost). This suggests that PD-1^{HI} T_{FH} cells do not directly contribute to the Tcm memory population, although more

adequate memory studies (with resting antigen-experienced cells in antigen-free environment for extended period of time before re-activation) are required to address the question fully.

Other published studies (discussed in the Introduction section 'T_{FH} memory', p. 37, (69,152) have clearly established that T_{FH} cells are able to persist in the absence of the antigen and upon activation give rise to cells with enhanced T_{FH} phenotype as well as 'classic' effector T cells. The existence of memory T_{FH} cells is an interesting phenomenon, since the GC reaction in the secondary response is of much lower magnitude than the one found in the primary response (27). Therefore, additional questions about the function of those T_{FH} memory cells arise.

6.5 T_{FH} subsets in humoral responses

An important aspect of T_{FH} biology, which has not been addressed directly in this thesis, regards the role of PD-1^{HI} T_{FH} and PD-1^{LO} T_{FH} cells in the antibody production. Ideally, adoptive transfers of these T_{FH} populations to congenic hosts would be followed by the assessment of antigen-specific antibody levels. Unfortunately, this approach is not feasible with SRBC as an antigen for several reasons. First of all, the transferred T_{FH} population size is small (3-4x10^5 cells) and therefore its effect on the GC output could be too modest to investigate. Secondly, SRBC generate a very robust humoral response and therefore the WT T_{FH} response concurrently taking place in the host could 'mask' the effects of the transferred population. Alternatively, an *in vitro* antibody production assay would provide some answers, but, as already discussed a few times before, this might not reflect the physiological situation observed *in vivo*.

6.6 Concluding remarks and unanswered questions

There are several important points in T_{FH} biology that still require answers. Firstly, the initial signals driving commitment to either the T_{FH} or effector T cell pool are not clear, and so far the strongest evidence point towards low IL-2 signalling (75,109,110). Secondly, signals governing the progression from T_{FH} cell to fully polarized GC T_{FH} cell are also elusive. Furthermore, the TCR repertoire of T_{FH} cells and GC T_{FH} cells in relation to T effector cells is also not well characterized. Finally, the ultimate differentiation state and the capacity to form memory by T_{FH} cells as

well as the possible conversion to other cell types is still under investigation. Therefore, although the T_{FH} function seems to be quite well understood, many questions focus on the origin and fate of the T_{FH} cells. These aspects of T_{FH} biology are highly significant for an optimal design of immune interventions. Expanding the fundamental knowledge about the T_{FH} population will further enhance the possibility to manipulate humoral responses, either by enhancing them when needed (e.g. during vaccine design) or blocking them when they are undesired (autoimmune conditions).

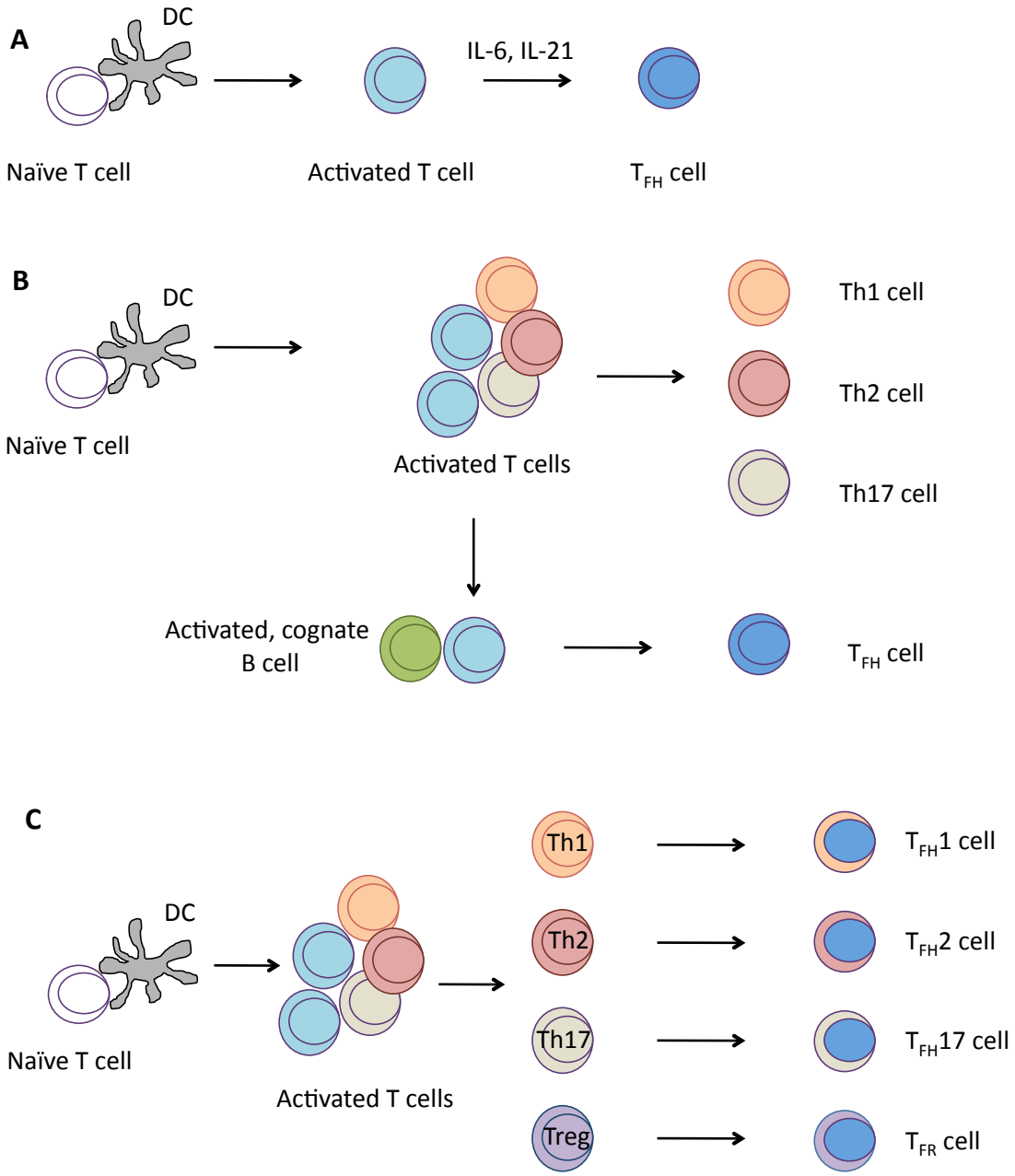

Fig 6.1.Models of T_{FH} differentiation.

(A) Linear model. Naïve T cells, following activation by dendritic cell (DC), differentiate into T_{FH} cells under the influence of IL-6 and IL-21. **(B) Pluripotent model**. Interactions between naïve T cells and DC establish a pool of activated T cell with separate precursors of each T cell subset. T_{FH} cells are generated after interaction with cognate B cells. **(C) Secondary program model.** Activated T cells differentiate into Th1, Th2, Th17 or Treg cells and then undergo re-programming to become T_{FH} cells (which retain some of the characteristics of the previous differentiation state).

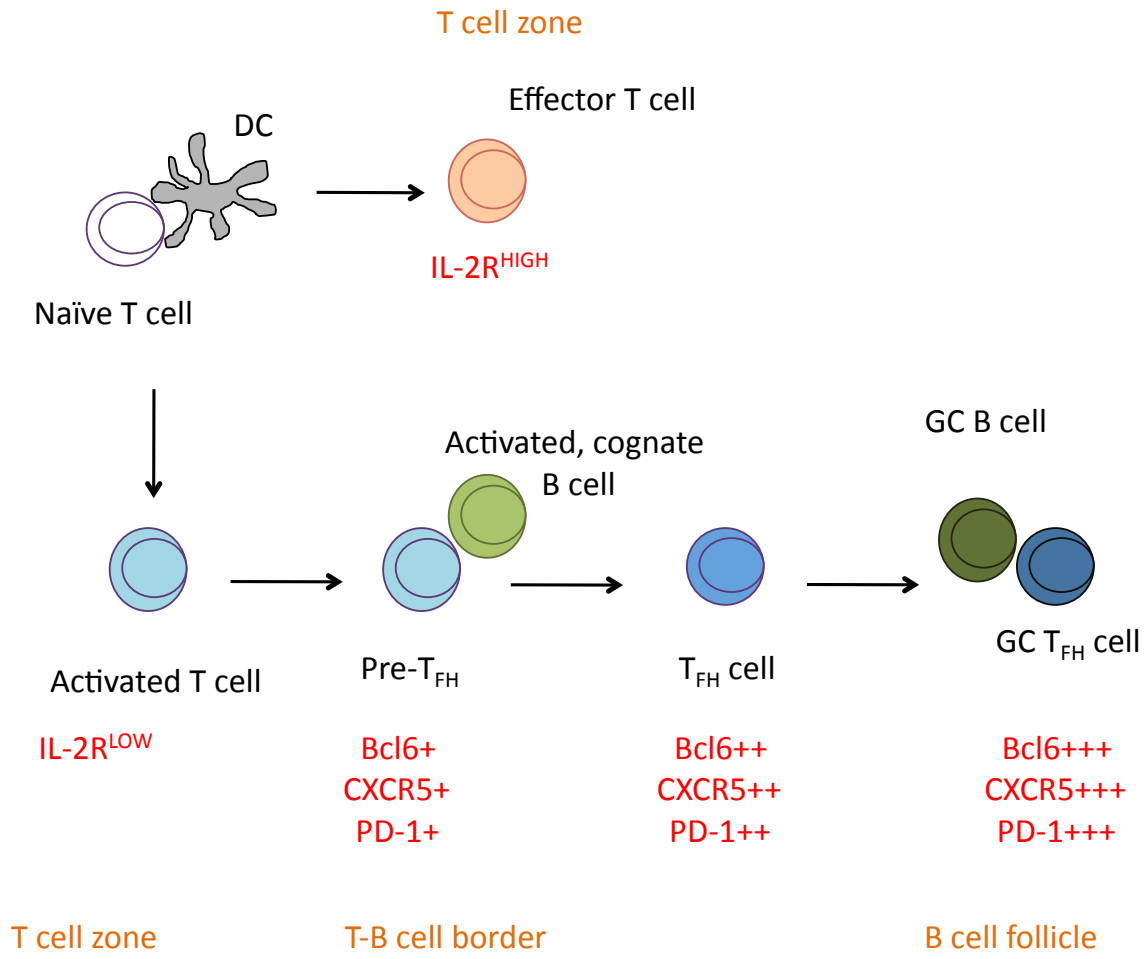

Fig 6.2.Integrated model of T_{FH} differentiation.

Naïve T cells during activation by DC commit to the effector T cell subset or the T_{FH} subset based on the amount of IL-2 signalling. IL-2R^{LOW} cells up regulate CXCR5, PD-1 and Bcl6 and move towards the T-B zone border, where they interact with activated cognate B cells. This interaction further enhances Bcl6, CXCR5 and PD-1 expression in T_{FH} cells. Full polarization of T_{FH} differentiation is displayed by GC T_{FH} cells, which upon interaction with GC B cells express maximum levels of CXCR5, Bcl6 and PD-1.

7 Appendix

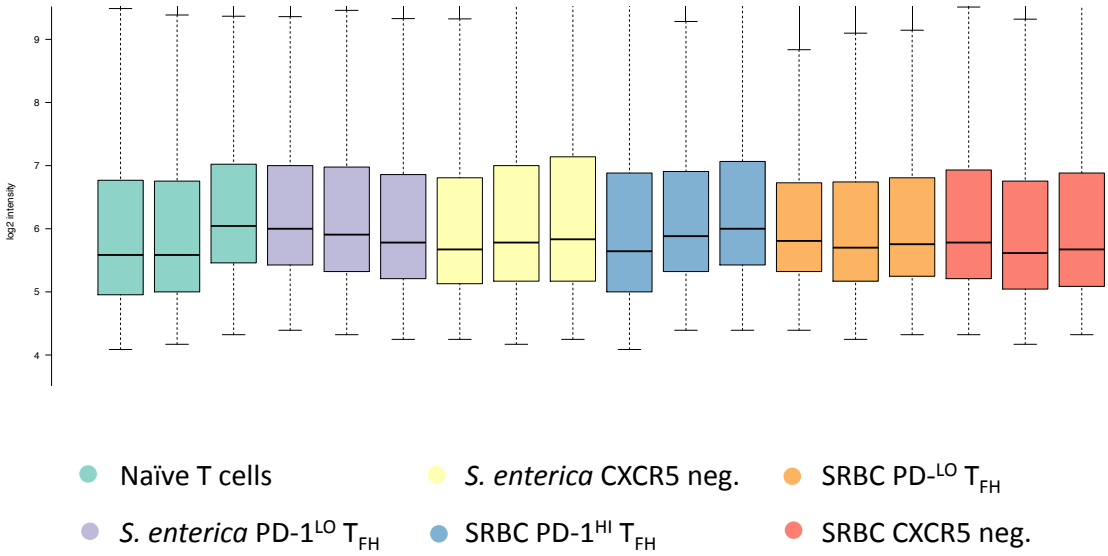

Fig 7.1 Quality control of microarrays: boxplots

Boxplots show the distribution of probe intensities (log2 intensity is plotted on Y axis) in each of the arrays (showed on X axis, one box plot symbolizes one array, each geoup is represented in triplicate). Boxes have similar size and variability (represented by interquartile range) and median (vertical line symbolizing central value). Boxplots are generated with raw, non-normalised data. Significant differences in the size or the position of the box suggest technical problem within the array. In this study no outliers were identified.

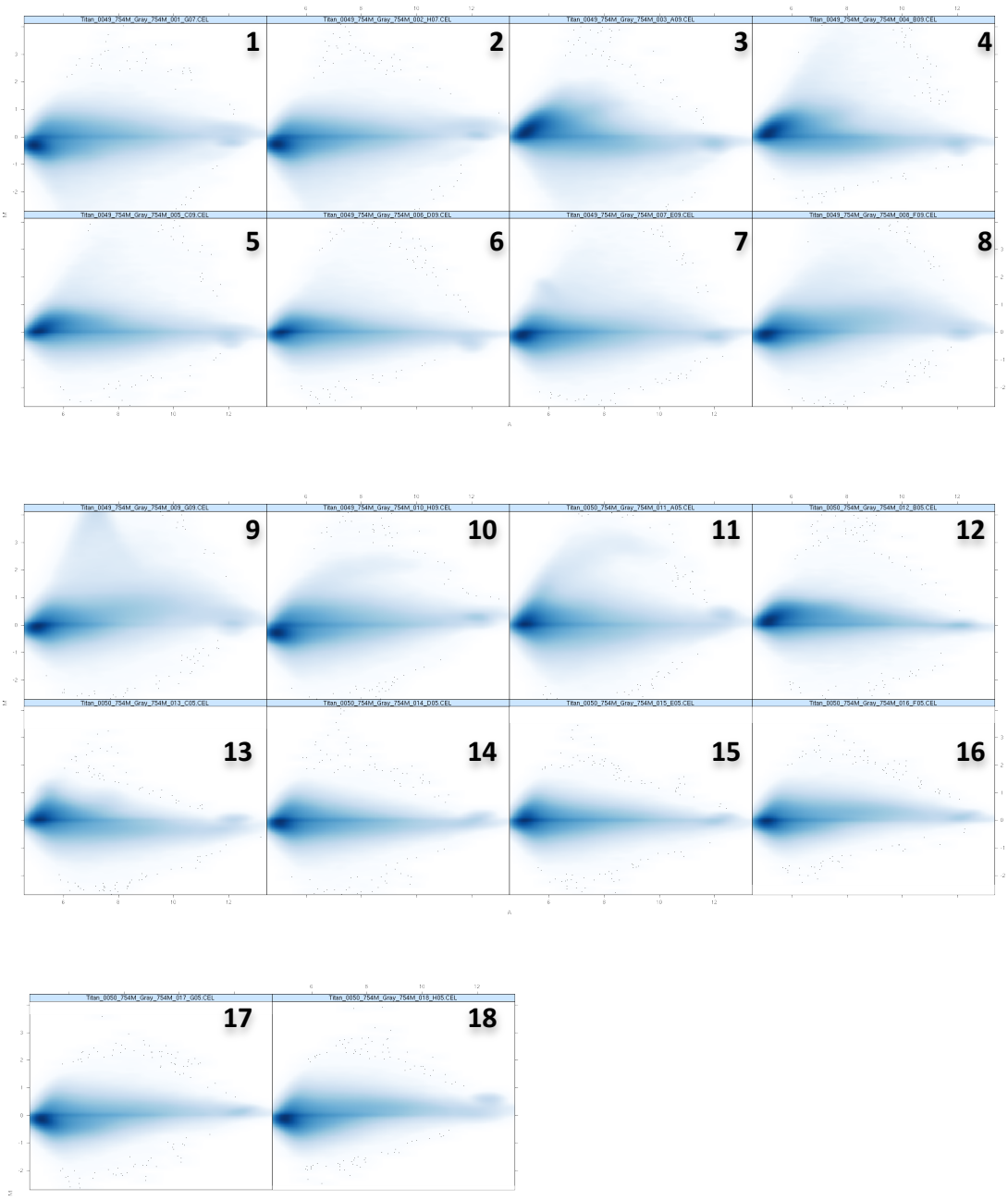

Fig 7.2 Quality control of microarrays: MA plots.

Individual array quality is assessed by MA plots. Y axis shows changes in the intensity (log2) for the array of interest and X axis shows average intensities across all arrays. Most of the genes (represented by single dots) are not differentially expresses and therefore are positioned along horizontal axis. The MA plot can identify issues with background intensity, saturation measurement or dye bias. In this study no outliers were identified based on MA plots. Each MA plot corresponds to one microarray. The code for the samples 1 to 18 is presented in Table 2.2 on p. 70.

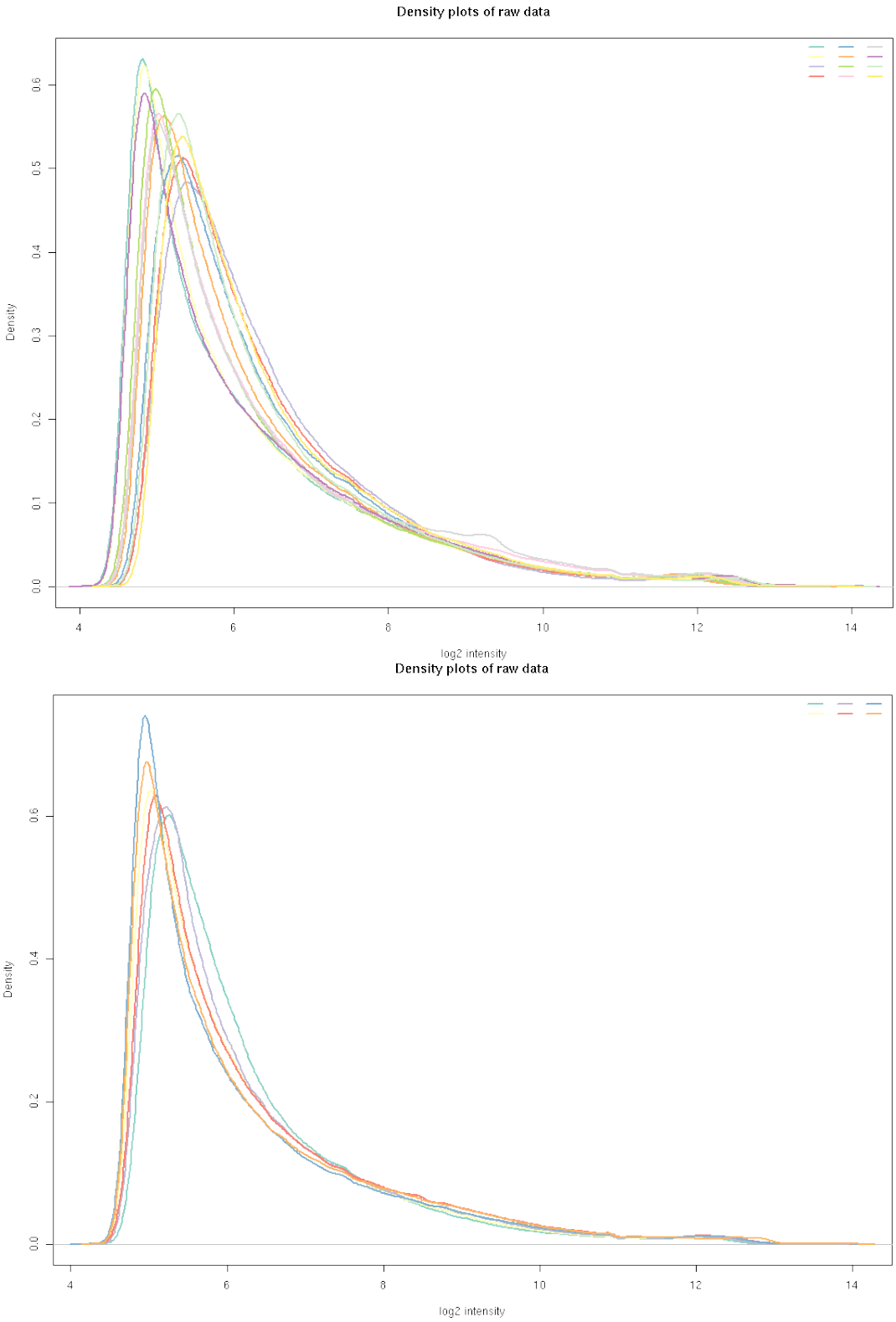

Fig 7.3. Quality control of microarrays: RNA density plots.

Density plots show how frequent certain intensity was measured for the samples. Each line represents one microarray. Y axis shows density and X axis shows log2 intensity. Samples should have similar size and range of the distribution. In this study no outliers were identified based on RNA density plots.

Fig 7.4. Quality control of microarrays: RNA degradation slopes.

RNA degradation plots illustrate RNA decay process. They are generated with normalised data. Each line represents one microarray. Lines should be parallel; significantly different slope indicates differences in handling samples. In this study no outliers were identified based on RNA degradation plots.

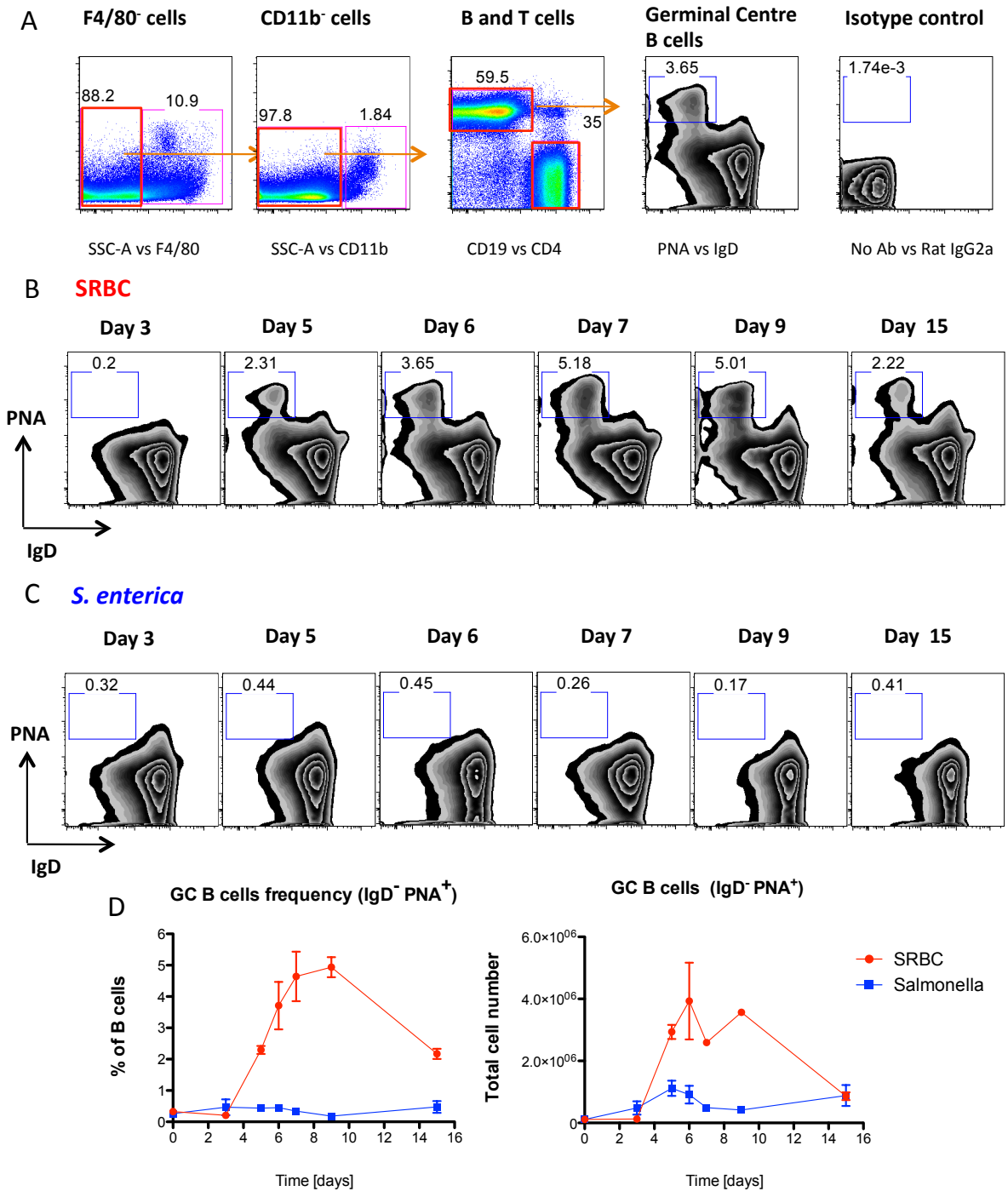

Fig. 7.5. Induction of GC B cell population (IgD$^-$ PNA$^+$) after immunisation with SRBC or *S. enterica* infection over time.

(A) Gating strategy for GC B cells (C57Bl/6 mouse on day 6 p.i with SRBC). **(B)** Representative flow cytometry plots GC B cell populations after SRBC immunisation **(B)** or *S. enterica* infection **(C)** over time. First two gating steps (lymphocytes and single cells, not shown) as in Fig. 3.1A. **(D)** Summary of GC B cell frequencies (left) or cell numbers (right) after SRBC immunisation (red) or *S. enterica* infection (blue) over time. Data representative of one experiment with at least three animals used per each time point.

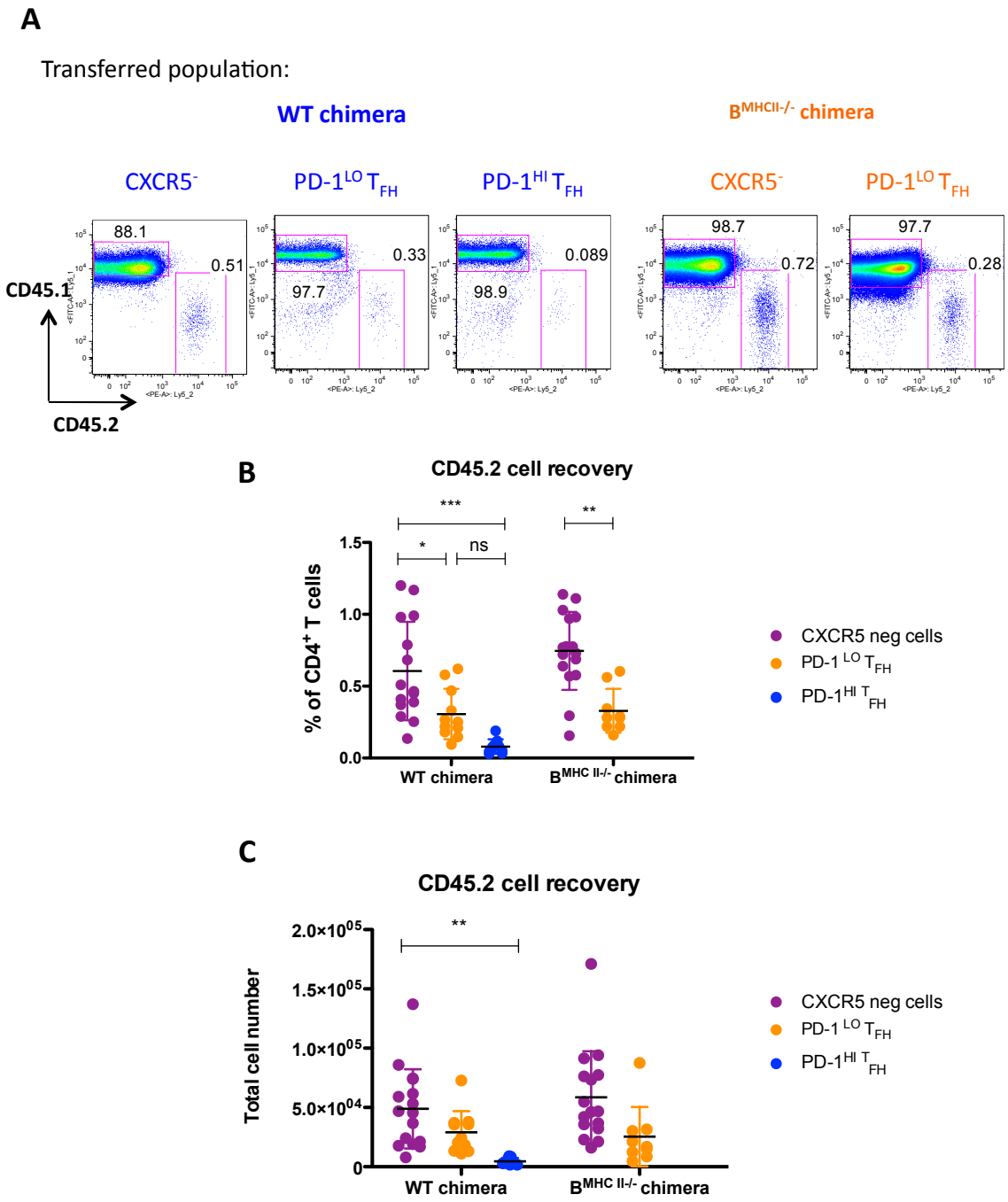

Fig 7.6. Differences in the recovery of transferred T cells populations.

(A) Representative flow cytometry plots of recovered transferred cells (CD45.2), gated on $CD19^{-}$ $CD4^{+}$ T cells from either WT chimeras (blue labels) or $B^{MHCII-/-}$ chimeras (orange labels). **(B)** Summary of recovered CD45.2 populations in terms of frequency or **(C)** total cell numbers. Data pulled from multiple experiments with at least 2 animals per group, each dot represents one mouse.

Statistical significance was determined by One-way ANOVA with post-ANOVA Tukey's test for multiple comparisons.

8 Bibliography

1. Mebius RE, Kraal G. Structure and function of the spleen. Nat Rev Immunol. 2005 Aug;5(8):606–16.

2. Luther SA, Bidgol A, Hargreaves DC, Schmidt A, Xu Y, Paniyadi J, et al. Differing activities of homeostatic chemokines CCL19, CCL21, and CXCL12 in lymphocyte and DC recruitment and lymphoid neogenesis. J Immunol. 2002 Jul 1;169(1):424–33.

3. Förster R, Mattis AE, Kremmer E, Wolf E, Brem G, Lipp M. A putative chemokine receptor, BLR1, directs B cell migration to defined lymphoid organs and specific anatomic compartments of the spleen. Cell. 1996 Dec 13;87(6):1037–47.

4. Cyster JG, Gunn MD, Ngo VN, Ansel KM, Ekland EH, Williams LT. A B-cell-homing chemokine made in lymphoid follicles activates Burkitt's lymphoma receptor-1 : Abstract : Nature. Nature. 1998 Feb 19;391(6669):799–803.

5. Ansel K, Ngo V, Hyman P, Luther S. A chemokine-driven positive feedback loop organizes lymphoid follicles. Nature. 2000.

6. Förster R, Davalos-Misslitz A. CCR7 and its ligands: balancing immunity and tolerance : Abstract : Nature Reviews Immunology. Nat Rev Immunol. 2008.

7. Baekkevold ES, Yamanaka T, Palframan RT, Carlsen HS, Reinholt FP, Andrian von UH, et al. The CCR7 ligand elc (CCL19) is transcytosed in high endothelial venules and mediates T cell recruitment. J Exp Med. 2001 May 7;193(9):1105–12.

8. Pillai S, Cariappa A, Moran ST. MARGINAL ZONE B CELLS. Annu Rev Immunol. 2005 Apr;23(1):161–96.

9. Cerutti A, Cols M, Puga I. Marginal zone B cells: virtues of innate-like antibody-producing lymphocytes. Nat Rev Immunol. 2013 Jan 25;13(2):118–32.

10. Borges da Silva H, Fonseca R, Pereira RM, Cassado ADA, Álvarez JM, D'Império Lima MR. Splenic Macrophage Subsets and Their Function during Blood-Borne Infections. Frontiers in Immunology. 2015 Sep 22;6(1):606.

11. Kang Y-S, Yamazaki S, Iyoda T, Pack M, Bruening SA, Kim JY, et al. SIGN-R1, a novel C-type lectin expressed by marginal zone macrophages in

spleen, mediates uptake of the polysaccharide dextran. International Immunology. 2003 Feb;15(2):177–86.

12. Seiler P, Aichele P, Odermatt B, Hengartner H, Zinkernagel RM, Schwendener RA. Crucial role of marginal zone macrophages and marginal zone metallophils in the clearance of lymphocytic choriomeningitis virus infection. Eur. J. Immunol. 1997 Oct;27(10):2626–33.

13. Martin F, Kearney JF. MARGINAL-ZONE B CELLS. Nat Rev Immunol. 2002 May;2(5):323–35.

14. Allman D, Pillai S. Peripheral B cell subsets. Curr Opin Immunol. 2008 Apr;20(2):149–57.

15. Gray M, Miles K, Salter D, Gray D, Savill J. Apoptotic cells protect mice from autoimmune inflammation by the induction of regulatory B cells. Proc. Natl. Acad. Sci. U.S.A. 2007 Aug 28;104(35):14080–5.

16. Kearney JF. B-cell subsets and the mature preimmune repertoire. Marginal zone and B1 B cells as part of a "natural immune memory." 2015 Nov 17;:1–10.

17. Zandvoort A, Timens W. The dual function of the splenic marginal zone: essential for initiation of anti-TI-2 responses but also vital in the general first-line defense against blood-borne antigens. Clin. Exp. Immunol. 2002 Oct;130(1):4–11.

18. Gil-Cruz C, Bobat S, Marshall JL, Kingsley RA, Ross EA, Henderson IR, et al. The porin OmpD from nontyphoidal Salmonella is a key target for a protective B1b cell antibody response. Proc. Natl. Acad. Sci. U.S.A. 2009 Jun 16;106(24):9803–8.

19. Baumgarth N, Herman OC, Jager GC, Brown LE, Herzenberg LA, Chen J. B-1 and B-2 cell-derived immunoglobulin M antibodies are nonredundant components of the protective response to influenza virus infection. J Exp Med. 2000 Jul 17;192(2):271–80.

20. Fu Y-X, Chaplin DD. DEVELOPMENT AND MATURATION OF SECONDARY LYMPHOID TISSUES. Annu Rev Immunol. Annual Reviews 4139 El Camino Way, P.O. Box 10139, Palo Alto, CA 94303-0139, USA; 1999 Apr;17(1):399–433.

21. Fillatreau S, Gray D. T cell accumulation in B cell follicles is regulated by DCs and is independent of B cell activation. J Exp Med. 2003 Jan 20;197(2):195–206.

22. Haynes NM, Allen CDC, Lesley R, Ansel KM, Killeen N, Cyster JG. Role of CXCR5 and CCR7 in follicular Th cell positioning and appearance of a programmed cell death gene-1high germinal center-associated subpopulation. J Immunol. 2007 Oct 15;179(8):5099–108.

23. Benson MJ, Erickson LD, Gleeson MW, Noelle RJ. Affinity of antigen encounter and other early B-cell signals determine B-cell fate. Curr Opin Immunol. 2007 Jun;19(3):275–80.

24. Allen CDC, Okada T, Cyster JG. Germinal-center organization and cellular dynamics. Immunity. 2007 Aug;27(2):190–202.

25. Qi H, Cannons JL, Klauschen F, Schwartzberg PL, Germain RN. SAP-controlled T–B cell interactions underlie GC formation. Nature. Nature Publishing Group; 2008 Oct 9;455(7214):764–9.

26. Crotty S, Johnston RJ, Schoenberger SP. Effectors and memories: Bcl-6 and Blimp-1 in T and B lymphocyte differentiation. Nat Immunol. 2010 Jan 19;11(2):114–20.

27. Liu YJ, Johnson GD, Gordon J, MacLennan IC. GC in T-cell-dependent antibody responses. Immunol. Today. 1992 Jan;13(1):17–21.

28. Cyster JG, Ansel KM, Reif K, Ekland EH, Hyman PL, Tang HL, et al. Follicular stromal cells and lymphocyte homing to follicles. Immunol. Rev. 2000 Aug;176:181–93.

29. Aguzzi A, Kranich J, Krautler NJ. Follicular DCs: origin, phenotype, and function in health and disease. Trends in Immunology. Elsevier Ltd; 2014 Mar 1;35(3):105–13.

30. Allen CDC, Cyster JG. Follicular DC networks of primary follicles and germinal centers: phenotype and function. Semin. Immunol. 2008 Feb;20(1):14–25.

31. Wang X, Cho B, Suzuki K, Xu Y, Green JA, An J, et al. Follicular DCs help establish follicle identity and promote B cell retention in germinal centers. J Exp Med. 2011 Nov 21;208(12):2497–510.

32. Klein U, Dalla-Favera R. GC: role in B-cell physiology and malignancy. Nat Rev Immunol. Nature Publishing Group; 2008 Jan;8(1):22–33.

33. Vinuesa CG, Sanz I, Cook MC. Dysregulation of GC in autoimmune disease. Nat Rev Immunol. Nature Publishing Group; 2009 Dec;9(12):845–57.

34. Yoshida T, Mei H, Dörner T, Hiepe F. Memory B and memory plasma cells - Yoshida - 2010 - Immunological Reviews - Wiley Online Library. Immunological …. 2010.

35. Cannons JL, Qi H, Lu KT, Dutta M, Gomez-Rodriguez J, Cheng J, et al. Optimal germinal center responses require a multistage T cell:B cell adhesion process involving integrins, SLAM-associated protein, and CD84. Immunity. 2010 Feb 26;32(2):253–65.

36. Swain SL. CD4 T cell development and cytokine polarization: an overview. J. Leukoc. Biol. 1995 May;57(5):795–8.

37. Kapsenberg ML. Dendritic-cell control of pathogen-driven T-cell polarization. Nat Rev Immunol. 2003 Dec;3(12):984–93.

38. Murphy KM, Stockinger B. Effector T cell plasticity: flexibility in the face of changing circumstances. Nat Immunol. 2010 Aug;11(8):674–80.

39. Zhu J, Yamane H, Paul WE. Differentiation of Effector CD4 T Cell Populations *. Annu Rev Immunol. 2010 Mar;28(1):445–89.

40. Nakayamada S, Takahashi H, Kanno Y, O'shea JJ. Helper T cell diversity and plasticity. Curr Opin Immunol. Elsevier Ltd; 2012 Jun 1;24(3):297–302.

41. Zhou L, Chong MMW, Littman DR. Plasticity of CD4+ T Cell Lineage Differentiation. Immunity. 2009 May;30(5):646–55.

42. Fontenot JD, Gavin MA, Rudensky AY. Foxp3 programs the development and function of CD4+CD25+ regulatory T cells. Nat Immunol. 2003 Apr;4(4):330–6.

43. Sakaguchi S, Yamaguchi T, Nomura T, Ono M. Regulatory T Cells and Immune Tolerance. Cell. 2008 May;133(5):775–87.

44. Askenasy N, Kaminitz A, Yarkoni S. Mechanisms of T regulatory cell function. Autoimmunity Reviews. 2008 May;7(5):370–5.

45. Kaplan MH. Th9 cells: differentiation and disease - Kaplan - 2013 - Immunological Reviews - Wiley Online Library. Immunol. Rev. 2013.

46. Hirota K, Turner J-E, Villa M, Duarte JH, Demengeot J, Steinmetz OM, et al. Plasticity of Th17 cells in Peyer's patches is responsible for the induction of T cell-dependent IgA responses. Nat Immunol. 2013 Apr;14(4):372–9.

47. Hutloff A, Dittrich AM, Beier KC, Eljaschewitsch B, Kraft R, Anagnostopoulos I, et al. ICOS is an inducible T-cell co-stimulator structurally and functionally related to CD28. Nature. 1999 Jan 21;397(6716):263–6.

48. Rudd CE, Schneider H. Unifying concepts in CD28, ICOS and CTLA4 co-receptor signalling. Nat Rev Immunol. 2003 Jul;3(7):544–56.

49. Greenwald RJ, Freeman GJ, Sharpe AH. THE B7 FAMILY REVISITED. http://dx.doi.org/10.1146/annurev.immunol.23.021704.115611. Annual Reviews; 2005.

50. McAdam AJ, Greenwald RJ, Levin MA, Chernova T, Malenkovich N, Ling V, et al. ICOS is critical for CD40-mediated antibody class switching. Nature. 2001 Jan 4;409(6816):102–5.

51. Tafuri A, Shahinian A, Bladt F, Yoshinaga SK, Jordana M, Wakeham A, et al. ICOS is essential for effective T-helper-cell responses. Nature. 2001 Jan 4;409(6816):105–9.

52. Dong C, Juedes AE, Temann UA, Shresta S, Allison JP, Ruddle NH, et al. ICOS co-stimulatory receptor is essential for T-cell activation and function. Nature. 2001 Jan 4;409(6816):97–101.

53. Akiba H, Takeda K, Kojima Y, Usui Y, Harada N, Yamazaki T, et al. The role of ICOS in the CXCR5+ follicular B helper T cell maintenance in vivo. J Immunol. 2005 Aug 15;175(4):2340–8.

54. Bosma MJ, Carroll AM. The SCID mouse mutant: definition, characterization, and potential uses. Annu Rev Immunol. 1991;9:323–50.

55. Nurieva RI, Chung Y, Hwang D, Yang XO, Kang HS, Ma L, et al. Generation of T Follicular Helper Cells Is Mediated by Interleukin-21 but Independent of T Helper 1, 2, or 17 Cell Lineages. Immunity. 2008 Jul;29(1):138–49.

56. Xu H, Li X, Liu D, Li J, Zhang X, Chen X, et al. Follicular T-helper cell recruitment governed by bystander B cells and ICOS-driven motility. Nature. 2013 Apr 25;496(7446):523–7.

57. Kerfoot SM, Yaari G, Patel JR, Johnson KL, Gonzalez DG, Kleinstein SH, et al. Germinal Center B Cell and T Follicular Helper Cell Development Initiates in the Interfollicular Zone. Immunity. 2011 Jun;34(6):947–60.

58. Weber JP, Fuhrmann F, Feist RK, Lahmann A, Baz Al MS, Gentz L-J, et al. ICOS maintains the T follicular helper cell phenotype by down-regulating Krüppel-like factor 2. J Exp Med. 2015 Feb 9;212(2):217–33.

59. Chen L. Co-inhibitory molecules of the B7–CD28 family in the control of T-cell immunity. Nat Rev Immunol. Nature Publishing Group; 2004 May;4(5):336–47.

60. Sharpe AH, Wherry EJ, Ahmed R, Freeman GJ. The function of programmed cell death 1 and its ligands in regulating autoimmunity and infection. Nat Immunol. 2007 Mar;8(3):239–45.

61. Sharpe AH, Freeman GJ. THE B7–CD28 SUPERFAMILY. Nat Rev Immunol. Nature Publishing Group; 2002 Feb;2(2):116–26.

62. Hams E, McCarron MJ, Amu S, Yagita H, Azuma M, Chen L, et al. Blockade of B7-H1 (Programmed Death Ligand 1) Enhances Humoral Immunity by Positively Regulating the Generation of T Follicular Helper Cells. The Journal of Immunology. 2011 May 3;186(10):5648–55.

63. Spolski R, Leonard WJ. Interleukin-21: basic biology and implications for cancer and autoimmunity. Annu Rev Immunol. 2008;26:57–79.

64. Ozaki K, Spolski R, Feng CG, Qi C-F, Cheng J, Sher A, et al. A critical role for IL-21 in regulating immunoglobulin production. Science. 2002 Nov 22;298(5598):1630–4.

65. Gharibi T, Majidi J, Kazemi T, Dehghanzadeh R, Motallebnezhad M, Babaloo Z. Biological effects of IL-21 on different immune cells and its role in autoimmune diseases. Immunobiology. 2015 Oct.

66. Ozaki K, Spolski R, Ettinger R, Kim H-P, Wang G, Qi C-F, et al. Regulation of B cell differentiation and plasma cell generation by IL-21, a novel inducer of Blimp-1 and Bcl-6. J Immunol. 2004 Nov 1;173(9):5361–71.

67. Zeng R, Spolski R, Casas E, Zhu W, Levy DE, Leonard WJ. The molecular basis of IL-21-mediated proliferation. Blood. 2007 May 15;109(10):4135–42.

68. Nurieva R, Yang XO, Martinez G, Zhang Y, Panopoulos AD, Ma L, et al. Essential autocrine regulation by IL-21 in the generation of inflammatory T cells. Nature. 2007 Jul 26;448(7152):480–3.

69. Lüthje K, Kallies A, Shimohakamada Y, Belz GT, Light A, Tarlinton DM, et al. The development and fate of follicular helper T cells defined by an IL-21 reporter mouse. Nat Immunol. 2012 Apr 1.

70. Vogelzang A, McGuire HM, Yu D, Sprent J, Mackay CR, King C. A fundamental role for interleukin-21 in the generation of T follicular helper cells. Immunity. 2008 Jul 18;29(1):127–37.

71. Ettinger R, Sims GP, Fairhurst A-M, Robbins R, da Silva YS, Spolski R, et al. IL-21 induces differentiation of human naive and memory B cells into antibody-secreting plasma cells. J Immunol. 2005 Dec 15;175(12):7867–79.

72. Zotos D, Coquet JM, Zhang Y, Light A, D'Costa K, Kallies A, et al. IL-21 regulates germinal center B cell differentiation and proliferation through a B cell-intrinsic mechanism. Journal of Experimental Medicine. 2010 Feb 15;207(2):365–78.

73. Zaretsky AG, Taylor JJ, King IL, Marshall FA, Mohrs M, Pearce EJ. T follicular helper cells differentiate from Th2 cells in response to helminth antigens. Journal of Experimental Medicine. 2009 May 11;206(5):991–9.

74. King IL, Mohrs M. IL-4-producing CD4+ T cells in reactive lymph nodes during helminth infection are T follicular helper cells. Journal of Experimental Medicine. 2009 May 11;206(5):1001–7.

75. Choi YS, Kageyama R, Eto D, Escobar TC, Johnston RJ, Monticelli L, et al. ICOS receptor instructs T follicular helper cell versus effector cell differentiation via induction of the transcriptional repressor Bcl6. Immunity. 2011 Jun 24;34(6):932–46.

76. Linterman MA, Denton AE, Divekar DP, Zvetkova I, Kane L, Ferreira C, et al. CD28 expression is required after T cell priming for helper T cell responses and protective immunity to infection. Elife. 2014;3.

77. Johnston RJ, Poholek AC, DiToro D, Yusuf I, Eto D, Barnett B, et al. Bcl6 and Blimp-1 are reciprocal and antagonistic regulators of T follicular helper cell differentiation. Science. 2009 Aug 21;325(5943):1006–10.

78. Kitano M, Moriyama S, Ando Y, Hikida M, Mori Y, Kurosaki T, et al. Bcl6 Protein Expression Shapes Pre-Germinal Center B Cell Dynamics and Follicular Helper T Cell Heterogeneity. Immunity. Elsevier Inc; 2011 Jun 24;34(6):961–72.

79. Poholek AC, Hansen K, Hernandez SG, Eto D, Chandele A, Weinstein JS, et al. In Vivo Regulation of Bcl6 and T Follicular Helper Cell Development. The Journal of Immunology. 2010 Jul 1;185(1):313–26.

80. Baumjohann D, Okada T, Ansel KM. Cutting Edge: Distinct Waves of BCL6 Expression during T Follicular Helper Cell Development. The Journal of Immunology. 2011 Sep 1;187(5):2089–92.

81. Goenka R, Barnett LG, Silver JS, O'Neill PJ, Hunter CA, Cancro MP, et al. Cutting Edge: DC-Restricted Antigen Presentation Initiates the Follicular Helper T Cell Program but Cannot Complete Ultimate Effector Differentiation. 2011 Aug 1;187(3):1091–5.

82. Fazilleau N, Mcheyzer-Williams LJ, Rosen H, Mcheyzer-Williams MG. The function of follicular helper T cells is regulated by the strength of T cell antigen receptor binding. Nat Immunol. Nature Publishing Group; 2009 Mar 1;10(4):375–84.

83. Ploquin MJ-Y, Eksmond U, Kassiotis G. B cells and TCR avidity determine distinct functions of CD4+ T cells in retroviral infection. The Journal of Immunology. 2011 Sep 15;187(6):3321–30.

84. Nurieva RI, Chung Y, Martinez GJ, Yang XO, Tanaka S, Matskevitch TD, et al. Bcl6 mediates the development of T follicular helper cells. Science. 2009 Aug 21;325(5943):1001–5.

85. Yu D, Rao S, Tsai LM, Lee SK, He Y, Sutcliffe EL, et al. The transcriptional repressor Bcl-6 directs T follicular helper cell lineage commitment. Immunity. 2009 Sep 18;31(3):457–68.

86. Mombaerts P, Iacomini J, Johnson RS, Herrup K, Tonegawa S, Papaioannou VE. RAG-1-deficient mice have no mature B and T lymphocytes. Cell. 1992 Mar 6;68(5):869–77.

87. Liu X, Yan X, Zhong B, Nurieva RI, Wang A, Wang X, et al. Bcl6 expression specifies the T follicular helper cell program in vivo. Journal of Experimental Medicine. 2012 Sep 17.

88. Hiramatsu Y, Suto A, Kashiwakuma D, Kanari H, Kagami S-I, Ikeda K, et al. c-Maf activates the promoter and enhancer of the IL-21 gene, and TGF-beta inhibits c-Maf-induced IL-21 production in CD4+ T cells. J. Leukoc. Biol. 2010 Apr;87(4):703–12.

89. Kroenke MA, Eto D, Locci M, Cho M, Davidson T, Haddad EK, et al. Bcl6 and Maf Cooperate To Instruct Human Follicular Helper CD4 T Cell Differentiation. The Journal of Immunology. 2012 Apr 4;188(8):3734–44.

90. Bauquet AT, Jin H, Paterson AM, Mitsdoerffer M, Ho I-C, Sharpe AH, et al. The costimulatory molecule ICOS regulates the expression of c-Maf and IL-21 in the development of follicular T helper cells and TH-17 cells. Nat Immunol. 2009 Feb;10(2):167–75.

91. Pot C, Jin H, Awasthi A, Liu SM, Lai C-Y, Madan R, et al. Cutting edge: IL-27 induces the TF c-Maf, cytokine IL-21, and the costimulatory receptor ICOS that coordinately act together to promote differentiation of IL-10-producing Tr1 cells. The Journal of Immunology. 2009 Jul 15;183(2):797–801.

92. Kim JI, Ho IC, Grusby MJ, Glimcher LH. The TF c-Maf controls the production of interleukin-4 but not other Th2 cytokines. Immunity. 1999.

93. Bollig N, Brüstle A, Kellner K, Ackermann W, Abass E, Raifer H, et al. TF IRF4 determines germinal center formation through follicular T-helper cell differentiation. Proc. Natl. Acad. Sci. U.S.A. 2012 May 29;109(22):8664–9.

94. Kwon H, Thierry-Mieg D, Thierry-Mieg J, Kim H-P, Oh J, Tunyaplin C, et al. Analysis of interleukin-21-induced Prdm1 gene regulation reveals functional cooperation of STAT3 and IRF4 TFs. Immunity. 2009 Dec 18;31(6):941–52.

95. Huber M, Brüstle A, Reinhard K, Guralnik A, Walter G, Mahiny A, et al. IRF4 is essential for IL-21-mediated induction, amplification, and stabilization of the Th17 phenotype. Proc. Natl. Acad. Sci. U.S.A. 2008 Dec 30;105(52):20846–51.

96. Betz BC, Jordan-Williams KL, Wang C, Kang SG, Liao J, Logan MR, et al. Batf coordinates multiple aspects of B and T cell function required for normal antibody responses. J Exp Med. 2010 May 10;207(5):933–42.

97. Ise W, Kohyama M, Schraml BU, Zhang T, Schwer B, Basu U, et al. The TF BATF controls the global regulators of class-switch recombination in both B cells and T cells. Nat Immunol. 2011 May 15;12(6):536–43.

98. Schraml BU, Hildner K, Ise W, Lee W-L, Smith WAE, Solomon B, et al. The AP-1 TF Batf controls TH17 differentiation. Nature. 2009 Jul 5.

99. Liu X, Chen X, Zhong B, Wang A, Wang X, Chu F, et al. TF achaete-scute homologue 2 initiates follicular T-helper-cell development. Nature. Nature

Publishing Group; 2014 Jan 19;:1–21.

100. Suto A, Kashiwakuma D, Kagami S-I, Hirose K, Watanabe N, Yokote K, et al. Development and characterization of IL-21-producing CD4+ T cells. J Exp Med. 2008 Jun 9;205(6):1369–79.

101. Batten M, Ramamoorthi N, Kljavin NM, Ma CS, Cox JH, Dengler HS, et al. IL-27 supports germinal center function by enhancing IL-21 production and the function of T follicular helper cells. Journal of Experimental Medicine. 2010 Dec 20;207(13):2895–906.

102. Eto D, Lao C, DiToro D, Barnett B, Escobar TC, Kageyama R, et al. IL-21 and IL-6 are critical for different aspects of B cell immunity and redundantly induce optimal follicular helper CD4 T cell (Tfh) differentiation. PLoS ONE. 2011;6(3):e17739.

103. Lu KT, Kanno Y, Cannons JL, Handon R, Bible P, Elkahloun AG, et al. Functional and Epigenetic Studies Reveal Multistep Differentiation and Plasticity of In Vitro-Generated and In Vivo-Derived Follicular T Helper Cells. Immunity. 2011 Oct 1;35(4):622–32.

104. Eddahri F, Denanglaire S, Bureau F, Spolski R, Leonard WJ, Leo O, et al. Interleukin-6/STAT3 signaling regulates the ability of naive T cells to acquire B-cell help capacities. Blood. 2009 Mar 12;113(11):2426–33.

105. Dienz O, Eaton SM, Bond JP, Neveu W, Moquin D, Noubade R, et al. The induction of antibody production by IL-6 is indirectly mediated by IL-21 produced by CD4+ T cells. J Exp Med. 2009 Jan 16;206(1):69–78.

106. Linterman MA, Beaton L, Yu D, Ramiscal RR, Srivastava M, Hogan JJ, et al. IL-21 acts directly on B cells to regulate Bcl-6 expression and germinal center responses. Journal of Experimental Medicine. 2010 Feb 15;207(2):353–63.

107. Yi JS, Du M, Zajac AJ. A vital role for interleukin-21 in the control of a chronic viral infection. Science. 2009 Jun 19;324(5934):1572–6.

108. Heinrich PC, Behrmann I, Haan S, Hermanns HM, Müller-Newen G, Schaper F. Principles of interleukin (IL)-6-type cytokine signalling and its regulation. Biochem. J. 2003 Aug 15;374(Pt 1):1–20.

109. Johnston RJ, Choi YS, Diamond JA, Yang JA, Crotty S. STAT5 is a potent negative regulator of TFH cell differentiation. Journal of Experimental Medicine. 2012 Feb 13;209(2):243–50.

110. Nurieva RI, Podd A, Chen Y, Alekseev AM, Yu M, Qi X, et al. STAT5 negatively regulates T follicular helper (Tfh) cell generation and function. Journal of Biological Chemistry. 2012 Feb 8.

111. Gong D, Malek TR. Cytokine-dependent Blimp-1 expression in activated T

cells inhibits IL-2 production. J Immunol. 2007 Jan 1;178(1):242–52.

112. Good-Jacobson KL, Song E, Anderson S, Sharpe AH, Shlomchik MJ. CD80 Expression on B Cells Regulates Murine T Follicular Helper Development, Germinal Center B Cell Survival, and Plasma Cell Generation. The Journal of Immunology. 2012 May 1;188(9):4217–25.

113. Good-Jacobson KL, Szumilas CG, Chen L, Sharpe AH, Tomayko MM, Shlomchik MJ. PD-1 regulates germinal center B cell survival and the formation and affinity of long-lived plasma cells. Nat Immunol. 2010 Jun;11(6):535–42.

114. Crotty S. Follicular helper CD4 T cells (TFH). Annu Rev Immunol. 2011 Apr 23;29(1):621–63.

115. Murphy KM, Nelson CA, Sedý JR. Balancing co-stimulation and inhibition with BTLA and HVEM. Nat Rev Immunol. 2006 Sep;6(9):671–81.

116. Kashiwakuma D, Suto A, Hiramatsu Y, Ikeda K, Takatori H, Suzuki K, et al. B and T lymphocyte attenuator suppresses IL-21 production from follicular Th cells and subsequent humoral immune responses. The Journal of Immunology. 2010 Sep 1;185(5):2730–6.

117. Foy TM, Laman JD, Ledbetter JA, Aruffo A, Claassen E, Noelle RJ. gp39-CD40 interactions are essential for germinal center formation and the development of B cell memory. J Exp Med. 1994 Jul 1;180(1):157–63.

118. Han S, Hathcock K, Zheng B, Kepler TB, Hodes R, Kelsoe G. Cellular interaction in germinal centers. Roles of CD40 ligand and B7-2 in established germinal centers. J Immunol. 1995 Jul 15;155(2):556–67.

119. van Essen D, Kikutani H, Gray D. CD40 ligand-transduced co-stimulation of T cells in the development of helper function. Nature. 1995 Dec 7;378(6557):620–3.

120. Renshaw BR, Fanslow WC, Armitage RJ, Campbell KA, Liggitt D, Wright B, et al. Humoral immune responses in CD40 ligand-deficient mice. J Exp Med. 1994 Nov 1;180(5):1889–900.

121. Whitmire JK, Slifka MK, Grewal IS, Flavell RA, Ahmed R. CD40 ligand-deficient mice generate a normal primary cytotoxic T-lymphocyte response but a defective humoral response to a viral infection. Journal of Virology. 1996 Dec;70(12):8375–81.

122. Choe J, Kim HS, Zhang X, Armitage RJ, Choi YS. Cellular and molecular factors that regulate the differentiation and apoptosis of germinal center B cells. Anti-Ig down-regulates Fas expression of CD40 ligand-stimulated germinal center B cells and inhibits Fas-mediated apoptosis. The Journal of …. 1996.

123. Randall TD, Heath AW, Santos-Argumedo L, Howard MC, Weissman IL, Lund FE. Arrest of B lymphocyte terminal differentiation by CD40 signaling: mechanism for lack of antibody-secreting cells in germinal centers. Immunity. 1998 Jun;8(6):733–42.

124. Good KL, Bryant VL, Tangye SG. Kinetics of Human B Cell Behavior and Amplification of Proliferative Responses following Stimulation with IL-21. The Journal of Immunology. 2006 Oct 2;177(8):5236–47.

125. Arpin C, Déchanet J, Van Kooten C, Merville P, Grouard G, Brière F, et al. Generation of memory B cells and plasma cells in vitro. Science. 1995 May 5;268(5211):720–2.

126. Veillette A. Immune regulation by SLAM family receptors and SAP-related adaptors. Nat Rev Immunol. Nature Publishing Group; 2006 Jan;6(1):56–66.

127. Cannons JL, Tangye SG, Schwartzberg PL. SLAM family receptors and SAP adaptors in immunity. Annu Rev Immunol. 2011;29:665–705.

128. Cannons JL, Yu LJ, Jankovic D, Crotty S, Horai R, Kirby M, et al. SAP regulates T cell-mediated help for humoral immunity by a mechanism distinct from cytokine regulation. J Exp Med. 2006 Jun 12;203(6):1551–65.

129. Yusuf I, Kageyama R, Monticelli L, Johnston RJ, DiToro D, Hansen K, et al. Germinal center T follicular helper cell IL-4 production is dependent on signaling lymphocytic activation molecule receptor (CD150). The Journal of Immunology. 2010 Jul 1;185(1):190–202.

130. Spolski R. IL-21 and T follicular helper cells. International Immunology. 2010.

131. Lee SK, Rigby RJ, Zotos D, Tsai LM, Kawamoto S, Marshall JL, et al. B cell priming for extrafollicular antibody responses requires Bcl-6 expression by T cells. Journal of Experimental Medicine. 2011 Jul 4;208(7):1377–88.

132. Reinhardt RL, Liang H-E, Locksley RM. Cytokine-secreting follicular T cells shape the antibody repertoire. Nat Immunol. 2009 Apr;10(4):385–93.

133. Kim H-J, Verbinnen B, Tang X, Lu L, Cantor H. Inhibition of follicular T-helper cells by CD8+ regulatory T cells is essential for self tolerance. Nature. 2010 Sep 16;467(7313):328–32.

134. Linterman MA, Pierson W, Lee SK, Kallies A, Kawamoto S, Rayner TF, et al. Foxp3+ follicular regulatory T cells control the germinal center response. Nat Med. 2011 Jul 24;17(8):975–82.

135. Chung Y, Tanaka S, Chu F, Nurieva RI, Martinez GJ, Rawal S, et al. Follicular regulatory T cells expressing Foxp3 and Bcl-6 suppress germinal center reactions. Nat Med. 2011 Jul 24;17(8):983–8.

136. Shaffer AL, Yu X, He Y, Boldrick J, Chan EP, Staudt LM. BCL-6 represses genes that function in lymphocyte differentiation, inflammation, and cell cycle control. Immunity. 2000 Aug;13(2):199–212.

137. Shaffer AL, Lin K-I, Kuo TC, Yu X, Hurt EM, Rosenwald A, et al. Blimp-1 orchestrates plasma cell differentiation by extinguishing the mature B cell gene expression program. Immunity. 2002 Jul;17(1):51–62.

138. Koch MA, Tucker-Heard G, Perdue NR, Killebrew JR, Urdahl KB, Campbell DJ. The TF T-bet controls regulatory T cell homeostasis and function during type 1 inflammation. Nat Immunol. 2009 Jun;10(6):595–602.

139. Zheng Y, Chaudhry A, Kas A, deRoos P, Kim JM, Chu T-T, et al. Regulatory T-cell suppressor program co-opts TF IRF4 to control T(H)2 responses. Nature. 2009 Mar 19;458(7236):351–6.

140. Chaudhry A, Rudra D, Treuting P, Samstein RM. CD4+ regulatory T cells control TH17 responses in a Stat3-dependent manner. Science. 2009.

141. Pelletier N, Mcheyzer-Williams LJ, Wong KA, Urich E, Fazilleau N, Mcheyzer-Williams MG. Plasma cells negatively regulate the follicular helper T cell program. Nature Publishing Group. 2010 Dec;11(12):1110–8.

142. Ma CS, Deenick EK, Batten M, Tangye SG. The origins, function, and regulation of T follicular helper cells. Journal of Experimental Medicine. 2012 Jul 2;209(7):1241–53.

143. Choi YS, Yang JA, Yusuf I, Johnston RJ, Greenbaum J, Peters B, et al. Bcl6 expressing follicular helper CD4 T cells are fate committed early and have the capacity to form memory. The Journal of Immunology. 2013 Apr 15;190(8):4014–26.

144. Lim HW, Kim CH. Loss of IL-7 receptor alpha on CD4+ T cells defines terminally differentiated B cell-helping effector T cells in a B cell-rich lymphoid tissue. J Immunol. 2007 Dec 1;179(11):7448–56.

145. Bentebibel SE, Schmitt N, Banchereau J, Ueno H. Human tonsil B-cell lymphoma 6 (BCL6)-expressing CD4+ T-cell subset specialized for B-cell help outside germinal centers. Proc. Natl. Acad. Sci. U.S.A. 2011 Aug 16;108(33):E488–97.

146. Godfrey DI, Stankovic S, Baxter AG. Raising the NKT cell family. Nat Immunol. 2010 Mar;11(3):197–206.

147. Chang P-P, Barral P, Fitch J, Pratama A, Ma CS, Kallies A, et al. Identification of Bcl-6-dependent follicular helper NKT cells that provide cognate help for B cell responses. Nat Immunol. 2011 Nov 27;13(1):35–43.

148. Barral P, Eckl-Dorna J, Harwood NE, De Santo C, Salio M, Illarionov P, et

al. B cell receptor-mediated uptake of CD1d-restricted antigen augments antibody responses by recruiting invariant NKT cell help in vivo. Proc. Natl. Acad. Sci. U.S.A. 2008 Jun 17;105(24):8345–50.

149. Barr TA, Brown S, Mastroeni P, Gray D. TLR and B Cell Receptor Signals to B Cells Differentially Program Primary and Memory Th1 Responses to Salmonella enterica. The Journal of Immunology. 2010 Sep 1;185(5):2783–9.

150. Crawford A, Macleod M, Schumacher T, Corlett L, Gray D. Primary T cell expansion and differentiation in vivo requires antigen presentation by B cells. J Immunol. 2006 Mar 15;176(6):3498–506.

151. Pepper M, Pagán AJ, Igyártó BZ, Taylor JJ, Jenkins MK. Opposing signals from the Bcl6 TF and the interleukin-2 receptor generate T helper 1 central and effector memory cells. Immunity. 2011 Oct 28;35(4):583–95.

152. Weber JP, Fuhrmann F, Hutloff A. T follicular helper cells survive as long-term memory cells. Eur. J. Immunol. 2012 Jun 25.

153. Hale JS, Youngblood B, Latner DR, Mohammed AUR, Ye L, Akondy RS, et al. Distinct Memory CD4+ T Cells with Commitment to T Follicular Helper- and T Helper 1-Cell Lineages Are Generated after Acute Viral Infection. Immunity. 2013 Apr;38(4):805–17.

154. Gray D. A role for antigen in the maintenance of immunological memory : Article : Nature Reviews Immunology. Nat Rev Immunol. 2002.

155. Vinuesa CG, Cook MC, Angelucci C, Athanasopoulos V, Rui L, Hill KM, et al. A RING-type ubiquitin ligase family member required to repress follicular helper T cells and autoimmunity. Nature. Nature Publishing Group; 2005 May 26;435(7041):452–8.

156. Linterman MA, Rigby RJ, Wong RK, Yu D, Brink R, Cannons JL, et al. Follicular helper T cells are required for systemic autoimmunity. J Exp Med. 2009 Mar 16;206(3):561–76.

157. Bossaller L, Burger J, Draeger R, Grimbacher B, Knoth R, Plebani A, et al. ICOS deficiency is associated with a severe reduction of CXCR5+CD4 germinal center Th cells. J Immunol. 2006 Oct 1;177(7):4927–32.

158. Hoiseth SK, Stocker BA. Aromatic-dependent Salmonella typhimurium are non-virulent and effective as live vaccines. Nature. 1981 May 21;291(5812):238–9.

159. Jones BD, Falkow S. Salmonellosis: host immune responses and bacterial virulence determinants. Annu Rev Immunol. 1996;14:533–61.

160. Gerold G, Zychlinsky A, de Diego JL. What is the role of Toll-like receptors in bacterial infections? Semin. Immunol. 2007 Feb;19(1):41–7.

161. Mastroeni P, Sheppard M. Salmonella infections in the mouse model: host resistance factors and in vivo dynamics of bacterial spread and distribution in the tissues. Microbes and Infection. 2004 Apr;6(4):398–405.

162. Jackson A, Nanton MR, O'Donnell H, Akue AD, McSorley SJ. Innate immune activation during Salmonella infection initiates extramedullary erythropoiesis and splenomegaly. The Journal of Immunology. 2010 Nov 15;185(10):6198–204.

163. Mastroeni P, Ugrinovic S, Chandra A. Resistance and susceptibility to Salmonella infections: lessons from mice and patients with immunodeficiencies. Reviews in Medical …. 2003.

164. Mastroeni P, Grant A, Restif O, Maskell D. A dynamic view of the spread and intracellular distribution of Salmonella enterica. Nat. Rev. Microbiol. 2009 Jan;7(1):73–80.

165. Bueno SM, Riquelme S, Riedel CA, Kalergis AM. Mechanisms used by virulent Salmonella to impair DC function and evade adaptive immunity. Immunology. 2012 Jun 16.

166. Mastroeni P, Ménager N. Development of acquired immunity to Salmonella. J. Med. Microbiol. 2003 Jun;52(Pt 6):453–9.

167. Kalupahana RS, Mastroeni P, Maskell D, Blacklaws BA. Activation of murine DCs and macrophages induced by Salmonella enterica serovar Typhimurium. Immunology. 2005 Aug;115(4):462–72.

168. Mastroeni P, Harrison JA, Robinson JH, Clare S, Khan S, Maskell DJ, et al. Interleukin-12 is required for control of the growth of attenuated aromatic-compound-dependent salmonellae in BALB/c mice: role of gamma interferon and macrophage activation. Infect Immun. 1998 Oct;66(10):4767–76.

169. Mastroeni P, Clare S, Khan S, Harrison JA, Hormaeche CE, Okamura H, et al. Interleukin 18 contributes to host resistance and gamma interferon production in mice infected with virulent Salmonella typhimurium. Infect Immun. 1999 Feb;67(2):478–83.

170. Nauciel C, Espinasse-Maes F. Role of gamma interferon and tumor necrosis factor alpha in resistance to Salmonella typhimurium infection. Infect Immun. 1992 Feb;60(2):450–4.

171. Cunningham AF, Gaspal F, Serre K, Mohr E, Henderson IR, Scott-Tucker A, et al. Salmonella induces a switched antibody response without germinal centers that impedes the extracellular spread of infection. J Immunol. 2007;178(10):6200–7.

172. Barr TA, Brown S, Mastroeni P, Gray D. B Cell Intrinsic MyD88 Signals Drive IFN- Production from T Cells and Control Switching to IgG2c. The

Journal of Immunology. 2009 Jul 15;183(2):1005–12.

173. Ugrinovic S, Ménager N, Goh N, Mastroeni P. Characterization and development of T-Cell immune responses in B-cell-deficient (Igh-6(-/-)) mice with Salmonella enterica serovar Typhimurium infection. Infect Immun. 2003 Dec;71(12):6808–19.

174. Pietro Mastroeni, Simmons C, Fowler R, Hormaeche CE, Dougan G. Igh-6 −/−(B-Cell-Deficient) Mice Fail To Mount Solid Acquired Resistance to Oral Challenge with Virulent Salmonella enterica Serovar Typhimurium and Show Impaired Th1 T-Cell Responses toSalmonella Antigens. Infection and …. 2000.

175. Sprent J, Boehmer von H. Helper function of T cells depleted of alloantigen-reactive lymphocytes by filtration through irradiated F1 hybrid recipients. I. Failure to collaborate with allogeneic B cells in a secondary response to sheep erythrocytes measured in vivo. J Exp Med. 1976 Sep 1;144(3):617–26.

176. Van Muiswinkel WB, Van Soest PL. The T cell-dependent period of the immune response to sheep erythrocytes. Immunology. 1976 Jul;31(1):111–8.

177. Chan TD, Gatto D, Wood K, Camidge T, Basten A, Brink R. Antigen Affinity Controls Rapid T-Dependent Antibody Production by Driving the Expansion Rather than the Differentiation or Extrafollicular Migration of Early Plasmablasts. The Journal of Immunology. 2009 Aug 20;183(5):3139–49.

178. Ismail N, Bretscher PA. The Th1/Th2 nature of concurrent immune responses to unrelated antigens can be independent. J Immunol. 1999 Nov 1;163(9):4842–50.

179. Adachi O, Kawai T, Takeda K, Matsumoto M, Tsutsui H, Sakagami M, et al. Targeted disruption of the MyD88 gene results in loss of IL-1- and IL-18-mediated function. Immunity. 1998 Jul;9(1):143–50.

180. Kitamura D, Roes J, Kühn R, Rajewsky K. A B cell-deficient mouse by targeted disruption of the membrane exon of the immunoglobulin mu chain gene. Nature. 1991 Apr 4;350(6317):423–6.

181. Cosgrove D, Gray D, Dierich A, Kaufman J, Lemeur M. Mice lacking MHC class II molecules. Cell. 1991.

182. Chtanova T, Tangye SG, Newton R, Frank N, Hodge MR, Rolph MS, et al. T follicular helper cells express a distinctive transcriptional profile, reflecting their role as non-Th1/Th2 effector cells that provide help for B cells. J Immunol. 2004 Jul 1;173(1):68–78.

183. Breitfeld D, Ohl L, Kremmer E, Ellwart J, Sallusto F, Lipp M, et al. Follicular B helper T cells express CXC chemokine receptor 5, localize to B

cell follicles, and support immunoglobulin production. J Exp Med. 2000 Dec 4;192(11):1545–52.

184. Schaerli P, Willimann K, Lang AB, Lipp M, Loetscher P, Moser B. CXC chemokine receptor 5 expression defines follicular homing T cells with B cell helper function. J Exp Med. 2000 Dec 4;192(11):1553–62.

185. Basso K, Dalla-Favera R. Roles of BCL6 in normal and transformed germinal center B cells. Immunol. Rev. 2012 May;247(1):172–83.

186. Schluns KS, Kieper WC, Jameson SC, Lefrançois L. Interleukin-7 mediates the homeostasis of naïve and memory CD8 T cells in vivo. Nat Immunol. 2000 Nov;1(5):426–32.

187. Tan JT, Dudl E, LeRoy E, Murray R, Sprent J, Weinberg KI, et al. IL-7 is critical for homeostatic proliferation and survival of naive T cells. Proc. Natl. Acad. Sci. U.S.A. 2001 Jul 17;98(15):8732–7.

188. Seddon B, Zamoyska R. TCR and IL-7 receptor signals can operate independently or synergize to promote lymphopenia-induced expansion of naive T cells. J Immunol. 2002 Oct 1;169(7):3752–9.

189. Bromley SK, Thomas SY, Luster AD. Chemokine receptor CCR7 guides T cell exit from peripheral tissues and entry into afferent lymphatics. Nat Immunol. Nature Publishing Group; 2005 Aug 14;6(9):895–901.

190. Yoshida R, Nagira M, Kitaura M, Imagawa N, Imai T, Yoshie O. Secondary lymphoid-tissue chemokine is a functional ligand for the CC chemokine receptor CCR7. J. Biol. Chem. 1998 Mar 20;273(12):7118–22.

191. Kim CH, Rott LS, Clark-Lewis I, Campbell DJ, Wu L, Butcher EC. Subspecialization of CXCR5+ T cells: B helper activity is focused in a germinal center-localized subset of CXCR5+ T cells. J Exp Med. 2001 Jun 18;193(12):1373–81.

192. Veerman KM, Williams MJ, Uchimura K, Singer MS, Merzaban JS, Naus S, et al. Interaction of the selectin ligand PSGL-1 with chemokines CCL21 and CCL19 facilitates efficient homing of T cells to TF. Nat Immunol. 2007 May;8(5):532–9.

193. Gallatin WM, Weissman IL, Butcher EC. A cell-surface molecule involved in organ-specific homing of lymphocytes. 1983. J. Immunol. 2006. pp. 5–9.

194. Kansas GS, Ley K, Munro JM, Tedder TF. Regulation of leukocyte rolling and adhesion to high endothelial venules through the cytoplasmic domain of L-selectin. J Exp Med. 1993 Mar 1;177(3):833–8.

195. Venturi GM, Tu L, Kadono T, Khan AI, Fujimoto Y, Oshel P, et al. Leukocyte migration is regulated by L-selectin endoproteolytic release. Immunity. 2003 Nov;19(5):713–24.

196. Bullwinkel J, Baron-Lühr B, Lüdemann A, Wohlenberg C, Gerdes J, Scholzen T. Ki-67 protein is associated with ribosomal RNA transcription in quiescent and proliferating cells. J. Cell. Physiol. 2006 Mar;206(3):624–35.

197. Gerdes J, Lemke H, Baisch H, Wacker HH, Schwab U, Stein H. Cell cycle analysis of a cell proliferation-associated human nuclear antigen defined by the monoclonal antibody Ki-67. J Immunol. 1984 Oct;133(4):1710–5.

198. Duchrow M, Schlüter C, Key G, Kubbutat MH, Wohlenberg C, Flad HD, et al. Cell proliferation-associated nuclear antigen defined by antibody Ki-67: a new kind of cell cycle-maintaining proteins. Arch. Immunol. Ther. Exp. (Warsz.). 1995;43(2):117–21.

199. Ringnér M. What is principal component analysis? Nat Biotechnol. New York, NY: Nature Pub. Co., 1996; 2008;26(3):303–4.

200. Gohlmann H, Talloen W. Gene Expression Studies Using Affymetrix Microarrays. CRC Press; 2010.

201. Levy S, Todd SC, Maecker HT. CD81 (TAPA-1): a molecule involved in signal transduction and cell adhesion in the immune system. Annu Rev Immunol. 1998;16:89–109.

202. VanCompernolle SE, Levy S, Todd SC. Anti-CD81 activates LFA-1 on T cells and promotes T cell-B cell collaboration. Eur. J. Immunol. 2001 Mar;31(3):823–31.

203. Deng J, Dekruyff RH, Freeman GJ, Umetsu DT, Levy S. Critical role of CD81 in cognate T–B cell interactions leading to Th2 responses. 2002.

204. Horie RAWT. CD30: expression and function in health and disease. 1998 Nov 19;:1–14.

205. Cerutti A, Schaffer A, Shah S, Zan H, Liou HC. CD30 is a CD40-inducible molecule that negatively regulates CD40-mediated immunoglobulin class switching in non-antigen-selected human B cells. Immunity. 1998.

206. Pellegrini P, Berghella AM, Contasta I, Adorno D. CD30 antigen: not a physiological marker for TH2 cells but an important costimulator molecule in the regulation of the balance between TH1/TH2 response. Transplant Immunology. 2003 Oct;12(1):49–61.

207. Weinstein JS, Bertino SA, Hernandez SG, Poholek AC, Teplitzky TB, Nowyhed HN, et al. B Cells in T Follicular Helper Cell Development and Function: Separable Roles in Delivery of ICOS Ligand and Antigen. The Journal of Immunology. 2014 Mar 7.

208. Deenick EK, Chan A, Ma CS, Gatto D, Schwartzberg PL, Brink R, et al. Follicular helper T cell differentiation requires continuous antigen presentation that is independent of unique B cell signaling. Immunity. 2010

Aug 27;33(2):241–53.

209. Barnett LG, Simkins HMA, Barnett BE, Korn LL, Johnson AL, Wherry EJ, et al. B cell antigen presentation in the initiation of follicular helper T cell and germinal center differentiation. The Journal of Immunology. 2014 Apr 15;192(8):3607–17.

210. Szakal AK, Kosco MH, Tew JG. Microanatomy of lymphoid tissue during humoral immune responses: structure function relationships. Annu Rev Immunol. 1989;7:91–109.

211. Hochweller K, Striegler J, Hämmerling GJ, Garbi N. A novel CD11c.DTR transgenic mouse for depletion of DCs reveals their requirement for homeostatic proliferation of natural killer cells. Eur. J. Immunol. 2008 Oct;38(10):2776–83.

212. Girard J-P, Moussion C, Förster R. HEVs, lymphatics and homeostatic immune cell trafficking in lymph nodes. Nat Rev Immunol. 2012 Nov;12(11):762–73.

213. Nikolich-Žugich J, Slifka MK, Messaoudi I. The many important facets of T-cell repertoire diversity. Nat Rev Immunol. 2004 Feb;4(2):123–32.

214. Felix NJ, Allen PM. Specificity of T-cell alloreactivity. Nat Rev Immunol. 2007 Dec;7(12):942–53.

215. Han A, Glanville J, Hansmann L, Davis MM. Linking T-cell receptor sequence to functional phenotype at the single-cell level. Nat Biotechnol. 2014 Jun 22;32(7):684–92.

216. Garcia KC, Teyton L, Wilson IA. Structural basis of T cell recognition. Annu Rev Immunol. 1999.

217. Rudolph MG, Wilson IA. The specificity of TCR/pMHC interaction. Curr Opin Immunol. 2002 Feb;14(1):52–65.

218. Calis JJA, Rosenberg BR. Characterizing immune repertoires by high throughput sequencing: strategies and applications. Trends in Immunology. 2014 Dec;35(12):581–90.

219. Freeman JD, Warren RL, Webb JR, Nelson BH, Holt RA. Profiling the T-cell receptor beta-chain repertoire by massively parallel sequencing. Genome Research. 2009 Oct 1;19(10):1817–24.

220. Newell EW, Davis MM. Beyond model antigens: high-dimensional methods for the analysis of antigen-specific T cells. Nat Biotechnol. 2014 Jan 19;32(2):149–57.

221. Fazilleau N, Eisenbraun MD, Malherbe L, Ebright JN, Pogue-Caley RR, Mcheyzer-Williams LJ, et al. Lymphoid reservoirs of antigen-specific

memory T helper cells. Nat Immunol. 2007 Jul;8(7):753–61.

222. Reiser J-B, Darnault C, Grégoire C, Mosser T, Mazza G, Kearney A, et al. CDR3 loop flexibility contributes to the degeneracy of TCR recognition. Nat Immunol. 2003 Mar;4(3):241–7.

223. Turcatti G, Romieu A, Fedurco M, Tairi A-P. A new class of cleavable fluorescent nucleotides: synthesis and optimization as reversible terminators for DNA sequencing by synthesis. Nucleic Acids Research. 2008 Mar;36(4):e25.

224. Shendure J, Ji H. Next-generation DNA sequencing. Nat Biotechnol. 2008 Oct;26(10):1135–45.

225. Bolotin DA, Shugay M, Mamedov IZ, Putintseva EV, Turchaninova MA, Zvyagin IV, et al. MiTCR: software for T-cell receptor sequencing data analysis. Nature Publishing Group. Nature Publishing Group; 2013 Jul 28;10(9):813–4.

226. Cookson BT, Bevan MJ. Identification of a natural T cell epitope presented by Salmonella-infected macrophages and recognized by T cells from orally immunized mice. J Immunol. 1997 May 1;158(9):4310–9.

227. McSorley SJ, Cookson BT, Jenkins MK. Characterization of CD4+ T cell responses during natural infection with Salmonella typhimurium. J Immunol. 2000 Jan 15;164(2):986–93.

228. Bergman MA, Cummings LA, Alaniz RC, Mayeda L, Fellnerova I, Cookson BT. CD4+-T-cell responses generated during murine Salmonella enterica serovar Typhimurium infection are directed towards multiple epitopes within the natural antigen FliC. Infect Immun. 2005 Nov;73(11):7226–35.

229. Lee S-J, McLachlan JB, Kurtz JR, Fan D, Winter SE, Baumler AJ, et al. Temporal expression of bacterial proteins instructs host CD4 T cell expansion and Th17 development. PLoS Pathog. 2012 Jan;8(1):e1002499.

230. Singh SP, Williams YU, Miller S, Nikaido H. The C-terminal domain of Salmonella enterica serovar typhimurium OmpA is an immunodominant antigen in mice but appears to be only partially exposed on the bacterial cell surface. Infect Immun. 2003 Jul;71(7):3937–46.

231. Leyva-Rangel JP, de Los Angeles Hernández-Cueto M, Galan-Enriquez C-S, López-Medina M, Ortiz-Navarrete V. Bacterial clearance reverses a skewed T-cell repertoire induced by Salmonella infection. Immun Inflamm Dis. 2015 Sep;3(3):209–23.

232. Wei L, Laurence A, Elias KM, O'shea JJ. IL-21 is produced by Th17 cells and drives IL-17 production in a STAT3-dependent manner. J. Biol. Chem. 2007 Nov 30;282(48):34605–10.

233. Perona-Wright G, Jenkins SJ, O'Connor RA, Zienkiewicz D, McSorley HJ, Maizels RM, et al. A pivotal role for CD40-mediated IL-6 production by DCs during IL-17 induction in vivo. The Journal of Immunology. 2009 Mar 1;182(5):2808–15.

234. Oestreich KJ, Mohn SE, Weinmann AS. Molecular mechanisms that control the expression and activity of Bcl-6 in TH1 cells to regulate flexibility with a TFH-like gene profile. Nat Immunol. Nature Publishing Group; 2012 Mar 11;13(4):405–11.

235. Toellner KM, Luther SA, Sze DM, Choy RK, Taylor DR, MacLennan IC, et al. T helper 1 (Th1) and Th2 characteristics start to develop during T cell priming and are associated with an immediate ability to induce immunoglobulin class switching. J Exp Med. 1998 Apr 20;187(8):1193–204.

236. Toellner K-M. Cognate interactions: extrafollicular IL-4 drives germinal-center reactions, a new role for an old cytokine. Eur. J. Immunol. 2014 Jul;44(7):1917–20.

237. Andoh A, Masuda A, Yamakawa M, Kumazawa Y, Kasajima T. Absence of interleukin-4 enhances germinal center reaction in secondary immune response. Immunology Letters. 2000 Jul 3;73(1):35–41.

238. Leddon SA, Sant AJ. The peptide specificity of the endogenous T follicular helper cell repertoire generated after protein immunization. PLoS ONE. 2012;7(10):e46952.

239. Sallusto F, Geginat J, Lanzavecchia A. C entralM emory andE ffectorM emoryT C ellS ubsets: Function, Generation, and Maintenance. Annu Rev Immunol. 2004 Apr;22(1):745–63.